THE STRUCTURAL ROOT SYSTEMS OF SITKA SPRUCE AND RELATED STOCHASTIC PROCESSES

by

ROBIN HENDERSON

Thesis Submitted for the Degree of Doctor of Philosophy

University of Edinburgh

1981

UNIV. EDINBURGEN EX BIBL

ABSTRACT OF THESIS

The research described in this thesis is in two parts. The first part is a study of the spatial patterns formed by the structural roots of Sitka spruce. The excavation and mensuration of eight Sitka spruce root systems are described, the variables which together determine the spatial pattern of a root system are identified and the data obtained are analysed by standard statistical methods. Our results indicate that the spatial spread of a root system may be more systematic than has been assumed previously. Computer simulation of rooting patterns is then discussed and examples are given to illustrate how simulation can be useful to forest scientists. The first part of the thesis is then concluded by an investigation into a method of describing a complex root system, namely the distribution of total root length against distance, depth and direction from the tree stem.

The second part of the thesis is a theoretical investigation into the properties of several stochastic processes suggested by an examination of rooting patterns and important to many other applications also. First, the correlated random walk in the plane is studied. In this type of walk the direction changes between steps are independent random variables whereas in classical random walks step directions are independent random variables. Results which are established include the recurrence of the walk and a central limit theorem. Next, correlated random walks on one- and two-dimensional lattices are investigated. Various results are derived and some interesting comparisons are made between correlated and simple random walks. In particular, it seems that correlation only has a scaling effect on many asymptotic properties of random walks. Finally, the effect of correlation in the branching random walk is considered. In this process particles perform correlated random walks and also produce random numbers of offspring after each step. Our main result for this process is an analogue to the central limit theorem. Two forms of this theorem are given: the first shows mean square and the second almost sure convergence.

ACKNOWLEDGEMENTS

I am sincerely grateful to my two supervisors, Dr. Ford and Dr. Renshaw, for their help, encouragement and constructive criticisms during the period of this research. Thanks are also due to Mr. J. D. Deans for the excavation of the root systems, assistance with their mensuration and for many useful discussions.

I would like to thank the Natural Environment Research Council for financial support.

CONTENTS

	DECLARATION	ii
	ABSTRACT OF THESIS	iii
	ACKNOWLEDGEMENTS	iv
CHAPTER 1	INTRODUCTION	1
	1.1 Statistical Analysis and Computer Simulation of the Rooting Patterns of Sitka Spruce	1
	1.2 Random Walks and Branching Random Walks with Correlated Step Directions	4
	1.3 Numbering and Notation	5
CHAPTER 2	STRUCTURAL ROOT MORPHOLOGY IN A SITKA SPRUCE PLANTATION	7
	2.1 A Summary of Earlier Work	7
	2.1.i The development of a structural root system	7
	2.1.ii Observed structural root systems	9
	2.2 Methods	10
	2.2.i Site and excavation	10
	2.2.ii Preliminary measuring system	12
	2.2.iii Measuring system employed	13
	2.3 Results	16
	2.3.i Gross dimensions	16
	2.3.ii Distribution of total root length	18
	2.3.iii Distribution of branching points	23
	2.3.iv Distribution of bends	28
	2.4 Discussion	30

CHAPTER 3 THE VARIABLES WHICH DETERMINE STRUCTURAL ROOT MORPHOLOGY 32

3.1 Initial Distribution Variables 33
3.1.i INROOT 33
3.1.ii STEMAZ and INAZ 34
3.1.iii INANG 36

3.2 Directional Variables 36
3.2.i BENDAZ and PARAZ 37
3.2.ii BRANCHAZ 39
3.2.iii FORKAZ 39
3.2.iv BENDANG, PARANG and FORKANG 40
3.2.v BRANCHANG 42

3.3 Path Reconstruction Variables 43
3.3.i GENLEN 44
3.3.ii ENDTYPE 45
3.3.iii NBRAN 46
3.3.iv NBEND 47
3.3.v DISTBRAN 48
3.3.vi DISTBEND 49

3.4 Sequential Step Variables 49
3.4.i STEPLEN 50
3.4.ii NOFF 52

3.5 Discussion 54

3.6 Figures 56

3.7 Tables 69

CHAPTER 4 COMPUTER SIMULATION OF ROOTING PATTERNS AND THE USE OF LENGTH CURVES AS DESCRIPTIVE STATISTICS 82

4.1 Simulation Models 82

4.2 Programming 83

4.3 Results 84
4.3.i Comparison of Models 84
4.3.ii Model application I: assessment of rules for generating rooting patterns 86

4.3.iii Model application II: the estimation of total root length from a partial sample 89

4.4 The Use of Length Curves As Descriptive Statistics of Spatial Patterns 91

4.4.i Convergence of the mean length curves 92

4.4.ii Sensitivity of the mean length curves 93

4.4.iii The use of length curves in numerical parameter estimation 95

4.5 Discussion 98

4.6 Figures 100

CHAPTER 5 A RANDOM WALK WITH CORRELATED STEP DIRECTIONS: CONTINUOUS CASE 137

5.1 Assumptions and Notation 138

5.2 Related Processes 143

5.3 The Problem of Determining the Distribution Function of $\underline{S}_n$ 144

5.4 Some Moments of the Process 148

5.4.i Mean of $\underline{S}_n$ 148

5.4.ii Dispersion matrix of $\underline{S}_n$ 150

5.4.iii Moments of R_n 157

5.5 Weak Law of Large Numbers 158

5.6 A Central Limit Theorem 159

5.7 Recurrence 165

CHAPTER 6 A RANDOM WALK WITH CORRELATED STEP DIRECTIONS: DISCRETE CASE 175

6.1 Correlated Random Walks on a One-Dimensional Lattice 176

6.1.i Probability distribution 176

6.1.ii Characteristic function of the probability distribution 181

6.1.iii Mean and variance 182
6.1.iv Occupation probability generating function 187
6.1.v Recurrence and first passage times 191
6.1.vi Asymptotic number of points visited 196
6.1.vii Diffusion approximation 200

6.2 Correlated Random Walks on a Two-Dimensional Square Lattice 201
6.2.i Characteristic function of the probability distribution 201
6.2.ii Mean and dispersion matrix 205
6.2.iii Occupation probability generating function 209
6.2.iv Recurrence and first passage times 219
6.2.v Asymptotic number of points visited 224
6.2.vi Diffusion approximation 228

6.3 Discussion 232

CHAPTER 7 BRANCHING CORRELATED RANDOM WALKS 236

7.1 Branching Processes 237

7.2 Related Work 241

7.3 Definitions, Notation and Basic Results 242

7.4 Limiting Results 249
7.4.i Weak law of large numbers 249
7.4.ii A central limit theorem: I, mean square convergence 251
7.4.iii A central limit theorem: II, almost sure convergence 259

7.5 Asymptotic Shape 269
7.5.i The shape of a spatial population distribution 269
7.5.ii Computer simulation of branching correlated random walks 270
7.5.iii Results 273

7.6 Discussion 283

CHAPTER 8 FURTHER WORK 285

8.1 Internal Control of Root Growth 285

8.2 External Control of Root Growth 286

8.3 Modelling Root Distributions 286

8.4 Correlation in the Random Walk 287

APPENDIX 1 IMP PROGRAM TO SIMULATE ROOT DISTRIBUTION 289

APPENDIX 2 EXPECTED VALUE OF R_n^4 315

APPENDIX 3 ROSEN'S CENTRAL LIMIT THEOREM FOR SUMS OF MULTIVARIATE RANDOM VARIABLES APPLIED TO THE CORRELATED RANDOM WALK 322

A3.1 Rosen's Theorem 322

A3.2 Correlated Random Walk Modification of Rosen's Theorem 324

REFERENCES 328

CHAPTER 1

INTRODUCTION

The work described in this thesis is in two parts. The first part, Chapters 2, 3 and 4, is a study of the rooting patterns of the United Kingdom's main forest tree species, Sitka spruce (Picea sitchensis (Bong.) Carr.). The second part, Chapters 5, 6 and 7, is a mathematical analysis of certain random walks and branching random walks which are important to studies of rooting patterns.

1.1 Statistical Analysis and Computer Simulation of the Rooting Patterns of Sitka Spruce

The major challenge to UK forestry is to reduce windthrow losses in upland forests (Fraser and Gardiner 1967). The stability of a tree is determined by the size and shape of its woody, structural root system (Potter and Lamb 1974). Thus to improve windthrow resistance we need to understand the mechanisms which govern the growth and spread of structural roots. Knowledge of these mechanisms is also important because trees exploit soil resources through their root systems and forest yield may be increased if the soil exploitation can be made more efficient.

There have been many investigations into root growth but progress, summarised in Chapter 2, has been limited. This is because of the difficulty of analysing such complex patterns as shown in Figure 1.1.1. A number of authors have described rooting patterns qualitatively but there have been no detailed analyses. Therefore our objective is to study the spatial patterns of eight excavated Sitka spruce structural root systems. Our work is mainly exploratory, to try and understand the mechanisms of root spread and to suggest areas for further research. The moisture and nutrient absorbing fine root systems (Ford and Deans 1977) will not be considered.

Structural root systems consist of a vertical taproot and a number of primary roots which originate at the tree stem, a number of secondary roots which are initiated on primaries, and so on. Each root consists of a series of segments between bends, where the root changes direction, and branching points where new roots are initiated. Hence when analysing rooting patterns the first problem is to find a method of accurately recording the positions of all root origins, bends and branching points. In Chapter 2 we describe a method which involves suspending the root system within an aluminium framework which acts as a basis for a three-dimensional coordinate system. Chapter 2 also includes a general description of the size and shape of the excavated root systems.

A detailed analysis of the patterns is described in Chapter 3. First, the component variables which together govern the size and shape of a root system are identified. For example, one component variable is the rate at which secondary roots are produced on

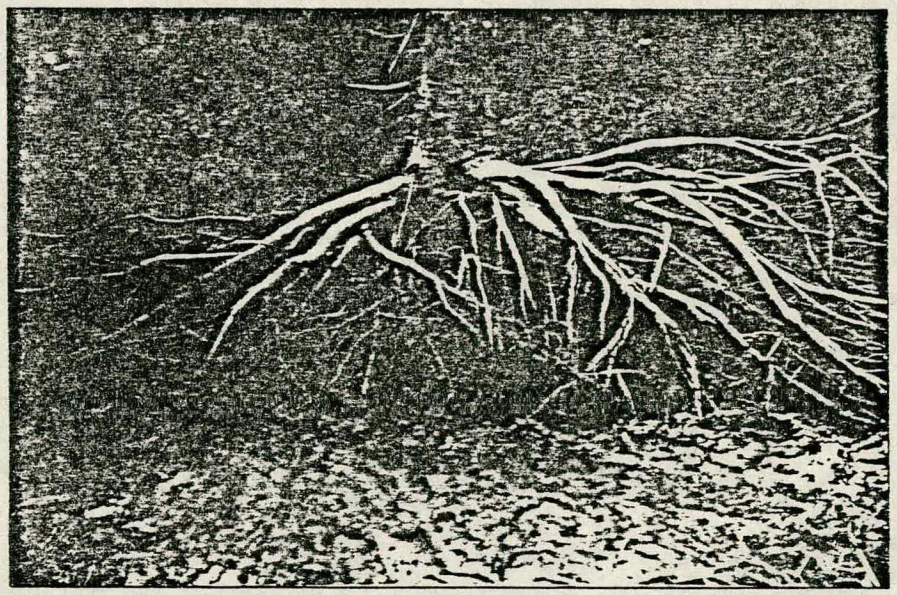


Figure 1.1.1
Structural root system of a 16-year-old Sitka spruce

primaries and another is the distribution around the stem of the primary root origins. After the component variables have been identified the data appropriate to each are analysed using standard statistical techniques.

Computer simulation of rooting patterns is discussed in Chapter 4. Honda (1971) simulated the above-ground branching structure of trees using a deterministic model based on the annual growth increments. Cochrane (1977) extended Honda's method to a stochastic model of the above-ground branching structure of Sitka spruce and obtained results of considerable biological interest. A similar model of root growth would be very useful. Unfortunately, we were not able to extend Honda and Cochrane's methods to the root systems of Sitka spruce for the annual growth increments could not be determined by a visual examination of a structural root system (see Section 2.4). An alternative method is to simulate rooting patterns using a distribution model which reproduces rooting patterns observed at a fixed time rather than the development over time. Two distribution models are proposed in the first part of Chapter 4. The models are then compared by visual examination of graph plots of simulated root systems. After the models have been compared we give two examples to illustrate how simulation can be useful to root growth studies.

Visual examination may be the best method of comparing simulated root systems for only a little experience is necessary to distinguish between realistic and unrealistic patterns. However, the method is subjective and statistical techniques such as hypothesis testing cannot be used. An objective method of describing a root system would be useful to experimentors who wish to compare root systems. For example, it is sometimes necessary to compare the root systems of various tree species (Kochenderfer 1973) or of the same species grown in different soils (Seth and Srivastava 1973). One method which may be useful was employed by ten Hoopen and Reuver (1970) to describe dendritic cells, which, like root systems, are types of spatial branching patterns. Ten Hoopen and Reuver's method of description was a histogram showing the frequency of branching points against distance from the centre of the cell. In the second part of Chapter 4 we suggest that a better description of a root system is

provided by histograms showing the distribution of total root length against distance and direction from the tree stem, and also against depth from the soil surface. A preliminary investigation into the use of these length distributions as descriptive statistics concludes the first part of the thesis.

1.2 Random Walks and Branching Random Walks with Correlated Step Directions

The second part of the thesis, Chapters 5, 6 and 7, describes a mathematical analysis of several stochastic processes suggested by an examination of the excavated root systems. For the path of any root may be described by a type of random walk (see Chapter 5) whilst an entire root system may be described by a type of branching random walk (see Chapter 7). Unfortunately, both random walks and branching random walks with fully realistic assumptions are too complicated for any important results to be directly obtained by theoretical analysis. Therefore in our investigation we will make some simplifying assumptions as a necessary basis to a complete analysis. Moreover, the random walks and branching random walks which we consider all have important applications to other fields of investigation.

During the simulations described in Chapter 4 we found that the most interesting feature of rooting patterns was the correlation between root directions before and after bends or branching points. At a bend or branching point a root changed direction by a random amount rather than taking a new direction which was completely independent of the previous direction. Hence our starting point is a random walk with this type of correlation between step directions, called the correlated random walk by Gillis (1955). The difference between the correlated random walk and classical, or independent-step, random walks is that in the correlated random walk direction changes between steps are independent and identically distributed random variables, whilst in classical random walks step directions are independent and identically distributed random variables.

The general correlated random walk is fully described in Chapter 5. Previous investigations are then summarised, the various applications

of correlated random walks are illustrated and several new results are derived. In particular, exact expressions for certain moments are obtained and used to show that correlated random walks are recurrent. In addition, a theorem of Rosen (1967) is used to show that the central limit theorem applies to the walk.

Random walks are often assumed to take place on lattices (see, for example, Feller 1968, p.342-371). In Chapter 6 we investigate the effect of correlated step directions on random walks on one- and two-dimensional lattices. As will be seen the algebra involved in our analysis is much more complicated than for random walks with independent steps. Nevertheless, several interesting results are obtained and compared with corresponding results for independent-step random walks.

Finally, in Chapter 7 the branching correlated random walk is considered. Branching random walks, which are mixtures of branching processes and random walks, are relevant to entire root systems rather than individual root paths. First, other work on branching random walks is summarised and the difficulty of a theoretical analysis is illustrated. Next, the main result of Chapter 7, an analogue to the central limit theorem, is obtained. Two forms of this theorem are given. The first, which shows mean square convergence, is obtained by a method based on the work of Asmussen and Kaplan (1976). The second form of the theorem shows almost sure convergence and is an extension of a theorem of Kaplan and Asmussen (1976). The possibility of using computer simulation to study the branching correlated random walk is also discussed in Chapter 7.

The thesis is then concluded by a short chapter of suggestions for further research.

1.3 Numbering and Notation

Chapters are divided into sections and sub-sections, with figures, tables and equations numbered consecutively within sections. Each of Chapters 3 and 4 includes a section of figures and tables at the end of the chapter. The other chapters have figures and tables inserted into the text.

Each of the mathematical chapters, 5, 6 and 7, includes an index of the main notation used in that chapter. Chapter 6 has one index for one-dimensional and another for two-dimensional correlated random walks. The important notation is consistent between chapters, although in some minor cases symbols have different interpretations in separate chapters. In those cases the usage will be clear from the context.

CHAPTER 2

STRUCTURAL ROOT MORPHOLOGY IN A SITKA SPRUCE PLANTATION

2.1 A Summary of Earlier Work

Research into the structure and habits of the root systems of forest trees can be classified into three areas of investigation: root physiology, fine root populations and structural root development or distribution. In this thesis we are concerned with the third area only. Root physiology is reviewed in Torrey and Clarkson (1975) and the fine root populations of Sitka spruce have been studied by, amongst others, Ford and Deans (1977) and Deans (1979). Only those features of structural root development and distribution which are relevant to a study of the morphology, or size and shape, of structural root systems will be summarised. Previous work on other aspects of structural root systems is reviewed by Kozlowski (1971, p.196-305).

2.1.i The development of a structural root system

Most commercially grown trees, including Sitka spruce, are developed from seed in nurseries for two or three years before transplanting to the field (Aldhouse 1972). At the time of transplanting the structural root systems consist of a taproot and a number of primary roots. After transplantation the taproot is initially important in providing moisture and nutrient and in supporting the tree (Eis 1974, Fayle 1975) but as the tree grows the primary roots spread and branch, reducing the taproot's dominance (Day 1962). Thus the morphology of a mature root system is determined by the extension, branching and growth directions of the primary roots and their offspring.

Root extension rates

Root extension rates govern the size of a root system. Primary root extension rate exceeds that of secondaries, which in turn exceeds that of tertiaries, and so on (Wilcox 1968). The growth rates of all roots vary throughout the year, with maximum extension rates of up to 2cm a day during the spring and autumn (Hilton and Khatamain 1973, Lyr and Hoffmann 1967). Competition between trees affects the extension rates of the above-ground shoots and may also affect root extension rates but to my knowledge this important question has not been considered.

Root branching

The frequency of root branching determines the complexity of a root system. The three separate types of branching, lateral production, adventitious and branching induced by damage to a root tip are described below.

Lateral branches arise a short distance behind the apex, or tip, of a growing root (Zimmermann and Brown 1971, p.53). Zimmermann and Brown (1971, p.56) have suggested that the root apex has a controlling influence on the positions of lateral root origins although the rate at which lateral roots are produced is modified by other factors. Factors which affect the rate of lateral production include the extension rate of the root (Wilcox 1968) and soil moisture and temperature (Wareing 1971). Lateral production may also depend upon the type of root, whether primary, secondary, etc., although no quantitative results have been established (McCully 1975). Not all of the newly initiated laterals develop into structural roots. Some quickly abort (Wilcox 1968) whilst others remain as fine, absorbtive roots (Wilson 1970). The factors which determine the fate of a newly initiated lateral are not understood (Kozlowski 1971, p.202) although Horsley and Wilson (1971) have suggested that size may be important, with only the larger laterals capable of becoming structurals.

The second type of branching, adventitious, occurs when a new root emerges from older wood. Fayle (1965) found 8-year-old roots growing from 40-year-old roots of yellow birch and similar cases have been noted in many other tree species, including Sitka spruce (Kozlowski 1971, p.210-215). Adventitious branching can be caused

by damage to an existing root and may also occur for other, unknown reasons (Kozlowski 1971, p.210-215).

The third type of branching is induced by damage to a root apex. This stimulates the production of two or more roots as replacements for the original (Wilson 1970). The frequency of such branching depends on soil type for damage is common in stony soils (Kozlowski 1971, p.239).

Growth directions

The growth directions of roots determine the spatial pattern of a root system. Laboratory experiments have shown that roots have a positive response to gravity and that growth direction can change in response to fluctuations in soil temperature, moisture and nutrient (Zimmermann and Brown 1971, p.56). Growth direction may also change when a lateral root is initiated (McCully 1975). Furthermore, Wilson (1967) showed that roots of red maple tended to return to their original direction of growth after being forced to deviate by an impenetrable barrier. To my knowledge there have been no further investigations to determine whether this characteristic is common to other species. Similarly, to my knowledge there has been no investigation into the distribution around the stem of the primary root origins, even though this distribution is important in determining root spread and resistance to windthrow.

2.1.ii Observed structural root systems

One of the main reasons for the poor understanding of root growth is the problem of following the development of a root system growing under natural conditions. Those results that have been established are mainly from laboratory experiments. There are two methods of following root development in the field, namely viewing windows (Hilton and Khatamain 1973, Mason, Bhar and Hilton 1970, Wilcox 1968) and radioactive tracers injected into the tree stem and followed by soil monitoring (Ueno and Yoshihara 1967, Waller and Olsen 1967). These techniques are inappropriate to a study of spatial pattern however for viewing windows allow only part of a root system to be observed whilst tracer methods are beset by

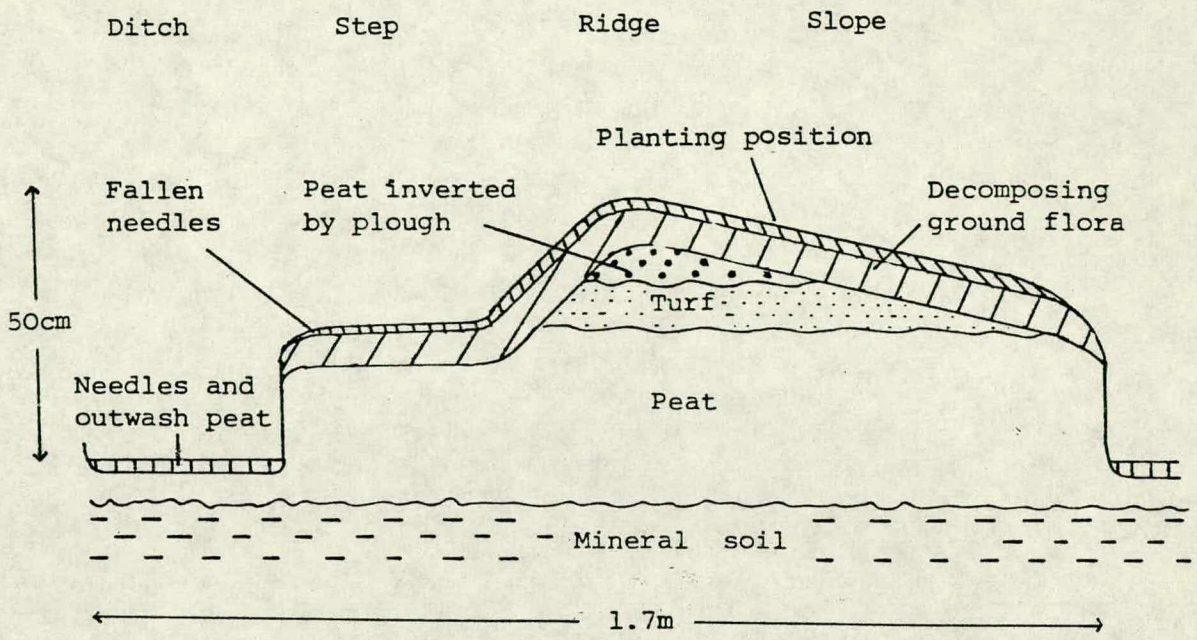
problems because the uptake and distribution of the radioactive material may be uneven.

Many authors have preferred to study root systems extracted from the soil rather than their temporal development. These studies, reviewed by Kozlowski (1971, p.196-305), have shown that whilst a basic shape is common to the root systems of forest trees their morphology is greatly modified by external factors. The basic shape is a central mass of large, rapidly tapering, many branched roots within about 1m of the stem with long, narrow, sparsely branched runners outside that region. The external factors which influence the morphology of a root system include soil type, soil moisture and planting techniques. Root systems are typically wide and deep in fine soils and are are usually flat when grown in a surface soil underlain by a more dense substratum (Lutz, Ely and Little 1937, Savill 1976, Stevens 1931, Wilde 1958,p.47). Large root systems are often found in soils with high moisture levels, very deep root systems in areas subject to droughts and very flat root systems in soils where rainfall penetrates a short distance only (Kozlowski 1949, Ponder and Kenworthy 1976, Wilde 1958,p.47). Faulty transplanting can result in a deformed root system (Bergmann and Haggstrom 1976); closely spaced apple trees have been found to produce deeper root systems than those of more widely spaced (Atkinson, Naylor and Coldrick 1976); and ploughing prior to planting reduces the extent of a root system (Savill 1976). Root systems may also be modified by competition between trees for light and soil resources (McMinn 1963). The relative importance of the ability of a tree to compete for soil resources to its ability to compete for light is not understood however (Wang 1952).

2.2 Methods

2.2.i Site and excavation

Eight trees were selected from a 6° south facing slope in the Rivox section of the Forestry Commission's Greskine Forest (National Grid reference NT016045). At Greskine the basic soil type is a layer of peat, 0.25-1.5m in depth, above a mineral soil (Figure 2.2.1). The



Before ploughing the soil type is a layer of peat above a mineral stratum, with turf above the peat. The ploughing forms a ditch with the ribbon of earth from the ditch forming a ridge into which the tree is planted.

Figure 2.2.1

Soil horizons at the planting site

land was ploughed at 1.5m intervals, with furrows running down the slope, before planting in 1962 with Picea sitchensis. Seedlings were spaced at 1.5m intervals with their roots planted in the inverted ribbon thrown up by the plough. Full details of site and soils are included in Ford and Deans (1977).

The eight chosen trees formed two adjacent rows of four, separated from drains and extraction routes by at least two guard rows. The trees were felled and their root systems excavated by hand during the spring and summer of 1978 by Mr. J. D. Deans of the Institute of Terrestrial Ecology. Before the trees were felled heights, crown projections, stem diameters at breast height and stem basal circumferences were recorded. Measurements of root lengths and directions made on site were inaccurate because many roots were obscured by others and access was difficult. Therefore the root

sytems were uplifted and removed for storage before individual laboratory analysis. Moisture loss and subsequent splitting were minimised by outside storage. Full details of the excavation of the root systems are included in Deans (1981).

Deans (1981) has investigated the radial thickening of roots within the extracted root systems. We will consider the spatial patterns of the root systems only. Only those roots with diameters greater than 5mm will be studied for smaller roots would not spring back to their original positions if displaced during the movement of the root systems from site to laboratory.

Taproots have different properties from other roots (Wilde 1958) and except where otherwise specified will not be considered in our analysis. This was because we only had eight taproots to study but several hundred other roots (Section 2.3).

2.2.ii Preliminary measuring system

Our first problem was to find an accurate method of recording the spatial patterns of the root systems. One of the root systems was used to determine a suitable method of measurement. The first method which was used involved suspending the root system from a beam at the same inclination to the horizontal as found in the field. A protractor, callipers, measuring tape and plumb-line were then used to record the following information:

i) the angle made to the horizontal plane, measured downwards, of each root at its origin and immediately after all bends and branching points along its path;

ii) the azimuths, i.e. directions of projections into the horizontal plane, measured clockwise from the forest north, at similar points; and

iii) the distances between successive bends and branching points along each root until the diameter reached 5mm.

In this way all the information necessary to reconstruct the individual root paths and the spatial pattern of the root system could be recorded. The method had several disadvantages however:

i) the method was very laborious;

ii) if touched the root system would oscillate until stopped by hand;

iii) estimation of the exact position of a root's origin was sometimes difficult because of subsequent diameter growth;

iv) measuring azimuths and angles with a hand held protractor was difficult; and

v) when reconstructing a root's path from the data measuring errors were cumulative.

To estimate measuring errors ten points on the root system were selected at random. The lengths and directions of the roots which formed paths between each point and the centre of the stem, which was defined to be the centre of the concentric growth rings at the depth of the top of the primary root with initial direction closest to north, were then measured six times. In each case the length, azimuth and angle of a line from the centre of the stem to the point were estimated from the data. Standard deviations of the sets of six repetitions were high: between 1.8 and 6.4cm for the length measurement, 7 and 14 degrees for the azimuth measurement and 3 and 8 degrees for the angle measurement. Therefore this measuring system was deemed unsuitable and a second method was employed.

2.2.iii Measuring system employed

The two main faults of the preliminary measuring system were its slowness because the root system oscillated until stopped by hand, and the cumulative measuring errors when root paths were reconstructed from the data. An alternative measuring system overcame these faults. First, the root system was rigidly fixed in the centre of a large framework (Figure 2.2.2). The root system was held by a triangular securing plate on a vertical rod passing through a hole bored through the tree stem. Screws in the securing plate were adjusted to ensure that the root system was held at its original inclination to the horizontal. After the root system was fixed in position three-dimensional coordinates of any point on the root system could be

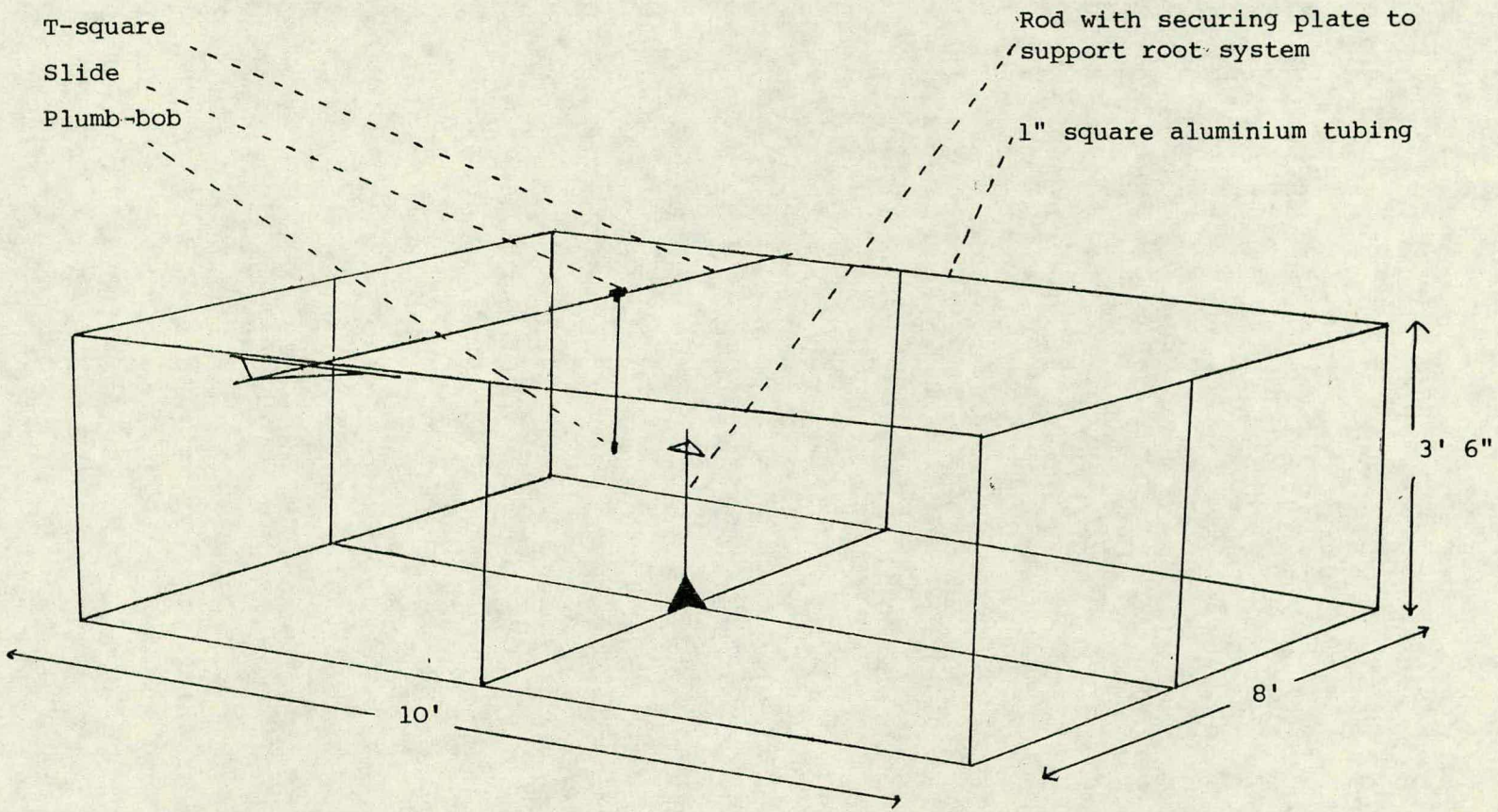


Figure 2.2.2

Framework used in the measurement of rooting patterns

determined using a T-square which moved along the top of the framework, a slide which moved along the T-square arm and a plumb-bob suspended frcm the slide. To determine the coordinates of any point the T-square, slide and plumb-bob were adjusted until the plumb-bob touched the point of interest. The coordinates were then read using steel measuring tapes attached to the frame and T-square arm. The X-coordinate was the position of the T-square along the frame, the Y-coordinate was the position of the slide on the T-square and the Z-coordinate was the depth from slide to plumb-bob.

This method was quicker than the preliminary measuring system, errors were not cumulative and the data obtained was in an easily manageable form. Errors could still occur in locating root origins and also in stopping the plumb-bob at the point of interest. To determine measuring errors 25 points on the test root system were randomly selected and their X, Y and Z coordinates measured six times. Standard deviations of each group of six measurements were very low, ranging from 0.3 to 1.2cm for X-coordinates, 0.3 to 1.1cm for Y-coordinates and 0.2 to 1.4cm for Z-coordinates. Hence the frame method was accepted as a suitable measuring system.

Because the test root system dried out and began to split during the attempt to find a suitable measuring system the numbers and initial directions of the primary roots were determined but no further measurements were taken. Four of the remaining seven root systems were then randomly selected and measured using the frame method. In each case three-dimensional coordinates of all root origins, branching points, bends and points at which root diameters reached 5mm were recorded. Whenever the plumb-bob was prevented from reaching a lower root by a higher the path of the higher root was recorded first. The higher root was then sawn off to allow the lower root's path to be recorded. Measurement within the frame took 60-80 hours for each root system.

It was only possible to measure four root systems before some drying, splitting and distortion of the three remaining root systems began to occur. The spatial patterns of those root systems were not recorded but some measurements which were not affected by splitting were taken. These were the number and initial directions of primary roots, the lengths between successive bends and branching points along

each root path and the angles between offspring and parent roots at the branching points where no splitting had occurred.

2.3 Results

A general description of the observed root systems is presented here before a detailed analysis of the data is described in Chapter 3. Throughout the following we will use the convention that significance levels are quoted in brackets. Only those roots with diameters greater than 5mm are considered.

2.3.i Gross dimensions

The eight root systems showed marked differences in both size and complexity with the largest root system having more than three times the total number of roots and total length of the smallest. Similar differences were found between the dimensions of the above-ground branching structures (Table 2.3.1). Spearman rank correlation coefficients (Kendall 1948,p.388-391) showed significant (5%) similarities between the rankings of the root systems by number of roots or total length with each of the rankings by stem basal circumference and north-south and east-west crown projections (Table 2.3.2). It is interesting to note that the Spearman rank correlation coefficients for ranking by both total length and number of roots with that by tree height were not significantly high.

Table 2.3.2

Spearman rank correlation coefficients for shoot-root relationships

Data does not include the test root system. Critical values are 0.714 (5%) and 0.893 (1%).

	Total root length	Total number of roots
Stem basal circumference	0.893	0.750
East-west crown projection	0.893	0.928
North-south crown projection	0.893	0.928
Tree height	0.430	0.642

	Tree							
	1	2	3	4	5	6	7	8
Tree height (m)	6.9	8.9	7.5	5.9	8.4	7.9	8.7	7.8
Stem diameter at breast height (cm)	9.0	10.5	11.5	7.0	10.0	9.0	13.0	11.0
Stem basal circumference (cm)	55	54	57	29	46	40	89	54
East-west crown projection (m)	2.9	3.4	3.2	2.0	2.6	2.2	4.3	2.8
North-south crown projection (m)	2.8	2.9	2.8	1.6	2.7	2.3	3.7	2.7
Total number of roots	134	156	132	45	61		142	80
Total length of roots (m)	34.0	31.7	28.2	11.6	17.0		39.4	23.2
East-west root projection (m)	1.5	1.3	1.4	1.4				
North-south root projection (m)	2.5	2.2	1.5	1.4				
Maximum depth penetrated (cm)	62	54	53	35				

Root systems 1, 2, 3 and 4 were measured by the frame method and root system 6 was the test root system.

Table 2.3.1

General dimensions of crowns and structural root systems

Depth and extent were recorded from the four root systems measured in the frame only. The extent from north to south of each of systems 1 and 2 was greater than their east-west extent whilst the north-south and east-west extent of systems 3 and 4 were similar (Table 2.3.1). Root systems 1, 2 and 3 penetrated to depths of 50-60cm whilst the smaller system 4 reached 35cm only. Depths penetrated by taproots were 40-50cm in systems 1, 2 and 3 and 34cm in system 4.

2.3.ii Distribution of total root length

The spatial distribution of root length was only recorded from the four root systems measured in the frame. Root length was classified in three ways. First, by radial distance: root length was classified by distance, measured in 10cm intervals from a vertical line, the central axis, passing through the centre of the stem. Second, by depth: root length was classified by depth, in 10cm intervals, from the depth of the centre of the stem. Third, by direction: root length was classified by direction from the central axis, measured in 30° arcs.

Root length first increased to a single maximum and then decreased with increasing radial distance (Figure 2.3.1). There were some differences between root systems but a basic pattern of a gradual increase followed by a smooth decline was common to all four root systems. Root system 1 had a later maximum than systems 2 and 3, which had similar length against radial distance distributions. As well as having less total length than the other systems root system 4 had a different pattern to its length against radial distance distribution, with an early maximum followed by a slow decline.

Root length also increased to a single maximum and then decreased with increasing depth (Figure 2.3.2). Again there were differences between root systems but a basic pattern was common to all four. The distribution of length against depth of system 3 had a broader peak than those of the other root systems, whilst system 2 was more flat than systems 1 and 3. Root system 4 had less total length than

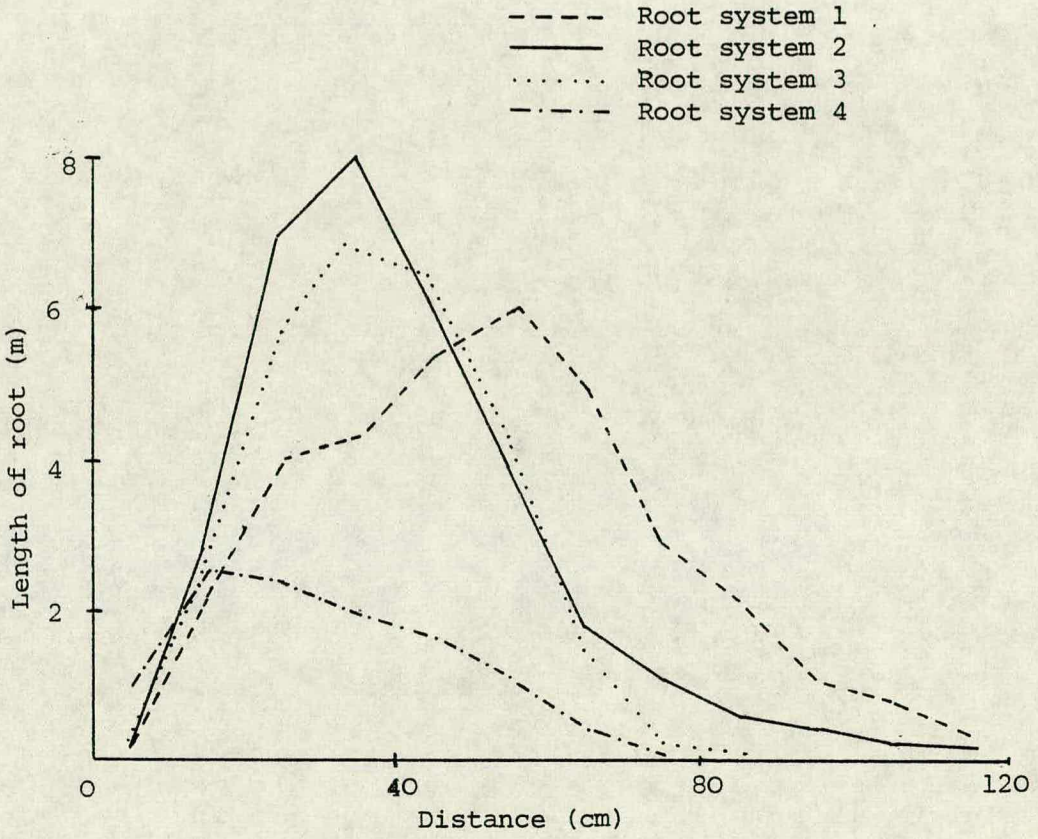


Figure 2.3.1

Length of root in successive 10cm intervals from the central axis

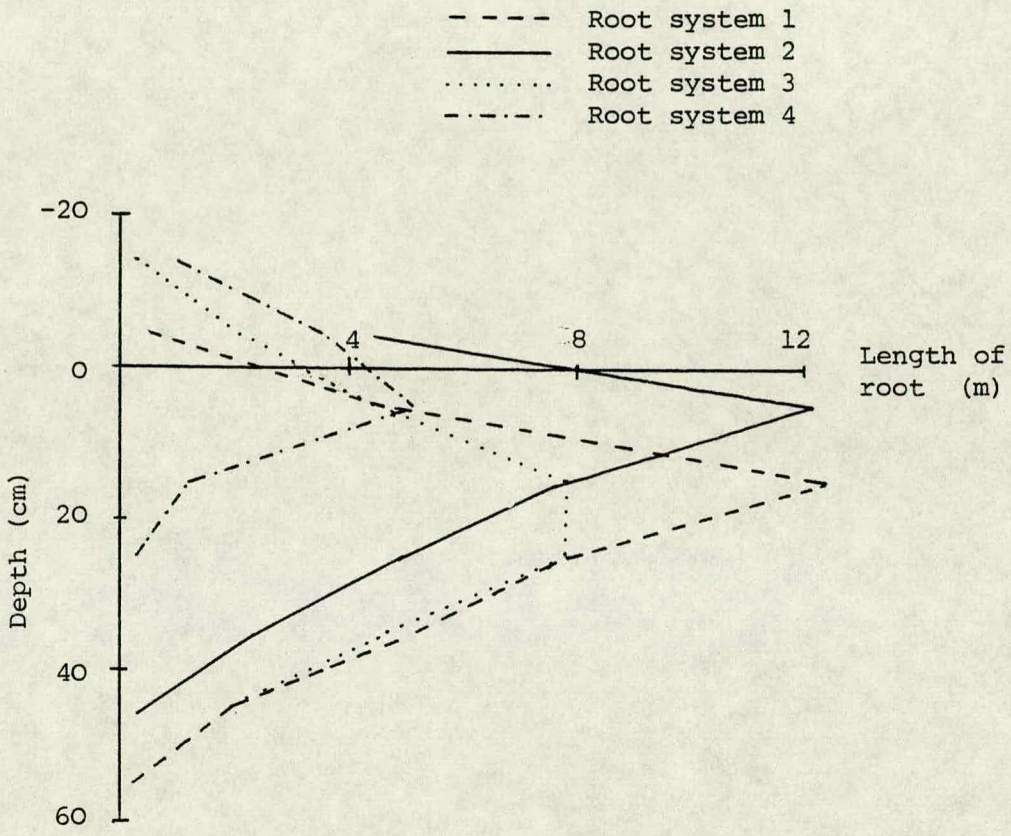


Figure 2.3.2

Length of root in successive 10cm depth intervals

the other root systems but had a similarly shaped length against distance distribution.

There was no pattern to the length against direction distributions common to all four root systems (Figure 2.3.3). Root system 1 had a high proportion of its length to the north of the stem, with lesser peaks to the west and south-east and a very sparsely populated region to the south-west. System 2 also had a sparsely populated region to the south-west but a more even distribution elsewhere. System 3 also included a sparse region, this time to the west, with most root length to the south and north-west. Most of the total root length of system 4 lay to the east and west of the stem, with little elsewhere.

Two- and three-way tables showing the distribution of total length against combinations of radial distance, depth and direction showed no pattern to be common to all root systems, except perhaps a lower percentage of deep roots to the north of the stems (Table 2.3.3). This could be explained by the 6° downward slope from north to south at the planting site, because depth was calculated relative to a horizontal plane.

Table 2.3.3

Proportion of root length with depth greater than 20cm in four 90° arcs

The northern arc includes all roots with azimuth from the central axis within the range $[-45°, 45°)$, the eastern the range $[45°, 135°)$, the southern $[135°, 225°)$ and the western $[225°, 315°)$.

Root system	Arc			
	North	East	South	West
1	0.55	0.86	0.77	0.96
2	0.37	0.40	0.62	0.43
3	0.73	0.70	0.84	0.77
4	0.00	0.39	0.11	0.09

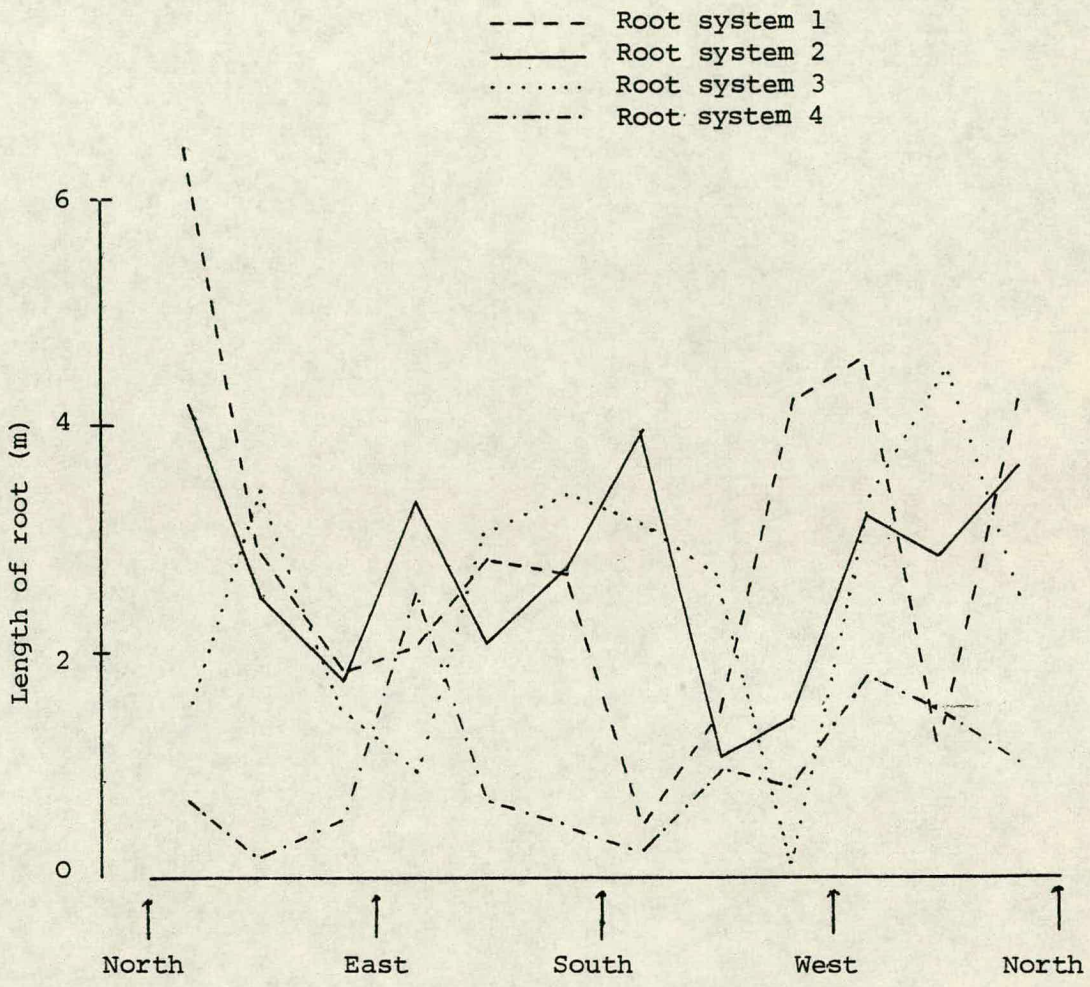


Figure 2.3.3

Length of root in successive 30° arcs

2.3.iii Distribution of branching points

Three distinct types of branching points were observed: ordinary branching points, forks and proliferations (Figure 2.3.4). At ordinary branching points a small root emerged from a larger, at forks a parent root apparently split into two equally sized roots which subtended equal angles to the parent, and at proliferations a root split into a number of much smaller roots. We will assume that ordinary branching points (often abbreviated to "branching points") were caused either by lateral production during growth or by later adventitious branching. The two types could not be distinguished because the irregular thickening properties of roots (Deans 1981). prevented the age of roots from being determined. We will assume that forks were caused by damage, with two new roots initiated as replacements for the damaged parent. We will also assume that damage caused the proliferations, which were much less common than either branching points or forks (Table 2.3.4) and will not be considered in our analysis.

Table 2.3.4

Frequency of three types of branching

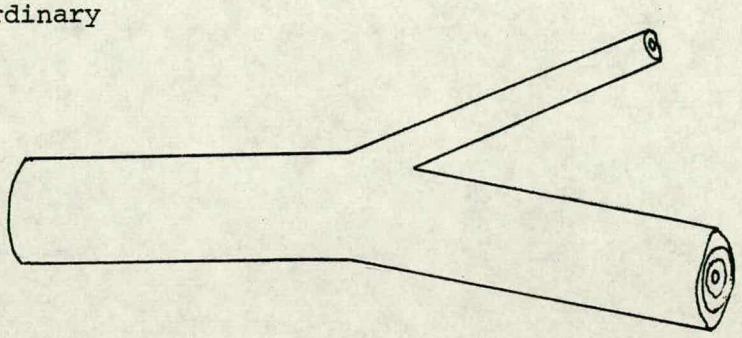
No data available from system 6.

Root system	Frequency			Mean length per type of branching (cm)		
	Branching point	Fork	Proliferation	Branching point	Fork	Proliferation
1	51	48	11	66.6	70.8	308.8
2	84	48	16	37.8	66.1	198.3
3	62	47	6	45.5	60.1	470.6
4	17	16	3	68.1	72.3	385.8
5	21	25	10	80.9	68.0	170.0
7	62	60	15	63.5	65.7	262.7
8	22	31	7	105.5	74.8	331.4

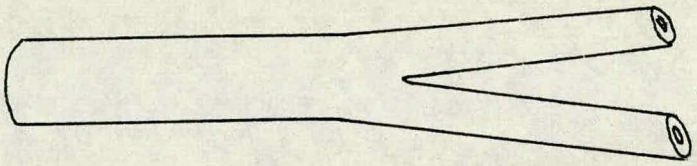
Figure 2.3.4

Three types of root branching

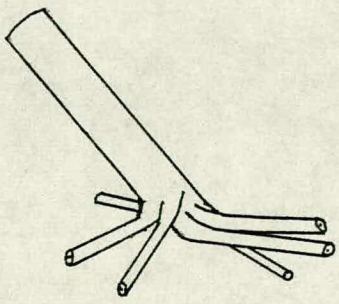
i) Ordinary



ii) Fork



iii) Proliferation



When the mean root length per type of branching (i.e. total root length ÷ frequency) is used to compare root systems (Table 2.3.4) two interesting points arise. First, the mean root length per branching point is more variable than the mean root length per fork. Second, the mean lengths per branching point or fork of the very small root system, number 4, were similar to those of the larger root systems.

We found no pattern to the positions of forks but considerable spatial variation in the frequency of branching points. The mean length per branching point was lowest to the west of all four root systems measured in the frame (Table 2.3 5) and decreased with increasing radial distance (Table 2.3.6). The mean length per branching point decreased with increasing depth for systems 1, 2 and 4 but conversely, increased for system 3 (Table 2.3.7).

Table 2.3.5

Mean length per branching point against direction

Bracketed figures denote frequencies. Direction groups are the four 90° arcs centred on the north, east, south and west directions respectively. Values plotted are the total length of root in each group, measured in cm, divided by the frequency.

Root system	Direction group			
	North	East	South	West
1	67(20)	75(8)	90(5)	56(18)
2	36(29)	70(10)	47(17)	22(28)
3	38(19)	69(8)	49(20)	38(15)
4	271(1)	72(5)	154(1)	38(10)

	Radial distance group								
Root system	1	2	3	4	5	6	7	8	9
1				146(3)	54(10)	25(23)	41(12)	98(3)	
2				264(3)	51(12)	21(15)	5(33)	5(21)	
3				114(6)	44(15)	26(16)	12(14)	3(10)	6(1)
4			240(1)	108(2)	29(6)	16(7)	47(1)		

Radial distance groups are 10cm intervals from the central axis. Values plotted are the total length of root in each group, measured in cm, divided by the frequency. Bracketed figures denote frequencies.

Table 2.3.6

Mean length per branching point against radial distance

Root system	Depth group							
	1	2	3	4	5	6	7	8
1	1(2)	16(3)	188(3)	126(11)	86(10)	42(10)	11(8)	4(4)
2	1(1)	417(1)	253(5)	59(13)	21(24)	7(27)	1(13)	
3	21(1)	20(10)	33(14)	52(16)	56(15)	62(6)		
4	52(2)	167(2)	130(4)	33(5)	9(4)			

Depth groups are 10cm intervals beginning at -10cm. Values plotted are the total length of root in each group, measured in cm, divided by the frequency. Bracketed figures denote frequencies.

Table 2.3.7

Mean length per branching point against depth

2.3.iv Distribution of bends

Bends were sharp and well defined rather than long smooth curves. Frequency varied between trees but was closely related to the size of a root system: with the exception of system 2, which included a higher bending rate, the mean lengths per bend of all root systems were similar (Table 2.3.8).

We found no systematic change in the bending rate with either radial distance or direction, but bending appeared to be more common at depths over 40cm (Table 2.3.9). Perhaps this can be explained by increased bending at the mineral soil stratum (Figure 2.2.1).

Table 2.3.8
Frequency of bends

No data available from system 6.

Root system	Frequency	Mean length per bend (cm)
1	145	23.4
2	182	17.4
3	119	23.7
4	48	24.1
5	68	25.0
7	183	21.5
8	105	22.1

Root system	Depth group							
	1	2	3	4	5	6	7	8
1			33(17)	20(67)	31(28)	16(27)	30(3)	6(3)
2		21(28)	20(31)	19(62)	15(40)	11(21)		
3	21(1)	28(7)	35(13)	32(26)	22(38)	15(24)	10(10)	
4	15(7)	21(21)	31(17)	27(2)	37 (1)			

Depth groups are 10cm intervals beginning at -10cm. Values plotted are the total length of root in each group, measured in cm, divided by the frequency. Bracketed figures denote frequencies.

Table 2.3.9

Mean length per bend against depth

2.4 Discussion

Bannan (1940) found that individual root systems of both black and white spruce had different sizes even when grown under identical conditions. Our observations are similar for we found a wide variety of sizes amongst the eight excavated Sitka spruce root systems (Table 2.3.1). Unlike similarly aged and spaced red pine (Fayle 1975) the sizes of the root systems were more highly correlated to stem basal circumferences and crown dimensions than to stem heights (Table 2.3.2). It is not clear how size variations are related to competition between trees for interaction between growing root systems could not be studied in our investigation.

Savill (1976) found that ploughing before planting restricted the horizontal spread of roots whilst a mineral stratum prevented deep penetration. He suggested that ploughing on a soil underlain by a mineral stratum reduces windthrow resistance even though the ribbon of earth thrown up by the plough provides extra depth at the planting position. Whilst no inference to the effect of ploughing on windthrow resistance is justified from our investigation because too few root systems were studied, we note that our results are similar to Savill's. Two of the four root systems measured in the frame had a much greater extent parallel to the ploughing direction than at right angles to it (Table 2.3.1). The maximum depth penetrated (Table 2.3.1) was similar to the depth of the mineral soil (Figure 2.2.1) and was much less than found in other soil types (Wilde 1958).

By examining the distributions of root length against radial distance, depth and direction (Figures 2.3.1, 2.3.2 and 2.3.3) the basic similarities and differences between the root systems can be seen. This suggests that a classification of root length by radial distance, depth and direction may be a useful method of describing a root system. This question is considered in Chapter 4.

We found little variation between trees in rates of bending and forking but considerable differences in branching rates (Tables 2.3.4 and 2.3.8). This could be because forking is caused by damage and bending by obstructions in the soil, and are thus properties of the site and soil type, whilst branching is a property of the tree. The

hypothesis that forking and bending occur randomly whilst branching is determined by other mechanisms is strengthened by considering the variation within the individual root systems. We found no systematic variation in forking rates or in bending except near the mineral soil surface but increased branching rate with radial distance in all four, and with depth in three, of the root systems measured in the frame (Tables 2.3.6 and 2.3.7). A number of authors, for example Reynolds (1975), have found that root branching rate is reduced at distances more than 1m from the stem. This was not apparent from our data, probably because at that distance most roots had diameters less than 5mm.

We were unable to use our data to reconstruct the development of the root systems. There were three reasons for this. First, unlike the aerial branching structure of Sitka spruce (Cochrane and Ford 1978), annual growth increments are not separated by whorls, or clusters, of branches. Second, roots thicken in a very irregular manner (Deans 1981) so that diameters or cross-sectional areas cannot be used to determine age. Third, annual growth rings of roots are often discontinuous (Fayle 1968) so that sectioning and counting growth rings is an unreliable method of determining root age. Besides, locating the exact origins of annual growth rings is likely to be very difficult. In the following chapters our analysis is based on the appearance of root systems at a fixed time, rather than on an assumed and possibly inaccurate development sequence.

CHAPTER 3

THE VARIABLES WHICH DETERMINE STRUCTURAL ROOT MORPHOLOGY

The variables which together determine the spatial pattern of a root system can be classified into three groups. First, the initial distribution variables, which are the numbers, dispersion around the stem and initial directions of the primary roots (Section 3.1). Second, the directional variables, which are the direction changes at bends and branching points (Section 3.2). Third, the root path variables, which are the root lengths and the bending and branching rates. We will consider two methods of analysing the root path variables, namely by path reconstruction or sequential steps (Sections 3.3 and 3.4). In the path reconstruction method entire roots are considered. Each root has a total length, ends at a fork, proliferation or, for this study, the 5mm diameter level, and has a number of bends and branching points distributed along its length. In the sequential steps method the straight-line segments between bends and branching points are considered separately rather than as components of entire roots. Each segment has a length, an orientation relative to the previous segment and ends with the initiation of a number of new segments. No new segments are produced at 5mm points, one new segment at bends and two or more at any of the types of branching point.

Both path reconstruction and sequential step methods are simply techniques in the analysis of spatial patterns, neither represents root growth. Nevertheless, each method is useful in helping us to understand the growth mechanisms. Path reconstruction allows the dispersion of bends and lateral branching points along a root's path to be investigated easily and also provides a simple method of examining the hierarchy of primaries, secondaries, etc. An analysis based on sequential steps allows relationships between successive root segments to be examined and also provides a simple method of

determining whether branching order (the number of branching points between the segment and the stem) affects extension rates or branch production.

To enable us to generate appropriate random numbers during the computer simulation of rooting patterns (Chapter 4) probability distributions are fitted to the data. In all cases the most simple probability distributions which fit the data will be chosen.

Throughout this chapter azimuths are measured clockwise from north and angles are measured downwards from a horizontal plane. Primary roots will sometimes be called generation 1 roots, secondaries generation 2, and so on.

3.1 Initial Distribution Variables

Four variables govern the initial distribution of the primary roots, whose origins are dispersed in a horizontal plane (the root collar) around the base of the tree stem. Each of the variables is allocated a mnemonic for easy reference:

i) the number of primary roots (INROOT);
ii) the azimuths subtended at the centre of the stem by the primary root origins (STEMAZ);
iii) the azimuths of the initial primary root directions (INAZ); and
iv) the angles of the initial primary root directions (INANG).

The relationship between STEMAZ and INAZ is illustrated in Figure 3.1.1.

3.1.i INROOT

The numbers of primary roots were

	Tree								
	1	2	3	4	5	6	7	8	Mean
INROOT	9	12	5	11	5	11	10	7	8.75

It is interesting to note that the number of primary roots was not

linearly related to the eventual size of the root system, having correlation coefficients 0.11 and 0.07 with the total number and total length of roots respectively. Neither of these correlation coefficients is significantly different from zero at the 10% level. We can suggest two possible reasons for the low correlation between the numbers of primary roots and the eventual size of the root systems. First, the eventual size may not be determined during the early development when the primary roots are formed but may be modified by later, external factors. Second, perhaps some of the primary roots found in the smaller root systems are adventitious, produced in later years in response to an already inadequate root system. Further experiments are necessary, especially because our sample of only eight root systems may have yielded misleading results.

3.1.ii STEMAZ and INAZ

L-statistics (Mardia 1972, p.189) may be used to test whether the STEMAZ and INAZ variables are clustered, uniformly distributed or evenly spaced. The L-statistic of a set of n ordered circular observations, $\theta_{(1)}, \theta_{(2)}, \ldots, \theta_{(n)}$, with spacings

$$T_i = \theta_{(i+1)} - \theta_{(i)}, \quad i = 1,2,\ldots,n-1, \quad T_n = 2\pi - (\theta_{(n)} - \theta_{(1)}),$$

is

$$L = \tfrac{1}{2} \sum_{i=1}^{n} |T_i - 2\pi/n| .$$

Significantly high values of L indicate clustered observations whilst significantly low values indicate regularly spaced observations. In each case the test is against a null hypothesis of independent circular uniform random variables.

L-statistics for the STEMAZ variables showed that the primary root origins of three root systems were significantly (5%) regularly spaced and that one root system had significantly (5%) clustered primary root origins (Table 3.1.1). L-statistics for the INAZ variables showed that three trees had significantly (5%) regularly spaced primary root initial azimuths, of which one tree also had regularly spaced origins and another had clustered origins (Table 3.1.1). The initial azimuth of a primary root (INAZ) could differ

from the corresponding STEMAZ value by up to two radians. (Table 3.1.2). Nevertheless, correlation coefficients between the STEMAZ and INAZ variables were significantly (1%) high for all seven root systems for which data are available:

	Tree						
	1	2	3	4	5	7	8
Correlation coefficient	0.95	0.96	0.98	0.96	0.94	0.99	0.96
1% significant point	0.75	0.66	0.93	0.69	0.93	0.72	0.79

The model which we fit is to assume that the STEMAZ variables are inherently regularly spaced, with wrapped Normal deviations from perfect regularity, whilst the INAZ variables differ from the corresponding STEMAZ values by independent wrapped Normal deviations. Thus if we denote the STEMAZ value of the ith of n primary roots by $X_n(i)$, with corresponding INAZ value $Y_n(i)$, the model is

$$X_n(i) = 2\pi i/n + \{\varepsilon_{xi} \text{ (modulus } 2\pi)\},$$

$$Y_n(i) = X_n(i) + \{\varepsilon_{yi} \text{ (modulus } 2\pi)\},$$

where ε_{xi}, ε_{yi} $(i = 1, 2, \ldots, n)$ are independent $N(0,\sigma_x^2)$ and $N(0,\sigma_y^2)$ random variables respectively.

Upon assuming that the observed order of primary root origins around the stems corresponded to the inherent order of the model we obtained the estimates

$$\sigma_x^2 = 0.07 \text{ (radians)}^2 \quad \text{and}$$

$$\sigma_y^2 = 0.11 \text{ (radians)}^2.$$

Each tree included too few primary roots to allow us to formally test for agreement between the model and the data. The model is biologically plausible however for inherently regularly spaced primary roots would help to ensure that the root system was evenly spread. The frequently large deviations between INAZ and STEMAZ variables may be caused by random changes in direction of the developing primary roots or may have occurred during the transplantation of seedlings

to the field, before the roots had become woody and rigid.

3.1.iii INANG

The initial angles to the horizontal of the primary roots varied between $-\pi/18$ and $5\pi/18$ radians (Table 3.1.3). There were no correlation coefficients between INANG and either STEMAZ or INAZ which were significantly (10%) different from zero. Thus the most simple model for the INANG data is to assume that the initial angles of all primary roots are independently uniformly distributed over the range $(-\pi/18, 5\pi/18)$. A Kolmogorov-Smirnov test of goodness of fit (Kendall and Stuart 1961, p.452) indicated no significant (5%) deviations of the sample distribution function from the distribution function of a $U(-\pi/18, 5\pi/18)$ random variable.

The initial angles of the primary roots of Sitka spruce are typically lower than those of other species (see, for example, McMinn 1963). Perhaps it is these low initial angles which cause the root systems of Sitka spruce to be characteristically flat (Day 1962). The upward growth of some primary roots allows the soil region above the root collar, which may be placed below the soil surface during transplantation, to be occupied and exploited. Upward growth of primary roots may also be useful when trees are planted on sloping ground; although we did not find upward growth to be to be more common to the north, or upslope, of the root systems.

Further experiments on INANG, and also STEMAZ and INAZ, variables may be useful. In particular, experiments to determine the influence of transplantation on primary root directions could have important applications to planting schemes.

3.2 Directional Variables

There are four types of direction change to consider, at each of which changes in both azimuths and angles must be investigated:

i) bends (BENDAZ, BENDANG);

ii) parent roots at branching points (PARAZ, PARANG);

iii) lateral roots at branching points (BRANCHAZ, BRANCHANG); and

iv) new roots at forks (FORKAZ, FORKANG).

These variables are illustrated in Figure 3.2.1.

The four root systems measured in the frame included 494 bends, 214 branching points and 159 forks. Of these 97 bends occurred at either the soil/atmosphere or peat/mineral soil boundaries and will be considered separately (Section 3.5).

Except where otherwise specified we found no significant spatial variation in the distributions of the variables. Similarly, except where otherwise specified χ^2-tests indicated no significant differences between the directional variable distributions of separate trees. Whenever possible the data from separate trees were pooled for more accurate estimation.

3.2.i BENDAZ and PARAZ

Roots changed azimuths at bends (BENDAZ) and when laterals were produced (PARAZ). The distributions of the BENDAZ and PARAZ variables were similar (Table 3.2.1) with most azimuth changes having small magnitudes although large deviations were possible.

The azimuth changes along a root's path, whether at bends or branching points, were not independent of each other. Let us consider pairs of successive azimuth changes and let CC denote two successive clockwise, or positive, changes, CA denote a clockwise change immediately followed by an anticlockwise change, etc. Then the frequencies were

Combination	CC	CA	AC	AA
Frequency	75	137	125	85

and the hypothesis of independence between successive changes was rejected at the 0.1% level by a χ^2-test. It seems that clockwise azimuth changes were more likely to be followed by anticlockwise than clockwise changes, and vice versa. Similarly, for sequences of three azimuth changes the frequencies were

Combination	CCC	CCA	CAC	CAA	ACC	ACA	AAC	AAA
Frequency	14	32	44	33	25	49	34	24.

The hypothesis that the third azimuth change was independent of the first two was also rejected at the 0.1% level by a χ^2-test. Again, sequences of alternately clockwise then anticlockwise changes were more common than could be explained by chance if the changes were independent of each other.

A sequence of alternately clockwise then anticlockwise azimuth changes often had the effect of giving a root overall azimuth, from first to last point, close to its original azimuth. Wilson (1967) found that the roots of red pine had similar properties and suggested that this may imply a mechanism whereby a tree maximises the outward spread of a root system.

The most simple model for the BENDAZ and PARAZ distributions is to assume that the sign of an azimuth change depends on the previous change only and that the magnitude of the change is independent of its sign. Then if θ_1 denotes any BENDAZ variable and θ_2 denotes any PARAZ variable our model is

$$\theta_i = \delta_i \varepsilon_i \text{ (modulus } 2\pi),$$

where ε_i $(i = 1, 2)$ are independent $N(\mu_i, \sigma_i^2)$ random variables and δ_i takes the values +1 or -1 with probabilities p and 1-p respectively. Parameter estimates from the BENDAZ data were

$$\mu_1 = 0.21 \text{ radians and}$$

$$\sigma_1^2 = 0.085 \text{ (radians)}^2,$$

and from the PARAZ data were

$$\mu_2 = 0.00 \text{ radians and}$$

$$\sigma_2^2 = 0.091 \text{ (radians)}^2.$$

From the pooled BENDAZ and PARAZ data we obtained the estimates

$$p = \begin{cases} 0.38 & \text{if the previous change in azimuth was clockwise} \\ 0.62 & \text{if the previous change in azimuth was anticlockwise} \\ 0.50 & \text{if there was no previous change in azimuth.} \end{cases}$$

A Kolmogorov-Smirnov test of goodness of fit showed no significant

differences between the model with these parameter estimates and the data.

3.2.ii BRANCHAZ

The distribution of the BRANCHAZ data appeared bi-modal (Table 3.2.1) with most lateral branches subtending azimuths with absolute values between $\pi/6$ and $\pi/2$ radians to their parent root direction and the frequencies of positive and negative directions roughly equal. Laterals were not found to emerge on alternate sides of the parent root or in any other regular pattern.

The most simple model for the BRANCHAZ data is to assume that the sign and the absolute value of the azimuth subtended by a lateral to its parent are independent. Thus if θ_3 denotes any BRANCHAZ variable our model is

$$\theta_3 = \delta_3 \varepsilon_3 \text{(modulus } 2\pi),$$

where ε_3 is an independent $N(\mu_3, \sigma_3^2)$ random variable and where δ_3 takes the values +1 or -1 with probabilities p_3 and $1-p_3$ respectively. The estimates of the model parameters were

$$\mu_3 = 0.83 \text{ radians},$$

$$\sigma_3^2 = 0.094 \text{ (radians)}^2 \text{ and}$$

$$p_3 = 0.49.$$

A Kolmogorov-Smirnov test indicated no significant (5%) differences between the model and sample distribution functions.

3.2.iii FORKAZ

The two new roots initiated at forks subtended symmetrical azimuths to the previous parent direction. The moduli of the FORKAZ variables were usually less than $\pi/6$ radians and no values greater than $\pi/2$ radians occurred (Table 3.2.1).

A simple model for any FORKAZ variable θ_4 is

$$\theta_4 = \pm|\varepsilon_4 \text{modulus}(2\pi)|$$

where ε_4 is an $N(\mu_4,\sigma_4^2)$ random variable and where one new root is allocated positive θ_4 and the other negative. The estimates obtained from the FORKAZ data were

$$\mu_4 = 0.34 \text{ radians and}$$

$$\sigma_4^2 = 0.082 \text{ (radians)}^2.$$

Again Kolmogorov-Smirnov tests indicated no significant (5%) differences between the model and sample distribution functions.

3.2.iv BENDANG, PARANG and FORKANG

We found no significant (5%) differences, using χ^2-tests, between the BENDANG, PARANG and FORKANG distributions. These data were therefore pooled for more accurate estimation.

The angle distributions were affected by the depth of the point and whether the previous direction of the root was upwards or downwards (Table 3.2.2). Changes in angles appeared to be more variable at depths over 15cm than at shallower depths: a hypothesis that the two population variances were equal was rejected at the 0.1% level by an F-test (Snedecor and Cochran 1967,p.116). When the previous direction was downwards the distribution of the BENDANG, PARANG and FORKANG variables was approximately symmetrical about zero. When the previous direction was upwards however, a sign test (Snedecor and Cochran 1967,p.125) showed that there were significantly (0.1%) more positive changes in angles than negative. Positive changes in angles of upward growing roots caused the direction to turn towards the horizontal.

The most simple suitable model for the data is to assume that the sign and absolute value of a change in angle are independent. The sign depends on the previous direction of the root and the absolute value depends on the depth. Let ϕ_{ij} denote any BENDANG, PARANG or FORKANG variable, where

$$i = \begin{cases} 1 & \text{if the previous direction was upwards} \\ 2 & \text{otherwise,} \end{cases}$$

and

$$j = \begin{cases} 1 & \text{if the depth of the point is less than 15cm} \\ 2 & \text{otherwise.} \end{cases}$$

Then our model is

$$\phi_{ij} = \delta_i \left| \varepsilon_j \text{modulus}(\pi) \right| ,$$

where δ_i takes the values +1 or -1 with probabilities p_i and $1-p_i$ respectively, and where ε_j is an independent $N(0,\sigma^2_{5,j})$ random variable. The parameter estimates for this model were

$$p_1 = 0.875,\ \sigma^2_{5,1} = 0.06\ (\text{radians})^2,$$

$$p_2 = 0.499,\ \sigma^2_{5,2} = 0.15\ (\text{radians})^2.$$

Kolmogorov-Smirnov tests indicated no significant (5%) differences between the model and sample distribution functions at any of the four i-j combinations.

Both the increased variability at greater depths and the higher proportion of positive changes in angles when growth is upward are consistent with previous work on root growth directions. Zimmermann and Brown (1971,p.56) suggested that whilst roots are positively responsive to gravity their directions, especially those of high generation roots, may be modified by moisture and nutrient availability. Most primary roots radiate almost horizontally from the stem but the higher order secondaries, tertiaries, etc., are typically deeper. Thus the high directional variability found at depths below 15cm may reflect the increased variability of the directions of the higher order roots. But all roots are to some extent positively responsive to gravity and it is reasonable to expect an upward growing root to return to downward growth when possible.

3.2.v BRANCHANG

The final directional variable is BRANCHANG, the angle subtended by a lateral root to its parent direction. Just as the BRANCHAZ variables were markedly different from the other azimuth variables, so too BRANCHANG had different properties from BENDANG, PARANG and FORKANG. BRANCHANG variables were asymmetrically distributed over the range $-\pi/3$ to $\pi/3$ radians (Table 3.2.3) and a sign test indicated that the number of positive BRANCHANG values was significantly (0.1%) greater than the number of negative values. The sign of a BRANCHANG variable was related to the angle of its parent root at the branching point (Table 3.2.4): the coefficient of correlation, - 0.749, between the proportion of lateral roots with positive BRANCHANG values and the parent root angles was significantly (0.1%) less than zero.

The most simple model which is consistent with the data is to assume that the absolute value of a BRANCHANG variable is uniformly distributed between 0 and $\pi/3$ radians whilst the sign depends on the parent angle only. Thus if Ψ denotes any BRANCHANG variable our model is

$$\Psi = \delta U ,$$

where U is a random variable uniformly distributed over the range 0 to $\pi/3$ radians and where δ takes the values +1 or -1 with probabilities p and 1-p respectively. The value of p is assumed to be linearly related to the angle of the parent root at the branching point, ϕ say. Regression of the proportion of positive BRANCHANG variables on the parent angles yielded

$$p = \begin{cases} 1 & \text{if } \phi<0 \\ 0.976-0.262\phi & \text{otherwise.} \end{cases}$$

For continuity at $\phi = 0$ the line $0.976-0.262\phi$ may be taken as $1-0.262\phi$. Using χ^2-tests we found no significant (5%) differences between the observed BRANCHANG frequencies in the groups shown in Table 3.2.3 and the expected frequencies under the model.

Our results on the directional variables suggest that Sitka spruce may possess some inherent mechanism to ensure that their root systems spread over a wide area and that the soil region within the area is evenly occupied. The direction changes at bends, of parent roots at lateral branching points and of replacement roots at forks are usually of small magnitude. Together with the alternately clockwise then anticlockwise changes in root azimuths this suggests that each root may have some preferred direction to enable the root system to spread as quickly as possible. The typically large azimuths and angles subtended by lateral roots to their parents suggests some form of inhibition to ensure that the lateral occupies a separate soil region to its parent. Further experiments are necessary for our results are based on a study of the four root systems measured by the frame method only.

3.3 Path Reconstruction Variables

As mentioned earlier we will use two methods of analysing the root lengths and the frequency of bends, branching points and forks, namely by path reconstruction in this section and by sequential steps in Section 3.4. The data which we use are mainly from the four root systems measured in the frame although in some cases data are available from the other root systems.

For each root there are six path reconstruction variables to consider. The variables are illustrated in Figure 3.3.1 and are as follows:

i) the total length of the root, which may depend upon the root generation (GENLEN);

ii) the type of termination of the root, i.e. 5mm diameter, fork or proliferation (ENDTYPE);

iii) the number of lateral roots initiated on the root (NBRAN);

iv) the number of bends in the root (NBEND);

v) the distances of the lateral root origins from the parent root origin, expressed as proportions of the total length of the root (DISTBRAN); and

vi) the distances of the bends from the parent root origin, also expressed as proportions of the total length of the root (DISTBEND).

Except where otherwise specified χ^2-tests indicated no significant differences between trees in the frequency distributions of the variables. Whenever possible the data from separate trees were pooled for more accurate estimation. Similarly, except where otherwise specified we found no significant spatial variation in the frequency distributions. The bends which occurred at the soil/atmosphere or peat/mineral soil boundaries are not considered here.

3.3.i GENLEN

With the exception of generation 1 roots, i.e. primaries, the mean root length decreased with increasing root generation as did the estimated standard deviations but not the coefficients of variation:

	Generation					
	1	2	3	4	5	6
Number of roots	59	202	241	156	62	30
Mean length (cm)	32.0	33.7	22.5	10.4	6.1	4.0
Estimated standard deviation (cm)	18.1	9.5	9.2	5.4	5.7	2.7
Coefficient of variation (%)	56	28	41	52	93	66

Primary root lengths were almost uniformly distributed over the range 0 to 65cm, secondary root lengths were almost symmetrically distributed about their mean and higher generation roots had positively skewed GENLEN distributions (Table 3.3.1). Standard probability distributions, with parameters estimated by maximum likelihood or method of moments, were found by χ^2-tests to fit the data well. These were as follows:

Generation	Probability distribution
1	Uniform over the range 0 to 65
2	Gamma with parameters 11 and 0.3
3	Gamma with parameters 7 and 0.3
4	Gamma with parameters 4 and 0.4
5	Exponential with parameter 0.16
6	Exponential with parameter 0.25

The GENLEN distributions of generations 2-6 were as expected because higher generation roots were younger and so typically shorter than earlier generation roots. The almost uniform distribution of primary roots is more suprising for primary roots were oldest and one would expect the frequency distribution to be concentrated about a high mean value. One possible reason for the high frequency of short primary roots is the transplantation of seedlings to the field which may have damaged several primaries. An alternative possibility is that some of the primary roots were of later, adventitious origin.

3.3.ii ENDTYPE

The proportion of roots ending at the 5mm diameter cut-off rather than in a fork or proliferation increased with root generation:

	Generation					
	1	2	3	4	5	6
Number of roots	59	202	241	156	62	30
Proportion ending at 5mm	0.22	0.71	0.82	0.92	0.90	1.00

This was as expected because higher generation roots were younger and narrower than earlier generation roots and so more likely to reach the 5mm diameter level before any damage occurred. The coefficient of correlation, 0.81, between root generation and the proportion of roots ending at the 5mm level was significantly (0.1%) greater than zero. However, the increase did not appear to be linear for a very low proportion of primary roots ended at the 5mm level. Perhaps the high proportion of primary roots which ended at forks or proliferations, almost 80%, explains the high frequency of short primary roots (Section 3.3.i).

ENDTYPE was also related to root length (Figure 3.3.2). The proportion of roots ending at the 5mm level decreased as length increased up to 50cm after which all roots terminated with a 5mm diameter. The initial decrease may have been caused by differences in the GENLEN distributions for high generation roots, as well as being narrow and likely to reach the 5mm level before any damage occurred, were also typically short. We can suggest no reason for

the sudden increase at 50cm and further experiments are required.

A suitable model for the ENDTYPE data is to assume an exponential relationship between root generation and the probability that a root ends at the 5mm cut-off, and also to take into account the observation that all generation 6 roots and roots over 50cm in length ended at the 5mm level. Thus for an ith generation root of length L say, our model is

$$\Pr(\text{root ends at 5mm}) = \begin{cases} 1 & \text{if } L>50\text{cm or } i = 6 \\ 1-\exp\{-\lambda(i-1)\} & \text{otherwise.} \end{cases}$$

The parameter λ was estimated to be 0.972 by maximum likelihood. With this estimate expected frequencies were very close to the observed frequencies (Figure 3.3.2).

The root systems included too few proliferitions (Section 2.3.iii) for a detailed investigation to be made into the relationships between forks and proliferations. During our simulations (Chapter 4) we will assume that roots which do not reach the 5mm level end in forks.

3.3.iii NBRAN

The third path reconstruction variable is the number of laterals initiated on the root, NBRAN. As expected longer roots usually produced more laterals than shorter roots: the correlation coefficient between NBRAN and parent root length, namely 0.641, was significantly (0.1%) greater than zero. Primary roots were less frequently branched than other roots (Tables 3.3.2 and 3.3.3) and no laterals were initiated on sixth generation roots. In addition, root system 4 included fewer lateral branches than the other trees.

The positive correlation between NBRAN and root length is obviously explained by a longer root having more time to produce laterals. The reduced frequency of laterals on primaries, which explains the low branching rate found near the tree stems from which the primaries originate (Section 2.3.iii), is less easily explained. Taken with the high proportion of primary roots found to end at forks (Section 3.3.ii) the reduced frequency of primary root branching may perhaps be explained by mis-classifications of lateral branching points as forks. Forks were deemed to occur when a root apparently split

into two roots of equal diameters and it is possible that the thickening of primary roots and their offspring caused some mis-classifications. However, the directional variables (Section 3.2) at primary root forks had similar properties to those at other forks and were markedly different from the corresponding variables at lateral branching points. This suggests that our classifications were correct.

Conditional upon root length the number of lateral roots had a positively skewed distribution (Tables 3.3.2 and 3.3.3). Hence a simple model is to assume that NBRAN has a Poisson distribution with parameter depending on tree and generation and proportional to root length. Let $P(x)$ denote a Poisson random variable with parameter x. Then our model for the NBRAN value of an ith generation root of length L say, of tree j, is

$$\text{NBRAN} = \begin{cases} 0 & \text{if } j = 4 \text{ and } i > 2 \\ P(\alpha_j L) & \text{if } i = 1 \\ P(\beta_j L) & \text{if } j \neq 4 \text{ and } 1<i<6, \text{ or if } j = 4 \text{ and } i = 2. \end{cases}$$

The parameter values were estimated by maximum likelihood to be

$\alpha_j = 0.0275$ (estimated standard error 0.0031) $(j \neq 4)$

$\beta_j = 0.0320$ (estimated standard error 0.0018) $(j \neq 4)$

$\alpha_j = 0.0181$ (estimated standard error 0.0042) $(j = 4)$

and

$\beta_j = 0.0241$ (estimated standard error 0.0038) $(j = 4)$.

Using χ^2-tests with suitable pooling we found no significant (5%) differences between observed and expected frequencies.

3.3.iv NBEND

As well as producing more laterals longer roots usually had more bends than shorter roots: the coefficient of correlation between NBEND and parent root length, namely 0.487, was significantly (0.1%) greater

than zero. Using χ^2-tests we found no significant (5%) differences between trees or generations in the NBEND distributions. These results support the hypothesis suggested in Section 2.4 that except at the soil/atmosphere and peat/mineral soil boundaries bending occurs randomly, in response to variations in the soil environment.

Conditional upon root length NBEND had a positively skewed distribution (Table 3.3.4). Thus a suitable model is to assume that NBEND has a Poisson distribution with parameter proportional to the length of the root. The constant of proportionality was estimated to be 0.055 by maximum likelihood. Using χ^2-tests with suitable pooling we found no significant (5%) differences between observed and expected frequencies.

3.3.v DISTBRAN

In the path reconstruction method the positions of lateral root origins are expressed as proportions of their parent root length (Figure 3.3.1) and DISTBRAN is used to denote the collection of lateral positions on any root.

Conditional upon the NBRAN value the laterals appeared to be almost regularly spaced whatever the length of the parent root (see, for example, Figures 3.3.3 and 3.3.4). These data are consistent with Zimmermann and Brown's (1971,p.56) hypothesis that some tree species may have a mechanism to control the positions of lateral roots. It seems that laterals are inherently regularly spaced, which may help in ensuring an even distribution and so improving windthrow resistance and allowing the soil region to be efficiently exploited. Further investigations should be made to determine the physiological processes which control the positions of laterals.

A simple model for DISTBRAN is to assume that lateral root origins are inherently regularly spaced with Normal deviations from perfect regularity. Thus if p(i,k) denotes the proportion of a root's length after which the ith of k lateral roots originates, our model is

$$p(i,k) = i/(k+1) + \varepsilon_i \qquad (i = 1, 2, \ldots, k).$$

Here ε_i is assumed to be an independent $N(0,\sigma^2)$ random variable

which is conditioned such that p(i,k) is between 0 and 1. The estimate of σ^2 was 0.0067 and a Kolmogorov-Smirnov test indicated no significant (5%) differences between the sample and model distribution functions.

3.3.vi DISTBEND

The final path reconstruction variable to consider is the positions of bends along roots. Conditional upon the number of bends in a root their positions were much more irregularly spaced than the lateral root origins (see, for example, Figures 3.3.5 and 3.3.6). Two bends could often occur close together and be separated by a long distance from a third. No bends occurred within 1cm of other bends however, nor within 1cm of root origins, lateral branching points, forks or proliferations. Perhaps this can be explained by the secondary thickening of roots for after thickening two close bends may appear as one.

Using Kolmogorov-Smirnov tests we found no significant (5%) differences between the uniform and sample distribution functions. Hence a suitable model for DISTBEND is the uniform distribution with appropriate modifications to prevent bends occurring too close to other bends, root origins, lateral branching points, forks or proliferations.

3.4 Sequential Step Variables

An alternative to path reconstruction as a basis of an analysis of the root path variables is to consider the straight-line segments, or steps, between bends and branching points individually. This method has the advantage that only two variables need be considered, namely the step lengths (STEPLEN) and, since each step ends with the initiation of a number of new steps, the numbers of offspring produced (NOFF). An additional advantage is that branching order, i.e. the number of forks, proliferations or lateral branching points between any step and the tree stem, may be investigated. Branching order may have an important influence on root growth for at each type of branching point the growth resources moving from the stem are divided

and reduced (see, for example, Vaadia and Itai 1969). Similarly, at at each branching point the nutrients moving from the root system to the stem are pooled and so increased.

Steps can begin at root origins, bends or lateral branching points and end at either 5mm points, bends, lateral branching points or forks or proliferations induced by damage. Throughout this section step type is used to denote how steps begin and end. For example, types include bend-bend, bend-lateral, lateral-damage and so on.

3.4.i STEPLEN

The steps which ended at the 5mm level were not considered in the analysis of the STEPLEN data for the choice of a 5mm cut-off was arbitrary. Other step lengths had a positively skewed distribution with most steps less than 15cm in length but lengths of up to 50cm possible (Figure 3.4.1).

Before the STEPLEN data from the four root systems measured in the frame were analysed in detail the data were transformed to be approximately Normal by a power transformation $y = x^{\lambda}$. The parameter λ was estimated to be 0.238 by Box and Cox (1964) methods but was chosen to be 0.25 for computing convenience. We then used multiple regression to investigate the effect on STEPLEN of distance and direction of the step origins from the central axis of the stem, depth, branching order and step type, and also to examine differences between trees. The direction of the step origin from the central axis was taken to be a qualitative variable, or factor, by classifying the direction into one of the four 90° arcs centred on the north, south, east and west directions. Tree and step type were also taken as factors whereas branching order, distance and depth were quantitative explanatory variables.

We began with a model which had 52 parameters and incorporated linear, quadratic and cubic terms in the quantitative explanatory variables and interaction between the factors. For example, the model took into account possible differences between trees in the effect of step type on STEPLEN. This model explained 38% of the total variation of the STEPLEN data. The step-down procedure (Snedecor and Cochran 1967,p.413) was then used to delete unnecessary terms from the model.

This procedure finally showed that only step type had a significant effect on the step lengths: a model incorporating only the factor step type explained 28% of the total variation.

The first steps of roots, whether ending at bends, lateral branching points or damage, were usually longer than subsequent steps (Table 3.4.1). Therefore our final model was

Step type	Model
Root origin to bend	Fourth power of an $N(\mu_1,\sigma^2)$ random variable
Root origin to lateral	" " " " $N(\mu_2,\sigma^2)$ " "
Root origin to damage	" " " " $N(\mu_3,\sigma^2)$ " "
Other	" " " " $N(\mu_4,\sigma^2)$ " "

The estimates of μ_1, μ_2, μ_3 and μ_4 were 1.664, 1.795, 1.654 and 1.630 $(cm)^{\frac{1}{4}}$ respectively. Corresponding estimated standard errors were 0.028, 0.032, 0.033 and 0.014 $(cm)^{\frac{1}{4}}$ respectively. The estimate of σ^2 was 0.091 $(cm)^{\frac{1}{2}}$. In each case a Kolmogorov-Smirnov test of goodness of fit showed no significant (5%) differences between the fitted distributions and the transformed data.

The estimates of μ_1 and μ_3 were not significantly greater than the estimate of μ_4 but the estimate of μ_2 was significantly (0.1%) greater than the other three estimates. With one exception these results are consistent with our hypothesis that lateral roots are regularly spaced along their parents whilst bends occur randomly (Sections 3.3.v and 3.3.vi). An argument consisting of the following four steps explains why.

1. Lateral roots are positioned at regular intervals on roots so the mean lengths between root origins and first lateral, between first and second laterals and so on, should be approximately equal.
2. The mean length of the last steps of roots should be less than the mean length between laterals. Otherwise another lateral would be produced.
3. Bends occur randomly along a root but must occur either before the first lateral, between two laterals or after the last lateral. Thus bends "break" the inter-lateral distances into two or more steps.

UNIV. EDINBURGH EX BIBL

4. Hence steps which start or end at a bend, and also the last steps of roots, should have mean length less than the mean inter-lateral length.

The above argument explains the high mean length of "unbroken" steps between root origins and first laterals but the exception to the argument is the low mean length of "unbroken" steps between two laterals (Table 3.4.1). By the argument the mean lateral-lateral step length should be approximately equal to the mean length of root origin to lateral steps. The frequency of lateral-lateral steps was low however, and we can suggest no other reason why steps from root origins to first laterals should be longer than other steps.

3.4.ii NOFF

The proportion of steps which ended with no new step initiated (i.e. 5mm points) increased in a curvilinear manner with branching order (Figure 3.4.2). The proportion ending with one new step initiated (i.e. bends) at first increased and then decreased as branching order increased whilst the proportion ending with more than one step initiated (i.e. lateral branching point, fork or proliferation) decreased. Conditional upon not ending at the 5mm cut-off the relative frequency of bends increased with branching order (Figure 3.4.3). Conditional upon not ending at either bends or the 5mm level the relative frequency of lateral branching points to forks or proliferations also increased with branching order (Figure 3.4.4).

The increase in the frequency of 5mm points as branching order increased was probably because high branching order steps were on young, narrow roots. The increase in the relative frequency of bends to any of the types of branching as branching order increased is less easily explained, particularly because we found no spatial variation in tha number of bends per unit root length (Section 2.3.iv). Perhaps the high frequency of forks on primary roots (Section 3.3.ii) reduced the relative frequency of bends at low branching orders. This could also explain the low relative frequency of lateral branches to forks or proliferations at low branching orders.

During our simulations (Chapter 4) we will assume that the probability that a step ends at the 5mm level is a geometrically increasing function of branching order. We will also assume that conditional upon not ending at the 5mm level the probability of ending in a bend increases linearly with branching order. Thus if $p_k(i)$ denotes the probability that a step of branching order k ends with the initiation of i new steps our model is

$$p_k(0) = 1-a^{(k-1)},$$

$$p_k(1)/\{1-p_k(0)\} = b+ck .$$

We were unable to model the relative proportions of branching points to forks because the frequencies were very low at high branching orders (Figure 3.4.4). During the simulations we will assume that the ratio of lateral branching points to forks is constant, namely 11:8. This ratio was obtained from the total frequencies of lateral branching points and forks found in the excavated root systems. Because the frequency of proliferations was very low (Section 2.3.iii) during the simulations we will assume that all steps end at either 5mm points, bends, lateral branching points or forks.

Estimates of a, b and c were obtained from the pooled data from six root systems (numbers 1, 2, 3, 5, 7 and 8), namely

$$a = 0.941,$$

$$b = 0.101,$$

$$c = 0.057.$$

The estimated standard errors of a, b and c were 0.014, 0.009 and 0.008 respectively. This model fit the data very well (Figure 3.4.2) except at the high branching orders where frequencies were low.

The small root system (number 4) had a higher proportion of 5mm points at low branching orders than the other root systems. Therefore the data from that root system were considered separately although the same general model was fitted. The estimates of a, b and c were in this case 0.923, 0.114 and 0.063 with estimated standard errors 0.032, 0.019 and 0.021 respectively.

3.5 Discussion

The above-ground branching structure of Sitka spruce develops in a regular and systematic manner (Cochrane and Ford 1978). Shoots extend in straight lines, clusters of branches separate annual growth increments and new shoots are regularly dispersed around their parent shoots. Taken together the component processes in the development of the branching structure produce a branching pattern with a high light and rainfall interception rate per unit of foliage.

The visual appearance of excavated root systems (recall Figure 1.1.1) suggests that root growth is much more haphazard than shoot growth. However, by considering the variables which determine root morphology individually we found that Sitka spruce may possess some mechanism to ensure that their root systems are well extended and evenly spread.

1. Primary roots are almost regularly spaced around the stems (Section 3.1.ii).
2. Primary roots radiate outwards rather than downwards (Sections 3.1.ii and 3.1.iii). Taken together 1 and 2 ensure a complete and even occupancy of the soil regions around the stems.
3. Lateral roots are almost evenly spaced along their parents (Section 3.3.v).
4. Lateral roots subtend large angles to their parent roots and so exploit separate soil regions (Sections 3.2.ii and 3.2.v).
5. If forced to change direction roots may attempt to return to their original direction, thus maintaining the direction of spread (Section 3.2.i).
6. Damage to a growing root results in the production of relacement roots which grow in directions similar to the parent direction, again maintaining the direction of spread (Sections 3.2.iii and 3.2.iv).

A detailed analysis of root behaviour at the ditch sides and mineral soil surface (Figure 2.2.1) was not possible because only few roots reached those boundaries. Those which did reach the ditch turned to follow the ploughing direction and those which reached the

mineral layer grew along that soil surface (Figure 3.5.1 and Table 3.5.1). No roots turned back into the occupied region. Perhaps this behaviour indicates an attempt to grow around the barriers, which is also evidence to suggest a mechanism whereby a root system develops in a non-random manner.

We suggest that the root growth of Sitka spruce is inherently regular and that the observed irregular patterns are caused by growth in a heterogeneous environment. Further experiments are necessary, in particular experiments in which roots are grown in a controlled, homogeneous environment may be useful. It may also be useful to extend Wilson's (1967) experiments to determine whether individual roots have preferred directions to enable the root system to spread outwards.

An important question is to ask whether the inherent regularity is necessary to ensure evenly spread root systems. Because root growth takes place in a heterogeneous environment a considerable variety of rooting patterns can occur, even of trees of the same species and grown under the same conditions (Section 2.3). Perhaps similar patterns would be produced if root growth was entirely random. As will be seen in the next chapter, computer simulation of rooting patterns is a technique which can help us to answer this question.

3.6 Figures

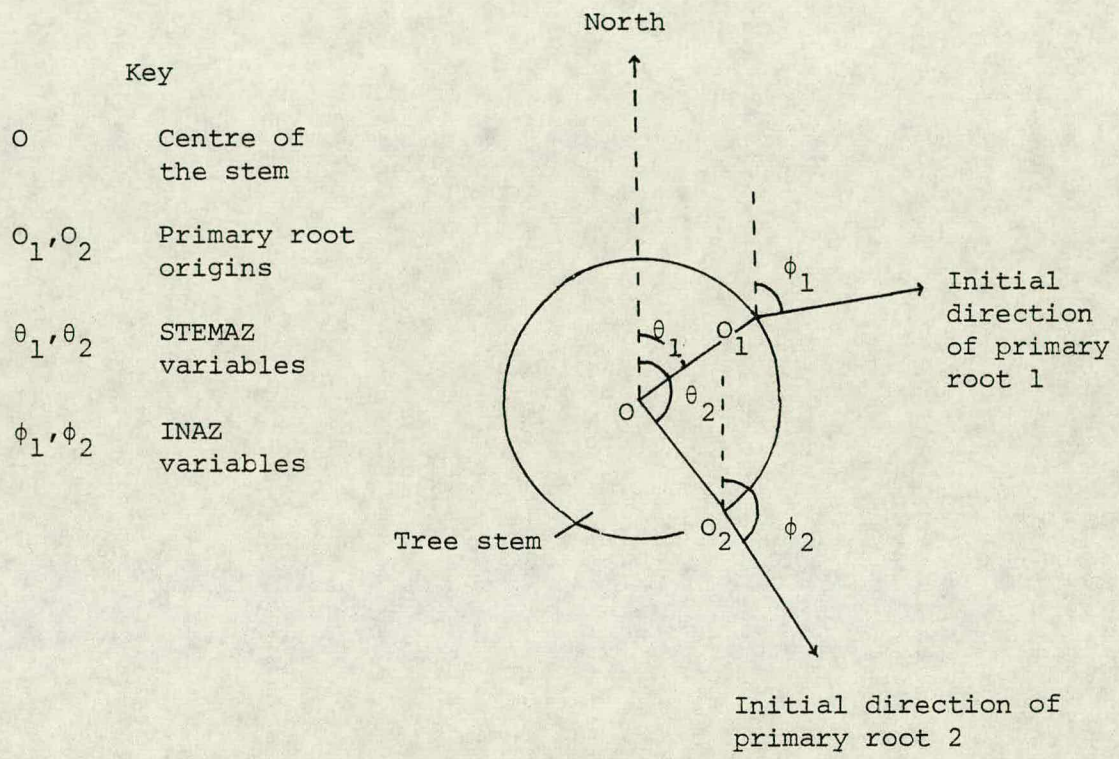
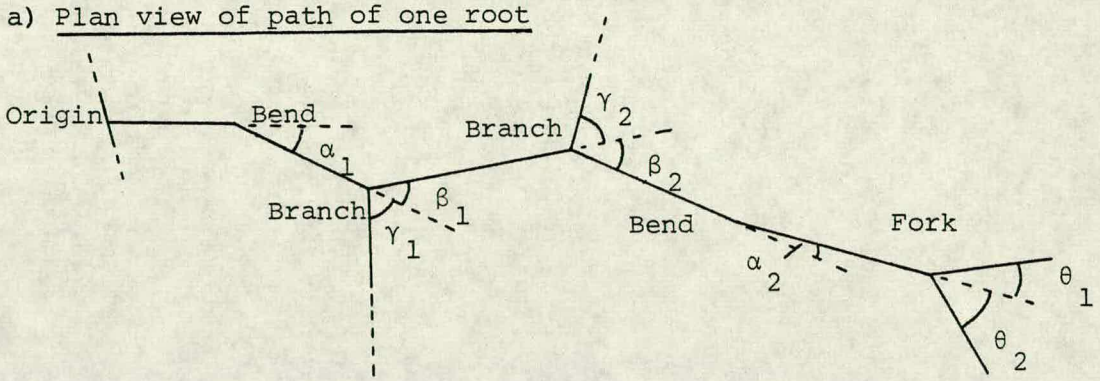


Figure 3.1.1

Diagram to illustrate STEMAZ and INAZ variables: plan view showing origins and initial directions of two primary roots

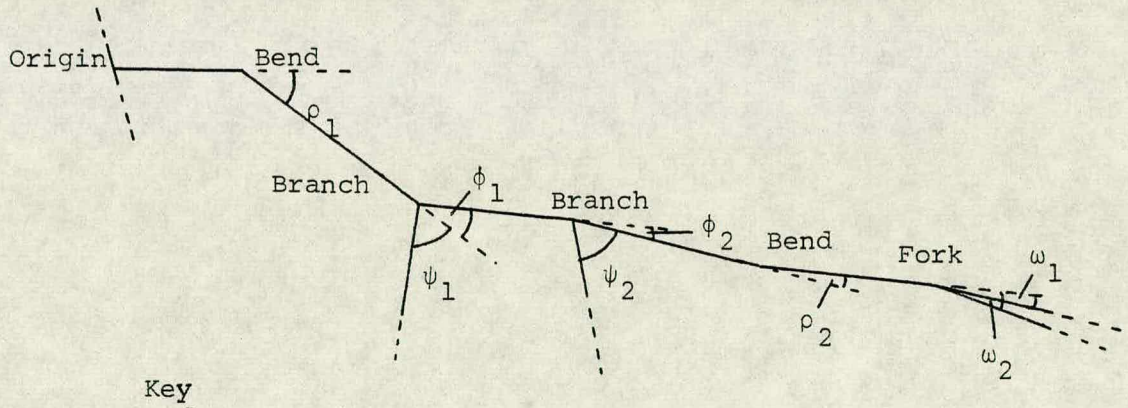
a) Plan view of path of one root



Key

α_1, α_2	BENDAZ variables
β_1, β_2	PARAZ variables
γ_1, γ_2	BRANCHAZ variables
θ_1, θ_2	FORKAZ variables

b) Transverse view of path of one root

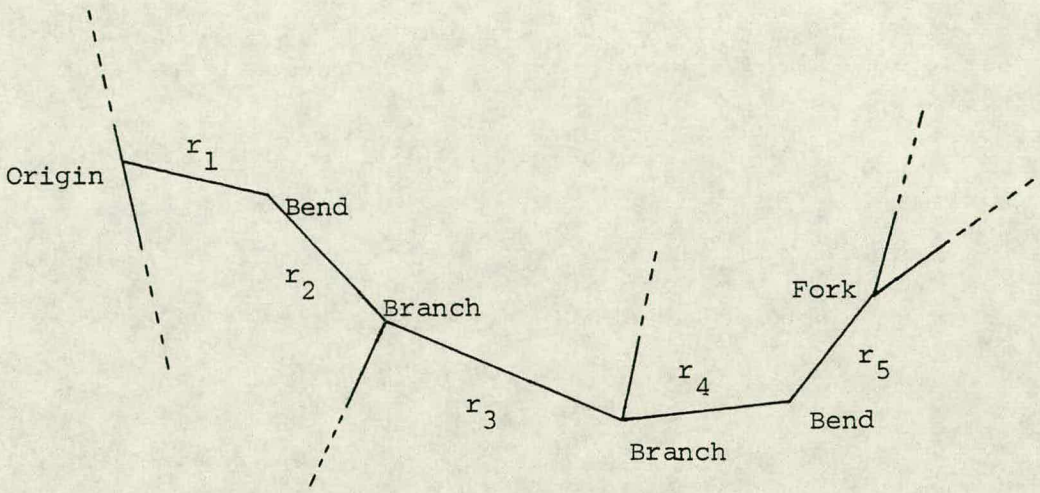


Key

ρ_1, ρ_2	BENDANG variables
ϕ_1, ϕ_2	PARANG variables
ψ_1, ψ_2	BRANCHANG variables
ω_1, ω_2	FORKANG variables

Figure 3.2.1

Diagram to illustrate the directional variables



The diagram illustrates the path of one root, made up of five segments, from its origin to its termination in a fork. The appropriate path reconstruction variables are:

GENLEN = $r_1+r_2+r_3+r_4+r_5$ (= r say);

ENDTYPE = Fork;

NBRAN = 2;

NBEND = 2;

DISTBRAN = $\{(r_1+r_2)/r, (r_1+r_2+r_3)/r\}$; and,

DISTBEND = $\{r_1/r, (r_1+r_2+r_3+r_4)/r\}$.

Figure 3.3.1

Path reconstruction variables

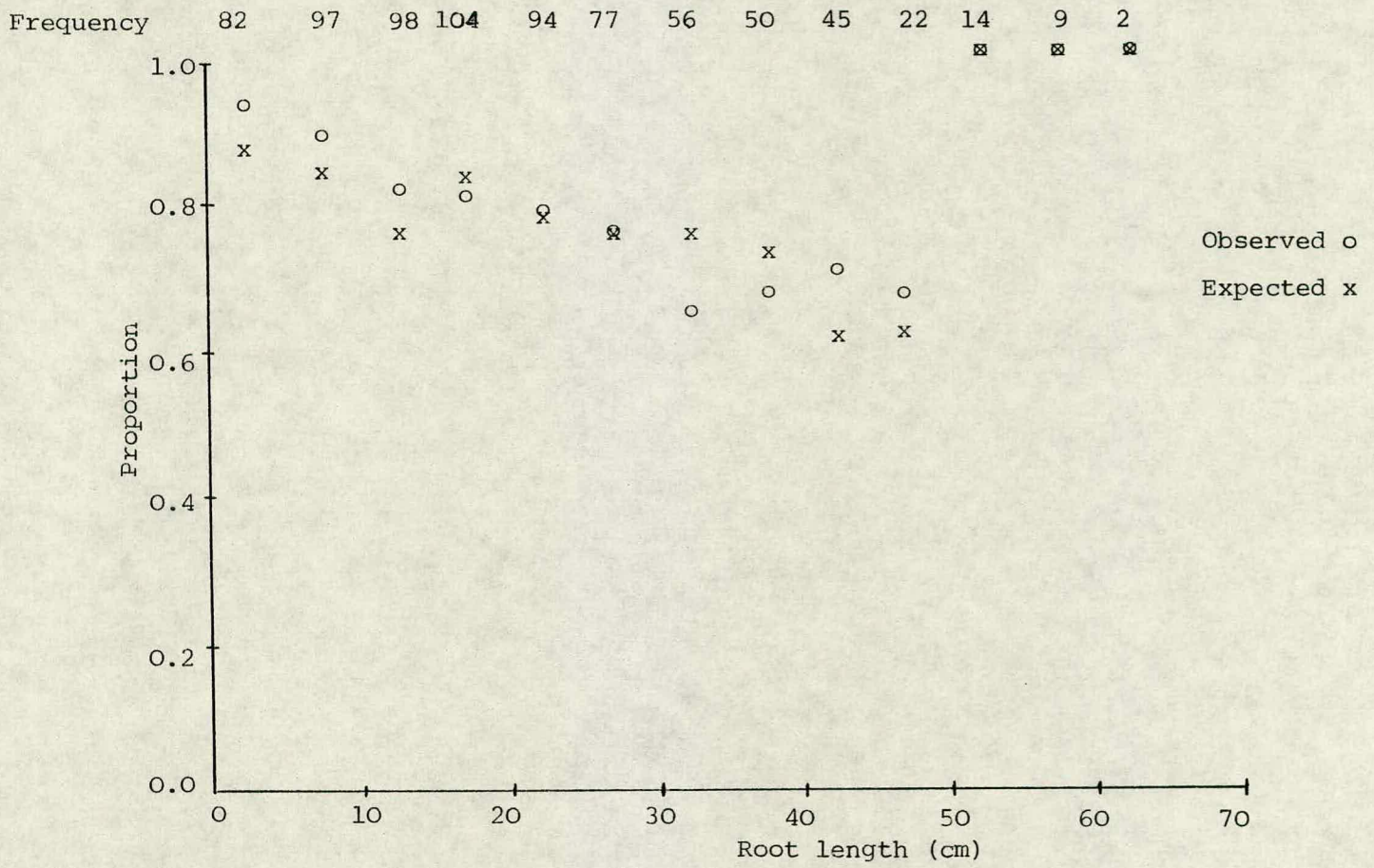


Figure 3.3.2

Proportion of roots ending at the 5mm diameter level against root length

Figure 3.3.3

DISTBRAN values for NBRAN = 2

(For explanation see Section 3.3.v)

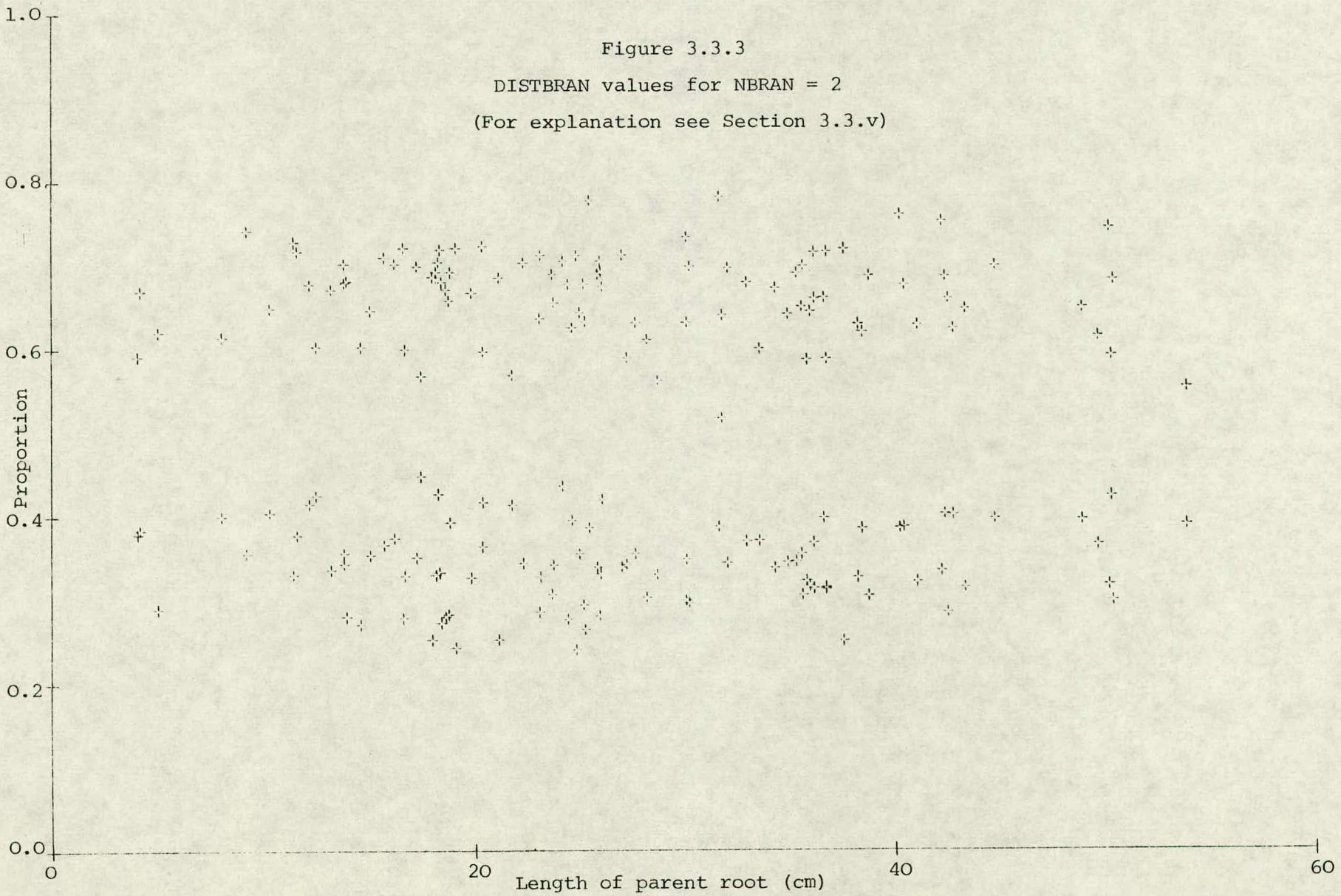


Figure 3.3.4

DISTBRAN values for NBRAN = 3

(For explanation see Section 3.3.v)

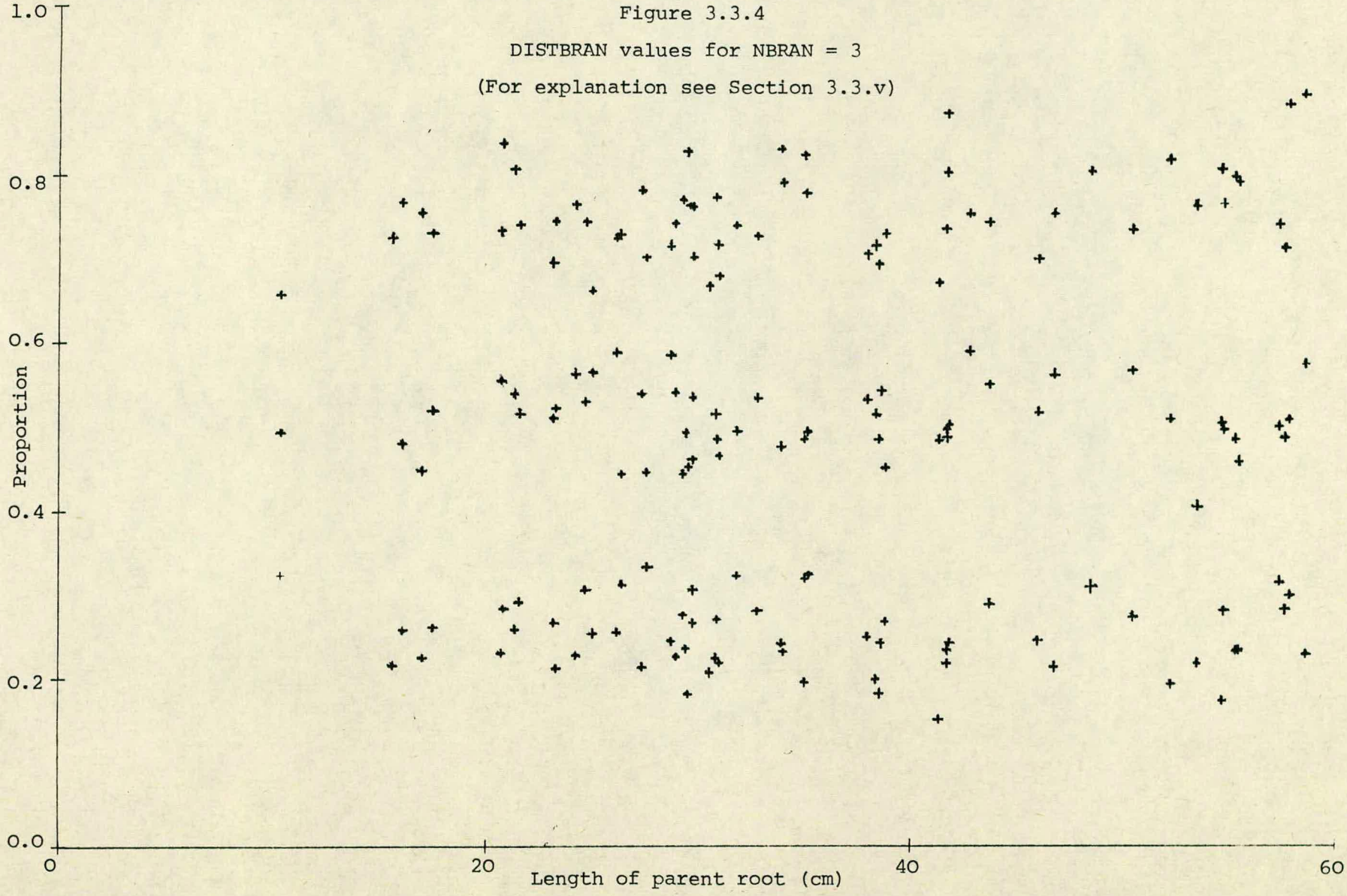


Figure 3.3.5

DISTBEND values for NBEND = 2

(For explanation see Section 3.3.vi)

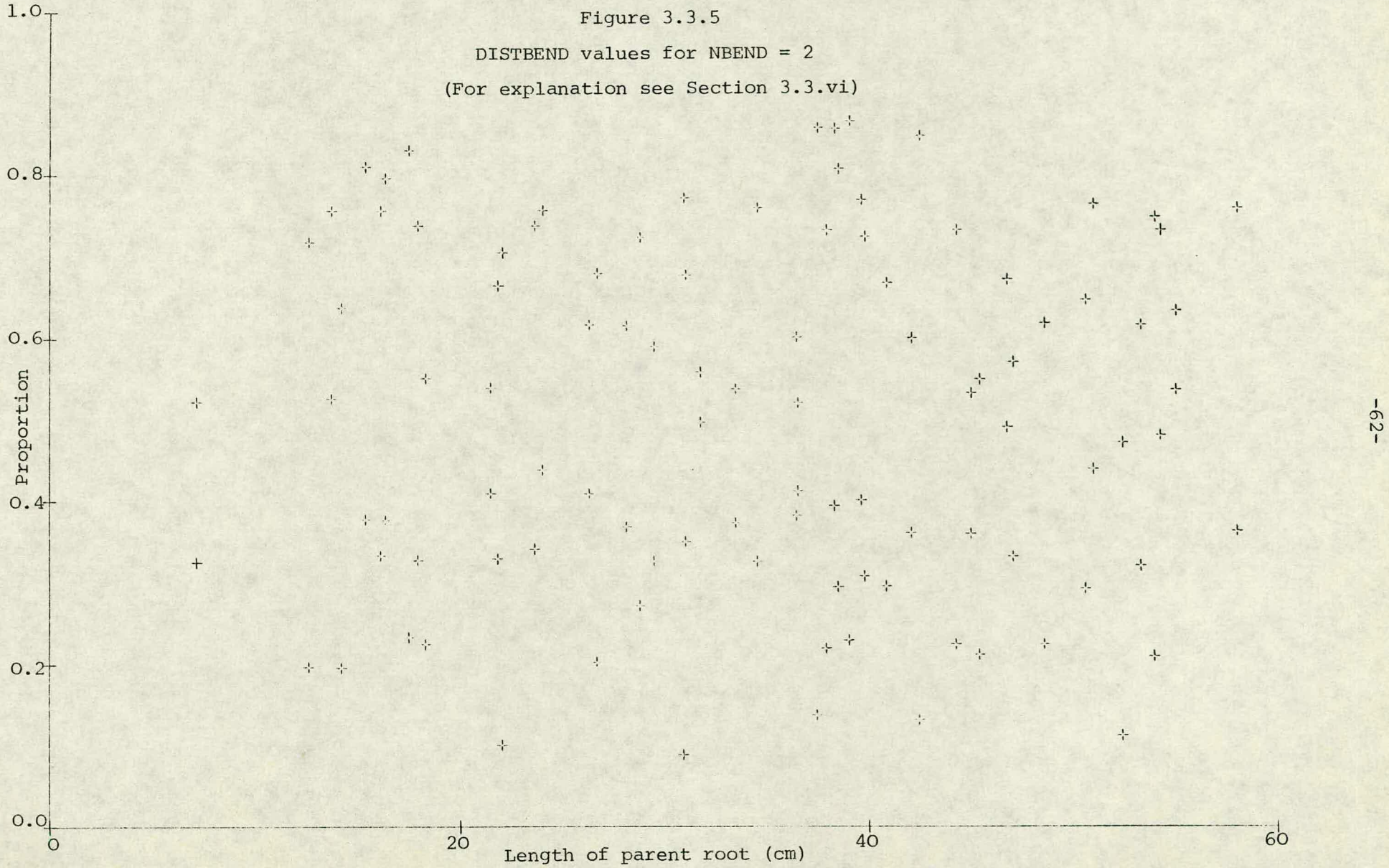
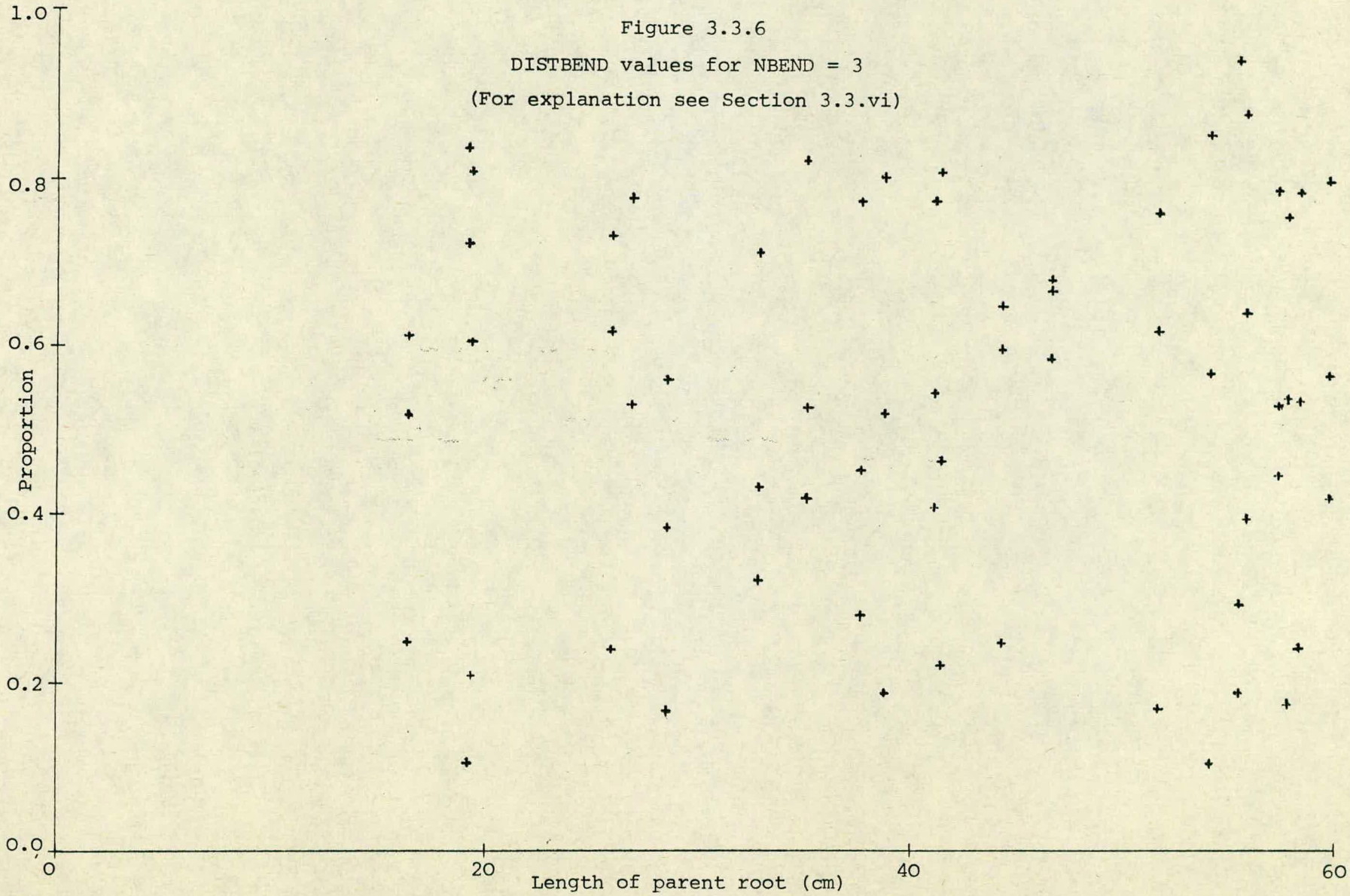


Figure 3.3.6

DISTBEND values for NBEND = 3

(For explanation see Section 3.3.vi)



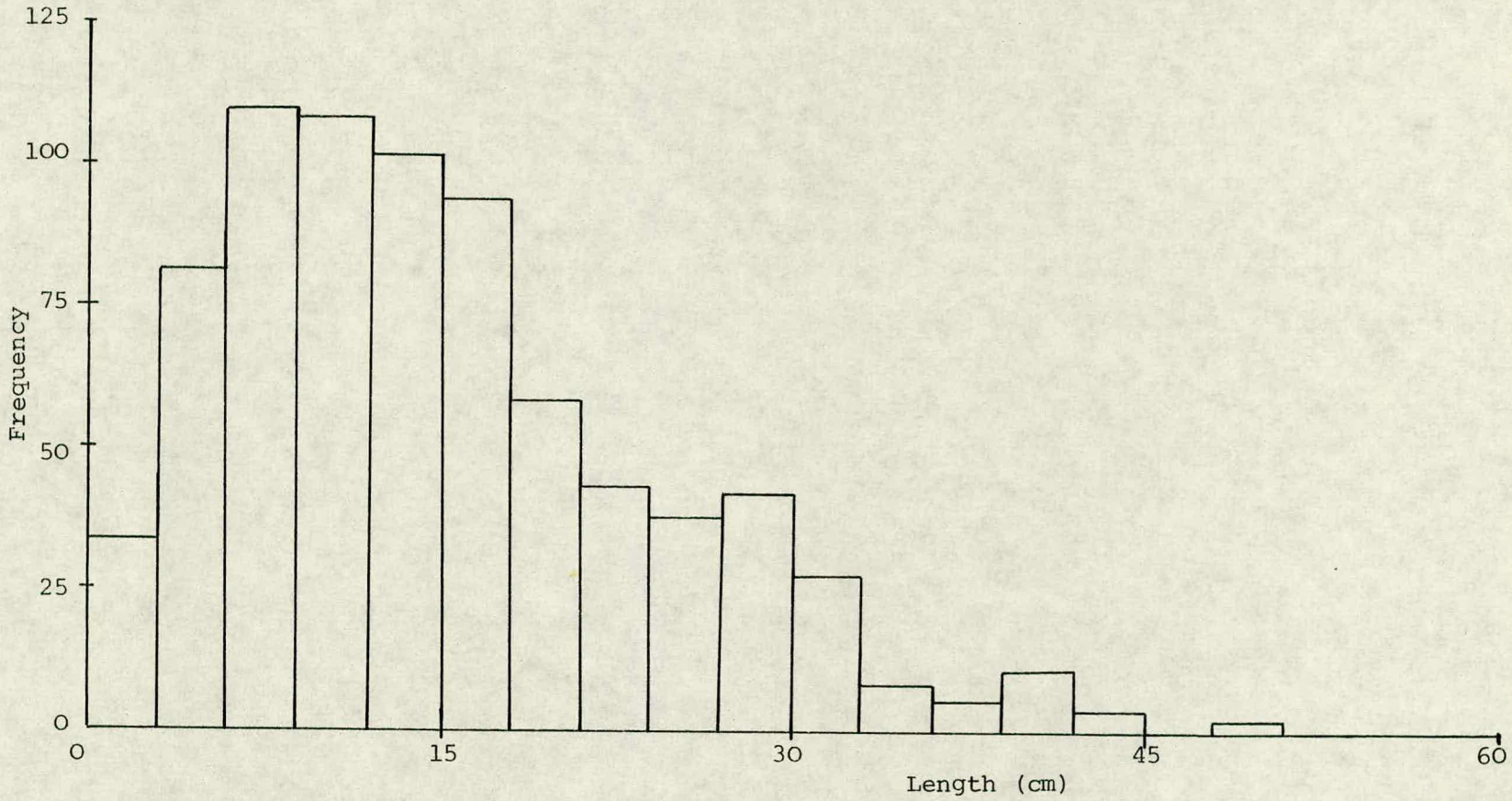


Figure 3.4.1

Length distribution of straight-line segments

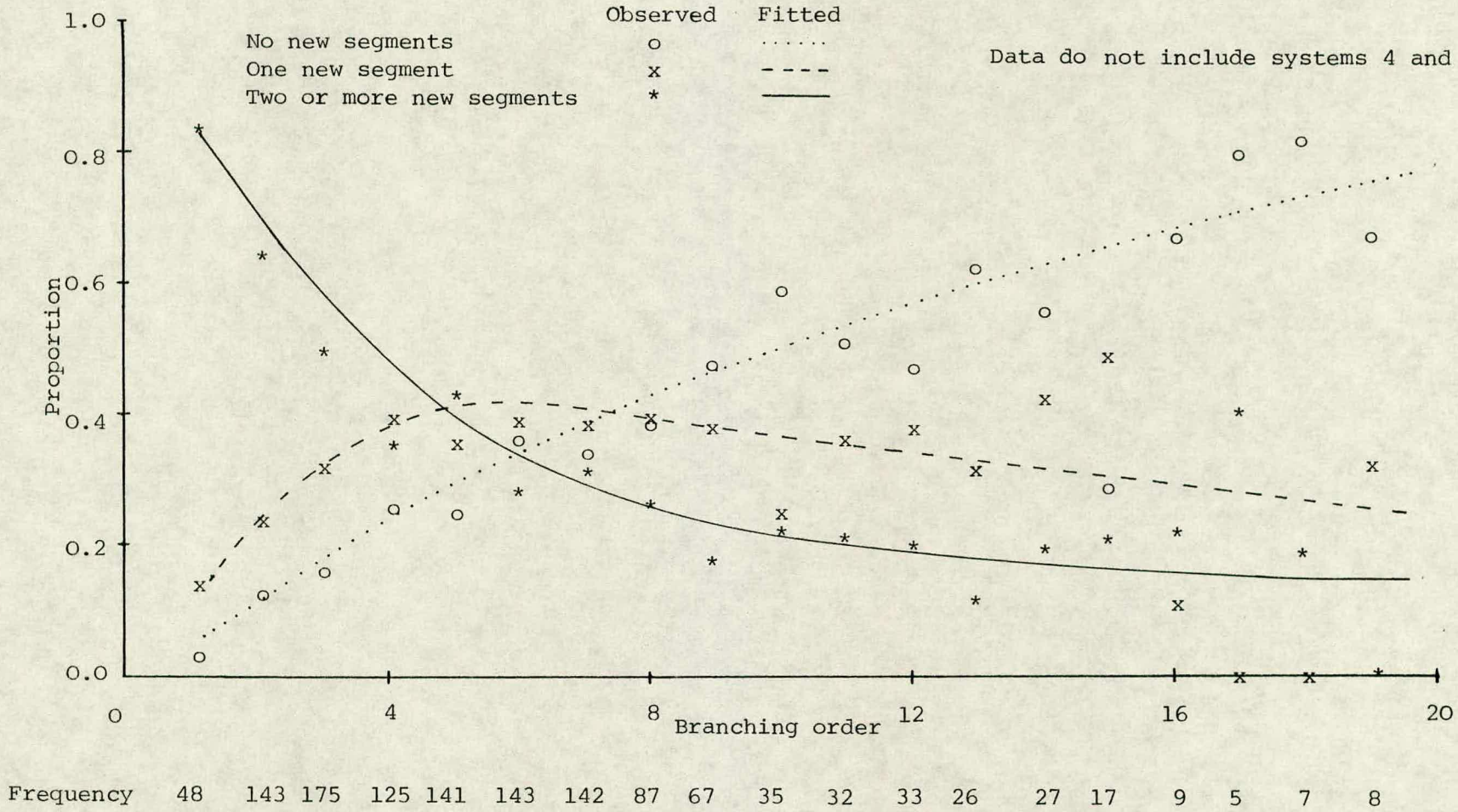


Figure 3.4.2

Proportion of root segments ending with zero, one or more than one new segments initiated, by branching order

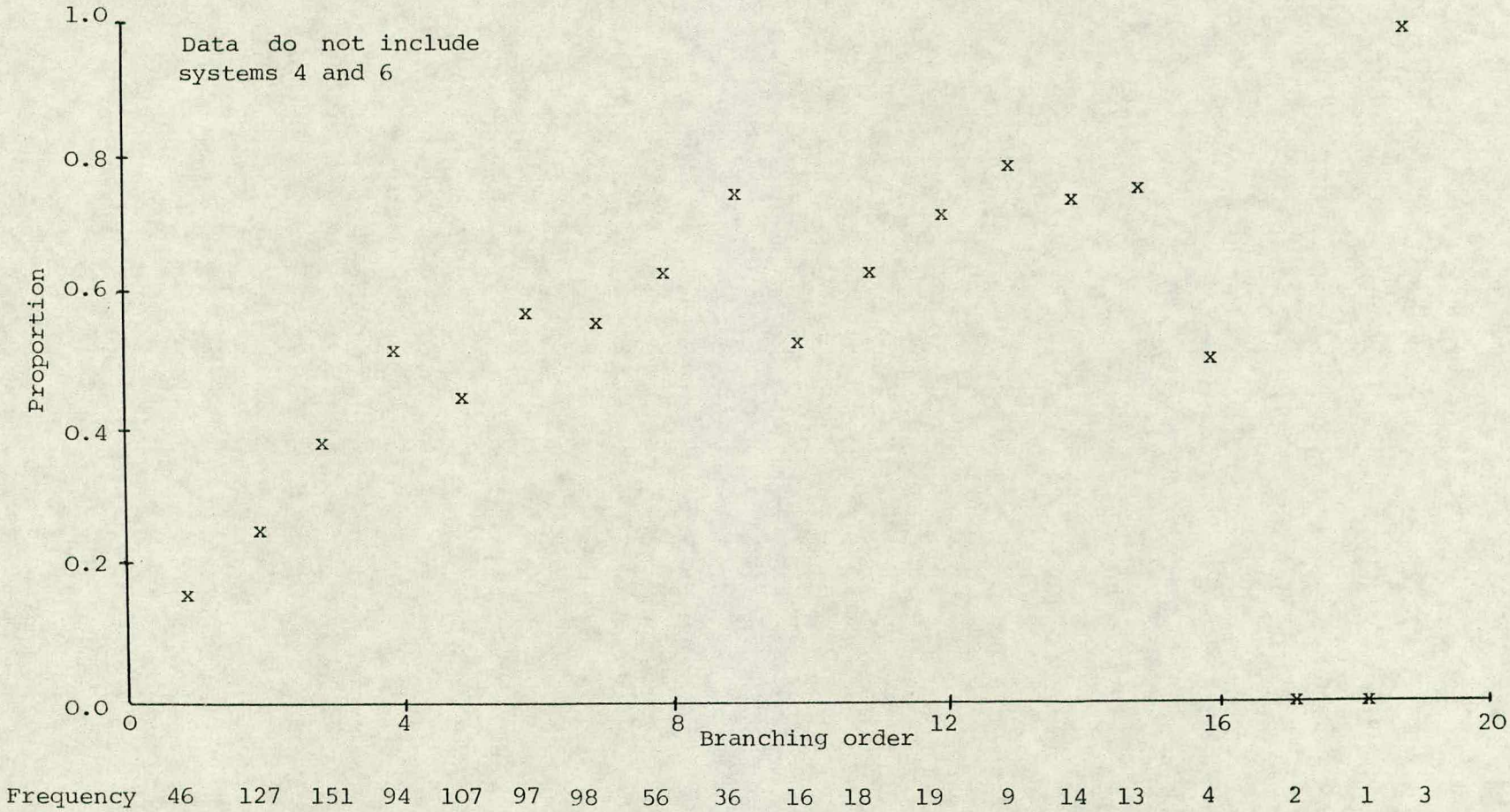


Figure 3.4.3

Proportion of root segments ending in bends conditional upon not ending at 5mm points, by branching order

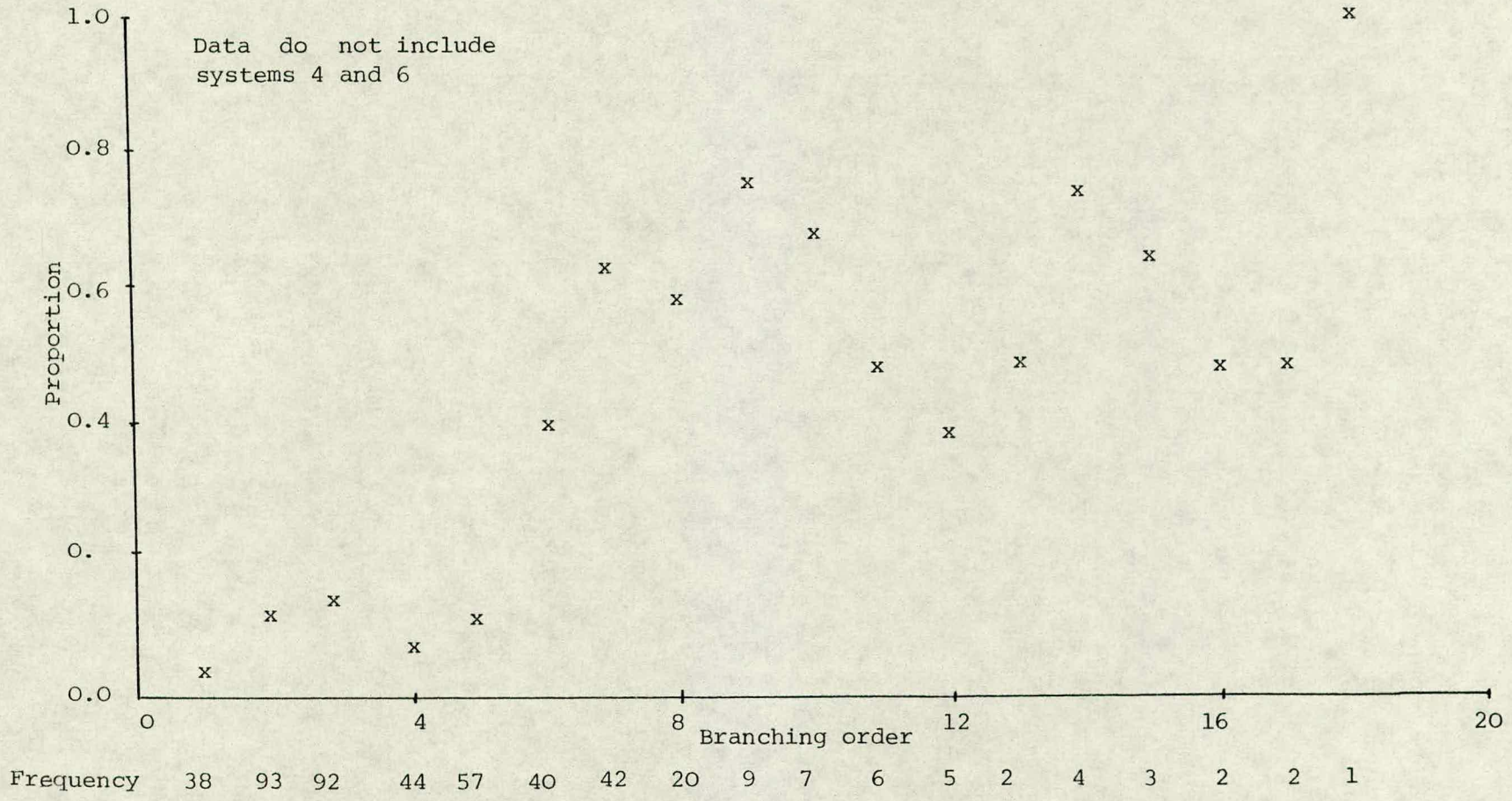
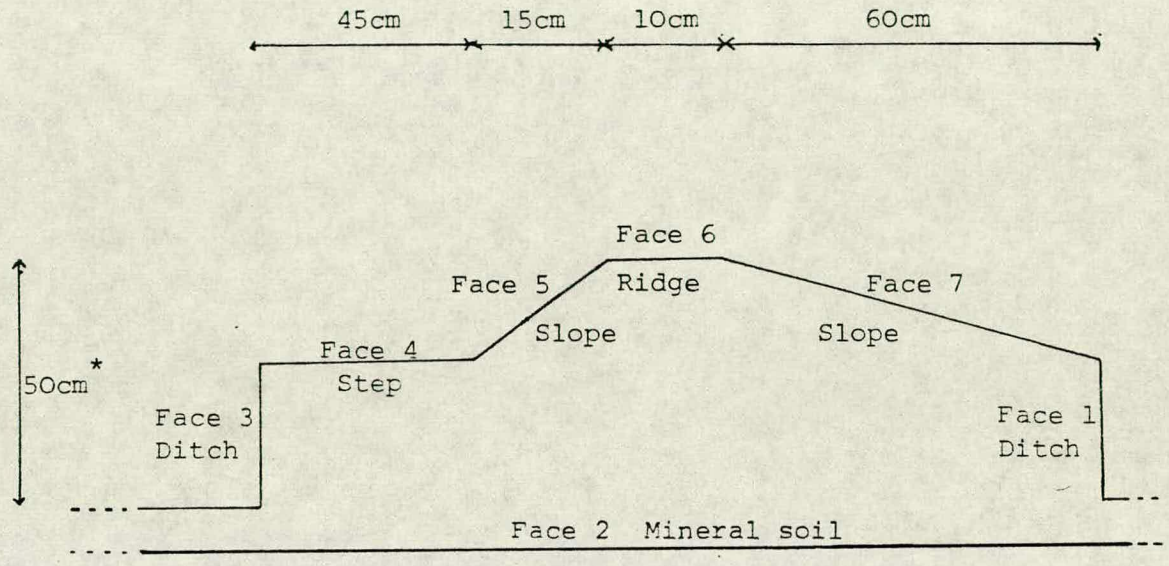


Figure 3.4.4

Proportion of root segments ending at lateral branching points conditional upon not ending at 5mm points or bends, by branching order



* This value is an approximation as the mineral soil and ploughing depths were variable.

Figure 3.5.1

Simplified diagram of the soil boundaries

No INAZ data for system 6

	Tree							
	1	2	3	4	5	6	7	8
STEMAZ L-statistic	2.23	1.36*	0.57*	2.58	3.74**	2.16	1.14*	1.99
INAZ L-statistic	1.46	2.02	0.78*	1.38*	0.98*		1.78	2.33
Significant points								
Upper 5%	3.03	2.95	3.21	2.97	3.21	2.97	3.00	3.10
Lower 5%	1.39	1.55	1.93	1.48	1.93	1.48	1.43	1.24

* Significant regularity

** Significant clustering

Upper 5% points are taken from Mardia (1972) and lower 5% points from Cochrane (1977).

Table 3.1.1

L-statistics for the STEMAZ and INAZ data

Tree

1		2		3		4	
STEMAZ	INAZ	STEMAZ	INAZ	STEMAZ	INAZ	STEMAZ	INAZ
0.63	0.98	0.76	1.48	0.08	6.02	2.23	1.68
0.81	2.40	0.91	0.98	1.24	1.27	2.69	1.26
3.00	2.94	1.16	1.41	2.96	2.50	2.71	2.53
4.12	3.97	1.93	2.03	3.80	4.29	3.48	2.72
4.59	4.85	2.53	2.81	5.00	4.81	3.99	3.90
4.96	5.29	2.65	2.22			4.75	5.17
5.11	5.02	2.86	3.20			4.92	4.92
5.17	6.17	3.65	2.97			5.00	0.38
5.98	0.45	4.24	3.58			5.28	1.00
		4.98	4.76			5.33	5.86
		5.59	5.91			5.74	0.23
		6.17	0.16				

5		6	7		8	
STEMAZ	INAZ	STEMAZ	STEMAZ	INAZ	STEMAZ	INAZ
1.70	6.02	0.18	0.28	0.14	1.33	1.45
1.19	0.98	0.77	1.85	1.89	2.47	2.68
1.19	2.06	1.49	2.46	2.20	2.65	2.96
5.03	3.72	1.50	3.06	2.97	3.32	3.39
5.04	5.55	1.86	3.72	3.38	3.59	3.60
		2.10	4.50	4.49	4.08	4.12
		2.30	5.02	5.51	5.20	5.08
		2.73	5.65	5.74		
		2.75	6.06	0.23		
		3.39	6.27	5.83		
		4.63				

No INAZ data for root system 6.

Table 3.1.2

Values of STEMAZ and INAZ (radians)

Angle (radians)	Frequency
less than $-\pi/18$	0
$-\pi/18$ and up to 0	9
0 " " " $\pi/18$	10
$\pi/18$ " " " $2\pi/18$	7
$2\pi/18$ " " " $3\pi/18$	15
$3\pi/18$ " " " $4\pi/18$	13
$4\pi/18$ " " " $5\pi/18$	5
$5\pi/18$ and over	0

Data are taken from all root systems except number 6.

Table 3.1.3

Distribution of INANG variables

Azimuth change from previous or parent direction (radians)	Frequencies			
	BFNDAZ	PARAZ	BRANCHAZ	FORKAZ
$-\pi$ and up to $-5\pi/6$	0	0	1	
$-5\pi/6$ " " " $-4\pi/6$	2	2	1	
$-4\pi/6$ " " " $-3\pi/6$	0	0	5	
$-3\pi/6$ " " " $-2\pi/6$	5	2	22	
$-2\pi/6$ " " " $-\pi/6$	26	10	73	
$-\pi/6$ " " " 0	173	95	8	
0 " " " $\pi/6$	155	90	13	127
$\pi/6$ " " " $2\pi/6$	30	8	65	25
$2\pi/6$ " " " $3\pi/6$	4	6	17	7
$3\pi/6$ " " " $4\pi/6$	1	0	6	0
$4\pi/6$ " " " $5\pi/6$	0	1	2	0
$5\pi/6$ and over	1	0	1	0

Data are from the four root systems measured in the frame. The two new roots initiated at forks subtended symmetrical azimuths to their parent: only the positive changes are included here.

Table 3.2.1

Azimuth change distributions

Change in angle (radians)	Depth < 15cm		Depth ⩾ 15cm	
	Previous direction		Previous direction	
	Positive	Negative	Positive	Negative
$-\pi/2$ and up to $-5\pi/12$	0	0	0	0
$-5\pi/12$ " " " $-4\pi/12$	0	0	1	0
$-4\pi/12$ " " " $-3\pi/12$	0	0	3	2
$-3\pi/12$ " " " $-2\pi/12$	0	0	28	1
$-2\pi/12$ " " " $-\pi/12$	2	7	67	3
$-\pi/12$ " " " 0	19	21	102	7
0 " " " $\pi/12$	18	134	98	45
$\pi/12$ " " " $2\pi/12$	3	40	69	35
$2\pi/12$ " " " $3\pi/12$	1	1	24	26
$3\pi/12$ " " " $4\pi/12$	0	0	5	4
$4\pi/12$ " " " $5\pi/12$	0	0	2	1
$5\pi/12$ and over	0	0	0	1

Data are from the four root systems measured in the frame.

Table 3.2.2

Pooled BENDANG, PARANG and FORKANG distribution

Change in angle (radians)	Frequency
less than $-\pi/3$	0
$-\pi/3$ and up to $-5\pi/18$	3
$-5\pi/18$ " " " $-4\pi/18$	3
$-4\pi/18$ " " " $-3\pi/18$	2
$-3\pi/18$ " " " $-2\pi/18$	5
$-2\pi/18$ " " " $-\pi/18$	4
$-\pi/18$ " " " 0	3
0 " " " $\pi/18$	33
$\pi/18$ " " " $2\pi/18$	30
$2\pi/18$ " " " $3\pi/18$	30
$3\pi/18$ " " " $4\pi/18$	38
$4\pi/18$ " " " $5\pi/18$	38
$5\pi/18$ " " " $\pi/3$	25
$\pi/3$ and over	0

Data are from the four root systems measured in the frame.

Table 3.2.3

Distribution of branching angles (BRANCHANG)

Parent angle (radians)	Frequency	Proportion with positive BRANCHANG
less than 0	85	1.000
0 and up to $\pi/12$	35	0.971
$\pi/12$ " " " $2\pi/12$	40	0.900
$2\pi/12$ " " " $3\pi/12$	28	0.786
$3\pi/12$ " " " $4\pi/12$	14	0.714
$4\pi/12$ " " " $5\pi/12$	10	0.700
$5\pi/12$ and over	2	0.000

Data are from the four root systems measured in the frame.

Table 3.2.4

Proportion of laterals with positive BRANCHANG

Length (cm)	Generation					
	1	2	3	4	5	6
0.00 to 4.99	3	0	0	21	36	22
5.00 " 9.99	4	0	8	63	15	7
10.00 " 14.99	8	4	36	42	7	1
15.00 " 19.99	4	12	65	21	2	0
20.00 " 24.99	6	20	59	8	1	0
25.00 " 29.99	3	38	35	1	0	0
30.00 " 34.99	6	35	14	0	1	0
35.00 " 39.99	1	41	8	0	0	0
40.00 " 44.99	0	36	9	0	0	0
45.00 " 49.99	12	5	5	0	0	0
50.00 " 54.99	8	6	0	0	0	0
55.00 " 59.99	2	5	2	0	0	0
60.00 " 64.99	2	0	0	0	0	0
65.00 and over	0	0	0	0	0	0

Values plotted are frequencies in each group. Data are taken from all systems except number 6. Root systems 1, 2, 3 and 7 had six generations of roots, numbers 5 and 8 had five and number 4 had three.

Table 3.3.1

GENLEN distribution

Length (cm)	Frequency	NBRAN					
		0	1	2	3	4	>4
0.00 to 4.99	3	0.67	0.33				
5.00 " 9.99	3	0.67	0.33				
10.00 " 14.99	6	0.83	0.17				
15.00 " 19.99	4	0.50	0.50				
20.00 " 24.99	5	0.60	0.20	0.20			
25.00 " 29.99	3	0.67	0.33				
30.00 " 34.99	5	0.40	0.40	0.20			
35.00 " 39.99	0						
40.00 " 44.99	0						
45.00 " 49.99	9	0.33	0.56	0.11			
50.00 " 54.99	6	0.16	0.33	0.16	0.16	0.16	
55.00 " 59.99	2		0.50		0.50		
60.00 " 64.99	2				1.00		
65.00 and over	0						

Values plotted are the proportions with each number of lateral branches (NBRAN). Zero proportions are omitted for clarity. Data are from all root systems except numbers 4 and 6.

Table 3.3.2

Numbers of lateral branches on primary roots

Length (cm)	Frequency	NBRAN					
		0	1	2	3	4	>4
0.00 to 4.99	75	0.97	0.03				
5.00 " 9.99	86	0.93	0.06	0.01			
10.00 " 14.99	81	0.67	0.31	0.02			
15.00 " 19.99	93	0.65	0.31	0.02	0.02		
20.00 " 24.99	88	0.53	0.40	0.07			
25.00 " 29.99	72	0.44	0.42	0.10	0.04		
30.00 " 34.99	48	0.40	0.46	0.10	0.04		
35.00 " 39.99	47	0.38	0.28	0.26	0.09		
40.00 " 44.99	45	0.29	0.44	0.18	0.07	0.02	
45.00 " 49.99	9	0.11	0.22	0.44	0.22		
50.00 " 54.99	6			0.50	0.17	0.17	0.17
55.00 " 59.99	7			0.29	0.29	0.29	0.14
60.00 and over	0						

Values plotted are the proportions with each number of lateral branches (NBRAN). Zero proportions are omitted for clarity. Data are from all root systems except numbers 4 and 6.

Table 3.3.3

Numbers of lateral branches on secondary or higher generation roots

Length (cm)	Frequency	NBEND					
		0	1	2	3	4	>4
0.00 to 4.99	82	0.87	0.10	0.04			
5.00 " 9.99	97	0.62	0.29	0.09			
10.00 " 14.99	98	0.62	0.18	0.17	0.02		
15.00 " 19.99	104	0.40	0.37	0.19	0.04		
20.00 " 24.99	94	0.26	0.45	0.21	0.06	0.02	
25.00 " 29.99	77	0.29	0.27	0.26	0.11	0.05	0.02
30.00 " 34.99	56	0.23	0.27	0.18	0.23	0.05	0.04
35.00 " 39.99	50	0.22	0.16	0.40	0.14	0.06	0.02
40.00 " 44.99	45	0.07	0.22	0.31	0.20	0.11	0.09
45.00 " 49.99	22	0.18	0.32	0.23	0.14		0.14
50.00 " 54.99	14	0.14		0.36	0.36	0.14	
55.00 " 59.99	9	0.11			0.33	0.33	0.22
60.00 " 64.99	2				0.50		0.50
65.00 and over	0						

Values plotted are the proportions with each number of bends (NBEND). Zero proportions are omitted for clarity. Data are from all root systems except number 6.

Table 3.3.4

Numbers of bends in roots

Means of transformed STEPLEN data ($(cm)^{\frac{1}{4}}$)

		Origin type		
		Root origin	Bend	Lateral position
End type	Bend	1.664	1.634	1.621
	Lateral position	1.795	1.641	1.639
	Damage	1.654	1.628	1.621

Frequencies

		Origin type		
		Root origin	Bend	Lateral position
End type	Bend	112	117	148
	Lateral position	87	109	18
	Damage	84	39	36

Data are from the four root systems measured in the frame.

Table 3.4.1

Effect of step origin and end types

Azimuth

Face	Behaviour
1, 3	Changes to almost parallel to the ditch, with north or south direction depending upon which was closest to the previous azimuth. Deviations from azimuths exactly parallel to the ditch could be modelled by the modulus of wrapped N(0,0.11) random variables with sign chosen to ensure that the root remained within the soil.
Others	No change in azimuth.

Angle

Face	Behaviour
1, 3	Takes a value in the range $7\pi/18$ to $\pi/2$ radians, i.e. changes to almost vertical.
2	Takes a value in the range 0 to $-\pi/12$ radians, i.e. changes to almost horizontal.
4, 6	Takes a value in the range 0 to $\pi/12$ radians, i.e. changes to almost horizontal.
5,7	Changes to parallel to the slope.

Roots which reached any of the seven soil boundaries, or faces, (see Figure 3.5.1) changed azimuth and angle as described above. Our estimates are based on the data from the four root systems measured in the frame. Frequencies were very low however, namely 13, 26, 5, 12, 20, 8 and 13 for faces 1 to 7 respectively.

Table 3.5.1

Estimated root behaviour at the soil boundaries

CHAPTER 4

COMPUTER SIMULATION OF ROOTING PATTERNS AND THE USE OF LENGTH CURVES AS DESCRIPTIVE STATISTICS

4.1 Simulation Models

Cochrane (1977) simulated the aerial branching patterns of Sitka spruce using a stochastic model of the development of the branching structure. A similar model for root growth is not possible in this study for we were unable to use our data to reconstruct the development of the excavated root systems (Section 2.4). Alternatives are either to base a model on an assumed growth sequence (development models) or to base a model on the appearance of a root system at a fixed time, without attempting to describe the actual sequence of development (distribution models). Until root growth is more fully understood the assumptions required to model development are likely to be arbitrary and distribution models will be of more use. In this chapter we will consider two distribution models based on our analysis of the variables which determine root morphology (Chapter 3).

Rooting patterns are simulated using the first model by generating the straight-line segments between bends and branching points sequentially (Figure 4.1.1a). Each segment has a length, an orientation relative to the previous segment and ends with the initiation of a number of new segments. If no new segments are produced then the point represents a 5mm diameter, one new segment represents a bend in a root and two new segments represents a fork or lateral branching point. This model will be called the sequential model of root distribution. The random numbers required when rooting patterns are simulated using this model are generated from the probability distributions fitted to the initial distribution, directional and sequential step variables (Sections 3.1, 3.2 and 3.4).

In the second model the path of a root is generated in the following manner. First, the total length and type of ending of the root are fixed. Then a number of bends and lateral branching points are distributed along the length. Finally, the shape is distorted by appropriate direction changes (Figure 4.1.1b). This model will be called the reconstruction model of root distribution. The reconstruction model also involves the initial distribution and directional variables but now the probability distributions fitted to the path reconstruction data (Section 3.3) are employed when random numbers are generated.

4.2 Programming

Edinburgh IMP programs were written to simulate rooting patterns using each model: Figure 4.2.1 is a flow chart for the program (Appendix 1) which uses the reconstruction model. The basis of both programs is a dynamic array, START, containing vectors of information on the origins of individual roots. The information stored in START is: the three-dimensional coordinates of the root origin; the initial azimuth and angle of the root; for the sequential program the branching order at the root origin; and for the reconstruction program the root generation. Each program cycles through the array, for each member generating the root's path and adding the initial information on any new offspring to START. The cycle continues until paths have been traced from all points in the array. Using this method the amount of store required is kept low.

Pseudo-random numbers from the probability distributions fitted to the initial distribution, directional and either path reconstruction or sequential step variables are generated by separately written subroutines and functions. Each subroutine also includes options to allow the user to generate random numbers from other distributions. For example, the azimuth changes at bends may be generated from the distribution fitted to the BENDAZ data, the circular uniform distribution or a circular lattice distribution.

Each program includes a routine to simulate root behaviour at the soil surface, ditch and mineral soil layer and so ensure that the development takes place within the soil. The programs also calculate

and print out several statistics after each simulation:

i) the maximum and minimum X, Y and Z coordinates reached;

ii) the number of roots; and,

iii) the distribution of simulated root length against radial distance, depth and direction (see, for example, Figures 2.3.1, 2.3.2 and 2.3.3), collectively called the length curves.

During the simulation of a rooting pattern the programs print the three-dimensional coordinates of all root origins, bends, lateral branching points, forks and 5mm points in such a way that diagrams of the simulated root system viewed in the X-Y, Y-Z and X-Z planes could be drawn on a Calcomp 936 graph plotter.

4.3 Results

4.3.i Comparison of models

Because no descriptive statistics of rooting patterns have previously been suggested we compared simulated root systems with each other and with the observed root systems by visually examining graph plots. Further comparisons were made using the overall dimensions, number of roots and length curves of the real and simulated root systems. The use of length curves as a method of describing a complex branching pattern is discussed in Section 4.4.

The graph plots illustrated the spatial patterns of the excavated and simulated root systems by representing each root segment as a single line, i.e. root diameters were not included. For example, Figures 4.3.1 to 4.3.6 are X-Y, X-Z and Y-Z views of two of the excavated root systems, one (number 1) with a greater extent of roots from north to south than from east to west, and another (number 3) with a more even north-south and east-west extent. The X-Y views (Figures 4.3.1 and 4.3.4) show the initial distribution of the primary roots and illustrate the relatively densely and sparsely populated areas. The X-Z views (Figures 4.3.2 and 4.3.5) show the characteristic flat bottom at the mineral soil layer and also illustrate the extent of the root systems parallel to the ploughing direction. The Y-Z views are sections at 90° to the direction of ploughing and illustrate the

soil contours, particularly the ridge of earth thrown up by the plough and the positions of the ditches (Figures 4.3.3 and 4.3.6).

Fifty root systems were simulated using the sequential model and although these were generally of the correct size and complexity, overall the patterns produced were unconvincing (for example, Figure 4.3.7). This was because:

i) the simulated root systems included a higher frequency of, often larger, sparse regions than seen in the actual root systems; and

ii) long sequences of bends could occur and end, with a flurry of branching perhaps, at a considerable distance from the stem.

The cause of both discrepancies may be the assumption in the sequential model that the number of segments produced after a previous segment depends on branching order only. This meant that after their initial directions had been determined the offspring produced at a branching point all behaved similarly. In reality one offspring should represent the continuation of the parent, which may have a different pattern of behaviour from the newly initiated laterals.

Fifty root systems were also simulated using the reconstruction model and in this case graph plots of the simulated root systems were realistic (see, for example, Figures 4.3.8 to 4.3.13). Most root length was within 60-70cm of the tree stem and no clusters of branches were found outside that region. Sparse regions occurred in the simulations but had similar sizes to the sparse regions within the excavated root systems. Moreover, the range of dimensions, number and total length of roots of the fifty simulated root systems included the corresponding values from the excavated root systems 1, 2 and 3:

Excavated root systems

	1	2	3	4
Number of roots	134	156	132	45
Total length (m)	34.0	31.7	28.2	11.6
North-south projection (m)	2.5	2.2	1.5	1.4
East-west projection (m)	1.5	1.3	1.4	1.4
Depth penetrated (cm)	62	54	53	35

Simulated root systems

	Minimum	Mean	Maximum
Number of roots	71	141	181
Total length (m)	16.8	31.2	42.4
North-south projection (m)	1.3	1.9	2.6
East-west projection (m)	1.3	1.4	1.6
Depth penetrated (cm)	30	48	60

It is interesting to note that no simulated root system had a smaller number or total length of roots than the excavated system 4. Perhaps this was because the data from which the parameters of the NBRAN distribution were estimated did not include the system 4 data, for root system 4 had fewer lateral branches than the other root systems (Section 3.3.iii).

We suggest that the reconstruction model is an acceptable empirical model for the spatial distribution of the structural roots of Sitka spruce. Having found an acceptable model we give two examples of how computer simulation of rooting patterns can be useful to tree growth studies. The first example (Section 4.3.ii) is an investigation into the necessity of the apparently regular growth mechanisms. The second example (Section 4.3.iii) is an illustration of how simulation can be used when considering the accuracy of soil sampling schemes. The simulation described in both examples is by the reconstruction method only. No attempt was made to improve the sequential model, which was abandoned.

4.3.ii Model application I: assessment of rules for generating rooting patterns

As mentioned in Section 3.5, perhaps rooting patterns are so modified by growth in a heterogeneous environment that the inherently regular growth mechanisms have little effect on the final patterns. One method of determining whether the regularity is necessary is to simulate rooting patterns with random variables drawn from probability distributions other than those fitted to the data. In this way we

can also assess which are the most important rules for generating realistic patterns.

Regularly distributed primary roots

When root systems were simulated with higher variances of the STEMAZ and INAZ distributions than those estimated from the data large sparse regions occurred and were interspersed with very densely populated regions (Figure 4.3.14). This suggests that the almost regular distribution of primary roots is important in ensuring an even spread of roots.

Root length distributions

The means and variances of the GENLEN distributions were more important to the final patterns than the precise form of the distributions. For example, we used Box and Cox (1964) methods to transform the GENLEN data to be approximately Normal and then fitted suitable Normal probability distributions to the transformed data. Root lengths were then simulated by generating random variables from the fitted Normal distributions and performing the inverse transformation. This had little effect on the final patterns (Figure 4.3.15).

Bending and Branching

When the parameters which determined the frequency of branching and bending were increased the simulated root systems were unrealistic (Figure 4.3.16). Root paths were irregular and very densely populated regions occurred although sparse regions could also occur. Whether bends and laterals were randomly or regularly spaced along a parent root had little effect on rooting patterns. For example, root systems simulated with the DISTBRAN and DISTBEND distributions (Sections 3.3.v and 3.3.vi) interchanged were similar to the excavated root systems (Figure 4.3.17).

Variances of the fitted distributions

The parameters which had most influence on the final patterns were the variances of the fitted distributions, especially the directional variable distributions. Root systems simulated with all variances reduced to zero had unrealistic, perfectly isotropic

patterns which included neither sparsely nor densely populated regions (Figure 4.3.18). When the variances of the azimuth distributions (Section 3.2) were very high simulated root systems were also unrealistic because the correlation between root directions before and after bends or lateral branching points was low. Many roots turned backwards towards the stem, which reduced the outward spread and caused the central region to become densely occupied (Figure 4.3.19). Similarly, root systems simulated with high angle variances were unrealistic because the central region was very densely populated (Figure 4.3.20). Low variances of the angle distributions also gave unrealistic simulations because fewer roots grew in almost horizontal directions than found in the excavated root systems (Figure 4.3.21).

Lateral branching angles and azimuths

Realistic patterns could only be simulated if lateral branches subtended large angles and azimuths to their parent directions. For example, when the BRANCHANG and BRANCHAZ distributions (Section 3.2) were chosen to be the same as FORKAZ and FORKANG the simulated root systems were unrealistic, for most roots followed the soil contours and few roots grew downwards (Figure 4.3.22).

Alternate azimuth changes

Finally, the tendency for azimuth changes to be alternately clockwise then anticlockwise was necessary for the simulation of realistic rooting patterns. If direction changes were assumed to be independent of all previous changes a high frequency of roots formed loops and turned back towards the stem (Figure 4.3.23).

Thus root growth is not entirely random and some regular growth mechanisms are necessary to produce a well extended and evenly spread root system. In particular, the correlation between root directions before and after bends and lateral branching points is extremely important to rooting patterns. Other important rules for generating realistic rooting patterns are: regularly distributed primary roots; large angles and azimuths between lateral roots and their parents; and alternate azimuth changes. It is interesting to note that the regular distribution of lateral root origins along other roots had little effect on the final pattern, perhaps because most roots

included only a few laterals (Section 3.3.v).

4.3.iii Model application II: the estimation of total root length from a partial excavation

Estimates of total root length are important to studies of forest development but accurate estimates are difficult to obtain because the excavation of complete structural root systems is both laborious and expensive. A method of partial excavation which can be shown to lead to accurate estimates would be a major development. Thus an important application of computer simulation of rooting patterns can be to assess the accuracy of estimates based on partial excavations. The technique is first to use simulation to find a method of estimating the total root length from the sample and then to use further simulations to assess the accuracy of the estimates. To illustrate the technique we consider two methods of estimating the total root length. The first method is based on the number of roots which intercept a vertical plane at 90° to the ploughing direction and 60cm north of the stem. In the field the number of intercepts may be determined by digging a suitable trench and counting the number of severed roots exposed on the trench wall. Similar methods of studying root distributions have been used by several authors, including Savill (1976). The method has the advantage that the tree need not be killed but the disadvantage that roots growing in the east-west direction are not likely to be included in the sample. The second estimate is based on the total length of root within the 90° segment between the north and east directions and within 1m of the central axis of the stem. Similar methods of sampling root systems by excavating pits have been used by many experimentors, including Bowen (1964). The method has the advantage that the estimate of total root length is based on a measurement of length rather than root numbers. A disadvantage is that if the root system is non-isotropic then a misleading estimate may be obtained.

To determine a method of estimating the total root length from the samples sixteen root systems were simulated using the reconstruction program. In each case ($i = 1, 2, \ldots, 16$) the total root length, y_i say, the number of roots which intercepted the plane,

x_{1i} say, and the total length of root within the segment, x_{2i} say, were determined. The results suggested that total root length was linearly related to both the number of intercepts and the length within the segment (Figures 4.3.24 and 4.3.25). Linear regression models were therefore fitted to the data, namely

$$y_i = \alpha_1 + \beta_1 x_{1i} + \varepsilon_{1i}$$

and

$$y_i = \alpha_2 + \beta_2 x_{2i} + \varepsilon_{2i} \ ,$$

where ε_{1i}, ε_{2i} $(i = 1, 2, \ldots, 16)$ are mutually independent $N(0,\sigma_1^2)$ and $N(0,\sigma_2^2)$ random variables respectively. The parameter estimates and their estimated standard errors were:

Parameter	Estimate	Estimated standard error
α_1	2.61m	2.45m
β_1	0.85m/intercept	0.10m/intercept
σ_1^2	$4.91m^2$	
α_2	16.41m	1.93m
β_2	1.03	0.40
σ_2^2	$14.86m^2$	

These results suggest that if x_1 intercepts are found when the trench method is used then the estimate of total root length should be $2.61+0.85x_1$ metres. Similarly, if a total length of x_2 metres is found within the 90° segment then the estimate should be $16.41+1.03x_2$ metres. The latter estimate is suprising for the chosen segment effectively includes one quarter of the available soil volume and so the intuitive estimate is $4x_2$ metres. We can suggest no explanation for why the estimate based on the fitted regression line should differ from the intuitive estimate unless perhaps sixteen simulations were insufficient.

A further sixteen root systems were simulated to assess the accuracy of the estimates. In each case the total root length was compared with estimates based on the trench and segment partial

excavation estimates. In thirteen out of the sixteen root systems the trench method led to a better estimate of total root length than the segment method (Figure 4.3.26). The mean square error of the trench method was $4.1m^2$ whilst the corresponding value of the segment method was $10.1m^2$. Therefore of the two partial excavation techniques considered here the trench method of estimating total root length is more accurate. Nevertheless, the discrepancy between estimated and actual total root length could be as high as 5m (Figure 4.3.26).

We suggest that further investigations should be made for many other partial excavation techniques are possible and simulation using the reconstruction model is a simple method of testing the accuracy of the techniques.

4.4 The Use of Length Curves As Descriptive Statistics of Spatial Patterns

Throughout Section 4.3 rooting patterns were compared by visually examining graph plots. Whilst only a little experience is necessary to distinguish between realistic and unrealistic patterns visual methods are inherently subjective. Moreover, visual methods require the relatively slow and expensive plotting of the simulated root systems. A method which uses a few statistics to summarise the information contained in a spatial branching pattern would be very useful in providing a more objective method of comparison and allowing a greater number of simulations to be examined. We require that such statistics:

i) describe the salient features of a branching pattern;
ii) are robust to random variations between root systems produced by the same model; and
iii) are sensitive to changes in the parameter values of the model.

The essential features of a rooting pattern are the number of roots and the distribution around the stem of its total length. The number of roots is easily determined and the distribution of root length is described by the three length curves of a root system, i.e. the distributions of root length against radial distance, depth and direction (for example Figures 2.3.1, 2.3.2 and 2.3.3). The length

curves are not robust to random variations however, for even though we found no significant differences between the component variables of root systems 1, 2 and 3 (Chapter 3) their length curves differed (Figures 2.3.1, 2.3.2 and 2.3.3).

An alternative summary of the rooting patterns produced by a model is provided by the mean length curves of a number of such patterns. To determine the usefulness of such mean length curves as descriptive statistics we must investigate:

i) whether the mean length curves converge as the number of root systems is increased and if so how many root systems are required before the mean curves become stable; and,

ii) if the mean length curves are sensitive to changes in parameter values.

Throughout the sequel the radial distance curve of a root system is its total length in successive 10cm intervals from the central axis; the depth curve is the length in successive 10cm horizontal layers; and the direction curve is the length in successive 30° arcs around the stem.

4.4.i Convergence of the mean length curves

The mean radial distance curve of the fifty root systems simulated by the reconstruction method was positively skewed with maximum length between 30 and 40cm from the central axis (Figure 4.4.1). The mean depth curve was more symmetrical with maximum at depths 10-20cm (Figure 4.4.2). The mean direction curve had almost constant value in each arc (Figure 4.4.3). Henceforth Figures 4.4.1, 4.4.2 and 4.4.3 will be called the "true" radial distance, depth and direction curves respectively. The true radial distance and depth curves had similar shapes to those of the actual root systems (Figures 2.3.1 and 2.3.2) but the true direction curve was more even than those of the excavated root systems (Figure 2.3.3). This was because over the fifty simulations no region was either sparsely or densely populated more often than any other.

Convergence to the true curves was measured by considering the sums of squared deviations between the true length curves and the corresponding mean length curves of an increasing number of simulated

root systems. Convergence of the radial distance and depth curves was rapid up to five simulations and was afterwards very gradual whereas the convergence of the distance curve did not become gradual until after ten root systems were included (Figure 4.4.4). These results suggest that the mean length curves converge and that the mean radial distance and depth curves of five root systems are stable, as is the mean distance curve of ten root systems.

4.4.ii Sensitivity of the mean length curves

The most important parameters of the reconstruction model (Section 4.3.ii) are the variances of the distributions fitted to the directional variable data (Section 3.2). Whenever any of these parameters were changed from the estimates obtained from the data unrealistic rooting patterns were simulated. Therefore it is interesting to investigate the sensitivity of the length curves to changes in these parameter values. This may be achieved by simulating a number, r say, of root systems at each stage as individual parameters are iteratively increased whilst all other parameters are fixed. Then by calculating the sums of squared deviations between the true length curves and the mean length curves of each group of r simulated root systems a measure of sensitivity is obtained.

We investigated the influence of the eight directional standard deviations listed below.

Variable	Standard deviation	Estimate (radians)
STEMAZ	σ_x	0.265
INAZ	σ_y	0.332
BENDAZ	σ_1	0.292
PARAZ	σ_2	0.302
BRANCHAZ	σ_3	0.307
FORKAZ	σ_4	0.286
PARANG, BENDANG and FORKANG (depth $<$ 15cm)	$\sigma_{5,1}$	0.245
PARANG, BENDANG and FORKANG (depth $\geqslant$ 15cm)	$\sigma_{5,2}$	0.387

Each parameter was increased by intervals of 0.1 from 0.0 to 1.0 radians whilst all others were kept at the estimated values. At each stage five root systems were simulated using the reconstruction model and the mean length curves were calculated. Although the mean direction curve of five root systems may not be stable (Section 4.4.i) the number of simulations at each stage was chosen to be five to reduce the computing time required. Even so a total of over three hours CPU time was used in simulating the 440 root systems.

The sums of squared deviations from the true curve of the mean radial distance curves increased sharply when any of the six directional variable parameters σ_1, σ_2, σ_3, σ_4, $\sigma_{5,1}$ and $\sigma_{5,2}$ were increased past their estimated values (Figure 4.4.5). Thus the mean radial distance curve was sensitive to increased variances of the directional distributions, which caused roots to turn back towards the stem and resulted in a densely populated central region (Figures 4.3.19 and 4.3.20). The radial distance curve was not affected by changes in the initial distribution parameters σ_x and σ_y.

The depth curve was affected only by low and high values of the two angle parameters $\sigma_{5,1}$ and $\sigma_{5,2}$ (Figure 4.4.6). When $\sigma_{5,1}$ and $\sigma_{5,2}$ were low the simulated root systems included a high proportion of deep roots (Figure 4.3.21) whilst at high values the volume near the stem became densely occupied (Figure 4.3.20).

The direction curve was sensitive to increases in the STEMAZ and INAZ parameters σ_x and σ_y (Figure 4.4.7). When the STEMAZ and INAZ variances were high simulated root systems included a high proportion of densely and sparsely populated regions (Figure 4.3.14) which caused the mean direction curves of groups of five simulated root systems to be much more irregular than the true direction curve.

Thus at least one of the three length curves was sensitive to changes in any of the parameter values but no length curve was sensitive to all parameters. We suggest therefore, that examination of all three mean length curves is a simple method of assessing the effect of changing the parameter values of a simulation model and may also be useful to experimentors who wish to compare root systems objectively. Further work is required, especially to obtain the length curves of more excavated root systems. In particular, it may be useful to determine whether individual tree species have

characteristic mean length curves, just as most species have characteristic crown morphologies (Zimmermann and Brown 1971,p.125-168). In addition, it may be useful to examine whether length curves change systematically as root systems develop.

4.4.iii The use of length curves in numerical parameter estimation

The reconstruction model of root distribution is of limited usefulness because the model does not represent the temporal development of a root system. There are two problems associated with modelling root development:

i) the dynamic aspects of root growth are not understood and any model must involve simplifications of the growth processes; and,

ii) some of the parameters of any specified model cannot be directly determined from a visual examination of an excavated root system. This is because annual growth increments cannot be determined (Section 2.4), adventitious roots are indistinguishable from others (Fayle 1968) and the proportion of lateral roots which did not become structurals is unknown (McCully 1975).

Until root growth mechanisms are more fully understood any specification of a development model will be almost entirely arbitrary. But if a plausible model could be specified then we suggest that length curves may be useful in the estimation of parameter values which cannot be directly determined. The technique is to find the parameter values which minimise some function of the difference between the true length curves and the mean length curves produced by the model. To illustrate how the technique may be applied we specify a simple growth model and use the length curves to estimate the unknown parameters. It is important to note that the model is chosen to illustrate the technique of parameter estimation only and does not accurately represent root growth. Our model is as follows.

1. Assume that the initial distribution, directional variables and behaviour at the soil boundaries are the same as for the reconstruction model.

2. Let Y_{ij} be the annual growth increment of the ith living root at year j (assuming a sixteen year growth period). Assume

$$Y_{ij} = INC+\sigma_j+\varepsilon_{ij} ,$$

where INC is some positive number and σ_j and ε_{ij} are independent zero mean Normal random variables with standard deviations YERR and RERR respectively.

3. Assume that each root produces a fixed number, NBR say, of lateral roots each year and that their origins are regularly spaced along the annual growth increment. Assume that each lateral has probability PSUR of surviving to become a structural. Also assume that lateral growth begins in the following year.
4. Assume that bends occur completely randomly so that distances between bends are exponentially distributed random variables. The parameter of the distribution can be directly estimated from the data to be 0.047 bends per centimetre.
5. Assign to each root at the beginning of each year a random distance, drawn from an exponential distribution with rate DAM. If the annual growth increment exceeds the random distance then assume that the root is damaged after that distance and a fork initiated.

There are six parameters which cannot be directly determined, namely INC, YERR, RERR, NBR, PSUR and DAM. Throughout the following $\underline{p}$ denotes any six-dimensional vector of estimates of the parameter values. Before the final estimates can be obtained a function must be specified to measure the difference between the true length curves and the mean length curves of a number, r say, of root systems simulated using the model with parameter values $\underline{p}$. We suggest that a suitable function, $F(\underline{p},r)$ say, is the total sum of squared deviations between the true radial distance and depth curves and the corresponding mean curves of the r simulations. The distance curve is not included because the mean distance curve of a small number of root systems is not robust to random variations (Figure 4.4.4). However, when choosing the value of $\underline{p}$ which minimises $F(\underline{p},r)$ constraints may be imposed to

ensure that values of $\underline{p}$ which lead to unrealistic distance curves are not chosen. We suggest that for root systems of similar size to the excavated root systems a suitable definition of a realistic direction curve is:

i) the total root length in any 30° arc is less than 8m; and,

ii) the total root length in any 90° arc exceeds 1m.

Similarly, constraints may be imposed to ensure that values of $\underline{p}$ which lead to simulated root systems of incorrect size are not chosen. We suggest that a suitable definition of the correct size of a root system is:

i) between 50 and 200 roots;

ii) total root length between 10 and 50m;

iii) maximum distance from the central axis less than 1.5m; and,

iv) between 10 and 60 forks.

A computer program was written to use the model to simulate five root systems at various values of $\underline{p}$ and proceed iteratively until $F(\underline{p},5)$ was minimised subject to the above constraints. The program also incorporated constraints on the possible parameter values: for example, NBR had to be a non-negative integer and PSUR had to be positive and not greater than unity. The iterative procedure was the simplex routine (Nelder and Mead 1965) as implemented in the NAG FORTRAN library of computer programs. In this routine the user provides a preliminary estimate of the six unknown parameters. An algorithm is then used to choose another six estimates and calculate the function values at all seven estimates. The function values are then compared, one of the estimates is deleted and a new estimate is obtained. The procedure continues until the function minimum is reached. This procedure is robust to inaccuracies in the function calculations which is important to our work for the mean length curves of two separate groups of five root systems simulated with the same parameter values, whilst similar, were not identical.

The final parameter estimates were 6.423cm, 1.347cm, 0.829cm, 1, 0.082 and 0.015 forks/cm for INC, YERR, RERR, NBR, PSUR and DAM respectively. The accuracy of the estimates is unknown and we have no data with which to compare values. Root systems simulated using these parameter estimates were realistic however, being of similar

size and complexity to the extracted root systems and also including densely and sparsely populated regions (Figure 4.4.8). Thus with even such a simple model of root development the use of length curves in parameter estimation leads to realistic patterns.

Much further work is necessary to determine the accuracy of this technique of parameter estimation. But the accuracy depends upon the choice of model and a more realistic development must first be specified. Thus more knowledge of the root growth mechanisms must be obtained from both laboratory experiments and field studies. In particular, quantitative rules to describe root extension rates, branch production and growth directions must be specified in a similar manner to Cochrane and Ford's (1978) specification of rules for the development of the aerial branching structure of Sitka spruce.

4.5 Discussion

Cohen (1967) simulated biological branching processes and included such factors as inhibition and interaction with a heterogeneous environment. Whilst such factors are intuitively plausible for root spread, we were able to reproduce patterns which were apparently indistinguishable from the actual root systems without including such complexities (Section 4.3.i). But of the two models which we considered realistic patterns could only be reproduced by the reconstruction model, the basis of which was the hierarchy of primary roots, secondary roots, etc. Thus it seems that root systems have a more ordered morphology than is obvious from visual examinations of rooting patterns. Further evidence to support the hypothesis of an inherently systematic growth mechanism is provided by using simulation to assess the rules for generating rooting patterns (Section 4.3.ii).

1. Realistic root systems could not be simulated without almost regularly spaced primary roots.
2. If the variance of the INAZ distribution was high primary roots did not necessarily radiate outwards and unconvincing patterns were produced.
3. The large angles and azimuths subtended by lateral roots to their parents were important to the final shape of the root systems.

4. The tendency for root azimuth changes to be alternately clockwise then anticlockwise prevented roots from turning back towards the stem.
5. The directions taken by roots after bends and lateral branching points, and by newly initiated roots at forks, were closely related to the previous directions. If direction changes were allowed to be more variable then totally unrealistic patterns were produced.

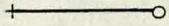
Thus regular growth mechanisms are necessary to effect a complete and even occupancy of the soil. This allows the soil resources to be efficiently exploited and improves windthrow resistance. The final patterns are considerably modified by the environment however, for when root systems were simulated with no random variation whatsoever the patterns produced (Figure 4.3.18) were as unrealistic as those simulated when growth directions were completely random (Figures 4.3.19 and 4.3.20). Cochrane (1977) found that the aerial branching structure of Sitka spruce had similar properties: unrealistic crown morphologies were simulated whenever the variance parameters of her growth model were either lower or higher than the estimated values.

Visual examination of graph plots may be the best method of determining whether a simulated root system is realistic but a useful method of describing a rooting pattern is to plot the three length curves (Section 4.4). Length curves of simulated root systems are more readily obtained than graph plots and are useful for comparative purposes for several curves may be examined on one diagram (for example, Figure 2.3.1). In addition, length curves may be useful in providing an objective summary of a rooting pattern so that statistical techniques such as hypothesis testing can be used in root growth studies. We suggest that further investigations should be made into the use of length curves as descriptive statistics in order that such techniques may be employed. Further investigations may be either Monte-Carlo studies using the reconstruction model with various parameter values, or theoretical investigations into the properties of length curves. A general theoretical analysis would be preferable for all possible parameter combinations cannot be studied by Monte-Carlo methods. As will be seen in the following chapters however, a theoretical analysis of even simple root distribution models is very difficult.

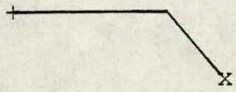
4.6 Figures

a) Sequential model

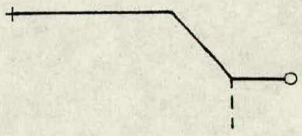
i)



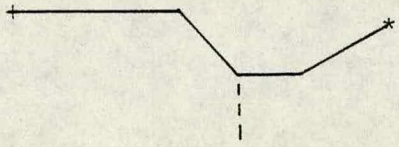
ii)



iii)

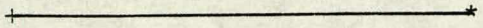


iv)



b) Reconstruction model

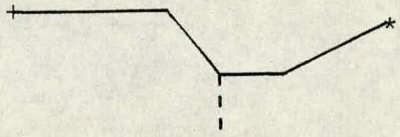
i)



ii)



iii)



+ = Root origin, * = 5mm point, o = bend, x = lateral branch.

i) Generate a step length and number of offspring.

ii,iii,iv) Generate changes in direction, length of next step and numbers of offspring sequentially until root ends in a 5mm point.

v) Return to any new roots.

i) Generate total length of root and type of ending.

ii) Distribute a number of bends and lateral branching points along the root length.

iii) Generate direction changes.

iv) Return to any new roots.

Figure 4.1.1

Simulation of one root by two methods

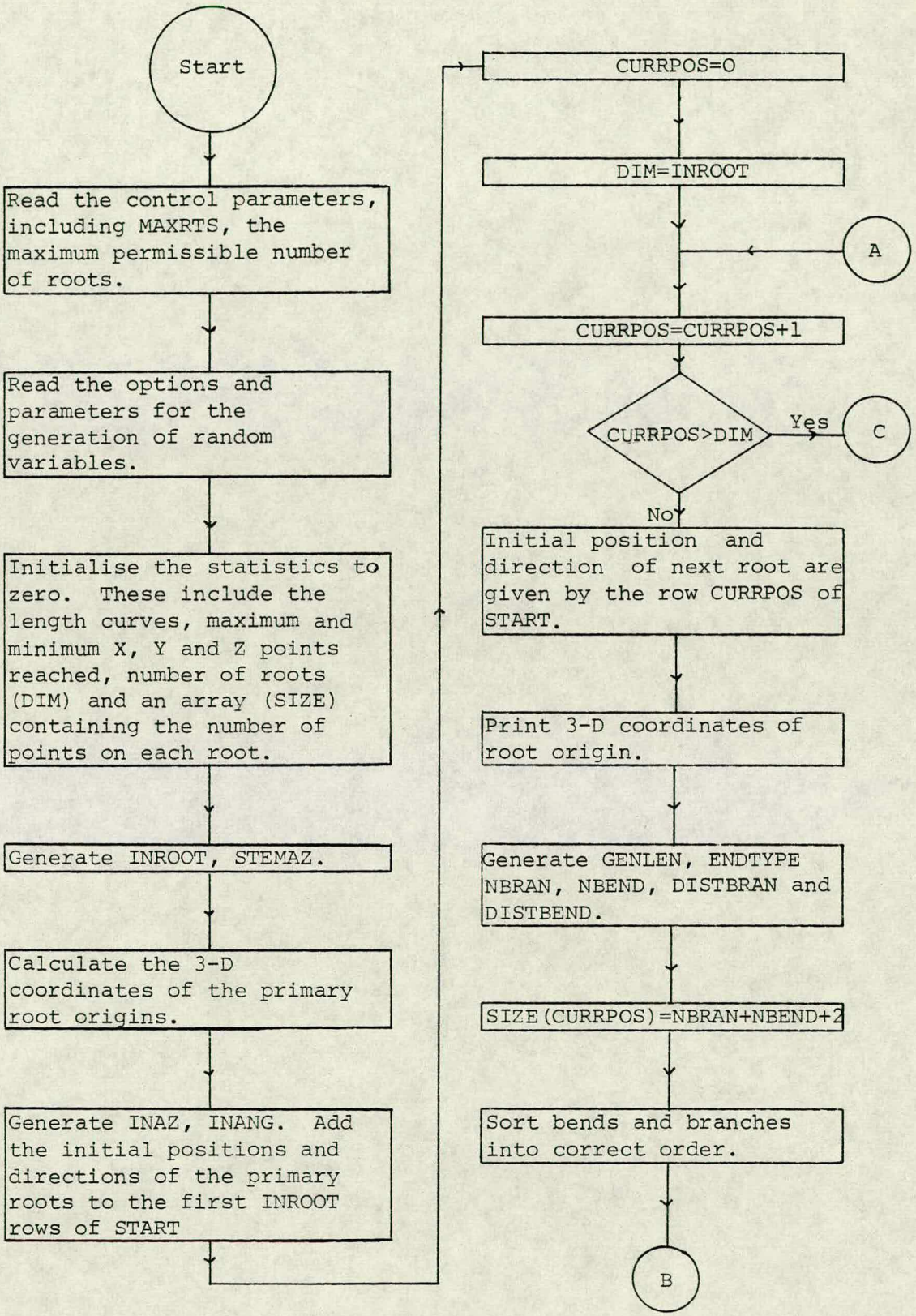


Figure 4.2.1

Flow chart of reconstruction program

(Continued overleaf)

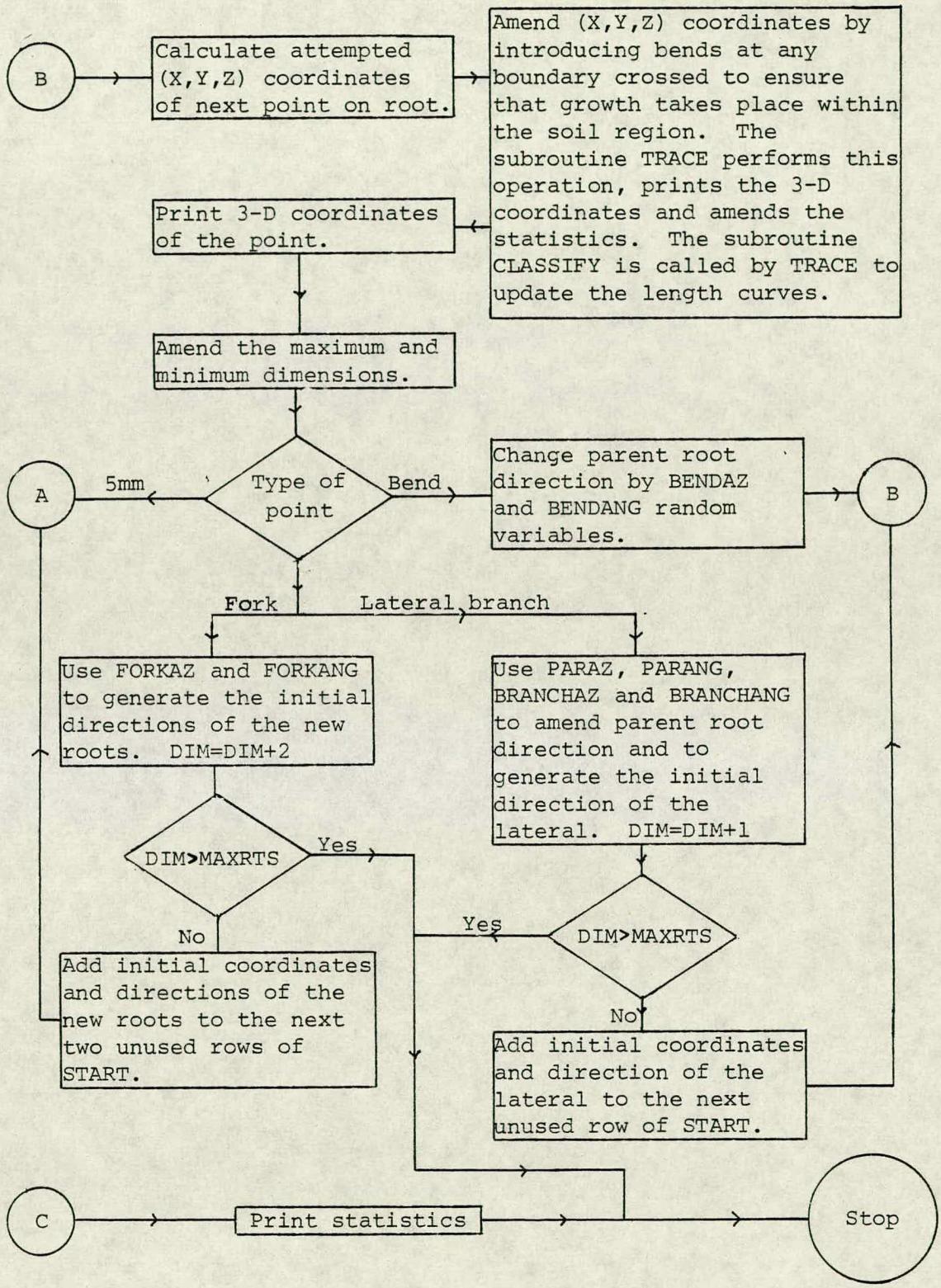


Figure 4.2.1

Flow chart of reconstruction program

(Continued)

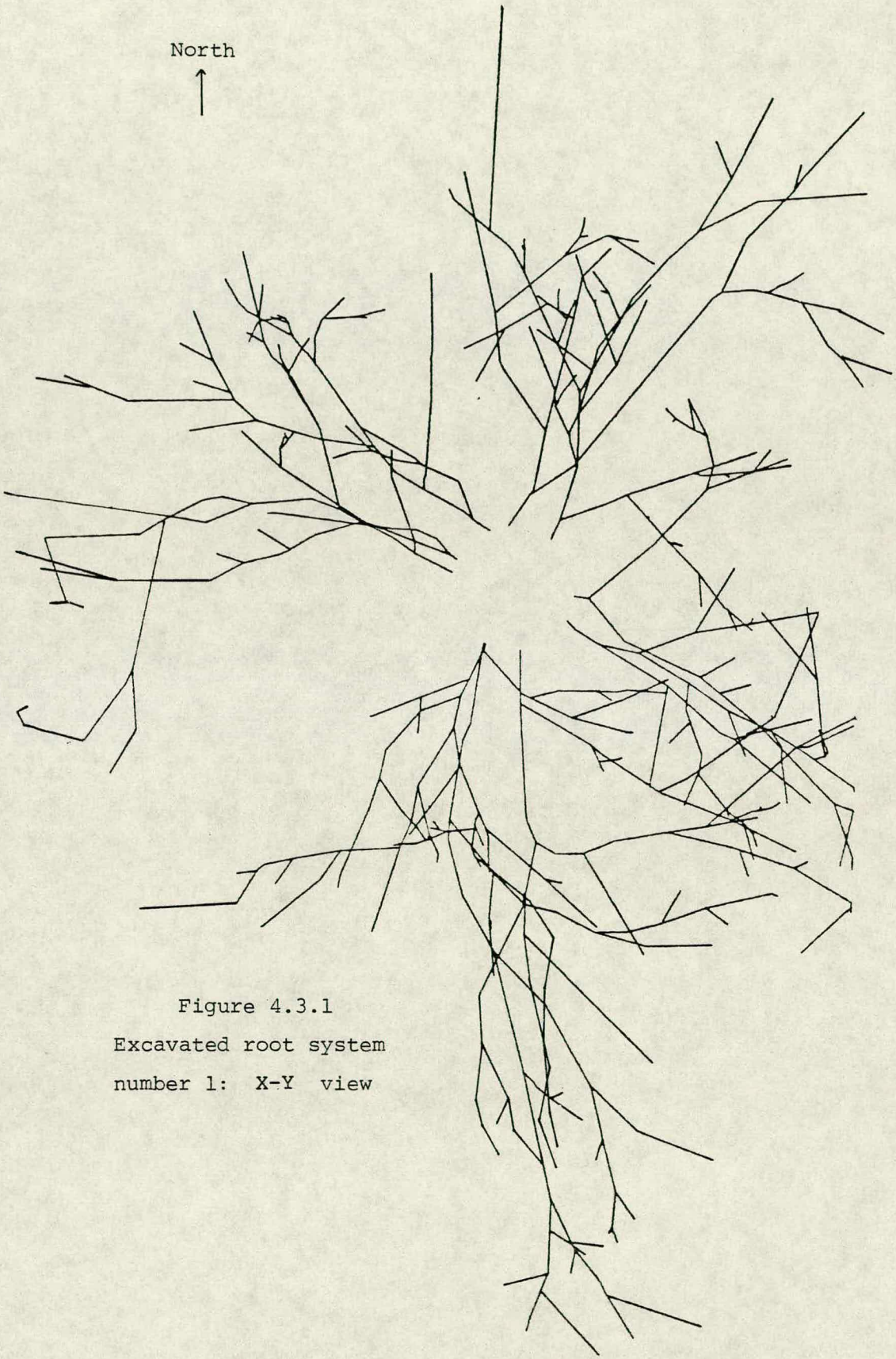


Figure 4.3.1
Excavated root system
number 1: X-Y view

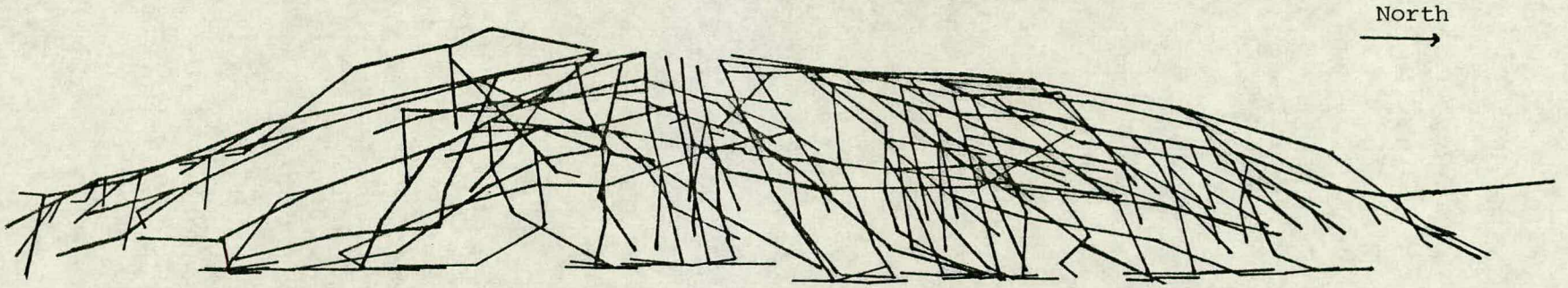


Figure 4.3.2

Excavated root system number 1: X-Z view

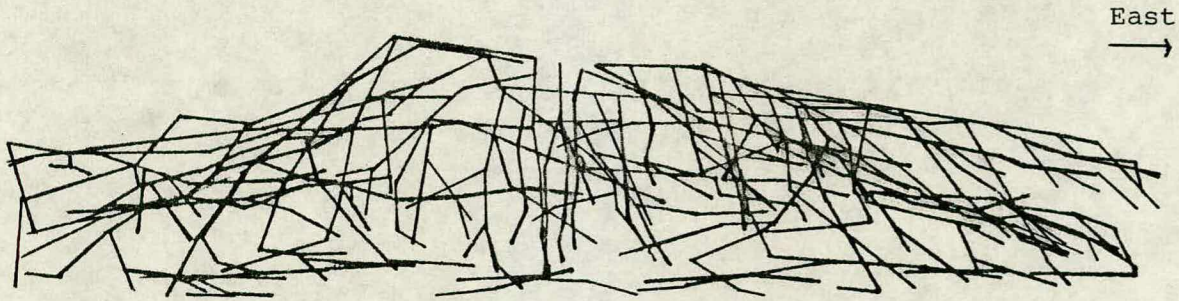


Figure 4.3.3

Excavated root system number 1: Y-Z view

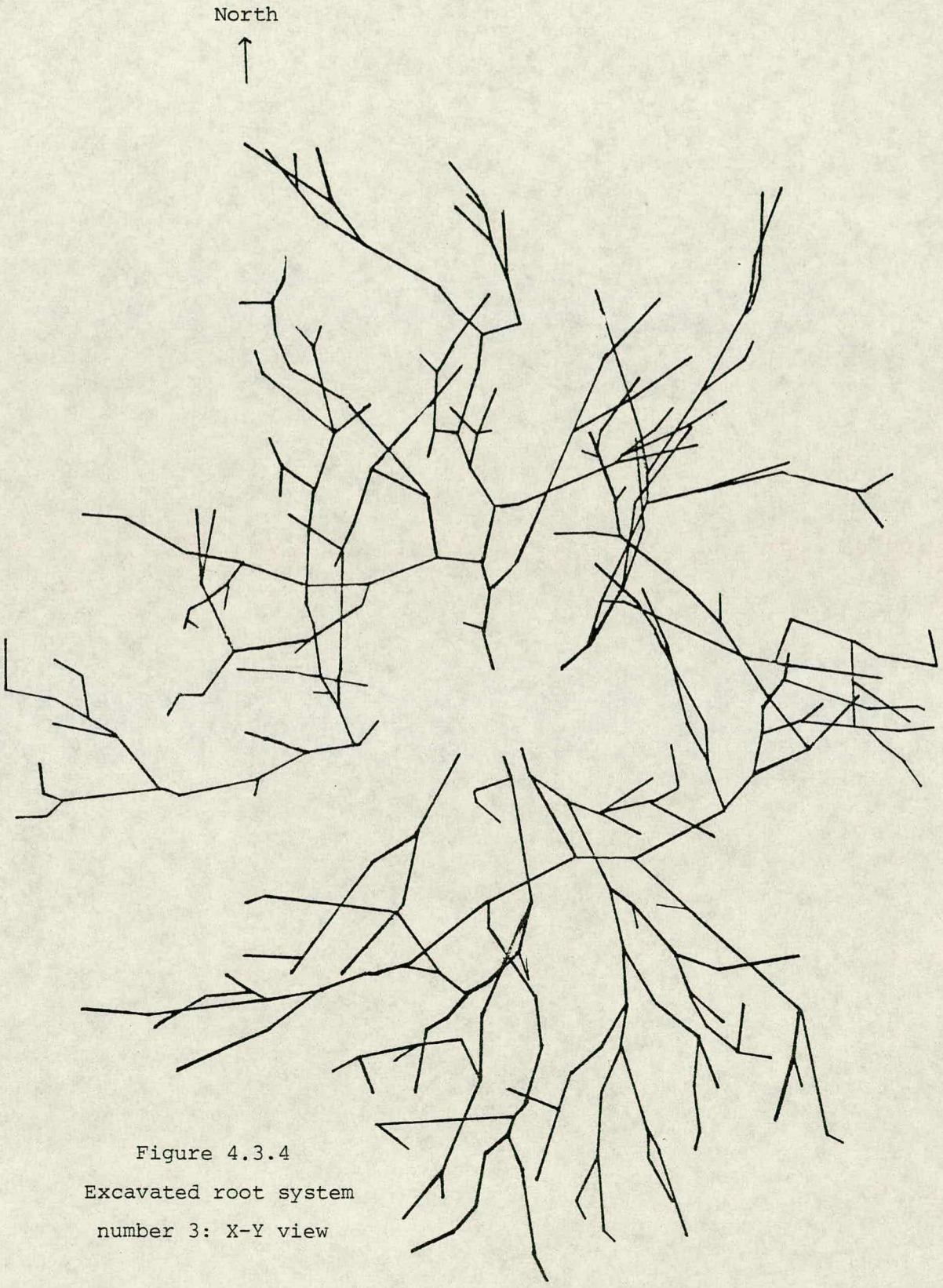


Figure 4.3.4
Excavated root system
number 3: X-Y view

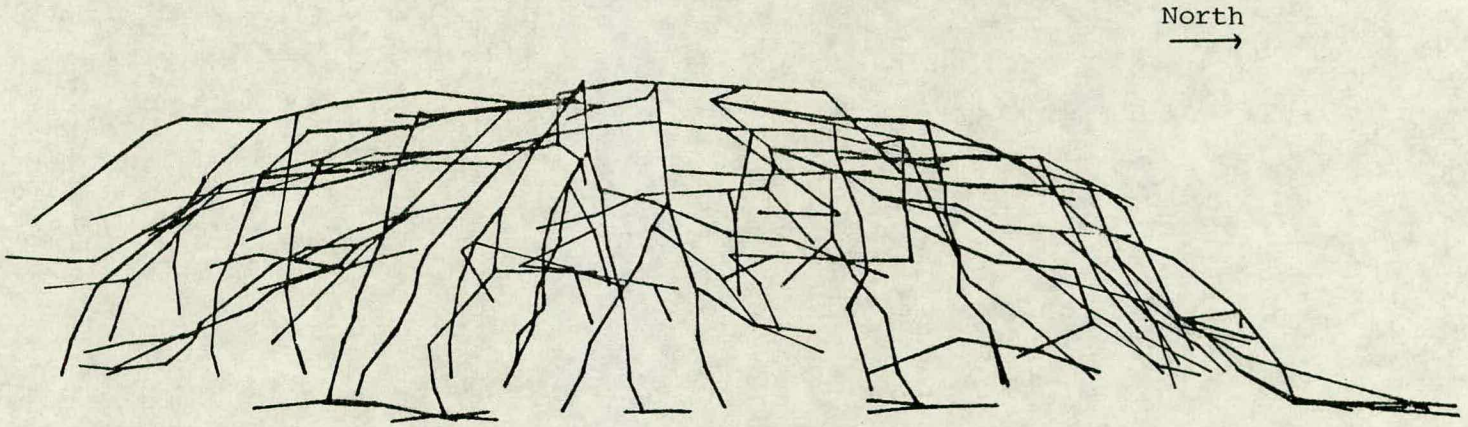


Figure 4.3.5

Excavated root system number 3: X-Z view

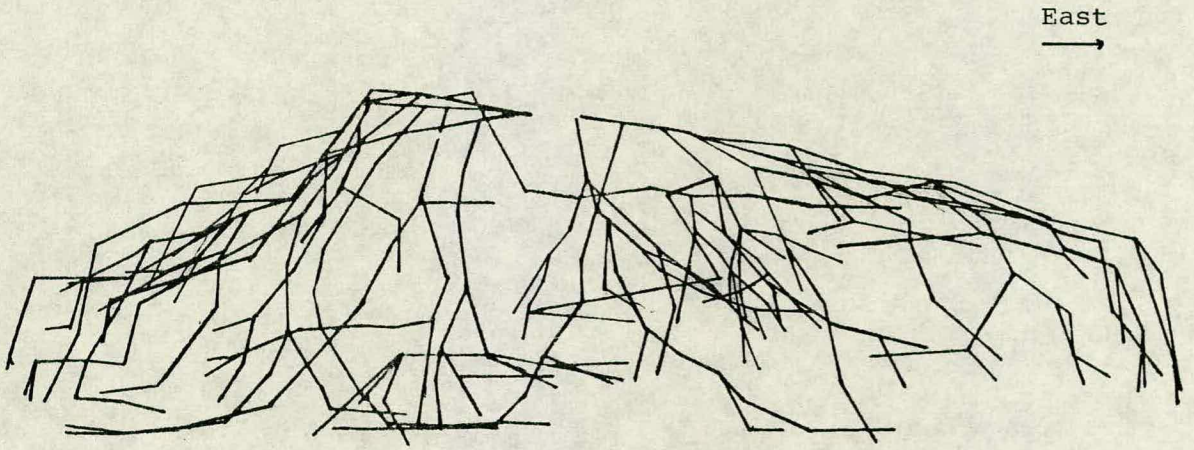


Figure 4.3.6

Excavated root system number 3: Y-Z view

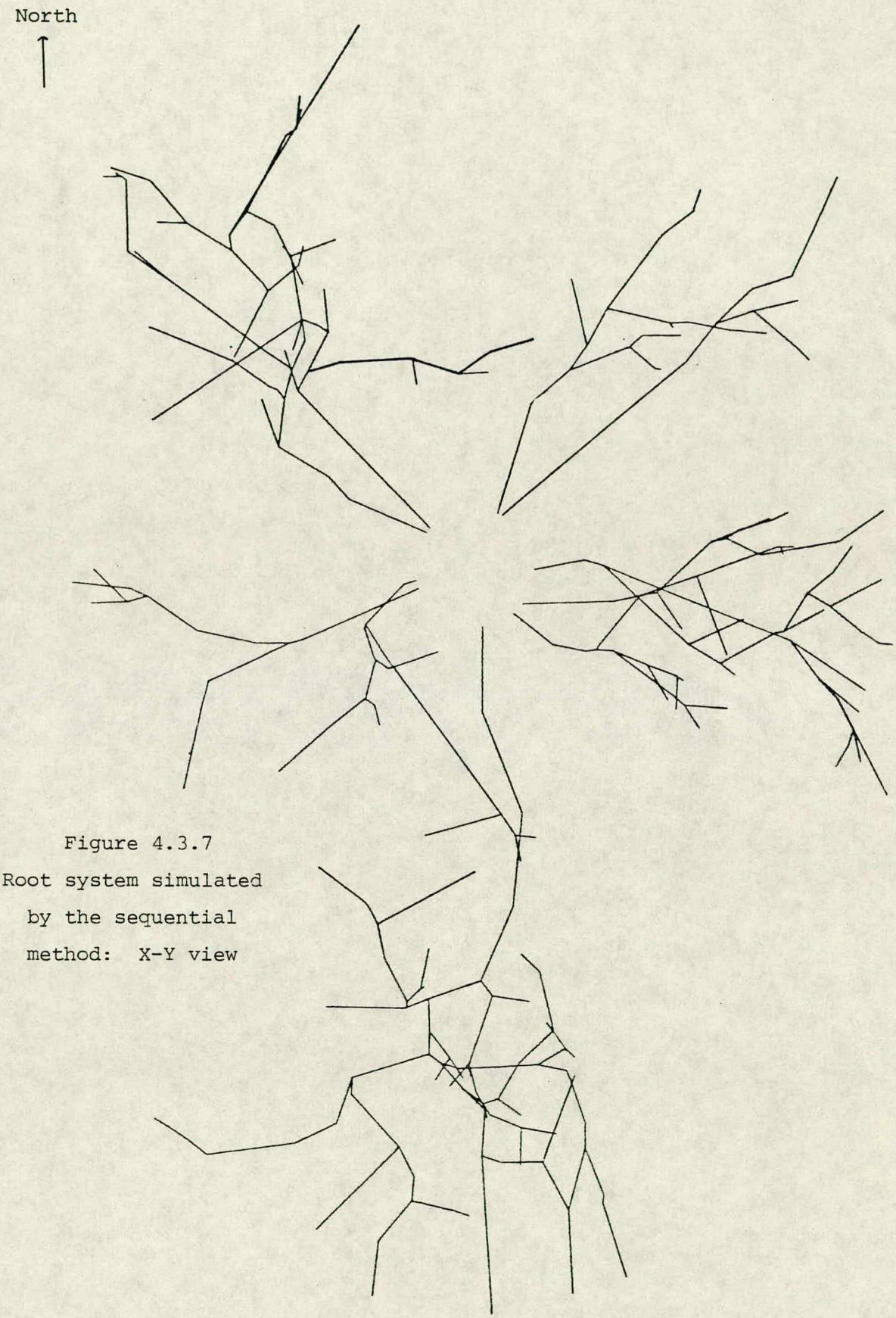


Figure 4.3.7
Root system simulated
by the sequential
method: X-Y view

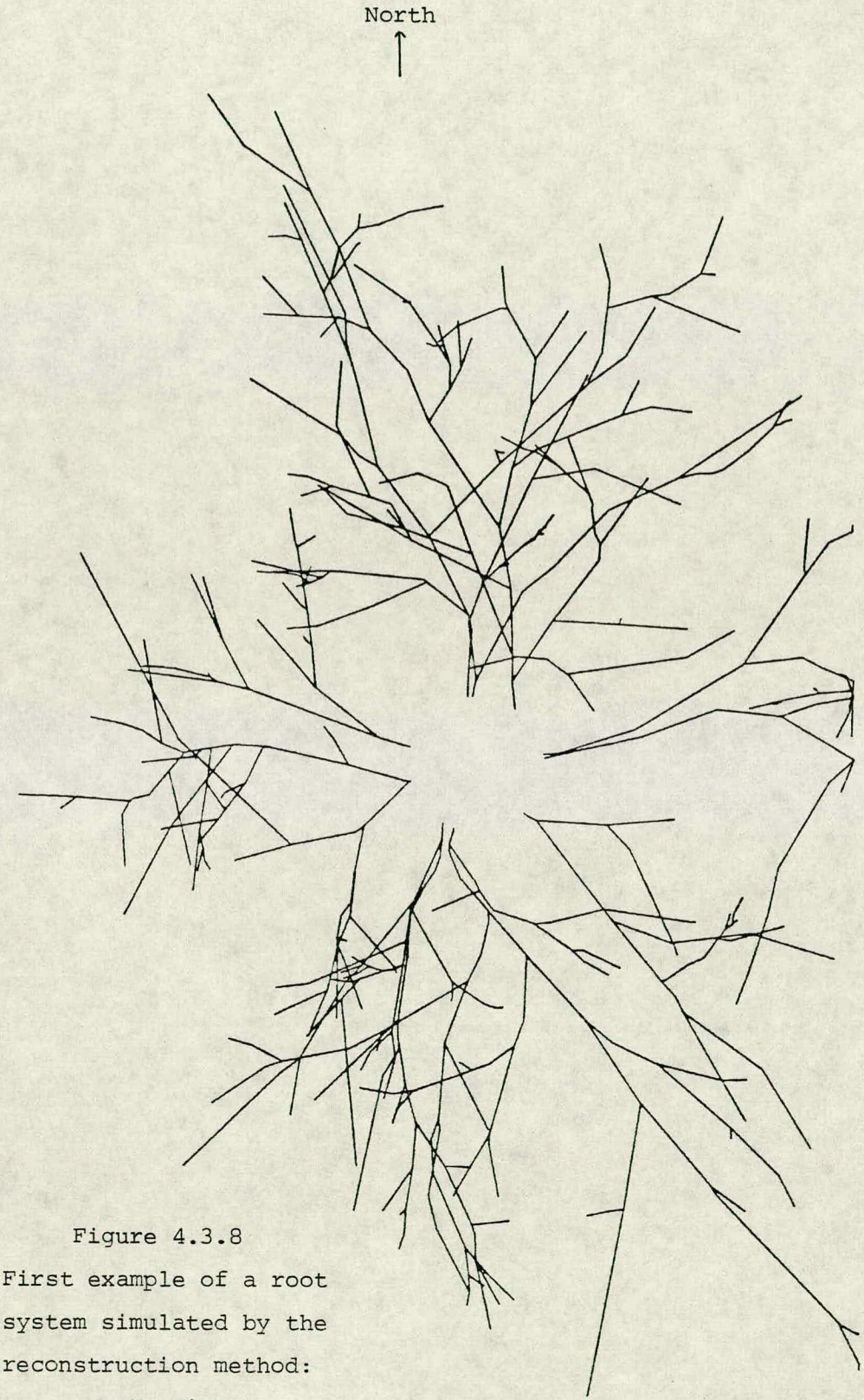


Figure 4.3.8
First example of a root system simulated by the reconstruction method:
X-Y view

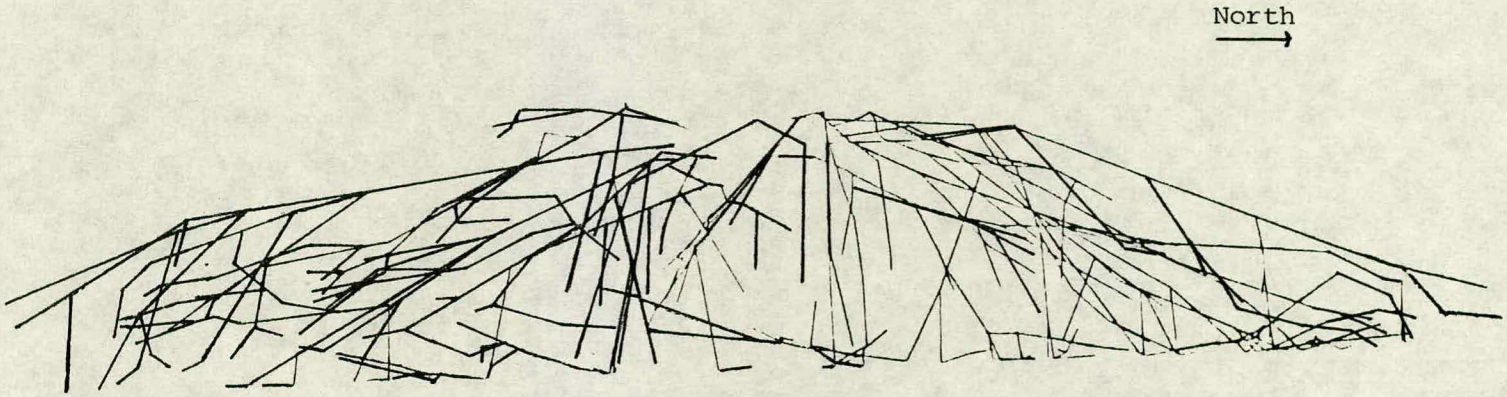


Figure 4.3.9

First example of a root system simulated by the reconstruction method: X-Z view

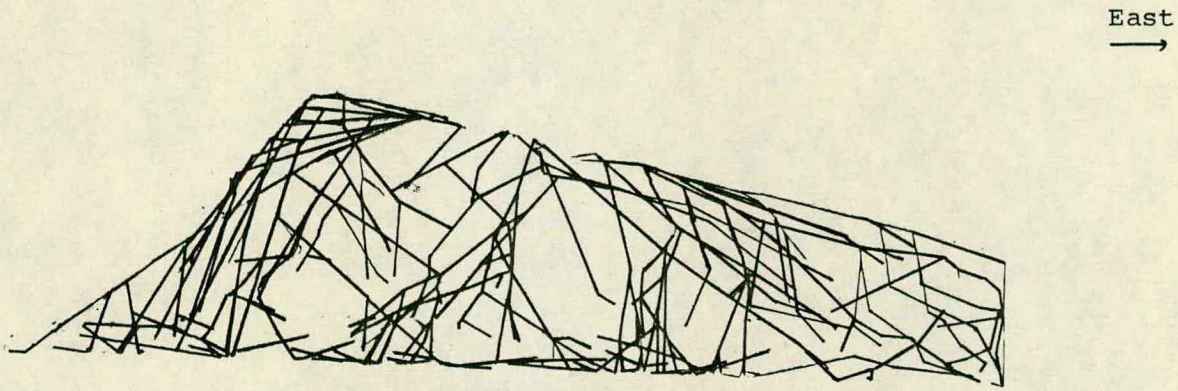


Figure 4.3.10

First example of a root system simulated by the reconstruction method: Y-Z view

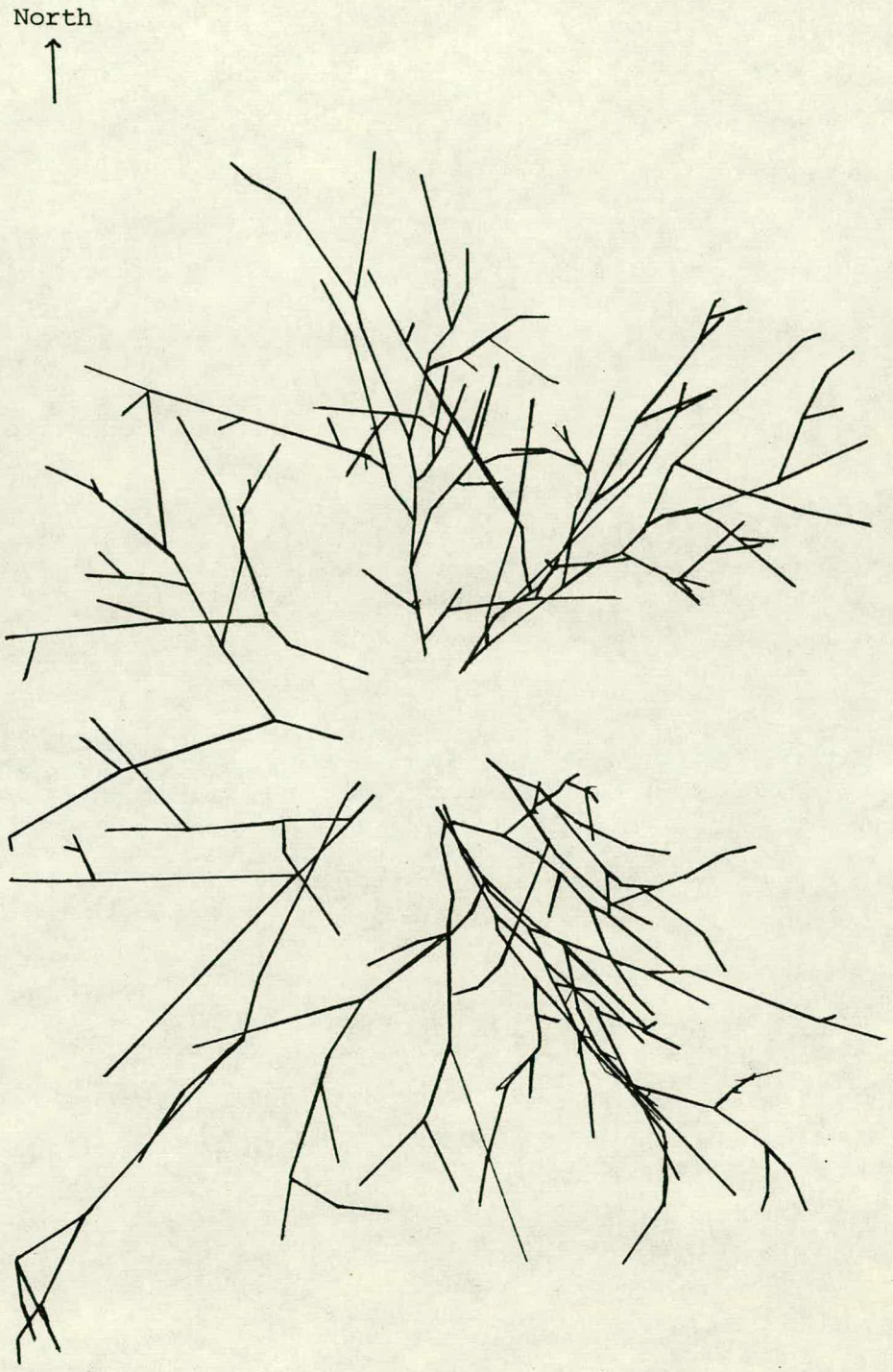


Figure 4.3.11

Second example of a root system simulated by the reconstruction method: X-Y view

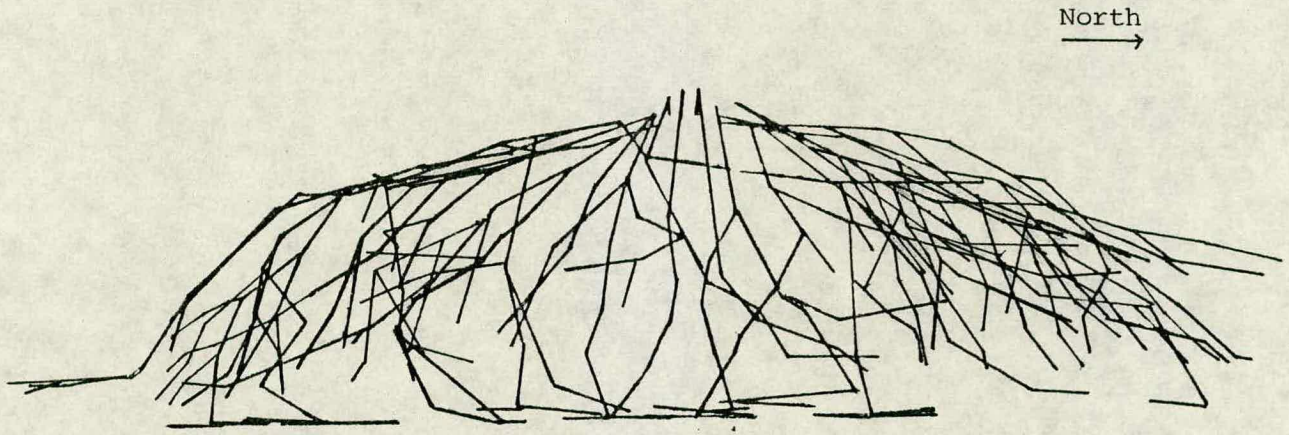


Figure 4.3.12

Second example of a root system simulated by the reconstruction method: X-Z view

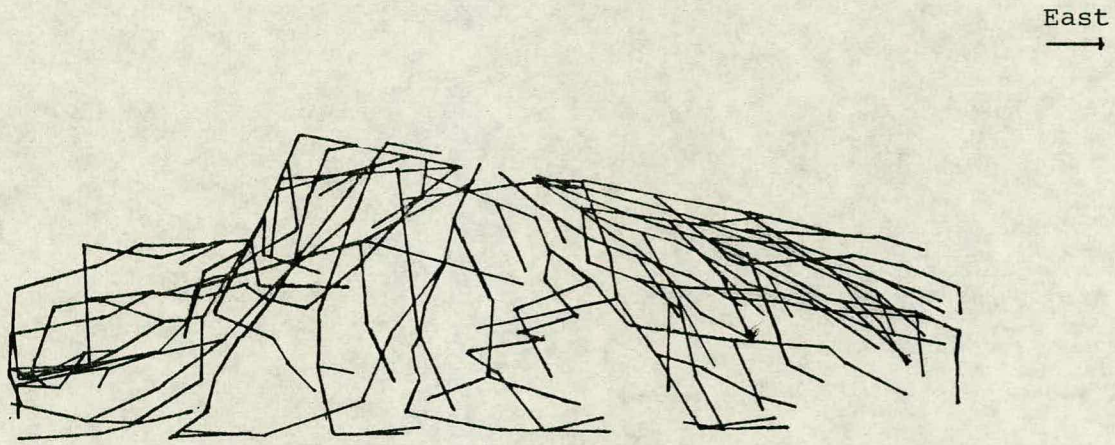


Figure 4.3.13

Second example of a root system simulated by the reconstruction method: Y-Z view

North

Estimated STEMAZ variance = 0.07 $(\text{radians})^2$

Value used in simulation = 0.30 $(\text{radians})^2$

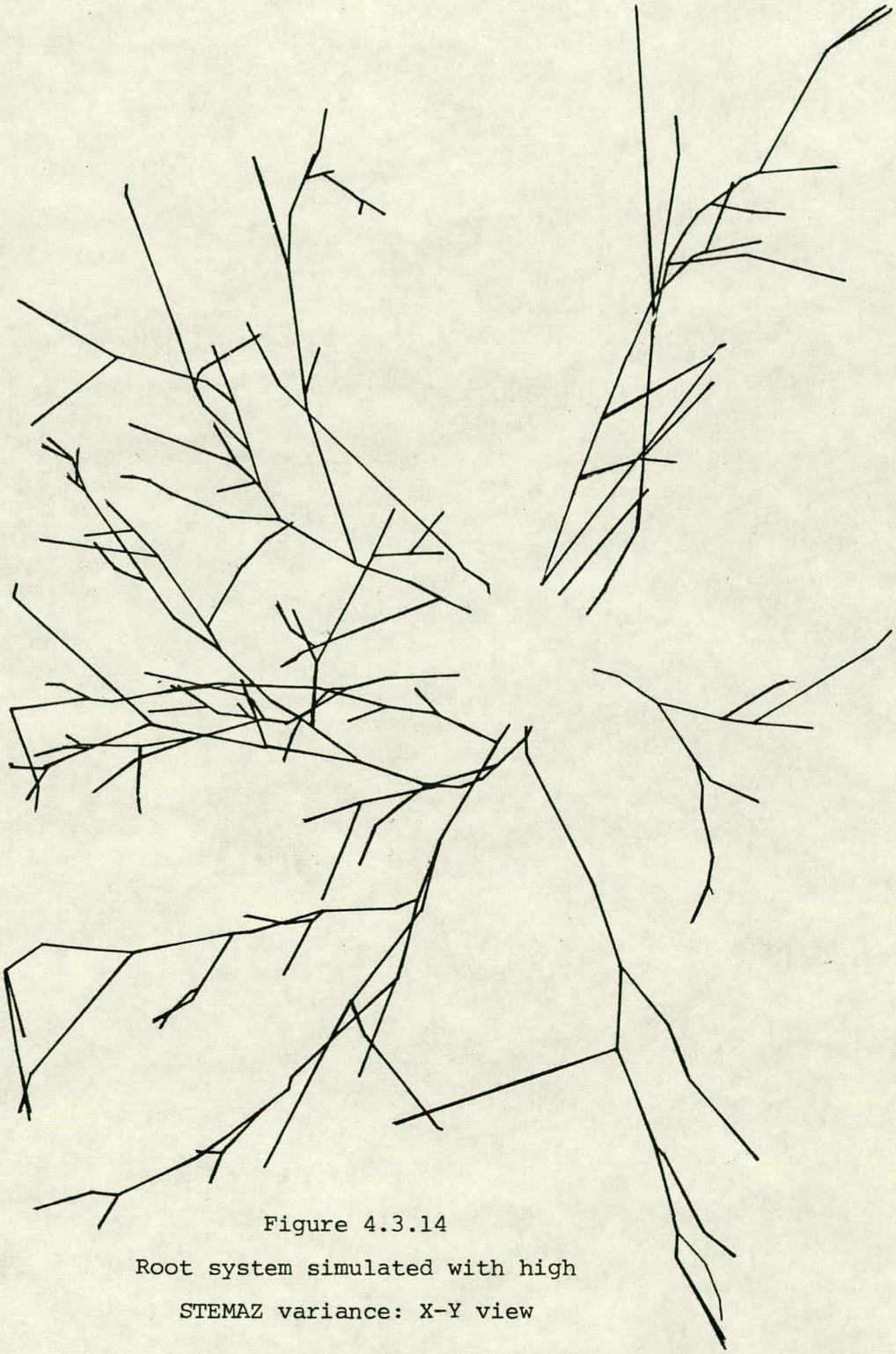


Figure 4.3.14

Root system simulated with high STEMAZ variance: X-Y view

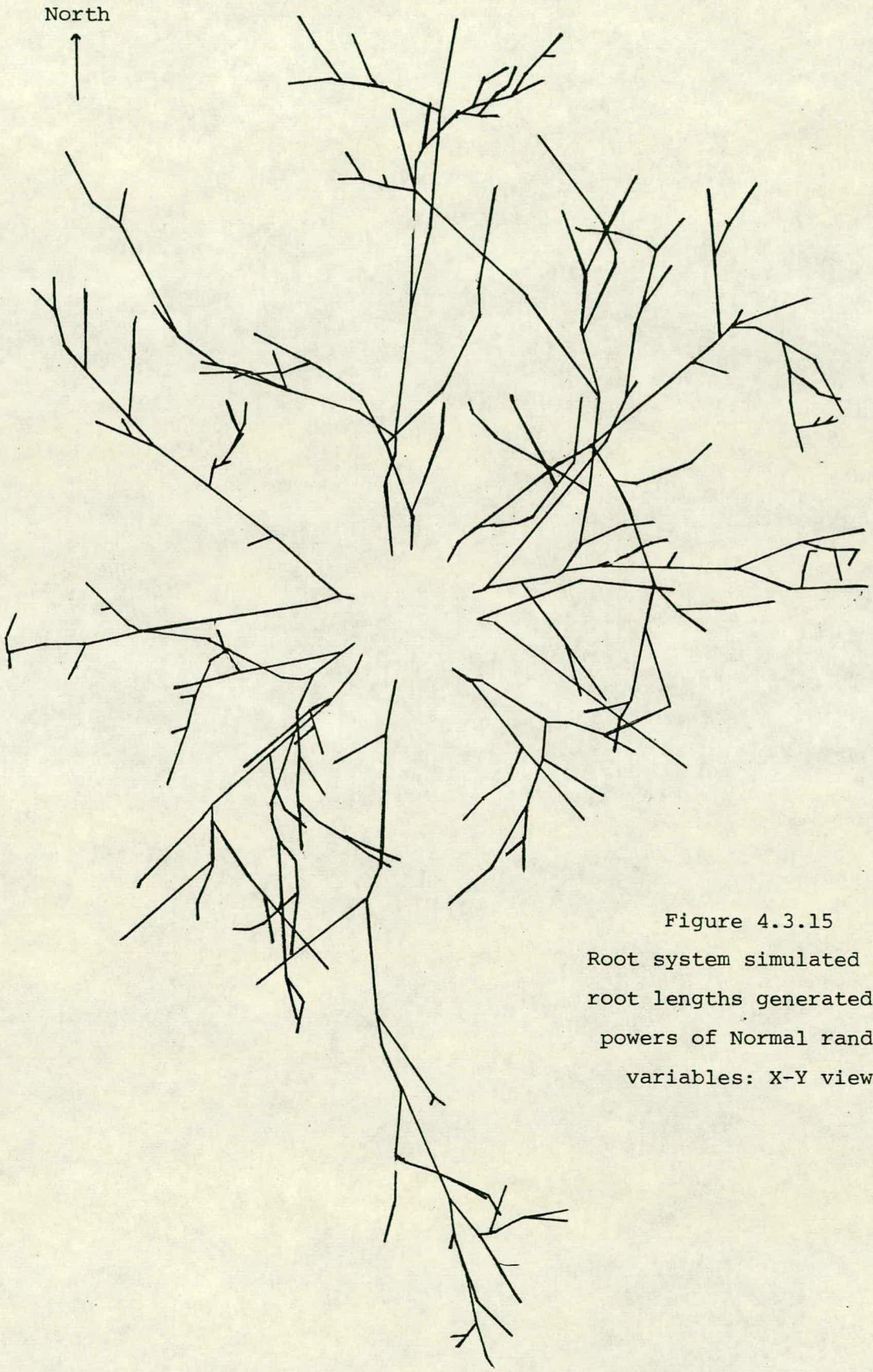


Figure 4.3.15
Root system simulated with root lengths generated as powers of Normal random variables: X-Y view

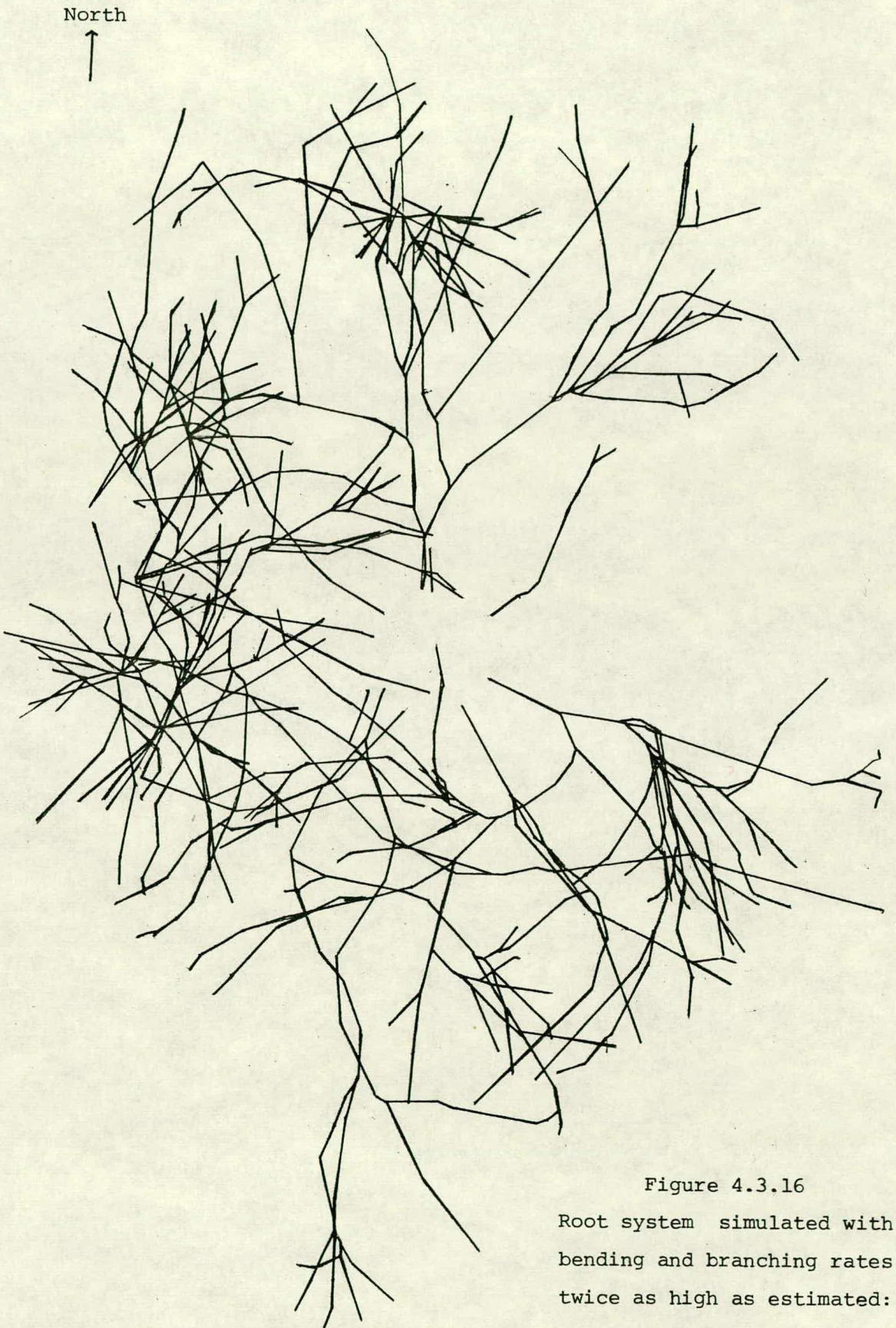


Figure 4.3.16
Root system simulated with bending and branching rates twice as high as estimated: X-Y view

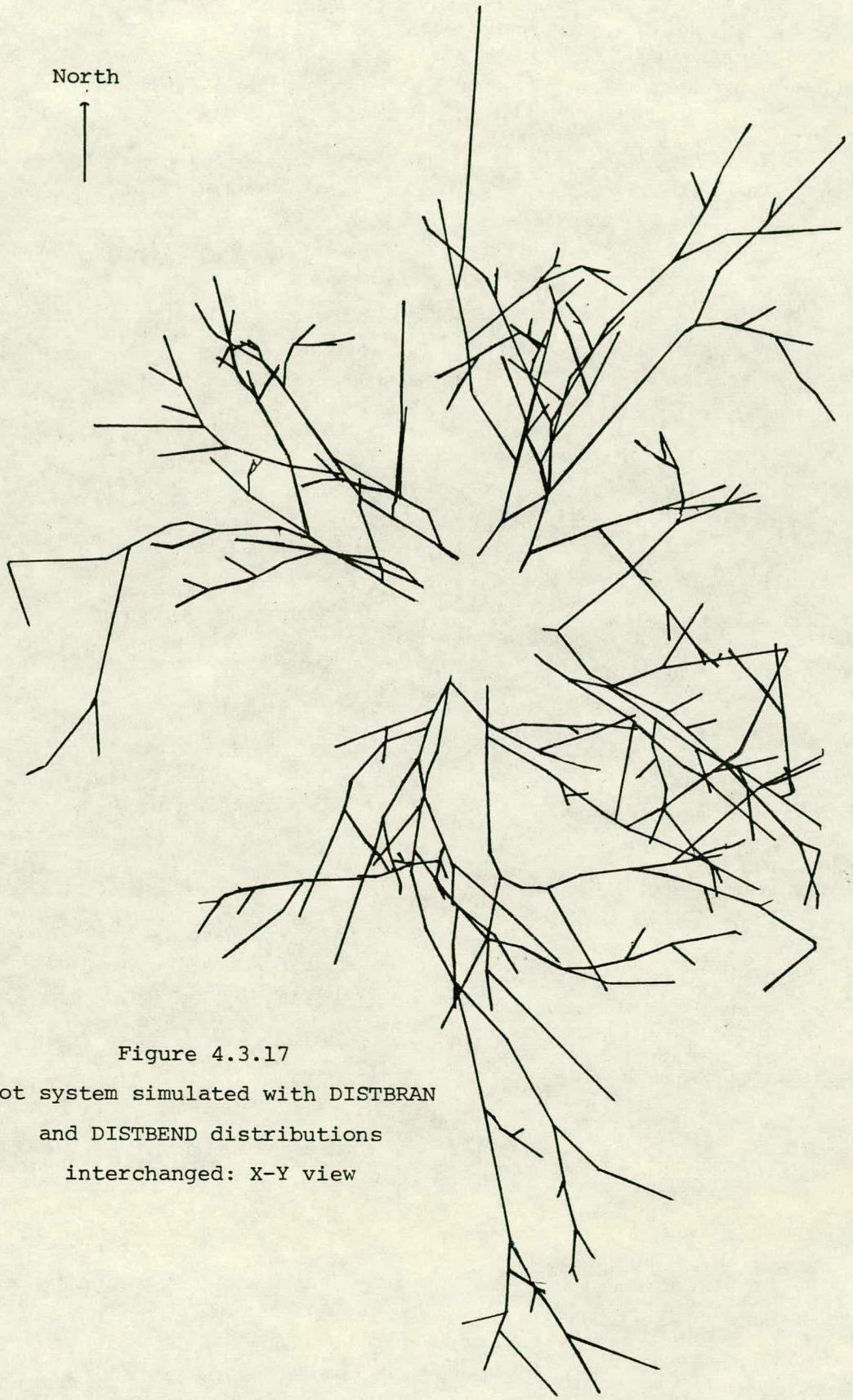


Figure 4.3.17
Root system simulated with DISTBRAN
and DISTBEND distributions
interchanged: X-Y view

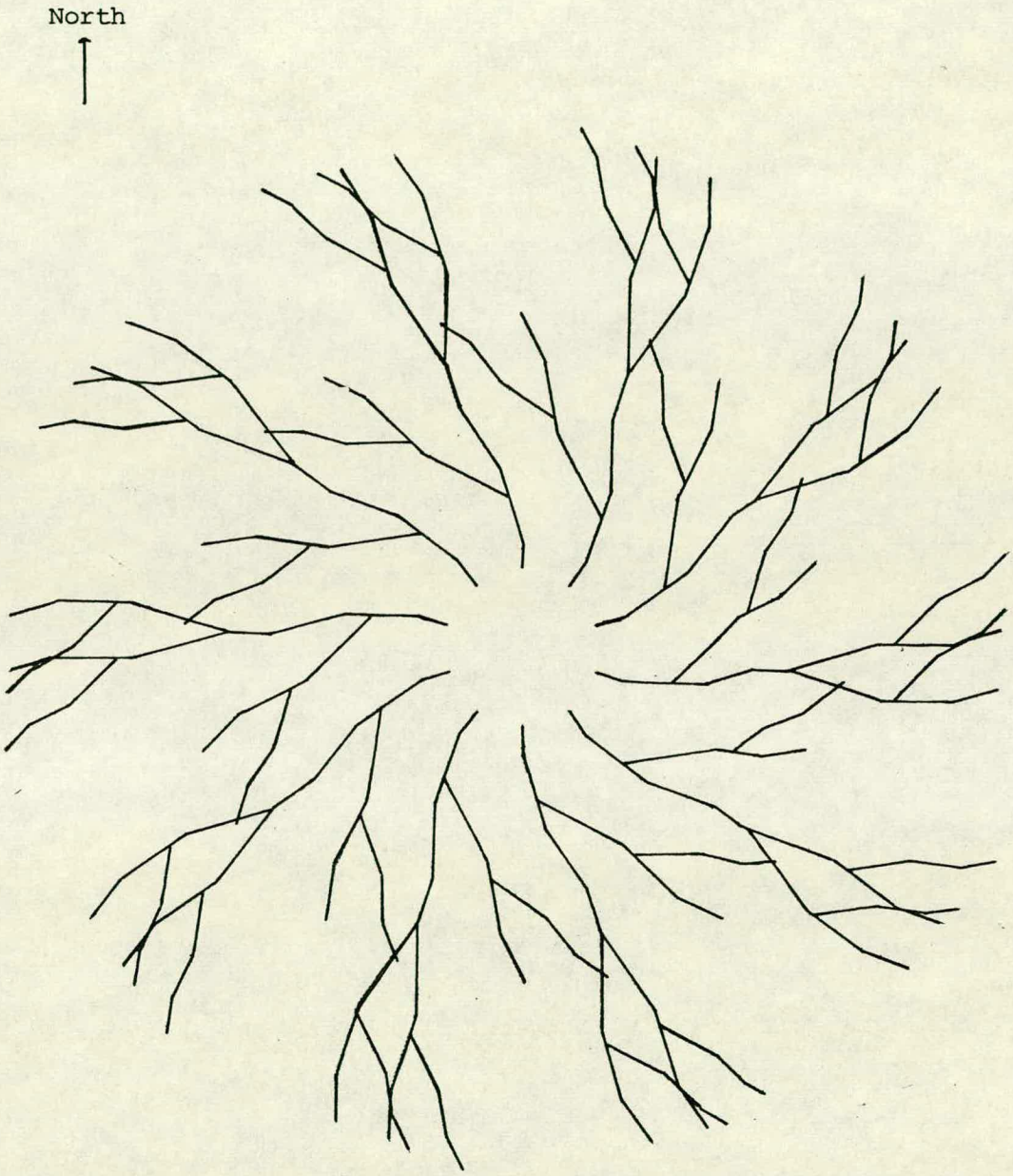


Figure 4.3.18

Root system simulated with all variances zero: X-Y view

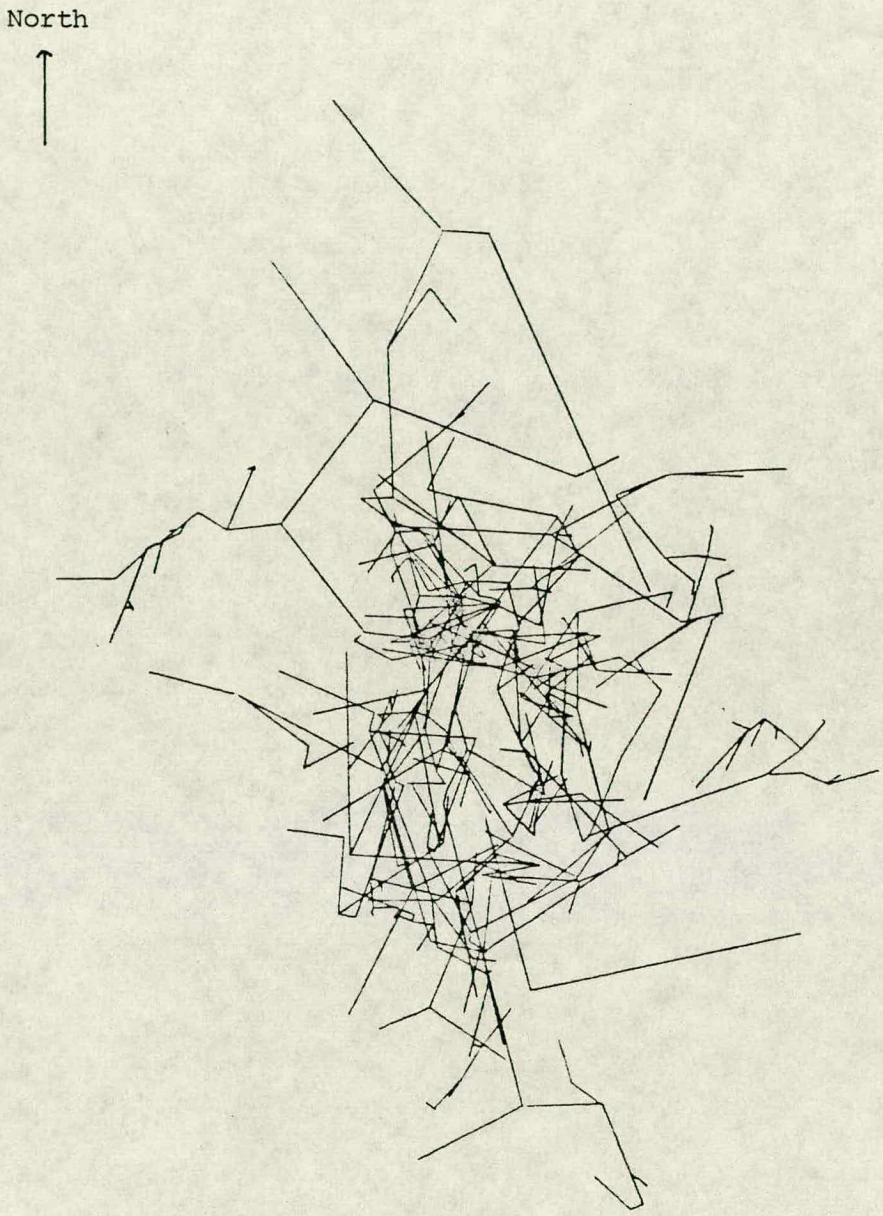


Figure 4.3.19

Root system simulated with all azimuth variances twice as high as estimated: X-Y view

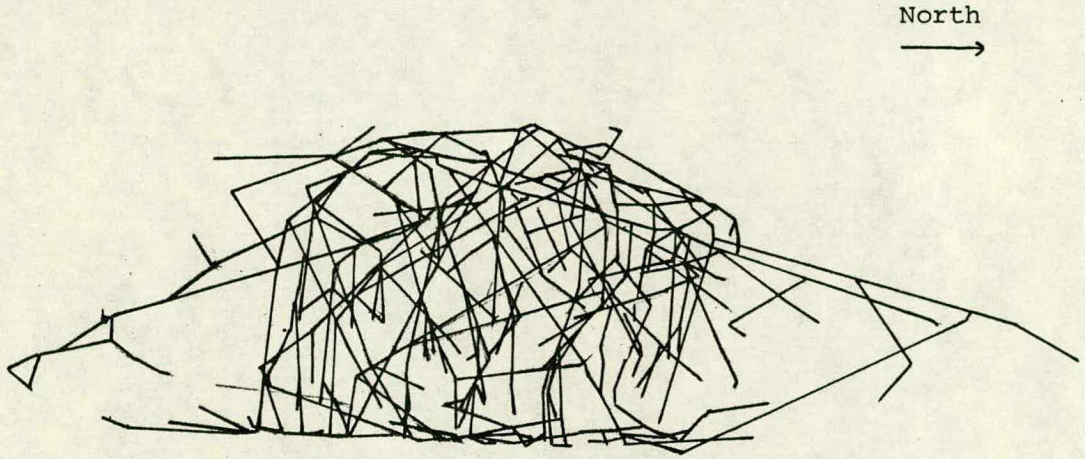


Figure 4.3.20

Root system simulated with all angle variances twice as high as estimated: X-Z view

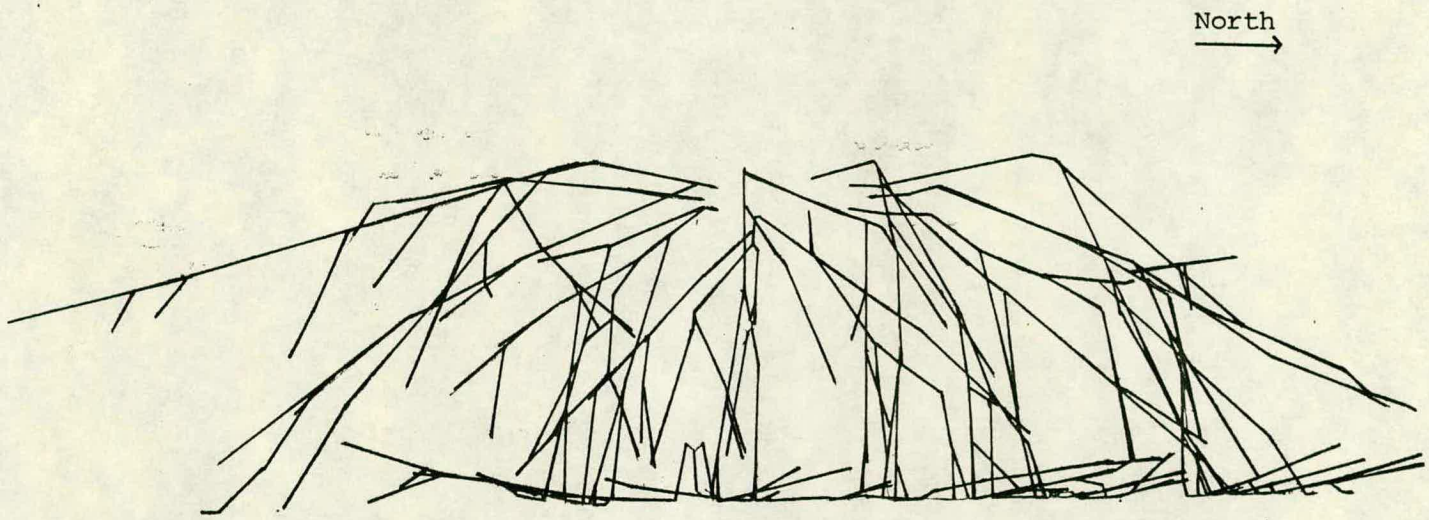


Figure 4.3.21

Root system simulated with all angle variances half the estimated values: X-Z view

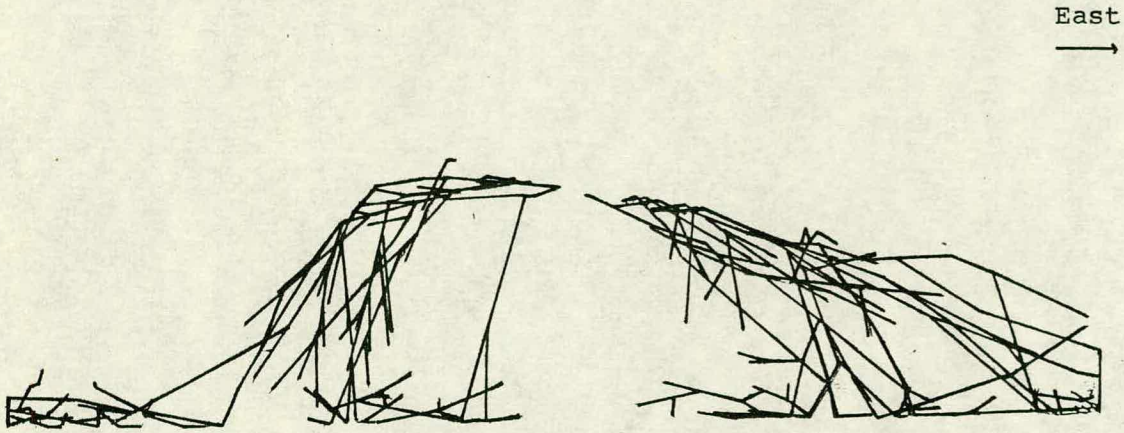


Figure 4.3.22

Root system simulated with branch directions having the same properties as fork directions: X-Y view

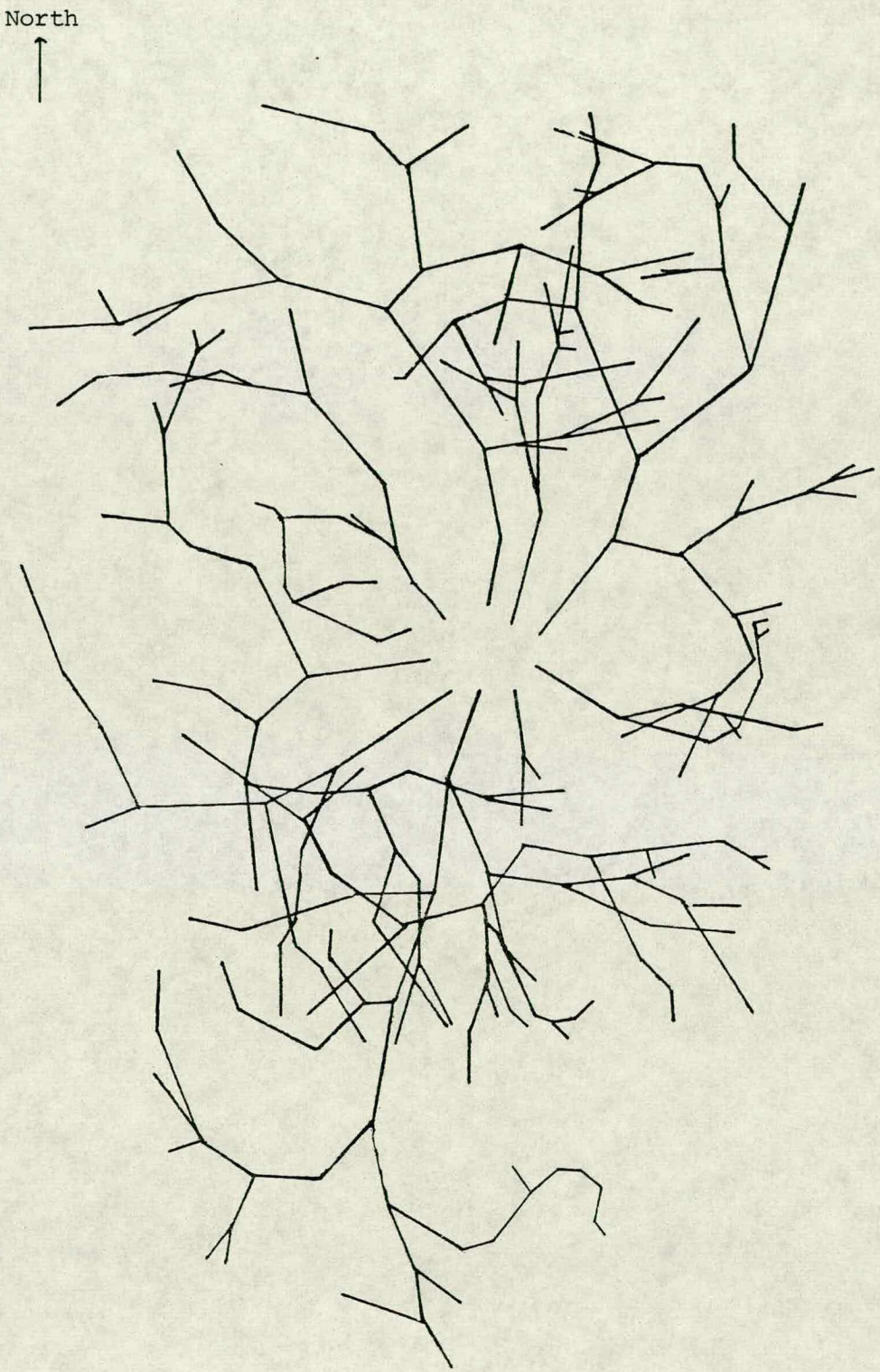


Figure 4.3.23

Root system simulated with independent azimuth changes: X-Y view

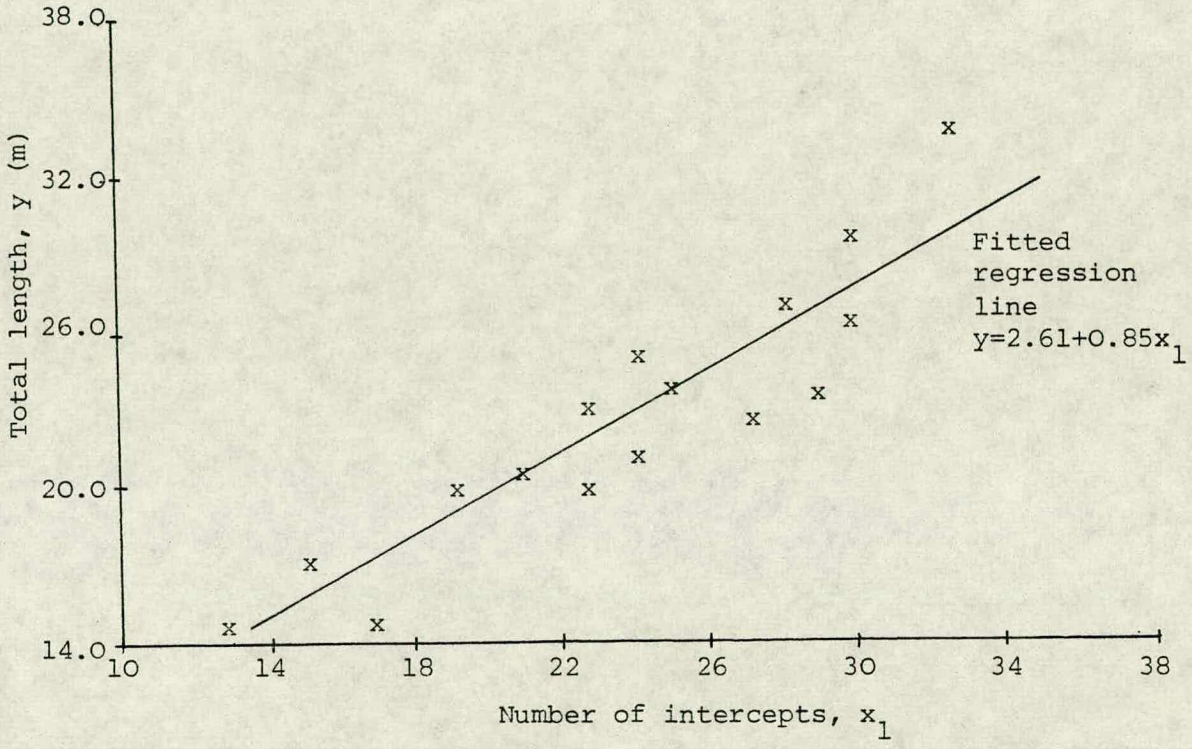


Figure 4.3.24

Total root length against number of intercepts with a vertical trench wall for 16 simulated root systems

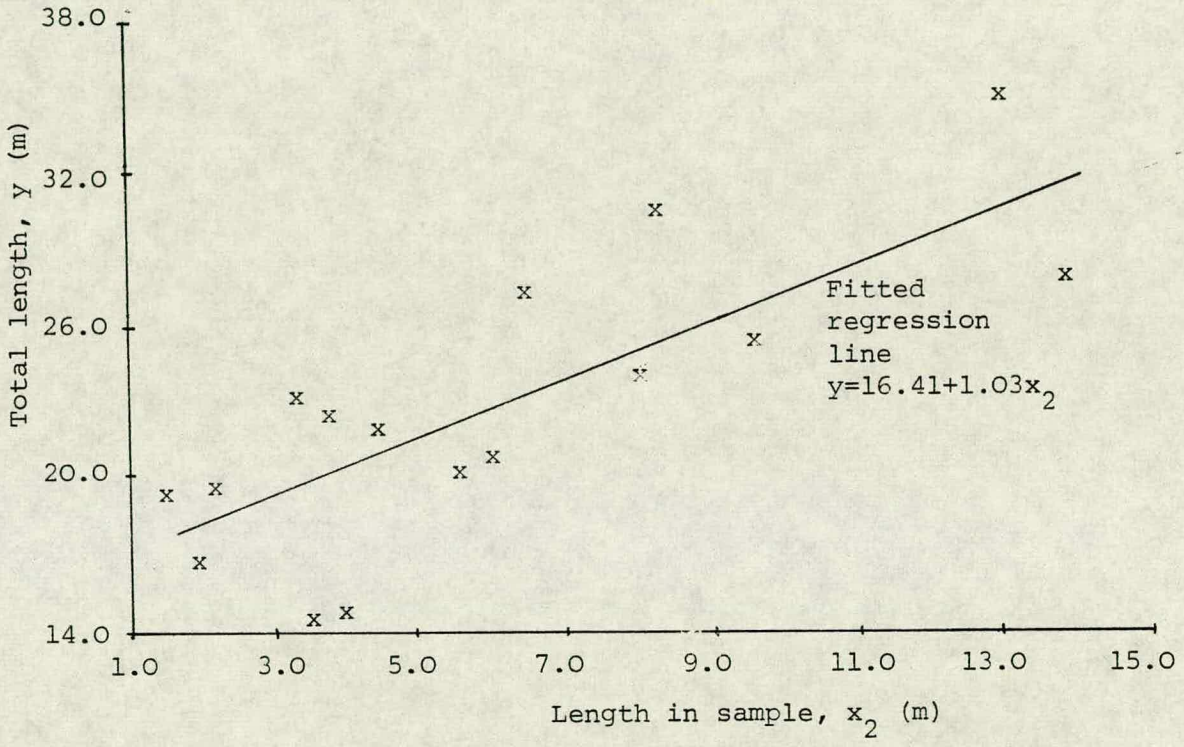


Figure 4.3.25

Total root length against length in a 90° segment for 16 simulated root systems

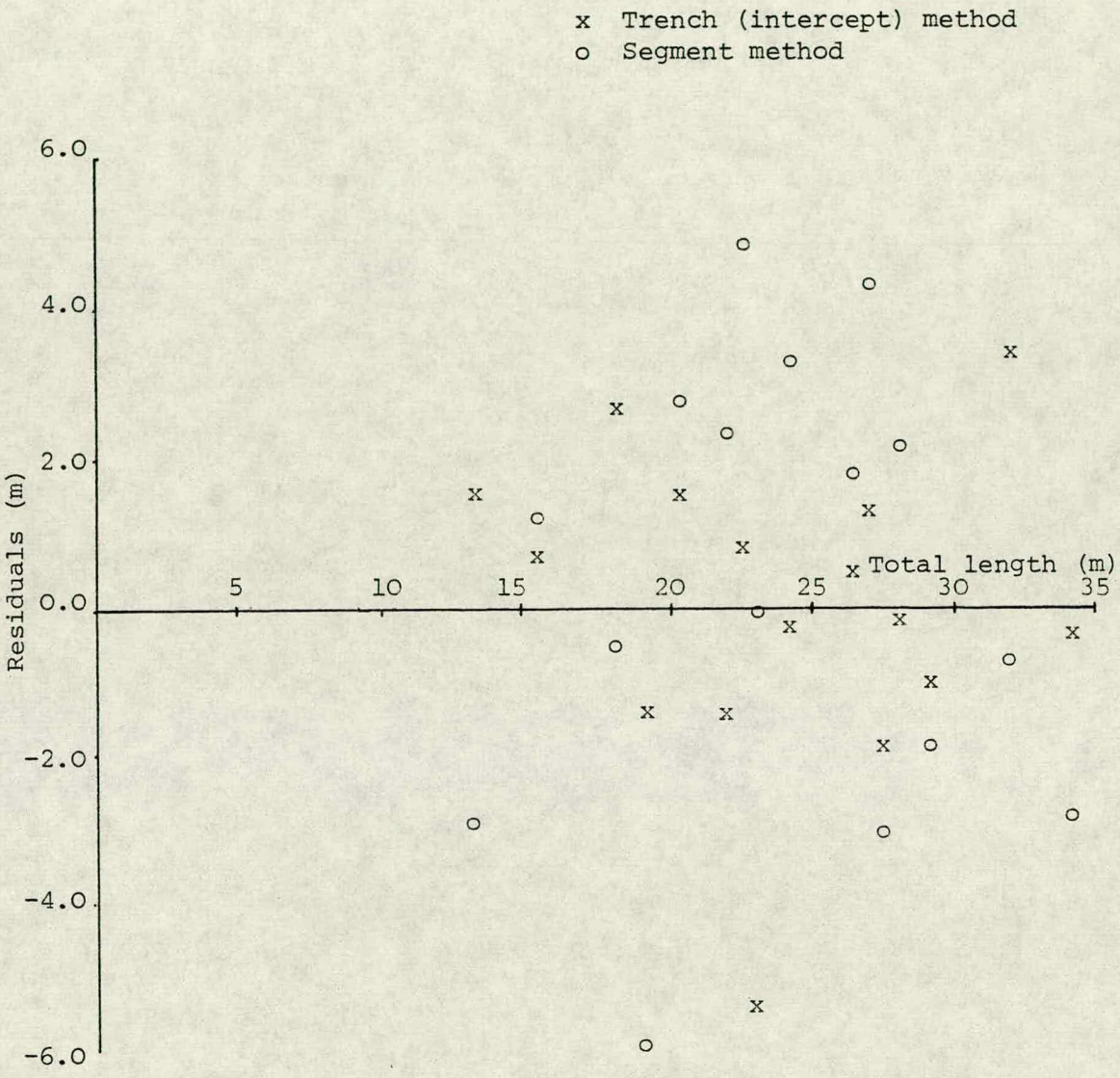


Figure 4.3.26

Residuals between actual and estimated total root lengths of 16 simulated root systems

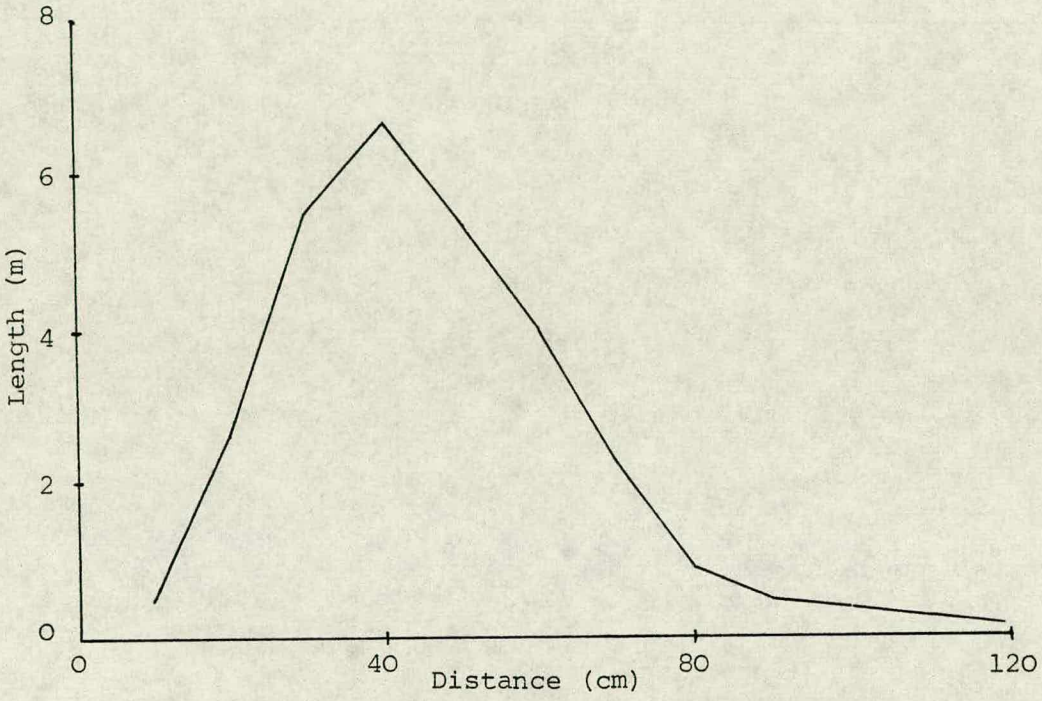


Figure 4.4.1

Length of root against radial distance: mean of 50 simulations

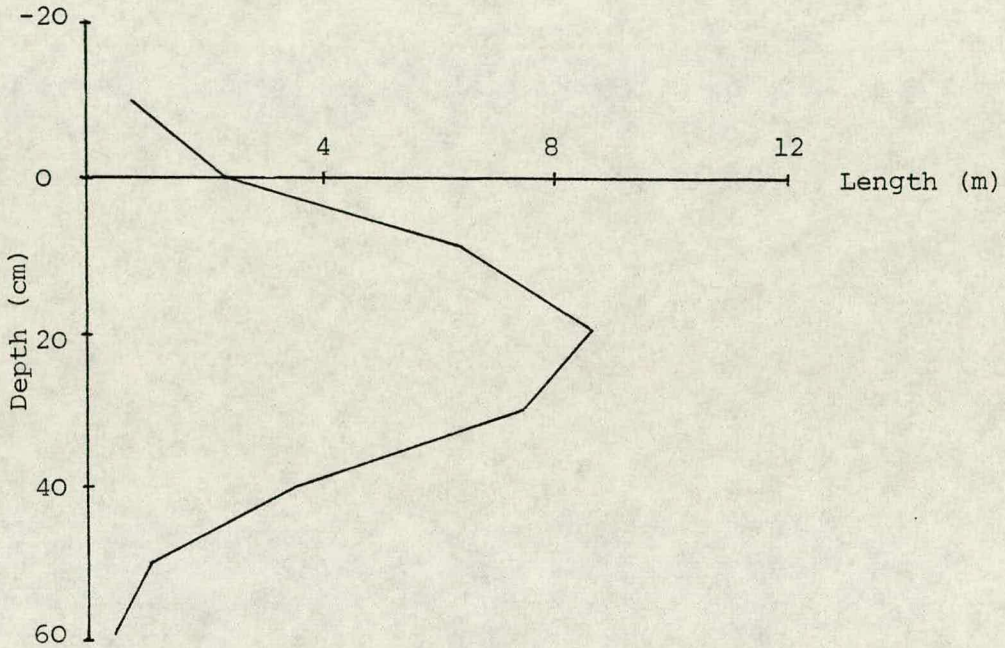


Figure 4.4.2

Length of root against depth: mean of 50 simulations

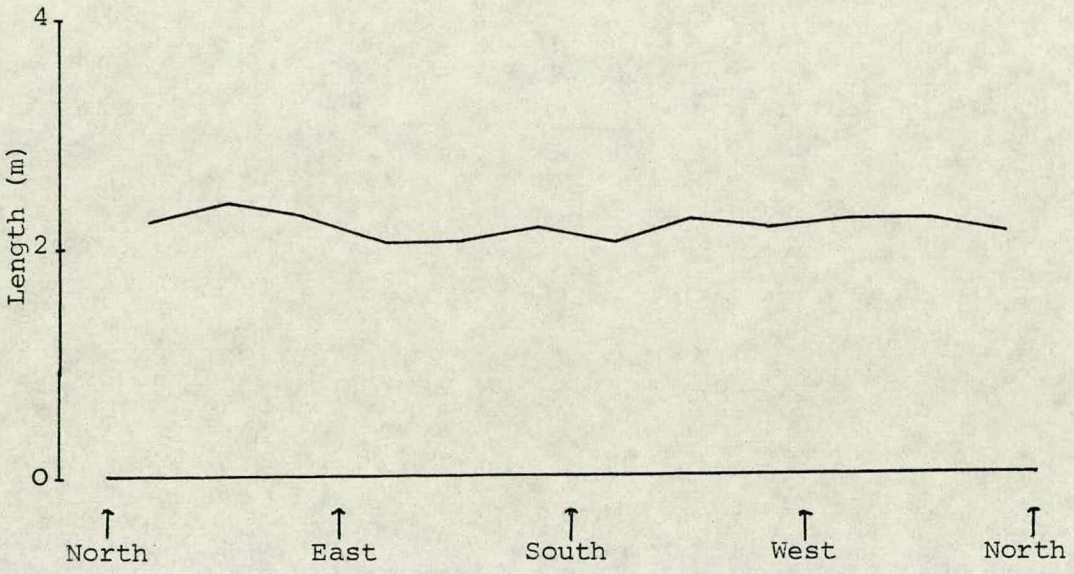
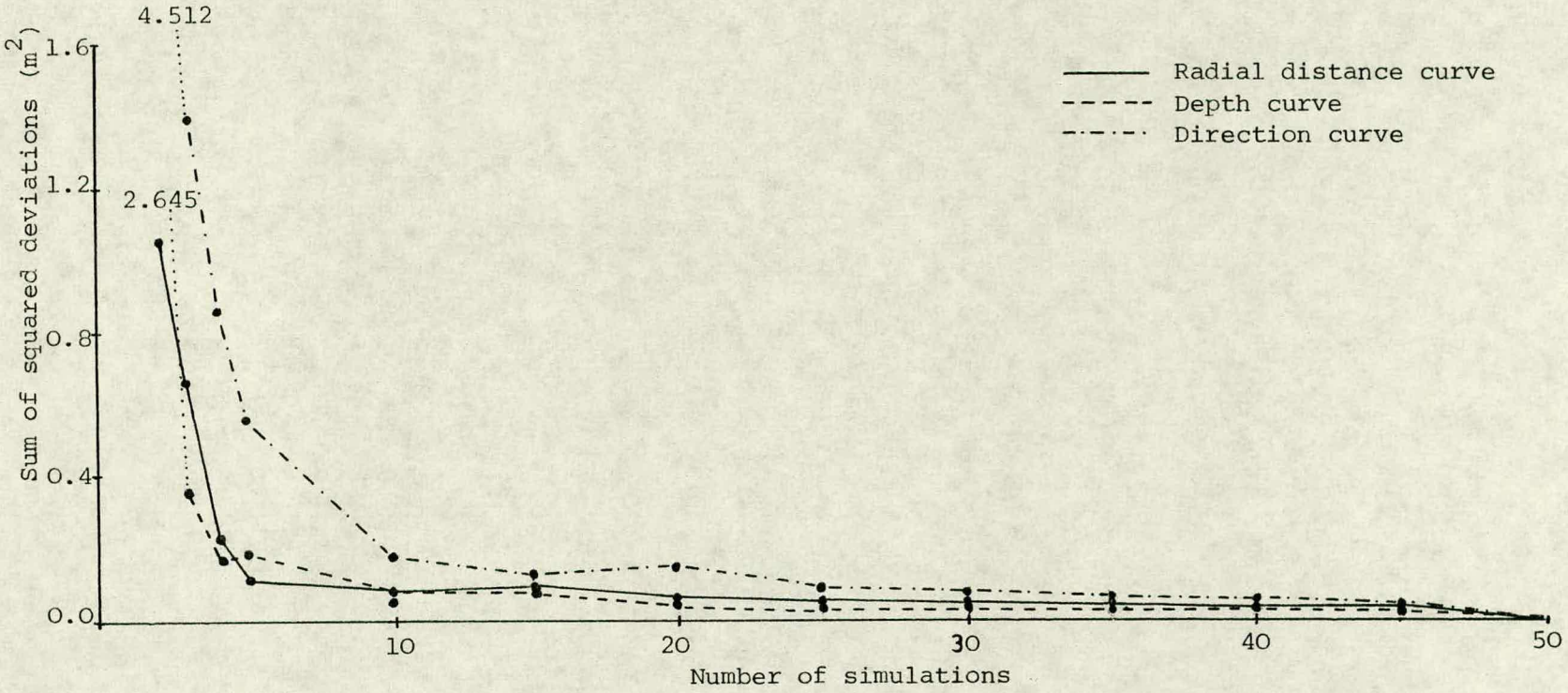


Figure 4.4.3

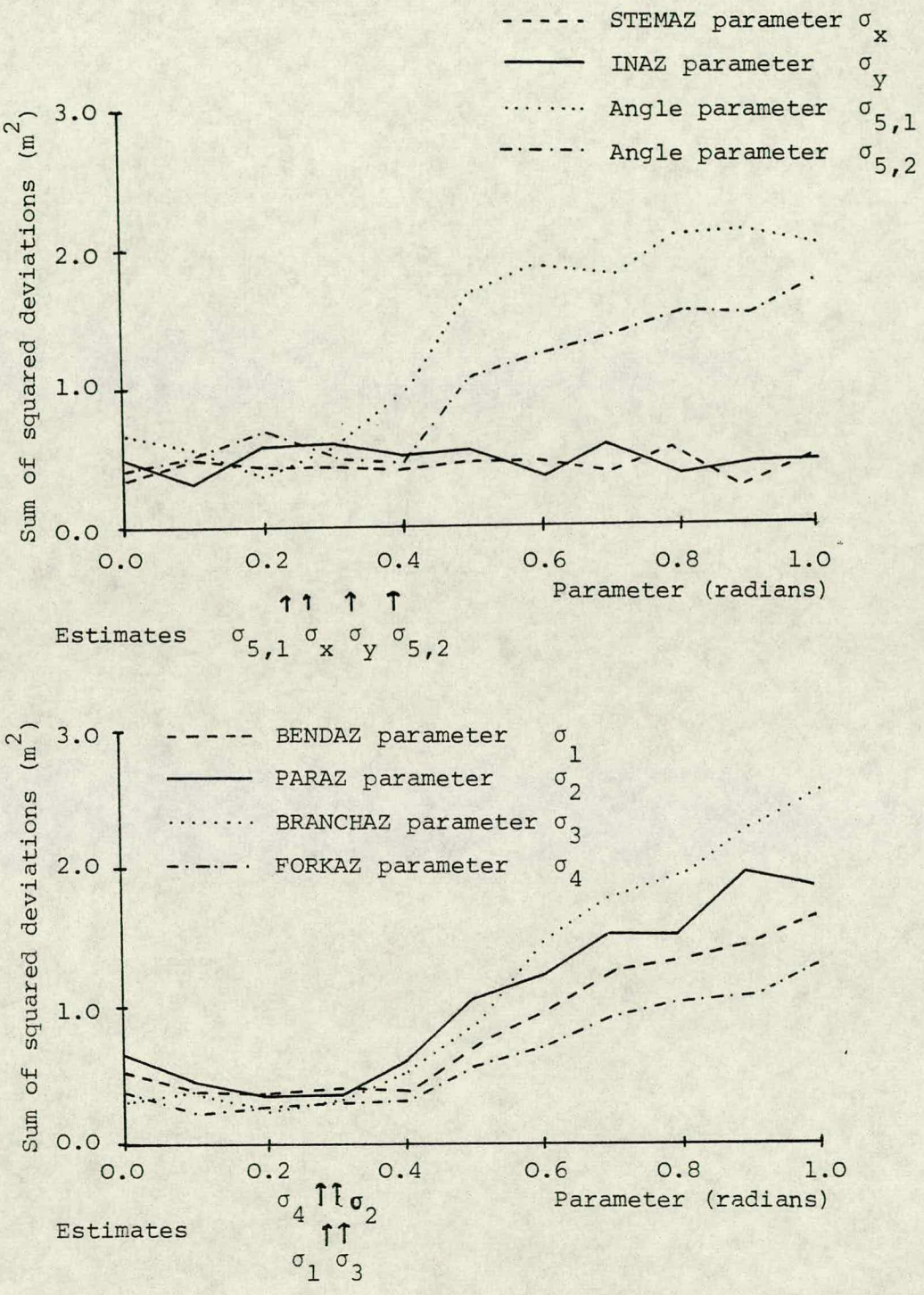
Length of root against direction: mean of 50 simulations



Values plotted are the sums of squared deviations between the true length curves and the corresponding mean length curves of r simulations for r = 2, 3, 4, 5, 10, 15,..., 45, 50.

Figure 4.4.4

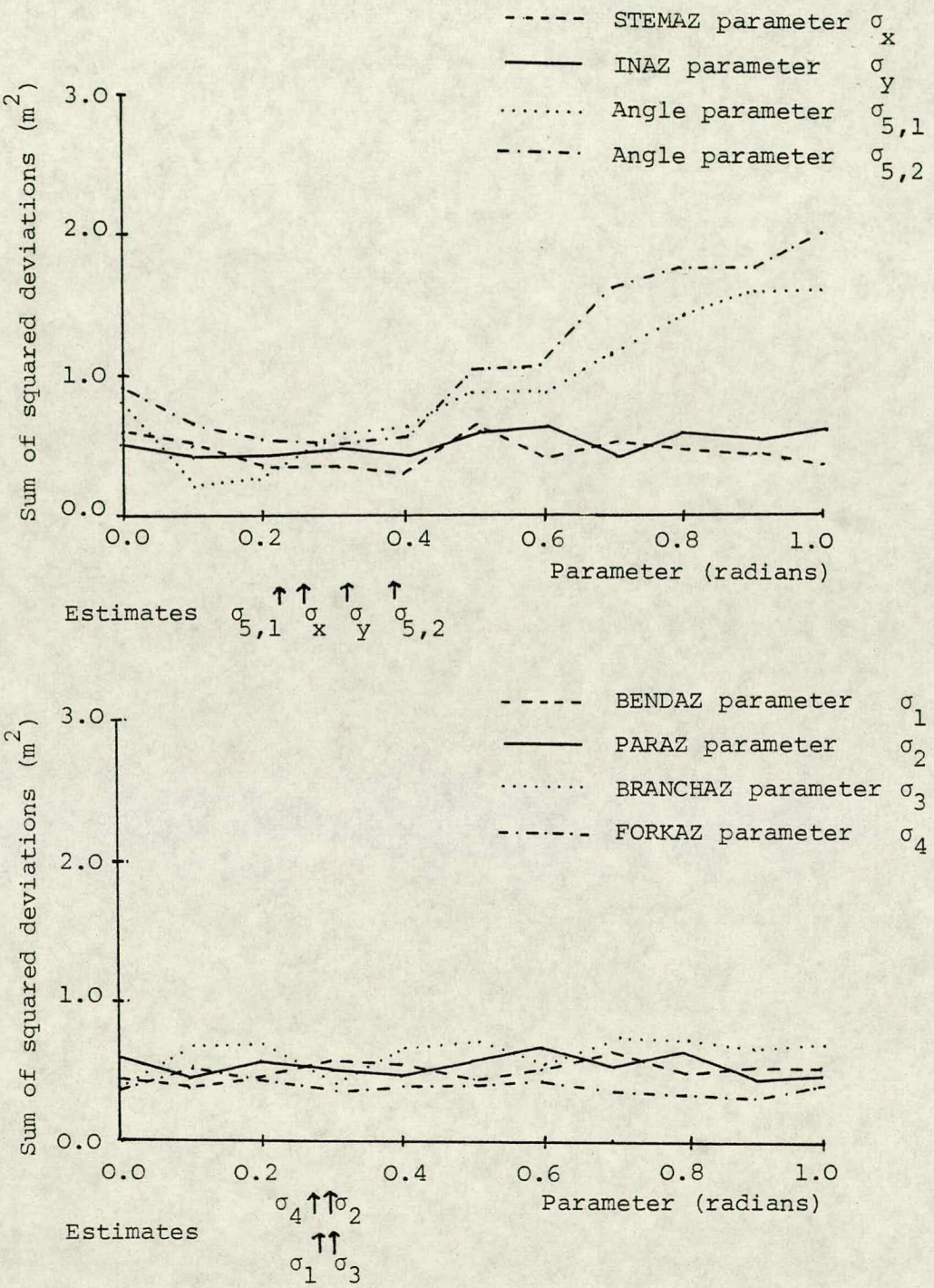
Convergence of the mean length curves



Values plotted are the sums of squared deviations between the true radial distance curve and the mean radial distance curves of groups of five simulations.

Figure 4.4.5

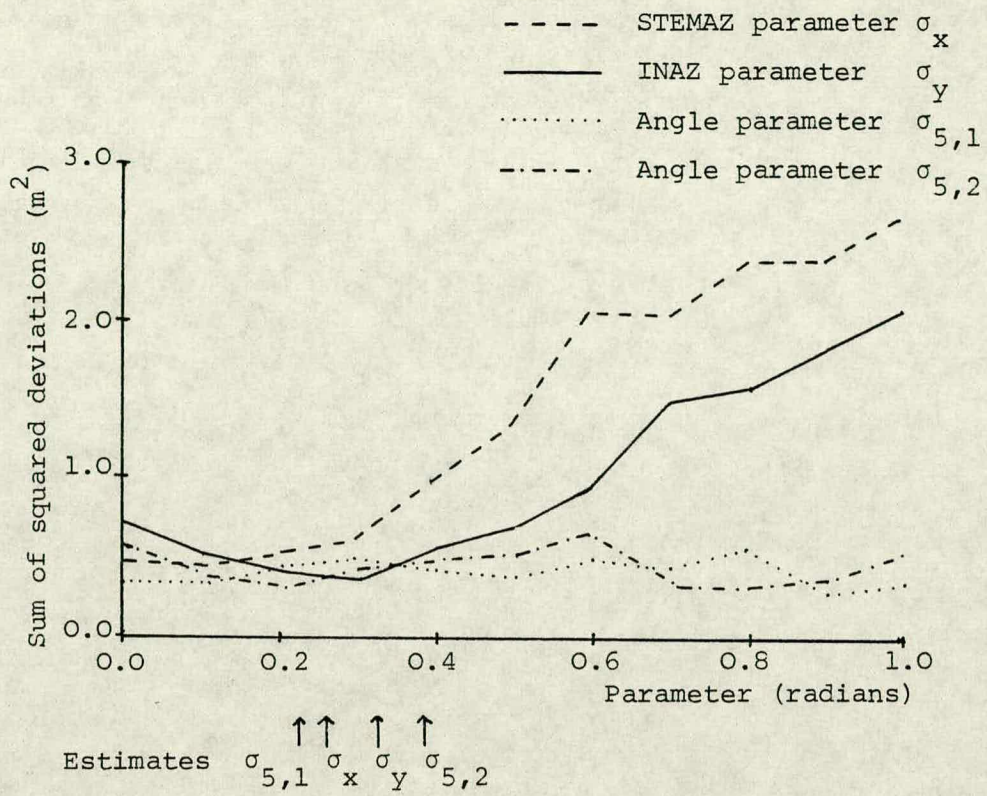
Sensitivity of the mean radial distance curve

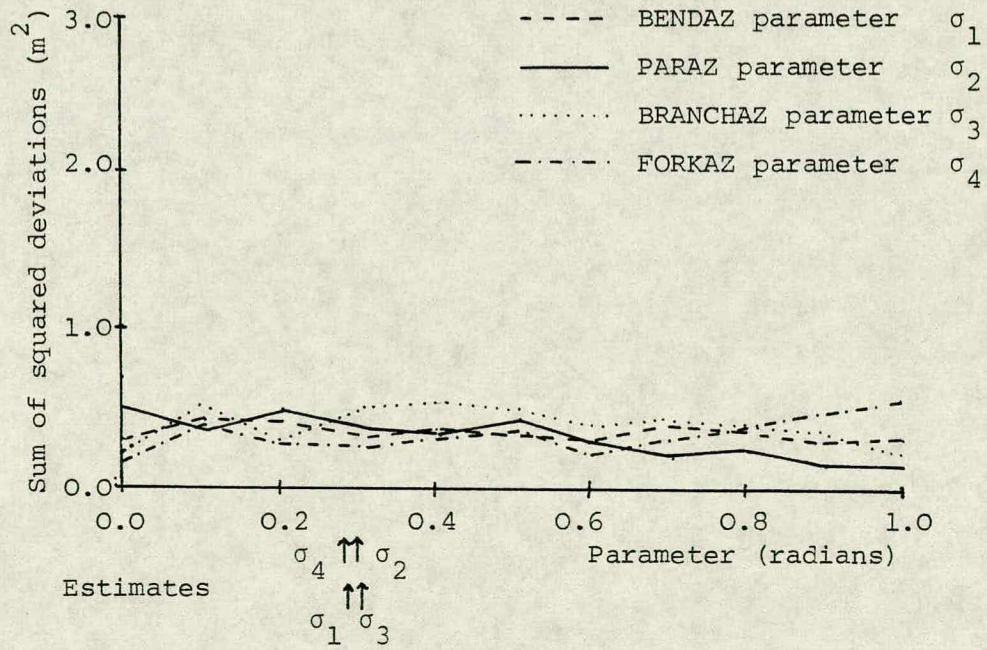


Values plotted are the sums of squared deviations between the true depth curve and the mean depth curves of groups of five simulations.

Figure 4.4.6

Sensitivity of the mean depth curve





Values plotted are the sums of squared deviations between the true direction curve and the mean direction curves of groups of five simulations.

Figure 4.4.7

Sensitivity of the mean direction curve



Figure 4.4.8

Root system simulated by the development model

CHAPTER 5

A RANDOM WALK WITH CORRELATED STEP DIRECTIONS: CONTINUOUS CASE

The following three chapters describe a theoretical analysis of several stochastic processes which were suggested by our study of rooting patterns and which have many important applications.

The two main mechanisms of the spread of a root system are the branching and extension of roots. A stochastic process which incorporates both of these mechanisms is the branching random walk which is fully described in Chapter 7. First we shall consider the paths of individual roots, which may be interpreted as examples of a type of random walk. For even though roots grow over continuous time periods each root consists of a series of distinct straight-line segments. Any straight-line segment may be represented by a three-dimensional vector, $\underset{\sim}{X}_i$ say, so that the position relative to its origin of the end-point of a root consisting of n segments, $\underset{\sim}{S}_n$ say, is given by $\underset{\sim}{S}_n = \underset{\sim}{X}_1+\underset{\sim}{X}_2+\ldots+\underset{\sim}{X}_n$. Hence the path taken by any root may be interpreted as a random walk with each segment representing one instantaneous jump of some particle performing the embedded random walk.

Most previous work on random walks (see, for example, Feller 1968, p.342-367) has involved the assumption that the steps $\{\underset{\sim}{X}_i\}$ are independent and identically distributed random variables. This assumption is not compatible with root growth for the following reasons.

i) Root growth is constrained by the soil boundaries (Figure 2.2.1) so that the distribution of step length or direction may depend upon position.

ii) The development takes place in a heterogeneous environment which contains regions which enhance or inhibit the frequency of bending and branching and therefore influence the step lengths.

iii) The growth process is non-stationary and depends upon season, soil moisture, root age, etc. Thus steps may not be identically distributed but may depend upon root age and position.

iv) Roots are prevented from passing through any previously occupied region and in particular must avoid their own paths.

v) Roots may interact with each other, for example they may be inhibited from growing too close together.

vi) Step directions are not independent: the direction taken by a root after a bend or branching point is correlated to that taken before.

Whilst there are techniques available for dealing to some extent with many of these difficulties individually, for example random walks in a random environment (Kesten, Kozlov and Spitzer 1975), absorbing or reflecting barriers (Cox and Miller 1965,p.45-67) or self-avoiding random walks (Edwards 1965), a random walk incorporating all of the factors is mathematically intractable.

When a root's path is interpreted as a random walk the most important factor is the correlation between step directions; for totally unrealistic rooting patterns were simulated when the directions of successive segments, or steps, were uncorrelated (Section 4.3.ii). Therefore we shall investigate a type of correlated random walk but will assume the other usual criteria of an infinite homogeneous space, stationarity, etc. to be true. First we shall formally describe the process which we consider (Section 5.1) before discussing its importance to other fields of investigation and describing related work (Section 5.2). The difficulties associated with an analysis are then illustrated (Section 5.3), explicit expressions for several moments of the process are derived (Section 5.4) and various limiting results are established (Sections 5.5, 5.6 and 5.7).

5.1 Assumptions and Notation

The walk which we shall investigate throughout this chapter is restricted to two-dimensional continuous space. Lattice walks are considered in Chapter 6 and most of the methods are easily extended to

higher dimensions.

The process is initiated from a particle situated at the origin of $\mathbb{R}^2$. At time n=1 the particle instantaneously jumps a random distance ℓ_1 in some direction ξ relative to a fixed line. At time n=2 the particle jumps a distance ℓ_2 in a direction $\xi+\theta_1$, where θ_1 denotes a random change in direction. At time n=3 the particle jumps distance ℓ_3 in direction $\xi+\theta_1+\theta_2$, and so on (Figure 5.1.1). We shall call the $\{\theta_i\}$ the turning variables, which are assumed to be independent and identically distributed, drawn from some probability distribution $G(\theta)$. The $\{\ell_i\}$, the length variables, are similarly assumed to be independent and identically distributed, drawn from some probability distribution $H(\ell)$.

This type of random walk involves independent changes in direction between steps rather than the usual assumption of independent step directions. The direction of the nth step, $\xi+\theta_1+\theta_2+\ldots+\theta_{n-1}$, is clearly correlated to those previously taken which explains the name "correlated random walk" for the process. The correlation is of a specific type however, and conditional upon the direction of the nth step the direction of the (n+1)st is independent of all previous steps.

We shall denote the position of the particle after n steps by

$$\underline{S}_n \equiv (S_{n1}, S_{n2})^T.$$

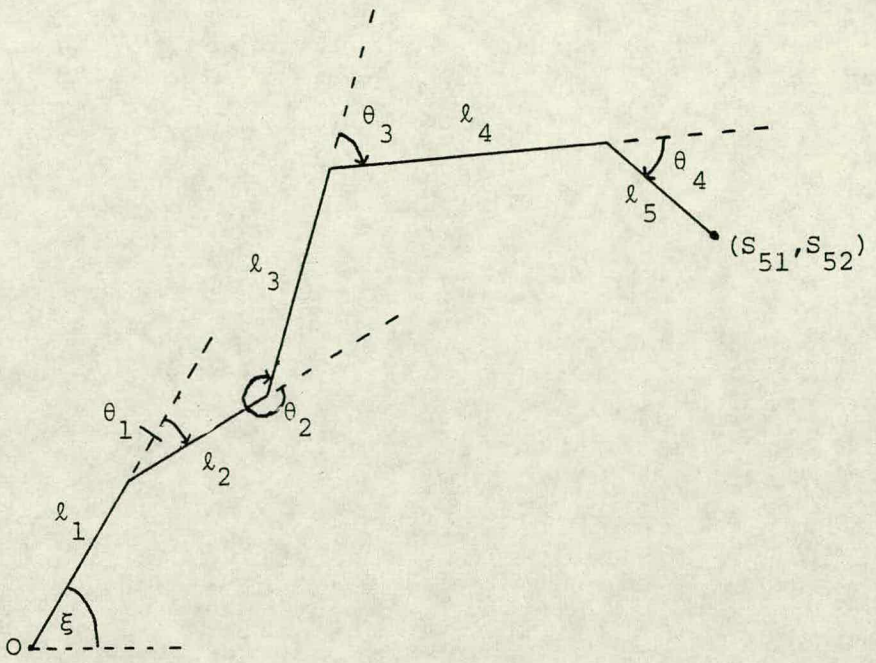
The contribution of the jth step, $\underline{X}_j$, to $\underline{S}_n$ is $(\ell_j\cos(\xi+\theta_1+\ldots+\theta_{j-1}), \ell_j\sin(\xi+\theta_1+\ldots+\theta_{j-1}))^T$ so that

$$(5.1.1) \qquad \begin{cases} S_{n1} = \sum_{j=1}^{n} \ell_j\cos(\xi+\theta_1+\ldots+\theta_{j-1}), \text{ and} \\ S_{n2} = \sum_{j=1}^{n} \ell_j\sin(\xi+\theta_1+\ldots+\theta_{j-1}). \end{cases}$$

Let the probability distribution of $\underline{S}_n$ be $F_n(.)$, where

$$F_n(I) \equiv \Pr(\underline{S}_n \in I)$$

for I any Borel set (Feller 1971,p.114) in $\mathbb{R}^2$. The assumption that the particle started from the origin with initial direction ξ is implicit in the definition of $F_n(.)$. More generally we can define



Notation

O	Origin
ξ	Initial direction
$\{\ell_i\}$	Length variables. Independent and identically distributed with probability distribution H(.)
$\{\theta_i\}$	Turning variables. Independent and identically distributed with probability distribution G(.)
(S_{n1}, S_{n2})	Coordinates of the particle after n steps

Figure 5.1.1

Correlated random walk in the plane: notation

$$F_n(I;\underline{u},\zeta) \equiv \Pr(\underline{S}_n \in I \text{ having started from } \underline{u} \in \mathbb{R}^2 \text{ with initial direction } \zeta),$$

so that

$$F_n(I) \equiv F_n(I;\underline{0},\xi).$$

(For simplicity we shall use "starting from $\underline{u},\zeta$" in the sequel as an abbreviated form of "starting with the particle at $\underline{u} \in \mathbb{R}^2$ and with initial direction ζ".)

In order to investigate the properties of $F_n(.)$ we will make the following assumptions.

Assumptions 5.1.1

1. The walk is not restricted to a subset of $\mathbb{R}^2$.
2. The turning variables are not confined to $\{0\}$ and $\{\pi\}$ or to $\{-\frac{1}{2}\pi\}$ and $\{\frac{1}{2}\pi\}$. This implies that
$$\max(E[|\cos\theta_i|],E[|\sin\theta_i|]) < 1 \qquad (i=1,2,\ldots).$$
3. $E[\ell_i^r] < \infty$ for $r = 1, 2, 3$ and 4.
4. $E[\sin\theta_i] = C$ $(i=1,2,\ldots)$ which implies that the distribution $G(.)$ is symmetrical about zero. This assumption is made in order to facilitate the derivation of expressions for the moments of $\underline{S}_n$ and does not affect any of the results obtained in Sections 5.5, 5.6 or 5.7.

These assumptions and our notation are summarised for easy reference in Table 5.1.1 where further notation is also introduced. Before proceeding with an analysis of the process we give a brief description of other relevant investigations and of the applications of correlated random walks.

Symbol	Interpretation
ξ	Initial direction of the particle.
$\{\theta_i\}$	Turning variables.
$G(.)$	Turning variable distribution. Assume $\int_0^{2\pi} \sin\theta dG(\theta) = 0$.
c	$E[\cos\theta_i]$ $(i=1,2,\ldots)$.
$\{\ell_i\}$	Length variables.
$H(.)$	Length variable distribution.
μ_r	$E[\ell_i^r]$. Assume $\mu_r < \infty$ $(r=1,2,3,4)$.
$\underline{X}_n = (X_{n1}, X_{n2})^T$	$(\ell_n \cos(\xi+\theta_1+..+\theta_{n-1}), \ell_n \sin(\xi+\theta_1+..\theta_{n-1}))^T$, the nth step of the particle.
$\underline{S}_n = (S_{n1}, S_{n2})^T$	The position of the particle after n steps.
$F_n(I;\underline{u},\zeta)$	$Pr(\underline{S}_n \in I$ having started from $\underline{u},\zeta)$.
$F_n(I)$	$F_n(I;\underline{0},\xi)$.
R_n	$\sqrt{(S_{n1}^2+S_{n2}^2)}$, the distance of the particle from the origin after n steps.
$\mathcal{L}_n$	The σ-field (Feller 1971,p.113) generated by the first n steps of the walk.

Table 5.1.1

Assumptions and notation for Chapter 5

5.2 Related Processes

Karl Pearson (1905) first formulated his "Problem of the random walk" as follows.

"A man starts from a point O and walks ℓ yards in a straight line; he then turns through any angle whatever and walks another ℓ yards in a straight line. He repeats this process n times. I require the probability that after these n stretches he is at a distance between r and $r+\delta r$ from his starting point O."

This definition describes a correlated random walk with fixed step lengths but if "any angle whatever" is assumed to imply a uniform distribution of the turning variables the important word "through" may be replaced by "to" without altering the mathematical analysis of the walk. If the turning variables had any other distribution then the replacement would have the effect of introducing independent step directions.

Rayleigh (1919) solved Pearson's problem for walks in one, two and three dimensions assuming uniformly distributed turning variables and so independent step directions. Since then more general solutions have been obtained by several authors, all of whom assumed step directions to be independently distributed. Chandrasekhar (1943) obtained asymptotic results for walks with random step lengths and Watson(1952, p.419-421) considered the walk to take place in a general p-dimensional space. Walks with step directions independently but not uniformly distributed have been studied by, amongst others, Stephens (1963) and Johnson (1966).

Improvements to Rayleigh's solution to Pearson's problem were developed by Spitzer (1964,p.104) who used Fourier analytic methods, Feller (1971,p.32-33) who considered the relationship between the length of a three-dimensional walk and its projection onto one axis, and by Mardia (1972,p.93-96) who developed a simple characteristic function method. None of these techniques can be applied when step directions are correlated.

Daniels (1952) and Hermans and Ullman (1952) studied the correlated random walk which we have described, using the name "stiff chains" for the process. These authors were mainly concerned with approximations to the distribution of the end to end distance, R_n, for

walks consisting of large numbers of short steps. Tchen (1952) investigated a similar process although he allowed a more general form of correlation, and further results were established by Gorostiza (1973) who considered particles moving in a p-dimensional space, undergoing random changes in direction at random times whilst maintaining constant speed.

A one-dimensional version of the correlated random walk in a continuous space, where particles reverse directions at random times, has been studied by Bartlett (1975,1978) and Cane (1967,1975). In this chapter we consider genuinely two-dimensional motion only: walks on a one-dimensional lattice are described in Chapter 6.

Correlated random walks have many applications, perhaps the most important of which is to polymer chemistry, where many results have been established for specific parametric forms of the length and turning variable distributions H(.) and G(.), respectively. See Freed (1971) and Fixman and Skolnick (1976) for references, and Flory (1962) for a discussion of the interpretation of a polymer chain as a mathematical process. Other applications in the biological, chemical and physical sciences include: the configuration of rubber molecules (Moran 1948); electron scattering (Goudsmit and Saunderson 1940); paths of cosmic ray particles (Moyal 1950); the resultant electrical moment of complex molecules (Eyring 1932); and diffusion of animals Skellam (1973).

5.3 The Problem of Determining the Distribution Function of S_n

An explicit expression for the distribution $F_n(.)$ of the particle's position after n steps, $\underline{S}_n$, would be very useful to all applications but we have been unable to derive such an expression. The difficulties are best illustrated by examining the relationship between $F_n(.)$ and $F_{n-1}(.)$, the easiest method of which evokes Daniels' (1952) system of coordinates. Instead of measuring the position of the particle relative to fixed axes Daniels defined a Cartesian coordinate system which was rotated and translated at every step of the particle so that the origin was kept at the particle's current position and the first axis always lay along the previous step of the particle. Then if we denote the position (with respect to the new coordinate system) of the

particle's initial position, i.e. the origin of the plane, by

$$\underset{-}{Z}_n \equiv (Z_{n1}, Z_{n2})^T,$$

a simple geometrical argument (Figure 5.3.1) shows that

$$(5.3.1)\begin{cases} Z_{n1} = \ell_n + Z_{n-1,1}\cos\theta_{n-1} - Z_{n-1,2}\sin\theta_{n-1}, \text{ and} \\ Z_{n2} = \quad Z_{n-1,1}\sin\theta_{n-1} + Z_{n-1,2}\cos\theta_{n-1}. \end{cases}$$

Thus the reason for the unusual choice of axes is that in this way the position of the particle at time n can be expressed as a function of the position at time (n-1), ℓ_n and θ_{n-1} only. The old and new coordinate systems are simply related (Figure 5.3.2) by

$$S_{n1} = Z_{n1}\cos(\xi+\theta_1+\ldots+\theta_{n-1}) - Z_{n2}\sin(\xi+\theta_1+\ldots+\xi_{n-1}), \text{ and}$$

$$S_{n2} = Z_{n1}\sin(\xi+\theta_1+\ldots+\theta_{n-1}) + Z_{n2}\cos(\xi+\theta_1+\ldots+\theta_{n-1}),$$

so that an expression for the probability distribution $F_n(.)$ may be derived if an expression can be obtained for the distribution of $\underset{-}{Z}_n$. Let us define the probability density function of $\underset{-}{Z}_n$ to be $f_n(Z_{n1}, Z_{n2})$. Then if Z_{n1}, Z_{n2}, $Z_{n-1,1}$, $Z_{n-1,2}$, ℓ_n and θ_{n-1} satisfy (5.3.1) it follows that

$$(5.3.2) \quad f_n(Z_{n1}, Z_{n2}) = \int_0^\infty \int_0^{2\pi} f_{n-1}(Z_{n-1,1}, Z_{n-1,2})\, dG(\theta_{n-1})\, dH(\ell_n),$$

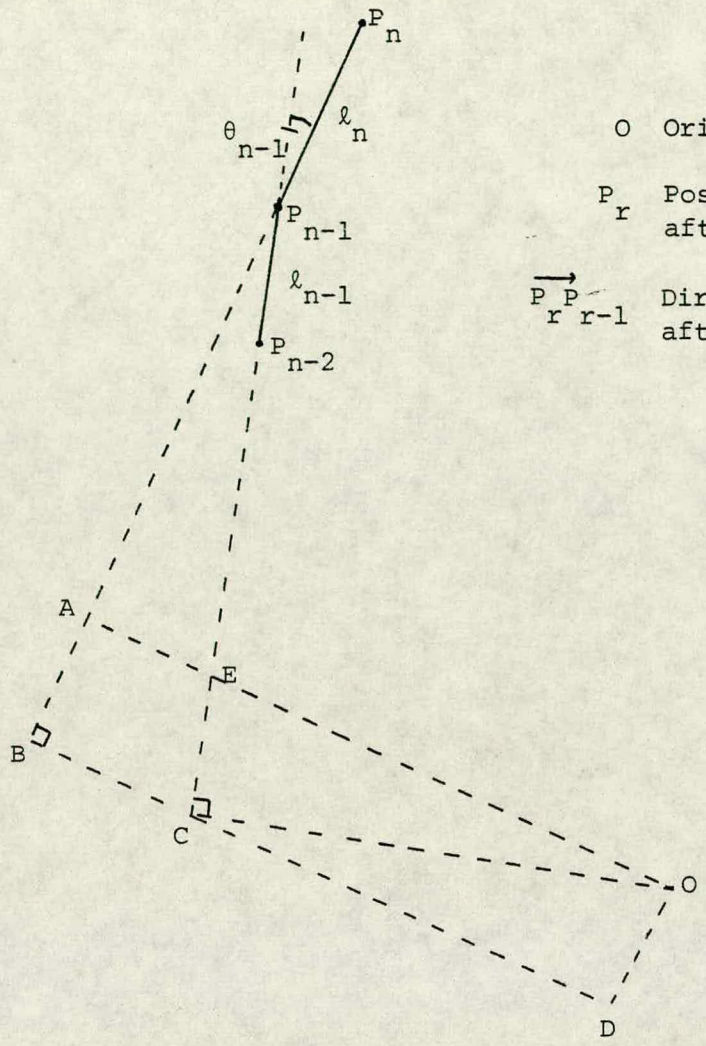
where G(.) and H(.) are the turning and length variable distribution functions introduced earlier.

Now let the characteristic function of Z_{n1} and Z_{n2} be

$$\psi_n(s,t) \equiv E[\exp(isZ_{n1}+itZ_{n2})]$$

$$= \iint_{R^2} \exp(isZ_{n1}+itZ_{n2}) f_n(Z_{n1}, Z_{n2})\, dZ_{n1}\, dZ_{n2}.$$

Transforming Z_{n1}, Z_{n2} and $f_n(Z_{n1}, Z_{n2})$ by (5.3.1) and (5.3.2) yields



O Origin

P_r Position of the particle after r steps

$\overrightarrow{P_r P_{r-1}}$ Direction of first axis after r steps

In the diagram the coordinates of the origin relative to the particles position after (n-1) steps, $(Z_{n-1,1}, Z_{n-1,2})$, are given by the lengths $P_{n-1}C$ and CO. Similarly the coordinates after n steps, (Z_{n1}, Z_{n2}), are given by the lengths P_nA and AO. Now

$$P_nA = P_nP_{n-1} + P_{n-1}B - AB \quad \text{and}$$

$$AO = BD = BC + CD \ .$$

Therefore

$$Z_{n1} = \ell_n + Z_{n-1,1}\cos\theta_{n-1} - Z_{n-1,2}\sin\theta_{n-1} \ , \quad \text{and}$$

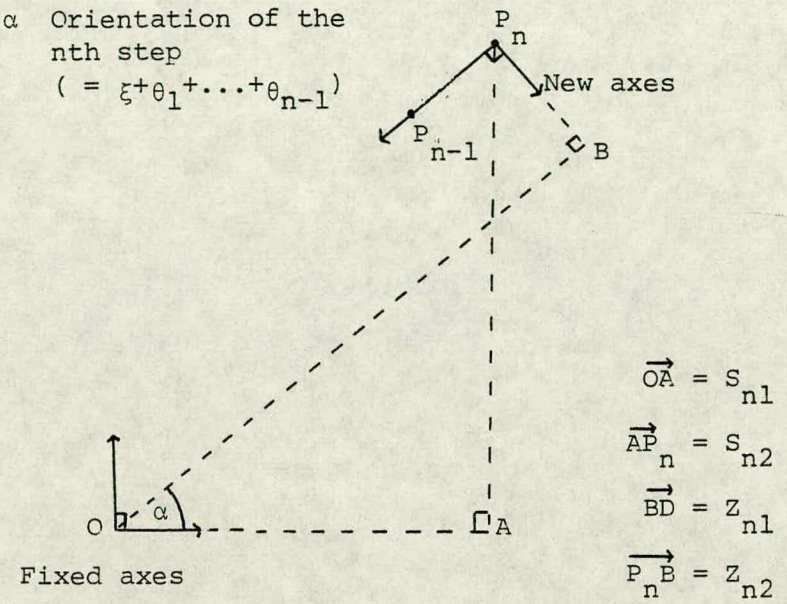
$$Z_{n2} = Z_{n-1,1}\sin\theta_{n-1} + Z_{n-1,2}\cos\theta_{n-1} \ .$$

Figure 5.3.1

Correlated random walk in the plane: Daniels' system of coordinates

P_{n-1}, P_n Positions of the particle after (n-1) and n steps respectively

α Orientation of the nth step ($= \xi + \theta_1 + \ldots + \theta_{n-1}$)



Now

$$OA = OB\cos\alpha - P_nB\sin\alpha \quad \text{and}$$

$$AP_n = OB\sin\alpha + P_nB\cos\alpha \ .$$

Therefore

$$S_{n1} = Z_{n1}\cos\alpha - Z_{n2}\sin\alpha \quad \text{and}$$

$$S_{n2} = Z_{n1}\sin\alpha + Z_{n2}\cos\alpha \ .$$

Figure 5.3.2

Relationship between Daniels' and original coordinate systems

$$\psi_n(s,t) = \int_0^\infty \int_0^{2\pi} \iint_{R^2} \exp(is\ell_n + iZ_{n-1,1}(s\cos\theta_{n-1}+t\sin\theta_{n-1}) + iZ_{n-1,2}(t\cos\theta_{n-1}-s\sin\theta_{n-1})\} \times f_{n-1}(Z_{n-1,1},Z_{n-1,2})dZ_{n-1,1}dZ_{n-1,2}dG(\theta_{n-1})dH(\ell_n)$$

because the Jacobian of the transformation is unity. Thus

$$\psi_n(s,t) = \int_0^\infty \int_0^{2\pi} \exp(is\ell_n)\psi_{n-1}(s\cos\theta_{n-1}+t\sin\theta_{n-1}, t\cos\theta_{n-1}-s\sin\theta_{n-1})dG(\theta_{n-1})dH(\ell_n). \tag{5.3.3}$$

Now choose λ and α such that $s = \lambda\cos\alpha$ and $t = \lambda\sin\alpha$. For simplicity write $\Psi_n(\lambda,\alpha)$ for $\psi_n(\lambda\cos\alpha,\lambda\sin\alpha)$ and use (5.3.3) to obtain

$$\Psi_n(\lambda,\alpha) = \int_0^\infty \int_0^{2\pi} \exp(i\ell_n\lambda\cos\alpha)\Psi_{n-1}(\lambda,\alpha-\theta_{n-1})dG(\theta_{n-1})dH(\ell_n) ,$$

which was established by Daniels (1952). This is the most simple relationship between the distributions of $\underline{S}_n$ and $\underline{S}_{n-1}$ which I have been able to establish. Even with simple parametric forms of the distributions G(.) and H(.) I have been unable to derive an expression for the probability distribution of $\underline{S}_n$.

5.4 Some Moments of the Process

Although no explicit expression has been found for the distribution of $\underline{S}_n$ exact expressions for several moments may be derived. The mean value of $\underline{S}_n$ has been calculated for walks with constant step lengths by Tchen (1952) and an expression for $E[R_n^2]$ was obtained by Skellam (1973). To my knowledge no other exact expressions have been derived.

5.4.i Mean of S_n

The assumption that $E[\sin\theta_j] = 0$ $(j=1,2,\ldots)$ is not essential to the derivation of moments of the particle's position but simplifies

the calculations. For when the assumption holds a simple trigonometrical argument shows that

$$(5.4.1)\qquad \begin{cases} E\left[\cos\left(\sum_{j=1}^{n}\theta_{j+k}\right)\right] = c^n \qquad (c = E[\cos\theta]), \text{ and} \\ E\left[\sin\left(\sum_{j=1}^{n}\theta_{j+k}\right)\right] = 0 \end{cases}$$

for any non-negative integers k and n.

The mean value of $\underline{S}_n$ $(= (S_{n1}, S_{n2})^T)$ is easily obtained from the expansions (5.1.1) which are

$$S_{n1} = \sum_{j=1}^{n} \ell_j \cos(\xi + \theta_1 + \ldots + \theta_{j-1}) \qquad \text{and}$$

$$S_{n2} = \sum_{j=1}^{n} \ell_j \sin(\xi + \theta_1 + \ldots + \theta_{j-1}).$$

First consider S_{n1}, take expectations and expand. This gives

$$\begin{aligned} E[S_{n1}] &= \sum_{j=1}^{n} E[\ell_j] E[\cos(\xi + \theta_1 + \ldots + \theta_{j-1})] \\ &= \sum_{j=1}^{n} E[\ell_j] E[\cos(\theta_1 + \ldots + \theta_{j-1})\cos\xi - \sin(\theta_1 + \ldots + \theta_{j-1})\sin\xi]. \end{aligned}$$

Thus by (5.4.1) and using the notation of Table 5.1.1 we have

$$\begin{aligned} E[S_{n1}] &= \sum_{j=1}^{n} \mu_1 c^{j-1} \cos\xi \\ &= \mu_1 \cos\xi (1-c^n)/(1-c), \end{aligned} \qquad (5.4.2)$$

which exists because we have ensured (Assumptions 5.1.1) that $c < 1$. Similarly, we can show that

$$E[S_{n2}] = \mu_1 \sin\xi (1-c^n)/(1-c), \qquad (5.4.3)$$

whence

$$E[\underline{S}_n] = \{\mu_1(1-c^n)/(1-c)\}(\cos\xi,\sin\xi)^T.$$

Hence the mean position of the particle is bounded and tends to a constant as the number of steps increases.

5.4.ii Dispersion matrix of $\underline{S}_n$

Gorostiza (1973) has determined an approximate asymptotic expression for the dispersion matrix of $\underline{S}_n$: in this section we shall establish an exact expression. We need to determine $E[S_{n1}^2]$, $E[S_{n2}^2]$ and $E[S_{n1}S_{n2}]$ and then use the appropriate mean values (5.4.2 and 5.4.3) to obtain expressions for the variances and covariance of the particle coordinates.

We begin by expanding (5.1.1) to give

$$S_{n1} = \{\ell_1 + \sum_{j=2}^{n} \ell_j \cos(\theta_1+\ldots+\theta_{j-1})\}\cos\xi - \{\sum_{j=2}^{n} \ell_j \sin(\theta_1+\ldots+\theta_{j-1})\}\sin\xi ,$$

which we may write as

$$S_{n1} \equiv A_n\cos\xi - B_n\sin\xi \qquad \text{(say)}. \tag{5.4.4}$$

Similarly, from (5.1.1),

$$S_{n2} = \{\ell_1 + \sum_{j=2}^{n} \ell_j \cos(\theta_1+\ldots+\theta_{j-1})\}\sin\xi + \{\sum_{j=2}^{n} \ell_j \sin(\theta_1+\ldots+\theta_{j-1})\}\cos\xi ,$$

which can be written as

$$S_{n2} \equiv A_n\sin\xi + B_n\cos\xi . \tag{5.4.5}$$

Therefore to calculate $E[S_{n1}^2]$, $E[S_{n2}^2]$ and $E[S_{n1}S_{n2}]$ we shall require expressions for $E[A_n^2]$, $E[B_n^2]$ and $E[A_nB_n]$. We can expand each of A_n^2, B_n^2 and A_nB_n to yield

$$A_n^2 = \{\ell_1^2 + \sum_{j=2}^{n} \ell_j^2 \cos^2(\theta_1+\ldots+\theta_{j-1})\}$$

$$+ \{2 \sum_{j=3}^{n} \sum_{k=2}^{j-1} \ell_j \ell_k \cos(\theta_1+\ldots+\theta_{j-1})\cos(\theta_1+\ldots+\theta_{k-1})\} \tag{5.4.6}$$

$$+ \{2 \sum_{j=2}^{n} \ell_1 \ell_j \cos(\theta_1+\ldots+\theta_{j-1})\} ,$$

$$B_n^2 = \{ \sum_{j=2}^{n} \ell_j^2 \sin^2(\theta_1+\ldots+\theta_{j-1})\}$$

$$+ \{2 \sum_{j=3}^{n} \sum_{k=2}^{j-1} \ell_j \ell_k \sin(\theta_1+\ldots+\theta_{j-1})\sin(\theta_1+\ldots+\theta_{k-1})\}, \text{ and} \tag{5.4.7}$$

$$A_n B_n = \{ \sum_{j=2}^{n} \ell_1 \ell_j \sin(\theta_1+\ldots+\theta_{j-1})\}$$

$$+ \{ \sum_{j=2}^{n} \ell_j^2 \cos(\theta_1+\ldots+\theta_{j-1})\sin(\theta_1+\ldots+\theta_{j-1})\}$$

$$+ \{ \sum_{j=3}^{n} \sum_{k=2}^{j-1} \ell_j \ell_k \cos(\theta_1+\ldots+\theta_{j-1})\sin(\theta_1+\ldots+\theta_{k-1})\} \tag{5.4.8}$$

$$+ \{ \sum_{j=3}^{n} \sum_{k=2}^{j-1} \ell_j \ell_k \sin(\theta_1+\ldots+\theta_{j-1})\cos(\theta_1+\ldots+\theta_{k-1})\} .$$

If we write (5.4.6), (5.4.7) and (5.4.8) as

$$A_n^2 = A_{n1} + A_{n2} + A_{n3} \qquad \text{(say)}, \tag{5.4.9}$$

$$B_n^2 = B_{n1} + B_{n2} \qquad \text{(say), and} \tag{5.4.10}$$

$$A_n B_n = C_{n1} + C_{n2} + C_{n3} + C_{n4} \qquad \text{(say)}, \tag{5.4.11}$$

then we need to determine the expected values of A_{n1}, A_{n2}, A_{n3}, B_{n1}, B_{n2}, C_{n1}, C_{n2}, C_{n3} and C_{n4}. We shall illustrate the method by deriving the expected values of A_{n1}, A_{n2} and A_{n3} and will quote the remaining results.

Expected value of A_{n1}

Recall that $\mu_r = E[\ell_i^r]$ $(r = 1, 2, 3 \text{ and } 4)$ and now let

$$(5.4.12) \quad \begin{cases} \eta = E[\exp(i2\theta)] \\ \nu = E[\exp(-i2\theta)] \end{cases},$$

where the expectation is with respect to the turning variable distribution $G(\theta)$. Note that from Assumptions 5.1.1 we have $|\eta|, |\nu| < 1$.

We have, from (5.4.6) and (5.4.9),

$$A_{n1} = \ell_1^2 + \sum_{j=2}^{n} \ell_j^2 \cos^2(\theta_1+\ldots+\theta_{j-1}) ,$$

whence by using the double angle formula for cosines

$$A_{n1} = \ell_1^2 + \tfrac{1}{2} \sum_{j=2}^{n} \ell_j^2 \{1 + \cos(2\theta_1+\ldots+2\theta_{j-1})\} ,$$

and so

$$A_{n1} = \ell_1^2 + \tfrac{1}{4} \sum_{j=2}^{n} \ell_j^2 \{2+\exp(2i\theta_1+\ldots+2i\theta_{j-1})+\exp(-2i\theta_1-\ldots-2i\theta_{j-1})\} .$$

Now take expectations to yield

$$E[A_{n1}] = \mu_2 + \tfrac{1}{4}\mu_2 \sum_{j=2}^{n} (2 + \eta^{j-1} + \nu^{j-1}) ,$$

and perform the summation to give

$$(5.4.13) \quad E[A_{n1}] = \tfrac{1}{4}\mu_2[2(n+1) + \{\eta(1-\eta^{n-1})/(1-\eta)\} + \{\nu(1-\nu^{n-1})/(1-\nu)\}].$$

Expected value of A_{n2}

From (5.4.6) and (5.4.9) we have

$$A_{n2} = 2 \sum_{j=3}^{n} \sum_{k=2}^{j-1} \ell_j \ell_k \cos(\theta_1+\ldots+\theta_{j-1}) \cos(\theta_1+\ldots+\theta_{k-1}) .$$

By writing $\cos(\theta_1+\ldots+\theta_{j-1})$ as $\cos\{(\theta_1+\ldots+\theta_{k-1})+(\theta_k+\ldots+\theta_{j-1})\}$ we may expand this expression as

$$A_{n2} = 2\sum_{j=3}^{n}\sum_{k=2}^{j-1} \ell_j\ell_k\{\cos^2(\theta_1+\ldots+\theta_{k-1})\cos(\theta_k+\ldots+\theta_{j-1})$$

$$- \sin(\theta_1+\ldots+\theta_{k-1})\sin(\theta_k+\ldots+\theta_{j-1})\cos(\theta_1+\ldots+\theta_{k-1})\}.$$

Upon taking expectations and recalling that $E[\cos(\theta_j+\ldots+\theta_{j+r-1})] = c^r$ whilst $E[\sin(\theta_j+\ldots+\theta_{j+r-1})] = 0$ for all positive integers j and r, we obtain

$$E[A_{n2}] = 2\mu_1^2\sum_{j=3}^{n}\sum_{k=2}^{j-1} c^{j-k}E[\cos^2(\theta_1+\ldots+\theta_{k-1})] .$$

Next, by the double angle formula for cosines and (5.4.12) we have

$$E[A_{n2}] = \tfrac{1}{2}\mu_1^2\sum_{j=3}^{n}\sum_{k=2}^{j-1} c^{j-k}(2 + \eta^{k-1} + \nu^{k-1}).$$

This series can be summed and the final result is

$$E[A_{n2}] = \frac{\mu_1^2 c}{2(1-c)}\{2(n-2) - \frac{2c(1-c^{n-2})}{(1-c)} + \frac{\eta c(1-c^{n-2})}{(c-\eta)} + \frac{\nu c(1-c^{n-2})}{(c-\nu)}$$

(5.4.14)

$$- \frac{\eta^2(1-\eta^{n-2})(1-c)}{(c-\eta)(1-\eta)} - \frac{\nu^2(1-\nu^{n-2})(1-c)}{(c-\nu)(1-\nu)}\} .$$

Expected value of A_{n3}

From (5.4.6) and (5.4.9) we have

$$A_{n3} = 2\sum_{j=2}^{n} \ell_1\ell_j\cos(\theta_1+\ldots+\theta_{j-1}) ,$$

and taking expectations gives

$$E[A_{n3}] = 2\mu_1^2\sum_{j=2}^{n} c^{j-1}.$$

This series can be summed to yield

$$E[A_{n3}] = 2\mu_1^2 c(1-c^{n-1})/(1-c). \tag{5.4.15}$$

In a very similar manner we can obtain the following expressions.

$$E[B_{n1}] = \tfrac{1}{4}\mu_2[2(n-1)-\{\eta(1-\eta^{n-1})/(1-\eta)\}-\{\nu(1-\nu^{n-1})/(1-\nu)\}], \tag{5.4.16}$$

$$E[B_{n2}] = \frac{\mu_1^2 c}{2(1-c)}\{2(n-2) - \frac{2c(1-c^{n-2})}{(1-c)} - \frac{\eta c(1-c^{n-2})}{(c-\eta)} - \frac{\nu c(1-c^{n-2})}{(c-\nu)} + \frac{\eta^2(1-\eta^{n-2})(1-c)}{(c-\eta)(1-\eta)} + \frac{\nu^2(1-\nu^{n-2})(1-c)}{(c-\nu)(1-\nu)}\}, \tag{5.4.17}$$

$$E[C_{n1}] = 0, \tag{5.4.18}$$

$$E[C_{n2}] = \tfrac{1}{4}\mu_2[\{\eta(1-\eta^{n-1})/(1-\eta)\}-\{\nu(1-\nu^{n-1})/(1-\nu)\}], \tag{5.4.19}$$

$$E[C_{n3}] = E[C_{n4}] = \frac{\mu_1^2 c}{4(1-c)}\{\frac{\eta c(1-c^{n-2})}{(c-\eta)} - \frac{\nu c(1-c^{n-2})}{(c-\nu)} - \frac{\eta^2(1-\eta^{n-2})(1-c)}{(c-\eta)(1-\eta)} + \frac{\nu^2(1-\nu^{n-2})(1-c)}{(c-\nu)(1-\nu)}\}. \tag{5.4.20}$$

We may now collect together results (5.4.2) to (5.4.5) and (5.4.13) to (5.4.20) to obtain exact expressions for the variances and covariance of the particle's coordinates after n steps, namely S_{n1} and S_{n2}. This procedure yields, after some simplification,

$$\mathrm{Var}(S_{n1}) = \tfrac{1}{4}\mu_2[\,2n + 2\cos 2\xi + \{1-\sin 2\xi\}\{\eta(1-\eta^{n-1})/(1-\eta)\}$$

$$+ \{1+\sin 2\xi\}\{\nu(1-\nu^{n-1})/(1-\nu)\]$$

$$+ \frac{\mu_1^2 c}{2(1-c)}\,[\,(\cos 2\xi - \sin 2\xi)\{\frac{\eta c(1-c^{n-2})}{(c-\eta)} - \frac{\eta^2(1-\eta^{n-2})(1-c)}{(c-\eta)(1-\eta)}\}$$

(5.4.21)

$$+ (\cos 2\xi + \sin 2\xi)\{\frac{\nu c(1-c^{n-2})}{(c-\nu)} - \frac{\nu^2(1-\nu^{n-2})(1-c)}{(c-\nu)(1-\nu)}\}$$

$$- \frac{2c(1-c^{n-2})}{(1-c)} + 2(n-2) + 4(1-c^{n-1})\cos^2\xi - \frac{2(1-c^n)\cos^2\xi}{(1-c)c}\,]\,,$$

$$\mathrm{Var}(S_{n2}) = \tfrac{1}{4}\mu_2[\,2n - 2\cos 2\xi + \{1+\sin 2\xi\}\{\eta(1-\eta^{n-1})/(1-\eta)\}$$

$$+ \{1-\sin 2\xi\}\{\nu(1-\nu^{n-1})/(1-\nu)\}]$$

$$+ \frac{\mu_1^2 c}{2(1-c)}\,[\,(\sin 2\xi - \cos 2\xi)\{\frac{\eta c(1-c^{n-2})}{(c-\eta)} - \frac{\eta^2(1-\eta^{n-2})(1-c)}{(c-\eta)(1-\eta)}\}$$

(5.4.22)

$$- (\cos 2\xi + \sin 2\xi)\{\frac{\nu c(1-c^{n-2})}{(c-\nu)} - \frac{\nu^2(1-\nu^{n-2})(1-c)}{(c-\nu)(1-\nu)}\}$$

$$- \frac{2c(1-c^{n-2})}{(1-c)} + 2(n-2) + 4(1-c^{n-1})\sin^2\xi - \frac{2(1-c^n)\sin^2\xi}{(1-c)c}\,]\,,$$

and finally

$$\mathrm{Cov}(S_{n1},S_{n2}) = \tfrac{1}{4}\mu_2[\,2\sin 2\xi + \{\eta(1-\eta^{n-1})/(1-\eta)\}\cos 2\xi$$

$$- \{\nu(1-\nu^{n-1})/(1-\nu)\}\cos 2\xi]$$

$$+ \frac{\mu_1^2 c}{2(1-c)}\,[\{\cos 2\xi+\sin 2\xi\}\{\frac{\eta c(1-c^{n-2})}{(c-\eta)} - \frac{\eta^2(1-\eta^{n-2})(1-c)}{(c-\eta)(1-\eta)}\}$$

(5.4.23)

$$+ \{\sin 2\xi-\cos 2\xi\}\{\frac{\nu c(1-c^{n-2})}{(c-\nu)} - \frac{\nu^2(1-\nu^{n-2})(1-c)}{(c-\nu)(1-\nu)}\}$$

$$+ 2(1-c^{n-1})\sin 2\xi - \frac{(1-c^n)\sin^2\xi}{(1-c)c}] \ .$$

From these expressions we can see that the covariance between S_{n1} and S_{n2} is bounded and that

$$\mathrm{Var}(S_{n1}) = \{\tfrac{1}{2}\mu_2 + \mu_1^2 c/(1-c)\}n + o(n) \ , \tag{5.4.24}$$

$$\mathrm{Var}(S_{n2}) = \{\tfrac{1}{2}\mu_2 + \mu_1^2 c/(1-c)\}n + o(n) \ , \text{ and} \tag{5.4.25}$$

$$\mathrm{Cov}(S_{n1},S_{n2}) = o(n) \ . \tag{5.4.26}$$

Hence the two coordinates of the particle's position are asymptotically uncorrelated and the initial direction, ξ, has no influence on the asymptotic variances of the coordinates. Let us write $D(\underset{\sim}{S}_n/\sqrt{n})$ for the dispersion matrix of the particle's position after n steps, $\underset{\sim}{S}_n$, when scaled by $\sqrt{n}$. Then it is apparent that

$$D(\underset{\sim}{S}_n/\sqrt{n}) = \{\tfrac{1}{2}\mu_2 + \mu_1^2 c/(1-c)\}I_2 \tag{5.4.27}$$

where I_2 denotes the 2×2 identity matrix. This is the asymptotic result obtained by Gorostiza (1973), who did not derive exact expressions first.

5.4.iii Moments of R_n

I have been unable to determine the expected value of R_n ($= \sqrt{(S_{n1}^2 + S_{n2}^2)}$), the distance of the particle from the origin after n steps. Skellam (1973) has calculated $E[R_n^2]$ for our type of correlated random walk and although this value can be obtained from the results for $E[S_{n1}^2]$ and $E[S_{n2}^2]$ Skellam's method, which is repeated below, is more direct.

For from (5.1.1) we have

$$S_{n1} + iS_{n2} = \sum_{j=1}^{n} \ell_j \exp\{i(\xi+\theta_1+\ldots+\theta_{j-1})\} , \quad \text{and}$$

$$S_{n2} - iS_{n2} = \sum_{j=1}^{n} \ell_j \exp\{-i(\xi+\theta_1+\ldots+\theta_{j-1})\} .$$

Therefore because the product of the left-hand terms of these two equations is R_n^2, and since $E[\exp(-i\theta)] = E[\exp(i\theta)]$ because $E[\sin\theta] = 0$ (Assumptions 5.1.1), we have

$$E[R_n^2] = E\Big[\sum_{j=1}^{n} \ell_j^2 + 2\sum_{j=2}^{n}\sum_{k=1}^{j-1} \ell_j \ell_k \exp\{i(\theta_k+\ldots+\theta_{j-1})\}\Big] .$$

In our earlier notation (Table 5.1.1) and upon using (5.4.1) this becomes

$$E[R_n^2] = n\mu_2 + 2\sum_{j=2}^{n}\sum_{k=1}^{j-1} \mu_1^2 c^{j-k}$$

$$= n\mu_2 + 2\mu_1^2 \sum_{j=2}^{n} c(1-c^{j-1})/(1-c) ,$$

so that we finally obtain

$$E[R_n^2] = n\mu_2 + 2\mu_1^2 c\{n - (1-c^n)/(1-c)\}/(1-c) . \qquad (5.4.28)$$

Fixman and Skolnick (1976) determined approximate expressions for several other even-order moments of R_n: we have been able to derive an exact expression for $E[R_n^4]$ (Appendix 2), which turns out to be of order n^2, but for no higher order moments. However, the

moments of both $\underset{\sim}{S}_n$ and R_n which we have derived are sufficient to enable us to obtain various asymptotic results.

5.5 Weak Law of Large Numbers

It is interesting to show that the weak law of large numbers (Feller 1968,p.243) applies to the particle position $\underset{\sim}{S}_n$, which is a sum of dependent variables (Table 5.1.1), as well as to sums of independent random variables.

Define the rectangle $I_n(\varepsilon_1,\varepsilon_2)$ for any $\varepsilon_1,\varepsilon_2 > 0$ by

$$I_n(\varepsilon_1,\varepsilon_2) \equiv \{(x_1,x_2): |x_1-E[S_{n1}]| < \varepsilon_1 n, |x_2-E[S_{n2}]| < \varepsilon_2 n\}$$

and recall that $F_n(I) \equiv \Pr(\underset{\sim}{S}_n \in I)$ for any set I in $\mathbb{R}^2$. We may now state the following analogue to the classical weak law of large numbers.

THEOREM 5.5.1 Under Assumptions 5.5.1

$$F_n(I_n(\varepsilon_1,\varepsilon_2)) \to 1$$

as n tends to infinity.

Proof

The proof uses the following bivariate Chebyshev-type inequality (Olkin and Pratt 1958) for any two variables y_1 and y_2 with variances σ_1^2 and σ_2^2 respectively, and correlation coefficient ρ:

$$\Pr(|y_1-E[y_1]| > k_1\sigma_1 \text{ or } |y_2-E[y_2]| > k_2\sigma_2) \leq \{k_1^2+k_2^2+\sqrt{[k_1^4+k_2^4+2(1-2\rho^2)k_1^2k_2^2]}\}/2k_1^2k_2^2 . \tag{5.5.1}$$

Denote the variances of S_{n1} and S_{n2} by σ_{n1}^2 and σ_{n2}^2 respectively, and their correlation coefficient by ρ_n. Now choose $k_1 = \varepsilon_1 n/\sigma_{n1}$ and $k_2 = \varepsilon_2 n/\sigma_{n2}$, whence from (5.5.1)

$$\Pr(\underset{\sim}{S}_n \notin I_n(\varepsilon_1,\varepsilon_2)) \leq \frac{\sigma_{n2}^2\varepsilon_1^2+\sigma_{n1}^2\varepsilon_2^2+\sqrt{\{\sigma_{n2}^4\varepsilon_1^4+\sigma_{n1}^4\varepsilon_2^4+2(1-2\rho_n^2)\sigma_{n1}^2\sigma_{n2}^2\varepsilon_1^2\varepsilon_2^2\}}}{2\varepsilon_1^2\varepsilon_2^2n^2} . \tag{5.5.2}$$

We know that σ_{n1}^2 and σ_{n2}^2 both have order of magnitude n (results 5.4.24 and 5.4.25) and that ρ_n tends to zero as n increases (5.4.26). Hence the right hand term must tend to zero as n tends to infinity. The left hand term is simply $1-F_n(I_n(\varepsilon_1,\varepsilon_2))$ and so the proof is complete.

□

5.6 A Central Limit Theorem

Having been unable to obtain an exact expression for the distribution of $\underline{S}_n$, the particle's position after n steps, the most important question to ask is whether the distribution is asymptotically Normal. Kac (1959,p.25-33) showed that this was so when all step lengths were equal and Gorostiza (1973) used a theorem of Rosen (1967) to show that the central limit theorem applied to the continuous time analogue of the correlated random walk, where particles move continuously and change directions at random times. Rosen showed that sums of dependent multivariate random variables converge to asymptotic Normality if certain moment conditions are met. By only a slight modification of his method (Appendix 3) it can be shown that the distribution of $\underline{S}_n/\sqrt{n}$ converges to that of a bivariate Normal random variable if the correlated random walk satisfies four conditions (C1 to C4 below). To state the conditions we require some new notation.

Let $\underline{S}_m^{(n)}$ denote the position of the particle after n steps relative to its position after m steps (m < n), i.e. if

$$\underline{S}_n = \sum_{j=1}^{n} \underline{X}_j$$

then

$$\underline{S}_m^{(n)} = \sum_{j=m+1}^{n} \underline{X}_j .$$

Also let $\underline{S}_m^{(n)} = (S_{m1}^{(n)}, S_{m2}^{(n)})^T$ so that $S_{m1}^{(n)} = S_{n1} - S_{m1}$ and $S_{m2}^{(n)} = S_{n2} - S_{m2}$, and define $R_m^{(n)} = \sqrt{\{(S_{m1}^{(n)})^2 + (S_{m2}^{(n)})^2\}}$. The moments of $\underline{S}_m^{(n)}$ and $R_m^{(n)}$ are derived in a similar manner to those of

$\underline{S}_n$ and R_n (Section 5.4): we simply replace n by (n-m) and ξ by $\xi+\theta_1+\ldots+\theta_m$.

We shall use the following conventions.

$$[a] \equiv \text{integer part of } a,$$

$$\langle \underline{u},\underline{v} \rangle \equiv \sum_{j=1}^{d} u_j v_j \quad \text{for } \underline{u} = (u_1,\ldots,u_d)^T \text{ and } \underline{v} = (v_1,\ldots,v_d)^T ,$$

$$\|\underline{u}\|_r \equiv \Big(\sum_{j=1}^{d} |u_j|^r \Big)^{1/r} \quad \text{for } \underline{u} = (u_1,\ldots,u_d)^T , \text{ and}$$

$$\|M\|_r \equiv \Big(\sum_{j,k=1}^{d} |m_{jk}|^r \Big)^{1/r} \quad \text{where } M = (m_{jk}) \quad (j,k = 1,2,\ldots,d) .$$

The conditions which must be satisfied by the correlated random walk are as follows.

Condition C1 There is a function $\kappa(s)$, which is bounded on $0 \leqslant s \leqslant 1$, and which tends to zero as s tends to zero, such that

$$\overline{\lim_{k\to\infty}} E[\| \underline{S}_{[\alpha k]} - \underline{S}_{[\beta k]} /\sqrt{k}\|_2^2] \leqslant \kappa(\alpha-\beta) \qquad (0 \leqslant \beta < \alpha \leqslant 1).$$

Condition C2 If $\mathcal{L}_n$ denotes the σ-field (Table 5.1.1) generated by the first n steps of the correlated random walk, then for all $0 \leqslant \alpha \leqslant 1$

$$\lim_{\Delta\downarrow 0} \frac{1}{\Delta} \overline{\lim_{k\to\infty}} \| E[E[\underline{S}_{[(\alpha+\Delta)k]} - \underline{S}_{[\alpha k]} /\sqrt{k} \,\big|\, \mathcal{L}_{[\alpha k]}]] \|_1 = 0.$$

Condition C3 There is a 2×2 function matrix $D(\alpha)$, defined and continuous for $0 \leqslant \alpha \leqslant 1$, such that

$$\lim_{\Delta\downarrow 0} \frac{1}{\Delta} \overline{\lim_{k\to\infty}} E[\| E[(\underline{S}_{[(\alpha+\Delta)k]} - \underline{S}_{[\alpha k]} /\sqrt{k}) (\underline{S}_{[(\alpha+\Delta)k]} - \underline{S}_{[\alpha k]} /\sqrt{k})^T \,\big|\, \mathcal{L}_{[\alpha k]}] - \Delta D(\alpha) \|_1] = 0.$$

Condition C4 For every $\varepsilon > 0$ and for $r = 1, 2$

$$\lim_{\Delta \downarrow 0} \frac{1}{\Delta} \overline{\lim_{k \to \infty}} \int_{|z_r| > \varepsilon} z_r^2 dF^{(k)}_{\alpha,\Delta}((z_1,z_2)^T) = 0$$

where $F^{(k)}_{\alpha,\Delta}(.)$ denotes the distribution function of $\underline{S}_{[\alpha k]}^{[(\alpha+\Delta)k]}$.

We shall show that these conditions are satisfied by the correlated random walk (Lemmas 5.6.1 to 5.6.4) before stating the central limit theorem formally.

Lemma 5.6.1 For $0 \leq \beta < \alpha \leq 1$

$$\overline{\lim_{k \to \infty}} E[\| \underline{S}_{[\beta k]}^{[\alpha k]} / \sqrt{k} \|_2^2] = (\alpha-\beta)\{\mu_2 + 2\mu_1^2 c/(1-c)\} ,$$

and condition C1 is satisfied by the correlated random walk with Assumptions 5.1.1.

Proof

Using the results of Sections 5.4.i and 5.4.ii, with $(n-m)$ replacing n, we have for $n > m$

$$E[(S^{(n)}_{m1})^2] = (n-m)\{\tfrac{1}{2}\mu_2 + \mu_1^2 c/(1-c)\} + o(n-m) , \quad \text{and} \tag{5.6.1}$$

$$E[(S^{(n)}_{m2})^2] = (n-m)\{\tfrac{1}{2}\mu_2 + \mu_1^2 c/(1-c)\} + o(n-m) . \tag{5.6.2}$$

Thus

$$E[\| \underline{S}_{[\beta k]}^{[\alpha k]} / \sqrt{k} \|_2^2] = E[(S^{[\alpha k]}_{[\beta k]1})^2 + (S^{[\alpha k]}_{[\beta k]2})^2]$$

$$= [([\alpha k] - [\beta k])\{\mu_2 + 2\mu_1^2 c/(1-c)\} + o(k)]/k ,$$

and as $[\alpha k] - [\beta k] \to (\alpha - \beta)k$ as $k \to \infty$ we have

$$\overline{\lim_{k \to \infty}} E[\| \underline{S}_{[\beta k]}^{[\alpha k]} / \sqrt{k} \|_2^2] = (\alpha-\beta)\{\mu_2 + 2\mu_1^2 c/(1-c)\} .$$

Now let $\kappa(s) = s\{\mu_2 + 2\mu_1^2 c/(1-c)\}$ and condition C1 is immediately satisfied. □

Lemma 5.6.2 For all $0 \leqslant \alpha \leqslant 1$

$$\lim_{\Delta \downarrow 0} \frac{1}{\Delta} \overline{\lim_{k \to \infty}} \| E[E[\underline{S}_{[\alpha k]}^{[(\alpha+\Delta)k]} / \sqrt{k} \,|\, \mathcal{L}_{[\alpha k]}]] \|_1 = 0$$

and condition C2 is satisfied by the correlated random walk with Assumptions 5.1.1.

Proof

By results (5.4.2) and (5.4.3) with n replaced by (n-m) and ξ by $(\xi+\theta_1+\ldots+\theta_m)$ we have

$$E[\underline{S}_m^{(n)} \,|\, \mathcal{L}_m] = \{\mu_1 (1-c^{n-m})/(1-c)\} (\cos(\xi+\theta_1+\ldots+\theta_m), \sin(\xi+\theta_1+\ldots+\theta_m))^T ,$$

for any positive integers n and m with $n > m$.

Thus for $0 \leqslant \alpha < \alpha+\Delta \leqslant 1$

$$E[\underline{S}_{[\alpha k]}^{[(\alpha+\Delta)k]} / \sqrt{k} \,|\, \mathcal{L}_{[\alpha k]}] = k^{-\frac{1}{2}} \{\mu_1 (1-c^{[\Delta k]})/(1-c)\} \times (\cos(\xi+\theta_1+\ldots+\theta_{[\alpha k]}), \sin(\xi+\theta_1+\ldots+\theta_{[\alpha k]}))^T ,$$

and upon using (5.4.1) to take expectations

$$E[E[\underline{S}_{[\alpha k]}^{[(\alpha+\Delta)k]} / \sqrt{k} \,|\, \mathcal{L}_{[\alpha k]}]] = k^{-\frac{1}{2}} \{\mu_1 (1-c^{[\Delta k]})/(1-c)\} c^{[\alpha k]} (\cos\xi, \sin\xi)^T .$$

Now

$$\| E[E[\underline{S}_{[\alpha k]}^{[(\alpha+\Delta)k]} / \sqrt{k} \,|\, \mathcal{L}_{[\alpha k]}]] \|_1 = k^{-\frac{1}{2}} \{\mu_1 (1-c^{[\Delta k]})/(1-c)\} c^{[\alpha k]} (|\cos\xi| + |\sin\xi|) ,$$

and as $|c| < 1$ (Table 5.1.1)

$$(1-c^{[\Delta k]})/(1-c) < [\Delta k]$$

whence

$$\| E[E[\underline{S}_{[\alpha k]}^{[(\alpha+\Delta)k]} / \sqrt{k} \,|\, \mathcal{L}_{[\alpha k]}]] \|_1 < \mu_1 (|\cos\xi| + |\sin\xi|) \Delta k^{\frac{1}{2}} c^{[\alpha k]} .$$

Because $k^{\frac{1}{2}} c^{[\alpha k]} \to 0$ as $k \to \infty$ we can take limits to yield

$$\lim_{\Delta\downarrow 0} \frac{1}{\Delta} \overline{\lim_{k\to\infty}} \| E[\, E[\, \underline{S}_{[\alpha k]}^{[(\alpha+\Delta)k]} / \sqrt{k} \,|\, \mathcal{L}_{[\alpha k]}\,]\,]\|_1 = 0 \ ,$$

and the lemma is proved. □

Lemma 5.6.3 There is a 2×2 function matrix $D(\alpha)$, defined and continuous for $0 \leq \alpha \leq 1$, such that

$$\lim_{\Delta\downarrow 0} \frac{1}{\Delta} \overline{\lim_{k\to\infty}} E[\, \| E[\, (\underline{S}_{[\alpha k]}^{[(\alpha+\Delta)k]} / \sqrt{k})\,(\underline{S}_{[\alpha k]}^{[(\alpha+\Delta)k]} / \sqrt{k})^T \,|\, \mathcal{L}_{[\alpha k]}\,] - \Delta D(\alpha) \|_1\,] = 0 \ ,$$

and condition C3 is satisfied by the correlated random walk with Assumptions 5.1.1.

Proof

Let $\sigma^2 = \{\frac{1}{2}\mu_2 + \mu_1^2 c/(1-c)\}$ and choose $D(\alpha) = \sigma^2 I_2$, where I_2 is the 2×2 identity matrix. Then by expanding the innermost expectation we have

$$E[\, \| E[\, (\underline{S}_{[\alpha k]}^{[(\alpha+\Delta)k]} / \sqrt{k})\,(\underline{S}_{[\alpha k]}^{[(\alpha+\Delta)k]} / \sqrt{k})^T \,|\, \mathcal{L}_{[\alpha k]}\,] - \Delta D(\alpha) \|_1\,]$$

$$= k^{-1}\{E[\, | E[\, (S_{[\alpha k]1}^{[(\alpha+\Delta)k]})^2 \,|\, \mathcal{L}_{[\alpha k]}\,] - \sigma^2 k\Delta |$$

$$+ | E[\, (S_{[\alpha k]2}^{[(\alpha+\Delta)k]})^2 \,|\, \mathcal{L}_{[\alpha k]}\,] - \sigma^2 k\Delta |$$

$$+ 2 | E[\, S_{[\alpha k]1}^{[(\alpha+\Delta)k]} S_{[\alpha k]2}^{[(\alpha+\Delta)k]} \,|\, \mathcal{L}_{[\alpha k]}\,] |\,]\} \ .$$

By the results of Section 5.4 with $(n-m)$ replacing n for any positive integers n and m with $n > m$, we have

$$E[\, S_{m1}^{(n)} S_{m2}^{(n)} \,|\, \mathcal{L}_m\,] = o(n-m). \qquad (5.6.3)$$

Therefore using (5.6.1), (5.6.2) and (5.6.3) to take expectations yields

$$E[\, \| E[\, (\underline{S}_{[\alpha k]}^{[(\alpha+\Delta)k]} / \sqrt{k})\,(\underline{S}_{[\alpha k]}^{[(\alpha+\Delta)k]} / \sqrt{k})^T \,|\, \mathcal{L}_{[\alpha k]}\,] - \Delta D(\alpha) \|_1\,]$$

$$= k^{-1} E[\, 2\sigma^2 |\, [\Delta k] - \Delta k | + o(\Delta k)\,] \ .$$

The result now follows upon taking limits. □

Lemma 5.6.4 For every $\varepsilon > 0$ and for $r = 1, 2$,

$$\lim_{\Delta \downarrow 0} \frac{1}{\Delta} \overline{\lim_{k \to \infty}} \int_{|s_r| > \varepsilon} s_1^2 dF_{\alpha,\Delta}^{(k)}((s_1,s_2)^T) = 0 \qquad (0 \leqslant \alpha \leqslant 1),$$

where $F_{\alpha,\Delta}^{(k)}$ denotes the distribution of $\underline{S}_{[\alpha k]}^{[(\alpha+\Delta)]}/\sqrt{k}$. Condition C1 is satisfied by the correlated random walk with Assumptions 5.1.1.

Proof

For $r = 1, 2$

$$\int_{|s_r| > \varepsilon} s_r^2 dF_{\alpha,\Delta}^{(k)}((s_1,s_2)^T) \leqslant \int_{|s_r| > \varepsilon} (s_1^2+s_2^2) dF_{\alpha,\Delta}^{(k)}((s_1,s_2)^T),$$

and by extending the range of integration of the right hand side from $|s_r| > \varepsilon$ to $s_1^2 + s_2^2 > \varepsilon^2$ we have

$$\int_{|s_r| > \varepsilon} s_r^2 dF_{\alpha,\Delta}^{(k)}((s_1,s_2)^T) \leqslant \int_{s_1^2+s_2^2>\varepsilon^2} (s_1^2+s_2^2) dF_{\alpha,\Delta}^{(k)}((s_1,s_2)^T).$$

Since $(s_1^2 + s_2^2)/\varepsilon^2 > 1$ whenever $s_1^2 + s_2^2 > \varepsilon^2$ we may increase the integrand on the right hand side by multiplying by $(s_1^2 + s_2^2)/\varepsilon^2$ and so obtain

$$\int_{|s_r| > \varepsilon} s_r^2 dF_{\alpha,\Delta}^{(k)}((s_1,s_2)^T) \leqslant \int_{s_1^2+s_2^2>\varepsilon^2} \varepsilon^{-2}(s_1^2+s_2^2)^2 dF_{\alpha,\Delta}^{(k)}((s_1,s_2)^T).$$

Next, extending the range of integration to the whole plane yields

$$\int_{|s_r| > \varepsilon} s_r^2 dF_{\alpha,\Delta}^{(k)}((s_1,s_2)^T) \leqslant \varepsilon^{-2} \int_{\mathbb{R}^2} (s_1^2+s_2^2)^2 dF_{\alpha,\Delta}^{(k)}((s_1,s_2)^T). \tag{5.6.4}$$

Because $F_{\alpha,\Delta}^{(k)}(.)$ denotes the probability distribution of $\underline{S}_{[\alpha k]}^{[(\alpha+\Delta)k]}/\sqrt{k}$ the right hand side above is just $\varepsilon^{-2}k^{-2}E[(R_{[\alpha k]}^{[(\alpha+\Delta)k]})^4]$. Now from Appendix 2 with $[\Delta k]$ replacing n we have

$$E[(R_{[\alpha k]}^{[(\alpha+\Delta)k]})^4] \leqslant a[\Delta k]^2$$

for some $a > 0$. Therefore from (5.6.4)

$$\int_{|s_r|>\varepsilon} s_r^2 dF^{(k)}_{\alpha,\Delta}((s_1,s_2)^T) \leqslant a\varepsilon^{-2}k^{-2}[\Delta k]^2 ,$$

whence

$$\lim_{\Delta\downarrow 0}\frac{1}{\Delta}\overline{\lim_{k\to\infty}}\int_{|s_r|>\varepsilon} s_r^2 dF^{(k)}_{\alpha,\Delta}((s_1,s_2)^T) \leqslant \lim_{\Delta\downarrow 0}\overline{\lim_{k\to\infty}}\frac{a[\Delta k]^2}{\Delta\varepsilon^2k^2} = 0$$

and the proof is complete. □

Thus the correlated random walk with Assumptions 5.1.1 satisfies the four conditions necessary to show that the distribution is asymptotically Normal (Appendix 3). The limiting moments are obtained from (5.4.24), (5.4.25) and (5.4.26) and we may state the following theorem.

THEOREM 5.6.1 If Assumptions 5.1.1 are satisfied by a particle undergoing a correlated random walk; and if

$$\sigma^2 = \{\tfrac{1}{2}\mu_2 + \mu_1^2 c/(1-c)\} ,$$

then as n increases $(S_{n1}/\sigma\sqrt{n}, S_{n2}/\sigma\sqrt{n})^T$ converges in distribution to that of two independent standard Normal random variables.

We note that this theorem also applies (with a different σ^2) under much less restrictive assumptions: in particular when $E[\sin\theta] \neq 0$.

5.7 Recurrence

One of the Assumptions 5.1.1 is that the motion of a paticle performing a correlated random walk is not restricted to a subset of $\mathbb{R}^2$. This implies that the whole of $\mathbb{R}^2$ is *accessible* to the particle, i.e. that for any point $\underline{x}$ in $\mathbb{R}^2$ and for any $\varepsilon > 0$ there is positive probability that a disc of radius ε centred at $\underline{x}$ is visited by the particle at some time. We now wish to know whether every such disc is *certain* to be visited, in which case the number of visits will be

infinite and the walk is recurrent (Spitzer 1964,p.7). To my knowledge the recurrence of random walks with correlated step directions has not been considered previously.

To prove that the walk is recurrent we will show that:

I) either all discs of positive radius are visited infinitely often or none are; and then

II) any disc of positive radius centred at the origin of $\mathbb{R}^2$ is visited infinitely often.

We will denote the disc of radius ε centred at $\underline{x}$ by $I_\varepsilon(\underline{x})$ and will define the point $\underline{x}$ to be a recurrent point if for any $\varepsilon > 0$ the disc $I_\varepsilon(\underline{x})$ is visited infinitely often with probability one. To prove result I (Lemma 5.7.2) we use a modified version of the methods of Chung and Fuchs (1954) for walks with independent steps. First we need to show that every point in $\mathbb{R}^2$ is accessible whatever the initial position and direction of the particle. Recall (Table 5.1.1) that $F_n(I;\underline{u},\zeta)$ denotes the probability that a particle performing a correlated random walk is in the set I after n steps, having started from $\underline{u}$ ($\in \mathbb{R}^2$) with initial direction ζ.

Lemma 5.7.1 Given any $\varepsilon > 0$, $\underline{u},\underline{x} \in \mathbb{R}^2$ and $0 \leqslant \zeta < 2\pi$, there is a positive integer m such that

$$F_m(I_\varepsilon(\underline{x});\underline{u},\zeta) > 0.$$

Thus every point in $\mathbb{R}^2$ is accessible whatever the initial position and direction of the particle.

Proof

By Assumptions 5.1.1 we know that for all $\underline{y} \in \mathbb{R}^2$ there is an m such that

$$F_m(I_\varepsilon(\underline{y});\underline{0},\xi) > 0. \tag{5.7.1}$$

Choose

$$\underline{y} = \begin{pmatrix} \cos(\xi-\zeta) & -\sin(\xi-\zeta) \\ \sin(\xi-\zeta) & \cos(\xi-\zeta) \end{pmatrix} \times (\underline{x} - \underline{u}),$$

which is the point $\underline{x}$ translated by $\underline{u}$ and rotated by $(\xi-\zeta)$ anticlockwise about the origin. By reversing the transformation we have

$$F_m(I_\varepsilon(\underline{y});\underline{0},\xi) = F_m(I_\varepsilon(\underline{x});\underline{u},\zeta)$$

and upon using (5.7.1) the lemma is proved. □

We can now prove result I.

Lemma 5.7.2 Either all points in $\mathcal{R}^2$ are recurrent or none are.

Proof

We shall suppose that $\underline{x}$ and $\underline{y}$ are two points in $\mathcal{R}^2$ and that $\underline{x}$ is recurrent, i.e. for all $\varepsilon > 0$

$$\Pr(\underline{S}_n \in I_\varepsilon(\underline{x}) \text{ for a finite number of indices n only}) = 0.$$

First we will show that at each visit to the set $I_\varepsilon(\underline{x})$ there is a positive probability of reaching $I_\varepsilon(\underline{y})$ within a fixed number, N_{min} say, of steps. For suppose the particle reaches a point $\underline{u}$ in $I_\varepsilon(\underline{x})$ and let the direction of the next step be ζ. Then by Lemma 5.7.1 there is a positive integer m such that

$$F_m(I_\varepsilon(\underline{y});\underline{u},\zeta) > 0 .$$

Therefore there is a minimum number of steps required to reach $I_\varepsilon(\underline{y})$ having started from $\underline{u},\zeta$, $m^*(\underline{u},\zeta)$ say, with

$$m^*(\underline{u},\zeta) = \min(m: F_m(I_\varepsilon(\underline{y});\underline{u},\zeta) > 0) .$$

Now choose the minimum number of steps, N_{min}, required for there to be positive probability of moving from any point in $I_\varepsilon(\underline{x})$ to $I_\varepsilon(\underline{y})$, i.e.

$$N_{min} = \sup_{\substack{\underline{u} \in I_\varepsilon(\underline{x}) \\ 0 \leqslant \zeta < 2\pi}} \{m^*(\underline{u},\zeta)\}$$

Next, choose the smallest positive probability, F_{min} say, of moving from $I_\varepsilon(\underline{x})$ to $I_\varepsilon(\underline{y})$ within the next N_{min} steps, i.e.

$$F_{min} = \inf_{\substack{\underline{u} \in I_\varepsilon(\underline{x}) \\ 0 \leqslant \zeta < 2\pi}} \{F_m(I_\varepsilon(\underline{y});\underline{u},\zeta): m=m^*(\underline{u},\zeta)\} .$$

Thus whenever the particle visits the set $I_\varepsilon(\underline{x})$ there is positive probability of at least F_{min} that the particle visits $I_\varepsilon(\underline{y})$ within the next N_{min} steps, where N_{min} is finite.

To show that $\underline{y}$ is recurrent we require that

$$\Pr(\underline{S}_n \in I_\varepsilon(\underline{y}) \text{ for a finite number of indices n only}) = 0.$$

Let us suppose that the particle visits $I_\varepsilon(\underline{y})$ only a finite number of times, and that the last visit occurs at the Nth step. We have

$$\Pr(\underline{S}_n \notin I_\varepsilon(\underline{y}) \text{ for } n > N \mid \underline{S}_N \in I_\varepsilon(\underline{y})) \leqslant \Pr(\text{No visits to } I_\varepsilon(\underline{y}) \text{ after the first return to } I_\varepsilon(\underline{x}) \text{ after the Nth step}),$$

and since $\underline{x}$ is a recurrent point and $I_\varepsilon(\underline{x})$ must be visited infinitely often

$$\Pr(\text{No visits to } I_\varepsilon(\underline{y}) \text{ after the first return to } I_\varepsilon(\underline{x}) \text{ after the Nth step}) = \Pr(\text{No visits to } I_\varepsilon(\underline{y}) \text{ within the next } N_{min} \text{ steps after the jth return to } I_\varepsilon(\underline{x}) \text{ after the Nth step for } j=1,2,\ldots)$$

At each return to $I_\varepsilon(\underline{x})$ there is probability of at least F_{min} that the particle visits $I_\varepsilon(\underline{y})$ during the next N_{min} steps, whence

$$\Pr(\text{No visits to } I_\varepsilon(\underline{y}) \text{ after the first return to } I_\varepsilon(\underline{x}) \text{ after the Nth step}) \leqslant \prod_{j=1}^{\infty}(1-F_{min}) = 0 .$$

This result is true whatever the value of N and therefore

$$\Pr(\underline{S}_n \in I_\varepsilon(\underline{y}) \text{ for a finite number of indices n only}) = 0 .$$

Thus if any point is recurrent then so too are all other points in $\mathbb{R}^2$ and the lemma is proved. □

To prove that the correlated random walk is recurrent we now need to prove result II, that for any $\varepsilon > 0$ the disc $I_\varepsilon(\underline{0})$ is visited infinitely often, i.e. that the origin is a recurrent point. Taken with Lemma 5.7.2 this shows that all points in $\mathbb{R}^2$ are recurrent. Our proof is based on a combination of the methods of Chung and Ornstein (1962) and Spitzer (1964,p.22-23). We require one preparatory lemma.

Lemma 5.7.3 The origin is a recurrent point if and only if for any $\varepsilon > 0$

$$\sum_{n=1}^{\infty} F_n(I_\varepsilon(\underline{0});\underline{0},\xi) = \infty .$$

Proof

i) Assume that the origin is a recurrent point. Then if

$$\sum_{n=1}^{\infty} F_n(I_\varepsilon(\underline{0});\underline{0},\xi) < \infty$$

the first Borel-Cantelli lemma (Kingman and Taylor 1966,p.337) implies that

$$\Pr(\underline{S}_n \in I_\varepsilon(\underline{0}) \text{ for infinitely many indices } n) = 0,$$

which contradicts our assumption for if the origin is a recurrent point then $I_\varepsilon(\underline{0})$ must be visited infinitely often. This shows that the condition is necessary.

ii) Assume that for any $\varepsilon > 0$

$$\sum_{n=1}^{\infty} F_n(I_\varepsilon(\underline{0});\underline{0},\xi) = \infty .$$

First we will show that the probability of never returning to any disc centred at the origin is zero, i.e. if

$$q(2\varepsilon) \equiv \Pr(\underline{S}_n \notin I_{2\varepsilon}(\underline{0}) \text{ for } n=1,2,\ldots) ,$$

then we wish to show that $q(2\varepsilon) = 0$ for any $\varepsilon > 0$.

Now,

$$1 \geqslant \Pr(\text{particle visits } I_\varepsilon(\underline{0}) \text{ a finite number of times only})$$

$$= \Pr(\text{particle never returns to } I_\varepsilon(\underline{0}))$$

$$+ \sum_{k=1}^{\infty} \Pr(\text{particle returns to } I_\varepsilon(\underline{0}) \text{ for the last time at step } k).$$

The probability of never returning to $I_\varepsilon(\underline{0})$ is non-negative whence

$$1 \geqslant \sum_{k=1}^{\infty} \Pr(\text{particle returns to } I_\varepsilon(\underline{0}) \text{ for the last time at step } k) ,$$

and by conditioning on $\underline{S}_k$ being in $I_\varepsilon(\underline{0})$ we have

$$(5.7.2)\quad 1 \geqslant \sum_{k=1}^{\infty} \Pr(\underline{S}_k \in I_\varepsilon(\underline{O}))\Pr(\underline{S}_{k+n} \notin I_\varepsilon(\underline{O}) \text{ for } n=1,2,\ldots \mid \underline{S}_k \in I_\varepsilon(\underline{O})).$$

Recall that $R_k^{(k+n)}$ denotes the distance between the particle's positions after k and (k+n) steps. Now, given that the particle is within distance ε of the origin after k steps, then it cannot be within distance ε of the origin after a further n steps if the distance $R_k^{(k+n)}$ exceeds 2ε. This is because if $\underline{S}_k \in I_\varepsilon(\underline{O})$ then the disc $I_\varepsilon(\underline{O})$ is entirely contained within the disc $I_{2\varepsilon}(\underline{S}_k)$. The distance $R_k^{(k+n)}$ exceeds 2ε when $\underline{S}_{k+n} \notin I_{2\varepsilon}(\underline{S}_k)$ and therefore we have the inequality

$$\Pr(\underline{S}_{k+n} \notin I_\varepsilon(\underline{O}) \text{ for } n=1,2,\ldots \mid \underline{S}_k \in I_\varepsilon(\underline{O}))$$

$$(5.7.3)\qquad \geqslant \Pr(\underline{S}_{k+n} \notin I_{2\varepsilon}(\underline{S}_k) \text{ for } n=1,2,\ldots \mid \underline{S}_k \in I_\varepsilon(\underline{O})) .$$

Conditional upon $\underline{S}_k$ the distribution of $\underline{S}_{k+n}$ is that of an n-step correlated random walk starting from $\underline{S}_k$ with initial direction $\xi+\theta_1+\ldots+\theta_k$. Thus

$$\Pr(\underline{S}_{k+n} \notin I_{2\varepsilon}(\underline{S}_k) \mid \underline{S}_k \in I_\varepsilon(\underline{O})) = 1 - F_n(I_{2\varepsilon}(\underline{S}_k); \underline{S}_k, \xi+\theta_1+\ldots+\theta_k)$$

$$= 1 - F_n(I_{2\varepsilon}(\underline{O}); \underline{O}, \xi+\theta_1+\ldots+\theta_k) .$$

By rotational symmetry the probability that an n-step correlated random walk ends in any disc centred at the origin is independent of the initial direction. Therefore

$$\Pr(\underline{S}_{k+n} \notin I_{2\varepsilon}(\underline{S}_k) \mid \underline{S}_k \in I_\varepsilon(\underline{O})) = 1 - F_n(I_{2\varepsilon}(\underline{O}); \underline{O}, \xi) ,$$

whence on recalling the definition of $q(2\varepsilon)$ as the probability that a correlated random walk never returns to the disc of radius 2ε centred at the origin, we have

$$\Pr(\underline{S}_{k+n} \notin I_{2\varepsilon}(\underline{S}_k) \text{ for } n=1,2,\ldots \mid \underline{S}_k \in I_\varepsilon(\underline{O})) = q(2\varepsilon).$$

Hence on returning to (5.7.2) and using (5.7.3) we now have

$$1 \geqslant \sum_{k=1}^{\infty} F_k(I_\varepsilon(\underline{O}); \underline{O}, \xi) q(2\varepsilon) .$$

Therefore because we have assumed that

$$\sum_{k=1}^{\infty} F_k(I_\varepsilon(\underline{0})) = \infty$$

it follows that for all $\varepsilon > 0$

$$q(2\varepsilon) = 0. \tag{5.7.4}$$

Thus the probability of never returning to any disc centred at the origin is zero.

We now use a similar method of conditioning on the time of the last entry to a disc centred at the origin to show that if

$$\sum_{k=1}^{\infty} F_k(I_\varepsilon(\underline{0})) = \infty$$

then

$$\Pr(\underline{S}_n \in I_\varepsilon(\underline{0}) \text{ for a finite number of indices n only}) = 0 ,$$

and the origin is a recurrent point. For

$$\Pr(\underline{S}_n \in I_\varepsilon(\underline{0}) \text{ for a finite number of indices n only}) = \Pr(\text{particle never returns to } I_\varepsilon(\underline{0})) + \sum_{k=1}^{\infty} \Pr(\text{particle returns to } I_\varepsilon(\underline{0}) \text{ for the last time at the kth step}).$$

By result (5.7.4) we know that the particle is certain to return to $I_\varepsilon(\underline{0})$ for all $\varepsilon > 0$, whence

$$\Pr(\underline{S}_n \in I_\varepsilon(\underline{0}) \text{ for a finite number of indices n only}) = \sum_{k=1}^{\infty} \Pr(\underline{S}_k \in I_\varepsilon(\underline{0}), \underline{S}_{k+n} \notin I_\varepsilon(\underline{0}) \text{ for } n=1,2,\ldots) . \tag{5.7.5}$$

For any integer $m > \varepsilon^{-1}$ denote the annulus between the two circles of radii $\varepsilon - m^{-1}$ and $\varepsilon - (m-1)^{-1}$, each centred at $\underline{x}$, by $A_{\varepsilon,m}(\underline{x})$. Conditional on $\underline{S}_k \in I_\varepsilon(\underline{0})$ there is a unique m such that $\underline{S}_k \in A_{\varepsilon,m}(\underline{0})$. Therefore by conditioning on the annulus in which the particle lies we have

$$\sum_{k=1}^{\infty} \Pr(\underline{S}_k \in I_\varepsilon(\underline{O}),\ \underline{S}_{k+n} \notin I_\varepsilon(\underline{O}) \text{ for } n=1,2,\ldots)$$

$$(5.7.6) \qquad = \sum_{m>1/\varepsilon} \sum_{k=1}^{\infty} \Pr(\underline{S}_{k+n} \notin I_\varepsilon(\underline{O}) \text{ for } n=1,2,\ldots \,|\, \underline{S}_k \in A_{\varepsilon,m}(\underline{O})) F_k(A_{\varepsilon,m}(\underline{O});\underline{O},\xi).$$

If $\underline{S}_k \in A_{\varepsilon,m}(\underline{O})$ the disc $I_{1/m}(\underline{S}_k)$ is contained entirely within the disc $I_\varepsilon(\underline{O})$ because the distance from the annulus to a circle of radius ε centred at the origin is $1/m$. Thus $\underline{S}_{k+n} \notin I_\varepsilon(\underline{O})$ implies that $\underline{S}_{k+n} \notin I_{1/m}(\underline{S}_k)$. Hence

$$\Pr(\underline{S}_{k+n} \notin I_\varepsilon(\underline{O}) \text{ for } n=1,2,\ldots \,|\, \underline{S}_k \in A_{\varepsilon,m}(\underline{O}))$$

$$(5.7.7) \qquad \leqslant \Pr(\underline{S}_{k+n} \notin I_{1/m}(\underline{S}_k) \text{ for } n=1,2,\ldots \,|\, \underline{S}_k \in A_{\varepsilon,m}(\underline{O})).$$

But conditional on the position of the particle after k steps the distribution of $\underline{S}_{k+n}$ is that of an n-step correlated random walk which began at $\underline{S}_k$ with initial direction $\xi+\theta_1+\ldots+\theta_k$. Therefore by rotational symmetry

$$\Pr(\underline{S}_{k+n} \notin I_{1/m}(\underline{S}_k) \,|\, \underline{S}_k \in A_{\varepsilon,m}(\underline{O})) = 1 - F_n(I_{1/m}(\underline{O});\underline{O},\xi) ,$$

and upon using (5.7.4) and (5.7.7) we have

$$\Pr(\underline{S}_{k+n} \notin I_\varepsilon(\underline{O}) \text{ for } n=1,2,\ldots \,|\, \underline{S}_k \in A_{\varepsilon,m}(\underline{O})) \leqslant q(m^{-1}) = 0 .$$

Therefore from (5.7.5) and (5.7.6)

$$\Pr(\underline{S}_n \in I_\varepsilon(\underline{O}) \text{ for a finite number of indices n only}) = 0 ,$$

and so the origin must be a recurrent point. This shows the sufficiency of the condition and completes the proof of Lemma 5.7.3. □

Now we may prove result II, that the origin is a recurrent point, and thus the following theorem.

THEOREM 5.7.1 The correlated random walk with Assumptions 5.1.1 is recurrent: all Borel sets of positive measure are visited infinitely often.

Proof

From Lemmas 5.7.2 and 5.7.3 we know that the walk is recurrent if and only if the series

$$\sum_{n=1}^{\infty} F_n(I_\varepsilon(\underline{0});\underline{0},\xi)$$

diverges for any $\varepsilon > 0$.

We may obtain a lower bound to the probability $F_n(I_\varepsilon(\underline{0});\underline{0},\xi)$ for large n using the central limit theorem for correlated random walk (Theorem 5.6.1). For the theorem states that as n increases

$$F_n(I_\varepsilon(\underline{0});\underline{0},\xi) \to \Pr(Z_1^2 + Z_2^2 < \varepsilon^2) \quad , \tag{5.7.8}$$

where Z_1 and Z_2 are independent zero mean Normal random variables, each with variance $n\sigma^2$ $(= n\{\tfrac{1}{2}\mu_2 + \mu_1^2 c/(1-c)\})$. Now the square of sides ε centred at the origin is entirely included within $I_\varepsilon(\underline{0})$, whence

$$\Pr(Z_1^2 + Z_2^2 < \varepsilon^2) > \{\int_{-\frac{1}{2}\varepsilon}^{\frac{1}{2}\varepsilon} (2\pi\sigma^2 n)^{-\frac{1}{2}} \exp(-x^2/2\sigma^2 n)\,dx\}^2 \quad .$$

Because $\exp(-x^2/2\sigma^2 n) > \exp(-\varepsilon^2/8\sigma^2 n)$ when $|x| < \tfrac{1}{2}\varepsilon$ we have

$$\Pr(Z_1^2 + Z_2^2 < \varepsilon^2) > \{\int_{-\frac{1}{2}\varepsilon}^{\frac{1}{2}\varepsilon} (2\pi\sigma^2)^{-\frac{1}{2}} \exp(-\varepsilon^2/8\sigma^2 n)\,dx\}^2 \quad .$$

The term within the braces is equal to $\varepsilon(2\pi\sigma^2 n)^{-\frac{1}{2}}\exp(-\varepsilon^2/8\sigma^2 n)$ which is greater than $\varepsilon(2\pi\sigma^2 n)^{-\frac{1}{2}}\exp(-1)$ when $n > \varepsilon^2/8\sigma^2$. Therefore

$$\Pr(Z_1^2 + Z_2^2 < \varepsilon^2) > bn^{-1} \tag{5.7.9}$$

for $n > \varepsilon^2/8\sigma^2$, where $b = \varepsilon^2(2\pi\sigma^2)^{-1}\exp(-2)$. The inequality in (5.7.9) is strict and so we may use (5.7.8) to find an n_o such that for all $n > n_o$

$$F_n(I_\varepsilon(\underline{0});\underline{0},\xi) > bn^{-1} \quad .$$

Therefore the series

$$\sum_{n=1}^{\infty} F_n(I_\varepsilon(\underline{0});\underline{0},\xi)$$

diverges and from Lemma 5.7.3 the origin is a recurrent point. Therefore from Lemma 5.7.2 all points in $\mathbb{R}^2$ must be recurrent. Finally, since any Borel set of positive measure must include a disc of positive radius and so must be visited infinitely often the proof of Theorem 5.7.1 is completed.

□

Theorem 5.7.1 completes our work on correlated random walks in a continuous space. The results which we have obtained will be discussed at the end of the following chapter, after similar results have been derived for correlated random walks on lattices.

CHAPTER 6

A RANDOM WALK WITH CORRELATED STEP DIRECTIONS: DISCRETE CASE

Classical random walk problems are usually concerned with motion over a discrete space: in this chapter we shall consider correlated random walks on one- and two-dimensional lattices.

Several of the results which are obtained for the one-dimensional case are also included in Renshaw and Henderson (1981). Other investigations into correlated random walks on a one-dimensional lattice have been made by Goldstein (1951), who obtained approximate expressions for the probabilities of being at any lattice point after a large number of steps, by Seth (1963), who derived the probability of return to the origin for the jth time at the nth step for any integers j and n, and by Cane (1967), who considered the effect of the initial conditions on the mean and variance of position after n steps. In addition, Mohan (1955), Jain(1971,1973) and Proudfoot and Lampard (1972) all considered the influence of an absorbing barrier.

For walks in higher dimensions Gillis(1955) established asymptotic expressions for the even-order moments and Domb and Fisher (1958), Domb, Gillis and Wilmers (1965) and Daley (1979) all studied walks with various types of correlation.

We shall consider the correlated random walk on a one-dimensional lattice in Section 6.1 and then extend the results to a two-dimensional walk in Section 6.2. In each case we shall use methods of difference equations and generating functions, although in some instances transition probability matrices are used in a similar manner to Nain and Kanwar Sen (1980). Each of Sections 6.1 and 6.2 includes an index of the main notation used in that section.

6.1 Correlated Random Walks on a One-Dimensional Lattice

The correlated random walk introduced in Section 5.1 may be confined to a one-dimensional lattice if all steps have unit length whilst the turning variable distribution, $G(.)$, is concentrated on $\{0\}$ and $\{\pi\}$ with weight p (say) at 0 and weight q $(= 1-p)$ at π. So

Pr(particle moves one unit in the same direction as the last step)

$$= p \text{ , and}$$

Pr(particle moves one unit in the opposite direction to the last step) $= q$.

If the walk satisfies these assumptions an exact expression for the probabilities

$$p_n(s) \equiv \Pr(\text{particle is at } s \text{ after } n \text{ steps})$$

may be derived and compared with the corresponding probabilities for the simple random walk (Section 6.1.i). Just as for the more general walk introduced in the previous chapter the mean and variance of the particle's position after n steps (for any n) may also be determined (Section 6.1.iii), the recurrence of the walk investigated (Section 6.1.v) and a limiting distribution for a large number of steps obtained (Section 6.1.vii). In addition, for this walk we may consider the number of lattice points visited by the particle during the first n steps of the walk (Section 6.1.vi).

We shall assume that the initial direction of the particle has probability $\frac{1}{2}$ of being in the positive direction and is otherwise in the negative direction.

The main notation to be used in this section is summarised for easy reference in Table 6.1.1.

6.1.i Probability distribution

An exact expression for the probability distribution $\{p_n(s)\}$ may be established by a conditioning argument based on the number of times the particle changes direction. For

Symbol	Interpretation
p	Pr(particle moves in the same direction as the previous step).
q	Pr(particle moves in the opposite direction to the previous step).
δ	$(p-q)$
$p_n(s)$	Pr(particle is at s after n steps).
μ_n	Mean of the distribution $\{p_n(s)\}$.
σ_n^2	Variance of the distribution $\{p_n(s)\}$.
$\Phi_n(\omega)$	Characteristic function of the distribution $\{p_n(s)\}$, i.e. $\Phi_n(\omega) \equiv \sum_{s=-\infty}^{\infty} \exp(i\omega s)p_n(s)$.
$U(z,s)$	Occupation probability generating function, i.e. $U(z,s) \equiv \sum_{j=0}^{\infty} z^j p_j(s)$.
E_1, E_2	The particle is in state E_1 if the previous step direction was positive and is otherwise in state E_2.
$p_{nj}(s)$	Pr(particle is at s and in state E_j after n steps),
$\phi_{nj}(s)$	Characteristic function of the distribution $\{p_{nj}(s)\}$, i.e. $\phi_{nj}(\omega) \equiv \sum_{s=-\infty}^{\infty} \exp(i\omega s)p_{nj}(s)$.
P	$\begin{pmatrix} p & q \\ q & p \end{pmatrix}$
$\Lambda(\omega)$	$\begin{pmatrix} \exp(i\omega) & 0 \\ 0 & \exp(-i\omega) \end{pmatrix}$
$f_n(s)$	Pr(point s is visited during the first n steps),
$r_n(s)$	Pr(first visit to s is at step n),
$R(z,s)$	$\sum_{n=1}^{\infty} z^n r_n(s)$
$N_E(n)$	Expected number of distinct lattice points visited during the first n steps.
Δ_n	$N_E(n) - N_E(n-1)$
$\Delta(z)$	$\sum_{n=1}^{\infty} z^n \Delta_n$

Table 6.1.1

Main notation for Section 6.1

$$p_{2n}(2s) = \sum_{k=0}^{\infty} \Pr(\text{particle is at } 2s \text{ after } 2n \text{ steps} \mid \text{particle changes direction } k \text{ times}) \times \Pr(k \text{ direction changes in } 2n \text{ steps}) .$$

Each walk of 2n steps has probability $\frac{1}{2}q^k p^{2n-k-1}$ of changing direction exactly k times. Let us therefore consider the number of such walks which end at position 2s, having made, of necessity, (n+s) positive and (n-s) negative steps.

Suppose that the first step is positive and that the particle then moves a_1 consecutive steps (including the first) in the positive direction until the first turn, followed by a_2 consecutive steps in the negative direction until the second turn, etc. We have conditioned on exactly k turns so that the

$$\text{total number of steps} = 2n = a_1+a_2+\ldots+a_{k+1} ,$$

$$\text{total number of positive steps} = n+s = a_1+a_3+\ldots+a_i ,$$

$$\text{total number of negative steps} = n-s = a_2+a_4+\ldots+a_j ,$$

where i = k+1 and j = k if k is even or else i = k and j = k+1 if k is odd.

Now the total number of ways in which (n+s) can be divided into $\frac{1}{2}(i+1)$ non-empty groups (because there must be at least one step between turns) is

$$\binom{n+s-1}{\frac{1}{2}(i+1)-1}$$

(Feller 1968,p.38). Similarly the total number of ways of dividing (n-s) into $\frac{1}{2}j$ non-empty groups is

$$\binom{n-s-1}{\frac{1}{2}j-1} .$$

Thus the total number of walks which end at 2s after 2n steps, having made exactly k turns and with the first step positive, is

$$\binom{n+s-1}{\frac{1}{2}(i+1)-1}\binom{n-s-1}{\frac{1}{2}j-1} .$$

Similarly, if the first step is in the negative direction there are

$$\binom{n-s-1}{\frac{1}{2}(i+1)-1}\binom{n+s-1}{\frac{1}{2}j-1}$$

such walks. Hence on summing over all possible values of k we have

$$p_{2n}(2s) = \tfrac{1}{2}\sum_{k=0}^{2n-2}{}^{|s|}\left\{\binom{n+s-1}{\frac{1}{2}(i+1)-1}\binom{n-s-1}{\frac{1}{2}j-1} + \binom{n-s-1}{\frac{1}{2}(i+1)-1}\binom{n+s-1}{\frac{1}{2}j-1}\right\}q^k p^{2n-k-1} .$$

By considering the two separate cases k even and k odd this expression may be written as

$$p_{2n}(2s) = \tfrac{1}{2}p^{2n-1}\delta_{|s|,n} + \tfrac{1}{2}\sum_{\ell=1}^{n-|s|} q^{2\ell}p^{2n-2\ell-1}\binom{n+s-1}{\ell}\binom{n-s-1}{\ell-1}$$

(6.1.1)

$$+ \binom{n-s-1}{\ell}\binom{n+s-1}{\ell-1} + 2pq^{-1}\binom{n+s-1}{\ell-1}\binom{n-s-1}{\ell-1}\Big\} ,$$

where

$$\delta_{|s|,n} = \begin{cases} 1 & \text{if } |s| = n \\ 0 & \text{otherwise,} \end{cases}$$

which is the Kronecker delta function.

By a similar method we have, for $s \geqslant 0$,

$$p_{2n+1}(-2s-1) = p_{2n+1}(2s+1) = \tfrac{1}{2}p^{2n}\delta_{s,n} + \tfrac{1}{2}\sum_{\ell=1}^{n-s} q^{2\ell}p^{2n-2\ell}\Big\{\binom{n+s}{\ell}\binom{n-s-1}{\ell-1}$$

(6.1.2)

$$+ \binom{n+s}{\ell-1}\binom{n-s-1}{\ell} + 2pq^{-1}\binom{n+s}{\ell-1}\binom{n-s-1}{\ell-1}\Big\} .$$

These expressions are also included in Renshaw and Henderson (1981).

By inspection we see that the distribution is symmetrical about the origin. When p is small the probability of the particle changing direction and so returning to a previously visited point is high and the distribution becomes concentrated about the origin (Figure 6.1.1). Conversely, for p close to unity the distribution is more evenly spread over the range $[-n,n]$. For p very close to unity the two end probabilities $p_n(-n)$ and $p_n(n)$ are each close to $\frac{1}{2}$ and the remaining total probability is evenly spread over the interior points $(-n,n)$.

When $p = \frac{1}{2}$ the correlated random walk is equivalent to the simple one-dimensional random walk and the distribution reduces to

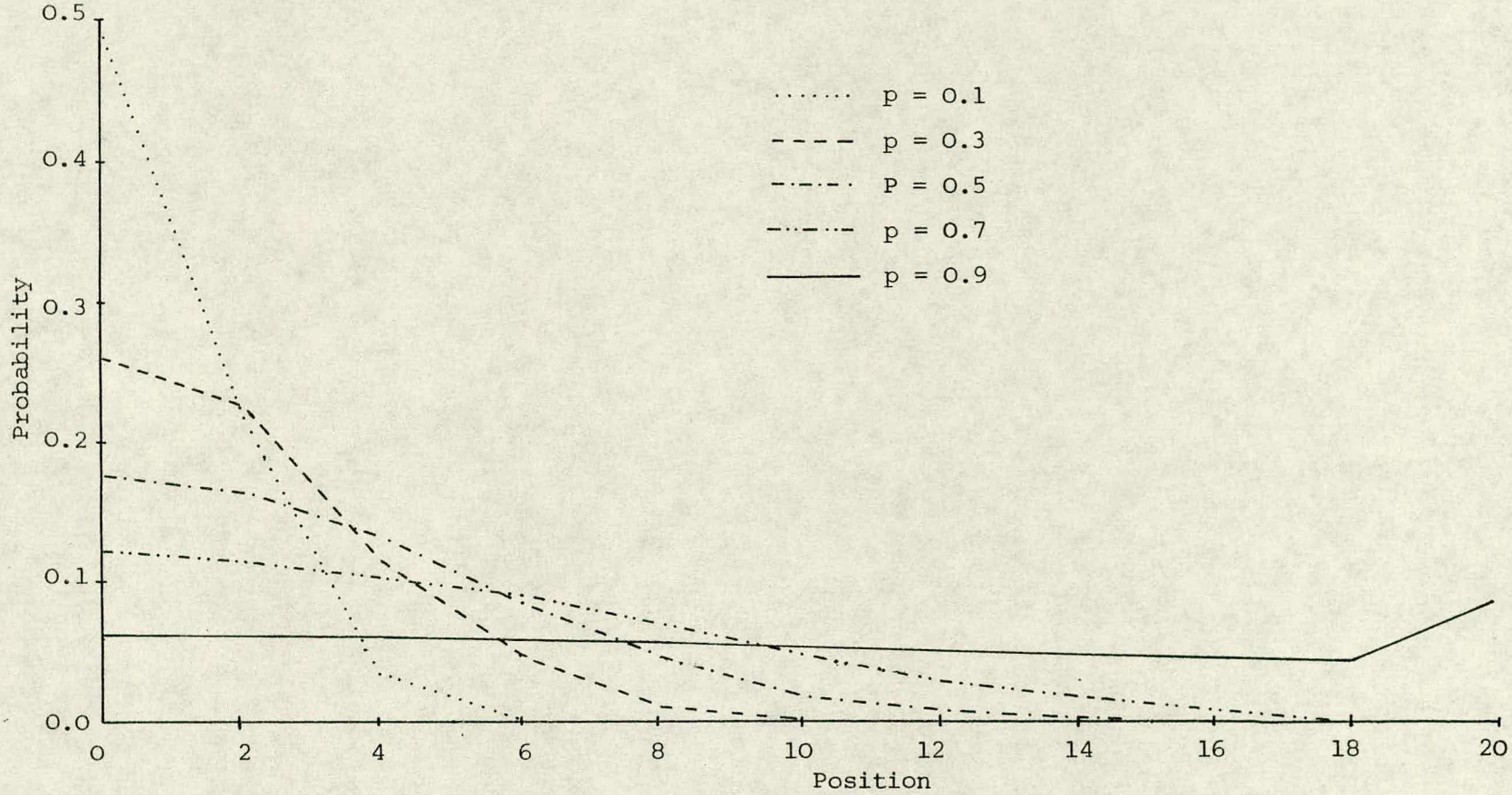


Figure 6.1.1

Values of $p_{20}(s)$ for s = 0(2)20

$$p_n(n-2\ell) = (\tfrac{1}{2})^n \binom{n}{\ell}$$

for $\ell = 0, 1, \ldots, n$.

6.1.ii Characteristic function of the probability distribution

In theory it should be possible to use expressions (6.1.1) and (6.1.2) to write down expressions for the moments of the distribution $\{p_n(s)\}$. In practice however it is much easier to differentiate the characteristic function

$$\Phi_n(\omega) \equiv \sum_{s=-\infty}^{\infty} \exp(i\omega s) p_n(s) \quad , \tag{6.1.3}$$

where ω is real and $i = \sqrt{(-1)}$.

In order to obtain an expression for $\Phi_n(\omega)$ we shall use the standard difference equation method. First let us define the particle to be in state E_1 if the previous step was in the positive direction, and to be in state E_2 if the previous step was in the negative direction. Then if

$$p_{nj}(s) \equiv \Pr(\text{particle is at } s \text{ and in state } E_j \text{ after } n \text{ steps})$$

for $j = 1, 2$, it follows that

$$p_n(s) = p_{n1}(s) + p_{n2}(s) \quad , \tag{6.1.4}$$

because the two states are mutually exclusive and exhaustive.

The particle may arrive at s in one step from either $(s-1)$ or $(s+1)$, whence

$$\begin{cases} p_{n1}(s) = pp_{n-1,1}(s-1) + qp_{n-1,2}(s-1) \\ p_{n2}(s) = qp_{n-1,1}(s+1) + pp_{n-1,2}(s+1) \end{cases} \tag{6.1.5}$$

for any $n > 1$. Now define

$$\phi_{nj}(\omega) \equiv \sum_{s=-\infty}^{\infty} \exp(i\omega s) p_{nj}(s)$$

for $j = 1, 2$, multiply each equation in (6.1.5) by $\exp(i\omega s)$ and sum over s. This procedure yields

$$(6.1.6)\qquad \begin{cases} \phi_{n1}(\omega) = pe^{i\omega}\phi_{n-1,1}(\omega) + qe^{i\omega}\phi_{n-1,2}(\omega) \\ \phi_{n2}(\omega) = qe^{-i\omega}\phi_{n-1,1}(\omega) + pe^{-i\omega}\phi_{n-1,2}(\omega) \ , \end{cases}$$

which may be rearranged as the two difference equations

$$(6.1.7)\qquad \phi_{n+1,j}(\omega) - 2p\cos(\omega)\phi_{nj}(\omega) + (p-q)\phi_{n-1,j}(\omega) = 0 \qquad (j=1,2).$$

The characteristic function $\Phi_n(\omega)$ of the probability distribution $\{p_n(s)\}$ may be obtained by solving (6.1.7) because from (6.1.4) we have

$$(6.1.8)\qquad \Phi_n(\omega) = \phi_{n1}(\omega) + \phi_{n2}(\omega).$$

However, a more concise expression for $\Phi_n(\omega)$ which is useful when the moments of $\{p_n(s)\}$ are determined (Section 6.1.iii) may be obtained by writing the equations (6.1.6) as

$$\underline{\phi}_n(\omega) = \Lambda(\omega)P\underline{\phi}_{n-1}(\omega) \ ,$$

where

$$\underline{\phi}_n(\omega) = (\phi_{n1}(\omega),\phi_{n2}(\omega))^T, \quad \Lambda(\omega) = \begin{pmatrix} e^{i\omega} & 0 \\ 0 & e^{-i\omega} \end{pmatrix} \text{ and } \quad P = \begin{pmatrix} p & q \\ q & p \end{pmatrix}.$$

For on solving recursively

$$\underline{\phi}_n(\omega) = (\Lambda(\omega)P)^n\underline{\phi}_0(\omega) \ ,$$

and since $\phi_{0j}(\omega) = \frac{1}{2}$ $(j=1,2)$, we have

$$\underline{\phi}_n(\omega) = \tfrac{1}{2}(\Lambda(\omega)P)^n\underline{h}_2 \ ,$$

where we use the symbol $\underline{h}_2$ to denote the vector $(1,1)^T$. Upon using (6.1.8) we finally obtain

$$(6.1.9)\qquad \Phi_n(\omega) = \tfrac{1}{2}\underline{h}_2^T(\Lambda(\omega)P)^n\underline{h}_2 \ .$$

6.1.iii Mean and Variance

The mean and variance of the particle's position after n steps, μ_n and σ_n^2 say, may be obtained by differentiating the characteristic

function $\Phi_n(\omega)$. For recall from (6.1.3) that

$$\Phi_n(\omega) = \sum_{s=-\infty}^{\infty} \exp(i\omega s) p_n(s) ,$$

whence

$$\frac{\partial \Phi_n(\omega)}{\partial \omega} = i \sum_{s=-\infty}^{\infty} s\exp(i\omega s) p_n(s)$$

and

$$\frac{\partial^2 \Phi_n(\omega)}{\partial \omega^2} = - \sum_{s=-\infty}^{\infty} s^2 \exp(i\omega s) p_n(s) .$$

Hence the mean and variance are given by

$$\mu_n = -i \frac{\partial \Phi_n(\omega)}{\partial \omega}\Big|_{\omega=0} \tag{6.1.10}$$

and

$$\sigma_n^2 = - \frac{\partial^2 \Phi_n(\omega)}{\partial \omega^2}\Big|_{\omega=0} - \mu_n^2 . \tag{6.1.11}$$

(For brevity we will write $\partial \Phi_n(0)/\partial\omega$ and $\partial^2 \Phi_n(0)/\partial\omega^2$ throughout the following for the first and second derivatives of $\Phi_n(\omega)$ evaluated at $\omega = 0$, respectively. In addition we will denote the matrix of derivatives $(\partial a_{jk}/\partial\omega)$ of any matrix A $(=(a_{jk}))$ by $\partial A/\partial\omega$.)

In order to evaluate μ_n and σ_n^2 we require expressions for $\partial \Phi_n(\omega)/\partial\omega$ and $\partial^2 \Phi_n(\omega)/\partial\omega^2$. To obtain these derivatives we shall use the formulation (6.1.9) of $\Phi_n(\omega)$ as a matrix product, because a similar method can be applied to find the moments of the two-dimensional lattice correlated random walk studied in Section 6.2.

Since the differential operator is linear we have from (6.1.9) that

$$\frac{\partial \Phi_n(\omega)}{\partial \omega} = \tfrac{1}{2} \underline{h}_2^T \{ \frac{\partial \{ (\Lambda(\omega)P)^n \}}{\partial \omega} \} \underline{h}_2 ,$$

and upon differentiating the matrix product we have

$$\frac{\partial \Phi_n(\omega)}{\partial \omega} = \tfrac{1}{2} \underline{h}_2^T \{ \sum_{k=0}^{n-1} (\Lambda(\omega)P)^k \frac{\partial (\Lambda(\omega)P)}{\partial \omega} (\Lambda(\omega)P)^{n-k-1} \} \underline{h}_2 . \tag{6.1.12}$$

The second derivative is more complicated. For

$$\frac{\partial^2 \Phi_n(\omega)}{\partial \omega^2} = \tfrac{1}{2}\underline{h}_2^T[\sum_{k=0}^{n-1}\{\frac{\partial(\Lambda(\omega)P)^k}{\partial\omega}\times\frac{\partial(\Lambda(\omega)P)}{\partial\omega}\times(\Lambda(\omega)P)^{n-k-1}$$

$$+ (\Lambda(\omega)P)^k\times\frac{\partial^2(\Lambda(\omega)P)}{\partial\omega^2}\times(\Lambda(\omega)P)^{n-k-1}$$

$$+ (\Lambda(\omega)P)^k\times\frac{\partial(\Lambda(\omega)P)}{\partial\omega}\times\frac{\partial(\Lambda(\omega)P)}{\partial\omega}^{n-k-1}\}]\underline{h}_2 .$$

By expanding the derivatives of $(\Lambda(\omega)P)^k$ and $(\Lambda(\omega)P)^{n-k}$ this may be written as

$$\frac{\partial^2 \Phi_n(\omega)}{\partial \omega^2} = \tfrac{1}{2}\underline{h}_2^T[\sum_{k=0}^{n-1}\{(\Lambda(\omega)P)^k\times\frac{\partial^2(\Lambda(\omega)P)}{\partial\omega^2}\times(\Lambda(\omega)P)^{n-k-1}$$

$$(6.1.13)\quad + \sum_{r=0}^{k-1}(\Lambda(\omega)P)^r\times\frac{\partial(\Lambda(\omega)P)}{\partial\omega}\times(\Lambda(\omega)P)^{k-r-1}\times\frac{\partial(\Lambda(\omega)P)}{\partial\omega}\times(\Lambda(\omega)P)^{n-k-1}$$

$$+ \sum_{r=0}^{n-k-2}(\Lambda(\omega)P)^k\times\frac{\partial(\Lambda(\omega)P)}{\partial\omega}\times(\Lambda(\omega)P)^r\times\frac{\partial(\Lambda(\omega)P)}{\partial\omega}\times(\Lambda(\omega)P)^{n-k-r-2}\}]\underline{h}_2 ,$$

where we use the convention that $\sum_{r=0}^{-1}(.) = 0$.

Considerable simplification is achieved at $\omega = 0$ because

$$\Lambda(0) = I_2 , \quad \frac{\partial\Lambda(0)}{\partial\omega} = \begin{pmatrix} i & 0 \\ 0 & -i \end{pmatrix} \text{ and } \frac{\partial^2\Lambda(0)}{\partial\omega^2} = -I_2 .$$

Also, the matrix P is independent of ω and so

$$\frac{\partial(\Lambda(\omega)P)}{\partial\omega} = \{\frac{\partial\Lambda(\omega)}{\partial\omega}\}P \quad \text{and} \quad \frac{\partial^2(\Lambda(\omega)P)}{\partial\omega^2} = \{\frac{\partial^2\Lambda(\omega)}{\partial\omega^2}\}P.$$

In addition, because P is doubly stochastic (Cox and Miller 1965,p.110) $\underline{h}_2^T P = \underline{h}_2^T$ and $P\underline{h}_2 = \underline{h}_2$. Thus when $\omega = 0$ terms such as

$$\frac{\partial(\Lambda(\omega)P)}{\partial\omega}\times(\Lambda(\omega)P)^{n-k-1}\ \underline{h}_2$$

reduce to

$$\frac{\partial \Lambda(0)}{\partial \omega}\, \underline{h}_2 \, .$$

Hence (6.1.12) and (6.1.13) evaluated at $\omega = 0$ become

$$\begin{aligned} \frac{\partial \Phi_n(0)}{\partial \omega} &= \tfrac{1}{2}\underline{h}_2^T \Big\{ \sum_{k=0}^{n-1} \frac{\partial \Lambda(0)}{\partial \omega} \Big\} \underline{h}_2 \\ &= \tfrac{1}{2} n \underline{h}_2^T \begin{pmatrix} i & 0 \\ 0 & -i \end{pmatrix} \underline{h}_2 \qquad (6.1.14) \\ &= 0 \, , \end{aligned}$$

and

$$\begin{aligned} \frac{\partial^2 \Phi_n(0)}{\partial \omega^2} = \tfrac{1}{2}\underline{h}_2^T \Big\{ \sum_{k=0}^{n-1} \frac{\partial^2 \Lambda(0)}{\partial \omega^2} \Big\} \underline{h}_2 + \tfrac{1}{2}\underline{h}_2^T \Big[\sum_{k=0}^{n-1} \Big\{ \sum_{r=0}^{k-1} \frac{\partial \Lambda(0)}{\partial \omega} \times P^{k-r} \times \frac{\partial \Lambda(0)}{\partial \omega} \\ + \sum_{r=0}^{n-k-2} \frac{\partial \Lambda(0)}{\partial \omega} \times P^{r+1} \times \frac{\partial \Lambda(0)}{\partial \omega} \Big\} \Big] \underline{h}_2 \, . \end{aligned}$$

The two double summations $\sum_{k=0}^{n-1} \sum_{r=0}^{k-1} P^{k-r}$ and $\sum_{k=0}^{n-1} \sum_{r=0}^{n-k-2} P^{r+1}$ are each equivalent to $\sum_{k=1}^{n-1} (n-k) P^k$, whence

$$\begin{aligned} \frac{\partial^2 \Phi_n(0)}{\partial \omega^2} &= -n + \underline{h}_2^T \begin{pmatrix} i & 0 \\ 0 & -i \end{pmatrix} \Big\{ \sum_{k=1}^{n-1} (n-k) P^k \Big\} \begin{pmatrix} i & 0 \\ 0 & -i \end{pmatrix} \underline{h}_2 \\ &= -n + (i,-i) \Big\{ \sum_{k=1}^{n-1} (n-k) P^k \Big\} (i,-i)^T \, . \end{aligned}$$

The spectral decomposition of the matrix P may be used to evaluate the term in braces. The spectral decomposition of any $d \times d$ matrix A, with eigenvalues λ_j $(j=1,2,\ldots,d)$ and corresponding left and right eigenvectors $\underline{x}_j^T$ and $\underline{y}_j$ respectively, is

$$A = \sum_{j=1}^{d} \lambda_j A_j \, ,$$

where $A_j = \underline{y}_j \underline{x}_j^T$ (Bailey 1964,p.48). With suitable scaling $A_j^2 = A_j$ and

because $A_j A_k = O$ when $j \neq k$ it follows that $A^k = \sum_{j=1}^{d} \lambda_j^k A_j$.

The matrix P has eigenvalues unity and (p-q), and spectral decomposition

$$P = \tfrac{1}{2}\begin{pmatrix} 1 & 1 \\ 1 & 1 \end{pmatrix} + \tfrac{1}{2}(p-q)\begin{pmatrix} 1 & -1 \\ -1 & 1 \end{pmatrix},$$

whence for any positive integer k

$$P^k = \tfrac{1}{2}\begin{pmatrix} 1 & 1 \\ 1 & 1 \end{pmatrix} + \tfrac{1}{2}(p-q)^k\begin{pmatrix} 1 & -1 \\ -1 & 1 \end{pmatrix}.$$

Therefore

$$\frac{\partial^2 \Phi_n(O)}{\partial \omega^2} = -n + \tfrac{1}{2}(i,-i)\begin{pmatrix} 1 & 1 \\ 1 & 1 \end{pmatrix}(i,-i)^T \sum_{k=1}^{n-1}(n-k)$$

$$+\tfrac{1}{2}(i,-i)\begin{pmatrix} 1 & -1 \\ -1 & 1 \end{pmatrix}(i,-i)^T \sum_{k=1}^{n-1}(n-k)(p-q)^k$$

$$= -n - 2\sum_{k=1}^{n-1}(n-k)(p-q)^k .$$

After a little algebra this expression reduces to

$$\frac{\partial^2 \Phi_n(O)}{\partial \omega^2} = \begin{cases} -[\,npq^{-1} + (p-q)\{(p-q)^n - 1\}/2q^2] & (q \neq O) \\ n^2 & (q = O). \end{cases} \tag{6.1.15}$$

Thus we have obtained expressions for the first two derivatives of $\Phi_n(\omega)$ evaluated at $\omega = O$ (6.1.14,6.1.15). Expressions (6.1.10) and (6.1.11) may now be used to yield the solutions

$$\mu_n = O \ , \quad \text{and}$$

$$\sigma_n^2 = \begin{cases} npq^{-1} + (p-q)\{(p-q)^n - 1\}/2q^2 & (q \neq O) \\ n^2 & (q = O). \end{cases}$$

These moments are also obtained (by another method) in Renshaw and Henderson (1981).

Thus the mean position of the particle after n steps is zero, which is obvious from the symmetry of the distribution $\{p_n(s)\}$ about

zero. If q is non-zero the variance is asymptotically proportional to n with constant of proportionality pq^{-1}. When $p = q = \frac{1}{2}$ the correlated random walk is equivalent to the simple random walk and so if $p > q$ the particle's position is more variable than for a simple random walk. Conversely, when $p < q$ the particle's position is less variable than for a simple random walk. When $q = 0$ each of the positions $\pm n$ is occupied with probability $\frac{1}{2}$ after n steps and the variance is n^2. When $q = 1$ the particle always changes direction and is situated at the origin after an even number of steps and at either ± 1 after an odd number of steps, whence $\sigma^2_{2n} = 0$ and $\sigma^2_{2n+1} = 1$.

6.1.iv Occupation probability generating function

The characteristic function $\Phi_n(\omega)$ is useful when the moments of the distribution $\{p_n(s)\}$ are investigated but when we consider the number of visits to any one lattice point the generating function

$$U(z,s) \equiv \sum_{j=0}^{\infty} z^j p_j(s) \qquad (0 \leq z < 1) \tag{6.1.16}$$

is more useful (Sections 6.1.v and 6.1.vi). We shall call U(z,s) the occupation probability generating function for the coefficient of z^j in U(z,s) is the probability that position s is occupied at time j.

An expression for U(z,s) may be derived from the matrix formulation (6.1.9) for the characteristic function $\Phi_n(\omega)$, namely

$$\Phi_n(\omega) = \tfrac{1}{2}\underline{h}_2^T(\Lambda(\omega)P)^n\underline{h}_2 .$$

For because

$$\int_{-\pi}^{\pi} \exp(ij\omega)\exp(-ik\omega)\,d\omega = \begin{cases} 2\pi & \text{if } j = k \\ 0 & \text{otherwise,} \end{cases}$$

the coefficient $p_n(s)$ of $\exp(i\omega s)$ may be extracted from $\Phi_n(\omega)$ by

$$p_n(s) = (2\pi)^{-1}\int_{-\pi}^{\pi} \Phi_n(\omega)\exp(-is\omega)\,d\omega .$$

Hence on multiplying each side of the above equation by z^n, summing over n and using the matrix formulation (6.1.9) for $\Phi_n(\omega)$, we have

$$U(z,s) = (4\pi)^{-1} \int_{-\pi}^{\pi} \{ \sum_{n=0}^{\infty} z^n \underline{h}_2^T (\Lambda(\omega)P)^n \underline{h}_2 \} \exp(-is\omega) d\omega$$

(6.1.17)

$$= (4\pi)^{-1} \int_{-\pi}^{\pi} \underline{h}_2^T \{ \sum_{n=0}^{\infty} z^n (\Lambda(\omega)P)^n \} \underline{h}_2 \exp(-is\omega) d\omega .$$

We may replace the matrix summation $\sum_{n=0}^{\infty} z^n (\Lambda(\omega)P)^n$ by $(I_2 - z\Lambda(\omega)P)^{-1}$ if this inverse exists. The existence is shown in the following lemma.

Lemma 6.1.1 The inverse of the matrix $(I_2 - z\Lambda(\omega)P)$ exists for all $0 \leqslant z < 1$.

Proof

The inverse obviously exists when $z = 0$, but suppose that there is a $0 < z_1 < 1$ such that no inverse exists. Then

$$|I_2 - z_1 \Lambda(\omega)P| = 0$$

and z_1^{-1} must be an eigenvalue of $\Lambda(\omega)P$.

Let $\underline{x}$ $(=(x_1, x_2)^T)$ be any two-dimensional vector and denote $\max\{|x_1|, |x_2|\}$ by $(\underline{x})_m$. We know that p and q are non-negative and less than unity and that $p + q = 1$, whence

$$(\underline{x})_m \geqslant \max\{|px_1 + qx_2|, |qx_1 + px_2|\},$$

and because $|\exp(i\omega)| = |\exp(-i\omega)| = 1$ we have

$$(\underline{x})_m \geqslant \max\{|(px_1 + qx_2)\exp(i\omega)|, |(qx_1 + px_2)\exp(-i\omega)|\} .$$

Therefore for any $\underline{x}$

$$(\underline{x})_m \geqslant (\Lambda(\omega)P\underline{x})_m . \qquad (6.1.18)$$

Now let us suppose that λ is an eigenvalue of $\Lambda(\omega)P$ with corresponding eigenvector $\underline{y}$. From (6.1.18) we have

$$(\underline{y})_m \geqslant (\Lambda(\omega)P\underline{y})_m = (\lambda\underline{y})_m = |\lambda| (\underline{y})_m .$$

Therefore no eigenvalue of $\Lambda(\omega)P$ has modulus greater than unity, and because $0 < z_1 < 1$ it follows that z_1^{-1} cannot be an eigenvalue of $\Lambda(\omega)P$. Hence the inverse of $(I_2 - z\Lambda(\omega)P)$ exists for all $0 \leqslant z < 1$ and the

proof of Lemma 6.1.1 is complete. □

On returning to (6.1.17) we now have

$$(6.1.19)\qquad U(z,s) = (4\pi)^{-1}\int_{-\pi}^{\pi} \underline{h}_2^T (I_2 - z\Lambda(\omega)P)^{-1}\underline{h}_2 \exp(-is\omega)\,d\omega .$$

In order to perform the integration we require the inverse of $(I_2 - z\Lambda(\omega)P)$. This matrix is

$$\begin{pmatrix} 1-zpe^{i\omega} & -zqe^{i\omega} \\ -zqe^{-i\omega} & 1-zpe^{-i\omega} \end{pmatrix}$$

which has determinant $1+z^2(p-q)-2zp\cos\omega$, and hence inverse

$$\{1+z^2(p-q)-2zp\cos\omega\}^{-1}\begin{pmatrix} 1-zpe^{-i\omega} & zqe^{i\omega} \\ zqe^{-i\omega} & 1-zpe^{i\omega} \end{pmatrix} .$$

Upon using this expression in (6.1.19) we see that

$$U(z,s) = (2\pi)^{-1}\int_{-\pi}^{\pi} \frac{\{1-z(p-q)\cos\omega\}\exp(-is\omega)\}}{\{1+z^2(p-q)-2zp\cos\omega\}}d\omega ,$$

and by writing $\exp(-is\omega)$ as $\cos(s\omega) - i\sin(s\omega)$ we have

$$(6.1.20)\qquad U(z,s) = (2\pi)^{-1}\int_{-\pi}^{\pi} \frac{\{1-z(p-q)\cos\omega\}\{\cos(s\omega)-i\sin(s\omega)\}}{\{1+z^2(p-q)-2zp\cos\omega\}}d\omega .$$

Now $\sin(s\omega) = -\sin(-s\omega)$ whilst $\cos(s\omega) = \cos(-s\omega)$. Therefore we may ignore the imaginary term in the above expression because

$$\int_{-\pi}^{\pi} \frac{\{1-z(p-q)\cos\omega\}\sin(s\omega)}{\{1+z^2(p-q)-2zp\cos\omega\}}\,d\omega = 0.$$

Therefore by writing $\cos\omega\cos(s\omega)$ as $\frac{1}{2}[\cos\{(s+1)\omega\}+\cos\{(s-1)\omega\}]$ we may reduce the expression (6.1.20) to

$$(6.1.21)\qquad U(z,s) = \pi^{-1}\int_{0}^{\pi} \frac{\{\cos(s\omega)-\frac{1}{2}z(p-q)[\cos\{(s+1)\omega\}+\cos\{(s-1)\omega\}]\}}{\{1+z^2(p-q)-2zp\cos\omega\}}\,d\omega .$$

The integration may now be performed with the use of the standard integral (Gradshteyn and Ryzhik 1965, result 3.613.1)

$$(6.1.22)\qquad \int_0^{\pi} \frac{\cos(nx)}{(1+u\cos x)}\,dx = \pi(1-u^2)^{-\frac{1}{2}}\left[\{(1-u^2)^{\frac{1}{2}}-1\}/u\right]^n \qquad (u^2 < 1).$$

First we need to show that $4z^2p^2/\{1+z^2(p-q)\}^2 < 1$, which is easily achieved. For

$$\begin{aligned} 1+z^2(p-q)-2zp &= 1+z^2(p^2-q^2)-2zp \\ &= (1-zp)^2-z^2q^2 \\ &= (1-z)\{1-z(p-q)\}. \end{aligned}$$

For $0 \leqslant z < 1$ the final term is positive and so by rearranging the first term we have

$$4z^2p^2/\{1+z^2(p-q)\}^2 < 1 .$$

Thus if (6.1.21) is written in the form

$$U(z,s) = \{1+z^2(p-q)\}^{-1}\pi^{-1}\int_0^{\pi} \frac{\{\cos(s\omega)-\frac{1}{2}z(p-q)[\cos\{(s+1)\omega\}+\cos\{(s-1)\omega\}]\}}{\{1+u\cos\omega\}}\,d\omega ,$$

where $u = -2zp/\{1+z^2(p-q)\}$, we may evaluate the integral with the use of (6.1.22). This procedure yields, with $\delta = (p-q)$,

$$\begin{aligned} U(z,s) = \frac{1}{\sqrt{\{(1+z^2\delta)^2-4z^2p^2\}}}\Bigg\{ &\left[\frac{1+z^2\delta-\sqrt{\{(1+z^2\delta)^2-4z^2p^2\}}}{2zp}\right]^{|s|} \\ &-\tfrac{1}{2}z\delta\left[\frac{1+z^2\delta-\sqrt{\{(1+z^2\delta)^2-4z^2p^2\}}}{2zp}\right]^{|s+1|} \\ &-\tfrac{1}{2}z\delta\left[\frac{1+z^2\delta-\sqrt{\{(1+z^2\delta)^2-4z^2p^2\}}}{2zp}\right]^{|s-1|}\Bigg\} . \end{aligned}$$

After some algebra the above expression reduces to

$$(6.1.23)\qquad U(z,s) = \frac{\{\sqrt{(1-z^2\delta^2)}\}[1+z^2\delta-\sqrt{\{(1-z^2)(1-z^2\delta^2)\}}]^{|s|}}{z^{|s|}(1+\delta)^{|s+1|}\sqrt{(1-z^2)}} \qquad (s \neq 0)$$

and

$$U(z,0) = (1+\delta)^{-1}\{\frac{\sqrt{(1-z^2\delta^2)}}{\sqrt{(1-z^2)}} + \delta\} . \tag{6.1.24}$$

Thus concise expressions for the occupation probability generating function have been derived and we may now consider the number of visits of the particle to any one lattice point.

6.1.v Recurrence and first passage times

Correlated random walks in a two-dimensional continuous space have been shown to visit all sets of positive measure infinitely often (Theorem 5.7.1). We now wish to know whether the one-dimensional lattice correlated random walk visits all lattice points infinitely often, i.e. whether the walk is recurrent.

Lemma 5.7.3 applies to the one-dimensional lattice walk as well as to the continuous space walk, whence the walk is recurrent if and only if

$$\sum_{n=0}^{\infty} p_n(0) = \infty .$$

By Chung and Fuchs (1951) this will be true if

$$\lim_{z\uparrow 1} \sum_{n=0}^{\infty} z^n p_n(0) = \infty .$$

Now, by using (6.1.16) and (6.1.24) we have

$$\sum_{n=0}^{\infty} z^n p_n(0) \equiv U(z,0) = (1+\delta)^{-1}\{\frac{\sqrt{(1-z^2\delta^2)}}{\sqrt{(1-z^2)}} + \delta\} ,$$

where, as earlier, $\delta = (p-q)$. Hence by inspection, provided that $p \neq 1$, we see that

$$\lim_{z\uparrow 1} U(z,0) = \infty ,$$

and so the walk is recurrent.

We note that it is possible to extend this result to a more general walk, where

$$\Pr(\text{particle moves one unit in the positive direction} \mid \text{last step positive}) = p_1 ,$$

$$\Pr(\text{particle moves one unit in the negative direction} \mid \text{last step positive}) = q_1 = (1-p_1) ,$$

$$\Pr(\text{particle moves one unit in the negative direction} \mid \text{last step negative}) = p_2 , \text{ and}$$

$$\Pr(\text{particle moves one unit in the positive direction} \mid \text{last step negative}) = q_2 = (1-p_2) .$$

The probability that a particle performing this type of random walk changes direction now depends upon the previous step direction. When $p_1 = p_2$ the new walk is equivalent to the correlated random walk which we have described, whilst when $p_1 = q_2$ the new walk is equivalent to an independent-step random walk on a one-dimensional lattice.

The occupation probability generating function of the new walk, $V(z,s)$ say, is given by analogy with (6.1.19) to be

$$V(z,s) = (4\pi)^{-1} \int_{-\pi}^{\pi} \underline{h}_2^T (I_2 - z\Lambda(\omega)Q)^{-1} \underline{h}_2 \exp(-is\omega) d\omega ,$$

where

$$Q = \begin{pmatrix} p_1 & q_2 \\ q_1 & p_2 \end{pmatrix} .$$

The integral may be evaluated for all s and we can show that

$$\lim_{z \uparrow 1} V(z,0) = \infty$$

if and only if $p_1 = p_2$.

Thus the new walk is recurrent only when it is equivalent to the correlated random walk.

Let us return to the correlated random walk, which is recurrent and therefore returns to the origin infinitely often with probability one. An interesting problem is to determine the expected number of

steps until the first return to the origin. This is well known to be infinite for the simple random walk even though the walk is recurrent (Cox and Miller 1965,p.41). But when $p < \frac{1}{2}$ the distribution $\{p_n(s)\}$ is more concentrated about the origin than the simple random walk equivalent (Figure 6.1.1) and perhaps the expected number of steps until the first return is finite.

Our methods are similar to those of Montroll (1964). Let

$$r_n(s) \equiv \Pr(\text{the particle visits point s for the first time at the nth step})$$

for $s \neq 0$, and

$$r_n(0) \equiv \Pr(\text{the particle returns to the origin for the first time at the nth step}) . \tag{6.1.25}$$

(We must distinguish between the origin and the other lattice points because the particle is initially situated at the origin and hence its first visit is at step zero). Next, define the probability generating function of the distribution $\{r_n(s)\}$ by

$$R(z,s) \equiv \sum_{n=1}^{\infty} z^n r_n(s) .$$

Now, by conditioning on the time until the first visit of the particle to position s we have

$$p_n(s) = \sum_{j=1}^{n} \Pr(\text{return to s after n steps} \mid \text{visit s for the first time after j steps}) \times \Pr(\text{visit s for the first time after j steps}) ,$$

and so by the definition of $r_j(s)$,

$$p_n(s) = \sum_{j=1}^{n} \Pr(\text{return to s after n steps} \mid \text{visit s for the first time after j steps}) \times r_j(s) .$$

The probability of return to the origin is independent of the initial direction of the particle as the axes may be rotated without affecting this probability. Thus the probability of return to s at the nth step conditional upon being at s after j steps must be independent of the direction of the jth step. Therefore

$$\Pr(\text{return to } s \text{ after } n \text{ steps} \mid \text{visit } s \text{ for the first time after } j \text{ steps}) = p_{n-j}(0) ,$$

whence

$$p_n(s) = \sum_{j=1}^{n} p_{n-j}(0) r_j(s) \qquad (n > 0) . \tag{6.1.26}$$

We can use this result to derive an expression for $R(z,s)$. For from the definition (6.1.16) we have

$$U(z,s) \equiv \sum_{n=0}^{\infty} z^n p_n(s) ,$$

which can be used in (6.1.26) to give

$$U(z,s) = \delta_{s,0} + \sum_{n=1}^{\infty} \sum_{j=1}^{n} z^n p_{n-j}(0) r_j(s) ,$$

where $\delta_{s,0}$ denotes the Kronecker delta function. If we write $k = (n-j)$ the right hand side above may be rearranged to yield

$$U(z,s) = \delta_{s,0} + \sum_{k=0}^{\infty} \sum_{j=1}^{\infty} z^j r_j(s) z^k p_k(0) .$$

Therefore by the definitions of $U(z,0)$ and $R(z,s)$ (Table 6.1.1) we have

$$U(z,s) = \delta_{s,0} + R(z,s)U(z,0) ,$$

and rearranging the terms yields

$$R(z,s) = \{U(z,s) - \delta_{s,0}\}/U(z,0) . \tag{6.1.27}$$

The expected number of steps until the first visit of the particle to any lattice point s (or first return to the origin if $s = 0$) is

$$\sum_{n=1}^{\infty} n r_n(s)$$

which is

$$\left.\frac{\partial R(z,s)}{\partial z}\right|_{z=1} .$$

Hence the expected number of steps until the first visit to any

lattice point may be determined by differentiating (6.1.27) with U(z,s) and U(z,0) replaced by their expansions (6.1.23) and (6.1.24) respectively.

In particular, the expected time until the first return to the origin is

$$\left.\frac{\partial R(z,0)}{\partial z}\right|_{z=1} .$$

From (6.1.27)

$$R(z,0) = 1 - \{U(z,0)\}^{-1} ,$$

whence

$$\frac{\partial R(z,0)}{\partial z} = \frac{\partial U(z,0)}{\partial z}\{U(z,0)\}^{-2} . \tag{6.1.28}$$

An expression for U(z,0) has been determined previously (6.1.24), namely

$$U(z,0) = (1+\delta)^{-1}\{\frac{\sqrt{(1-z^2\delta^2)}}{\sqrt{(1-z^2)}} + \delta\} ,$$

where, as usual, $\delta = (p-q)$. Differentiation yields

$$\frac{\partial U(z,0)}{\partial z} = (1-\delta)z/\{(1-z^2)^{3/2}(1-z^2\delta^2)^{\frac{1}{2}}\} .$$

Using these last two expressions in (6.1.28) we find that

$$\frac{\partial R(z,0)}{\partial z} = \frac{(1+\delta)^2(1-\delta)z}{(1-z^2)^{\frac{1}{2}}(1-z^2\delta^2)^{\frac{1}{2}}[1+\delta^2-2z^2\delta^2+2\{(1-z^2)^{\frac{1}{2}}(1-z^2\delta^2)^{\frac{1}{2}}\}]} .$$

Provided that $p \neq 0$ the right hand side tends to infinity as z is increased to unity. Therefore the expected time until the first return to the origin is infinite.

It is interesting to note that no matter how small the value of p, and therefore how high the probability, q, of immediate return to the origin after two steps, as long as p is positive the expected time until the first return to the origin is infinite.

6.1.vi Asymptotic number of points visited

The distribution $\{p_n(s)\}$ becomes more concentrated about zero as the parameter p is decreased (Figure 6.1.1). Therefore we expect the number of distinct lattice points visited by the particle during the first n steps of the walk to be typically lower at lower than at higher values of p. I have not been able to derive an expression for the expected number of distinct lattice points visited during the first n steps for all n, but by a similar method to that used by Montroll (1964) for independent-step random walks, an asymptotic expression may be obtained.

Define

$N_E(n) \equiv$ Expected number of distinct lattice points visited during the first n steps ,

and

$f_n(s) \equiv$ Pr(particle visits lattice point s at least once during the first n steps) .

By recalling the definition (Table 6.1.1) of $r_n(s)$ as the probability that the point s is visited for the first time at the nth step, we have

$$f_n(s) = \sum_{j=1}^{n} r_n(s). \tag{6.1.29}$$

Also, the expected number of lattice points visited by the particle during the first n steps may be expressed as a sum of the probabilities $\{f_n(s)\}$. For by definition

$$N_E(n) = \sum_{s=-\infty}^{\infty} \text{Pr(s is visited at least once during the first n steps)}$$

whence

$$N_E(n) = \sum_{s=-\infty}^{\infty} f_n(s) . \tag{6.1.30}$$

Our aim is to find an asymptotic expression for $N_E(n)$. First, we denote $N_E(n) - N_E(n-1)$ by Δ_n for $n > 0$ so that

$$N_E(n) = 1 + \Delta_1 + \Delta_2 + \ldots + \Delta_n \ .$$

Each of the terms Δ_j may be expanded by the use of expression (6.1.30), i.e.

$$\Delta_j = \sum_{s=-\infty}^{\infty} f_j(s) - \sum_{s=-\infty}^{\infty} f_{j-1}(s) \ ,$$

and upon using the expansion (6.1.29) for $f_j(s)$ and $f_{j-1}(s)$ we have

$$\Delta_j = \sum_{s=-\infty}^{\infty} \{ \sum_{k=1}^{j} r_k(s) - \sum_{k=1}^{j-1} r_k(s) \}$$

$$= \sum_{s=-\infty}^{\infty} r_j(s) \ .$$

Now let us define the generating function of the $\{\Delta_n\}$ by

$$\Delta(z) \equiv \sum_{n=1}^{\infty} z^n \Delta_n \ ,$$

whence

$$\Delta(z) = \sum_{s=-\infty}^{\infty} \sum_{n=1}^{\infty} z^n r_n(s) \ .$$

We may now find an expression for $\Delta(z)$ involving z and the generating function $U(z,0)$ only. For from the definition (Table 6.1.1) of the generating function $R(z,s)$ as

$$\sum_{n=1}^{\infty} z^n r_n(s)$$

we have

$$\Delta(z) = \sum_{s=-\infty}^{\infty} R(z,s) \ .$$

We know from (6.1.27) that

$$R(z,s) = \{U(z,s) - \delta_{s,0}\}/U(z,0)$$

and so we may write

(6.1.31) $$\Delta(z) = \{ \sum_{s=-\infty}^{\infty} U(z,s) - 1\}/U(z,0) \ .$$

The occupation probability generating function U(z,s) has been defined (6.1.16) as

$$\sum_{j=0}^{\infty} z^j p_j(s) \quad .$$

Therefore

$$\sum_{s=-\infty}^{\infty} U(z,s) = \sum_{j=0}^{\infty} z^j \{ \sum_{s=-\infty}^{\infty} p_j(s) \} = \sum_{j=0}^{\infty} z^j = (1-z)^{-1} \ ,$$

and from (6.1.31) we have

$$\Delta(z) = \{(1-z)^{-1} - 1\}/U(z,0) = z/\{(1-z)U(z,0)\} \ .$$

From the expression (6.1.24) for U(z,0) we see that as z is increased towards unity

$$U(z,0) \sim q^{\frac{1}{2}}/\{(1-z^2)p\}^{\frac{1}{2}} \ ,$$

and so for z close to unity

$$\Delta(z) \sim z\{(1-z^2)p\}^{\frac{1}{2}}/\{(1-z)q^{\frac{1}{2}}\}$$

$$\sim [2p/\{(1-z)q\}]^{\frac{1}{2}} \ .$$

We require an asymptotic expression for $N_E(n)$, which is

$$\sum_{j=1}^{n} \Delta_j \ ,$$

and we now have an approximate expression for

$$\sum_{j=1}^{\infty} z^j \Delta_j \ .$$

The required expression can be obtained from our expression for $\Delta(z)$ with the use of Theorem 108 of Hardy (1949), which states the following.

"Let the sum

$$S(y) = \sum_{n=1}^{\infty} a_n \exp(-ny)$$

be convergent for all $y > 0$, and let a_n be non-negative for all n. If, as $y \to 0$, $S(y) \sim \phi(y^{-1})$, where $\phi(x) \equiv \sigma^n L(x)$ is a positive increasing function of x for $x > x_0$, tending to infinity as x tends to infinity,

and if $\sigma > 0$ and $L(cx) \sim L(x)$ as $x \to \infty$, then as $n \to \infty$

$$a_1+\ldots+a_n \sim \phi(n)/\Gamma(\sigma+1) \ ."$$

In order to obtain an asymptotic expression for $N_E(n)$ $(=1+\Delta_1+\ldots+\Delta_n)$ we replace a_n in the above by Δ_n, $S(y)$ by $\Delta(z)$ and write $\exp(-y)$ for z. Then it is easy to show that the conditions of the theorem are satisfied. First, $\Delta(z)$ is convergent for all $0 \leqslant z < 1$. Second, $N_E(n)$ is an increasing function of n, whence Δ_n is non-negative. Third, as z increases to unity

$$\Delta(z) \sim [\,2p/\{(1-z)q\}]^{\frac{1}{2}} \ ,$$

so by writing $z = \exp(-y)$ we see that as $y \to 0$ so that $(1-e^{-y}) \sim y$ then

$$\Delta(e^{-y}) \sim \{2p/(yq)\}^{\frac{1}{2}}$$

$$= \phi(y^{-1}) \quad \text{(say)}.$$

Finally, the function $\phi(x) \equiv \{2p/q\}^{\frac{1}{2}}x^{\frac{1}{2}}$ satisfies the remaining conditions.

Hence by the above theorem

$$N_E(n) = 1+\Delta_1+\ldots+\Delta_n \sim \{2p/q\}^{\frac{1}{2}}n^{\frac{1}{2}}/\Gamma(3/2).$$

The gamma function may be evaluated with the use of result 8.339.2 of Gradshteyn and Ryzhik (1965) and the final result is

(6.1.32) $$N_E(n) \sim \{8np/\pi q\}^{\frac{1}{2}}$$

as n tends to infinity.

Thus the asymptotic expected number of distinct lattice points visited is proportional to the square root of the number of steps. The constant of proportionality is $\{8p/\pi q\}^{\frac{1}{2}}$ which is $\{8/\pi\}^{\frac{1}{2}}$ when $p = q$ and the correlated random walk is equivalent to the simple random walk. When $p < \frac{1}{2}$ then $p/q < 1$ and, as expected, the particle typically visits fewer lattice points during the first n steps than the simple random walk because the probability of changing direction and returning to a previously visited point is high. When $p > \frac{1}{2}$ then $p/q > 1$ and the particle typically visits more lattice points during

the first n steps, for large n, than a particle performing a simple random walk.

It is interesting to note that the asymptotic expected number of distinct lattice points visited is closely related to the standard deviation of the probability distribution $\{p_n(s)\}$, which was found (Section 6.1.iii) to be asymptotically equal to $\{pn/q\}^{\frac{1}{2}}$. Both are measures of the concentration of $\{p_n(s)\}$ about zero and we see that the scaling factor of the distribution $\{p_n(s)\}$ in comparison to the simple random walk is $\{p/q\}^{\frac{1}{2}}$.

6.1.vii Diffusion approximation

It is interesting to ask whether the limiting distribution as the number of steps increases whilst the distance between lattice points decreases is also the same as for the simple random walk except for the introduction of a scaling factor.

The limiting distribution when the distance between consecutive lattice points is chosen to be δx whilst the time interval between steps is δt (chosen to be of the same order of magnitude as $(\delta x)^2$), has been studied by Renshaw and Henderson (1981). We shall omit full details of the argument because the diffusion approximation technique is illustrated in Section 6.2.vi for two-dimensional correlated random walks. The final result is that as $\delta x, \delta t \to 0$ in such a way that $\delta t = O(\delta x^2)$ then the probability density of the particle being at x at time t is given by

$$p(x,t) = (2\pi\sigma^2 t)^{-\frac{1}{2}} \exp(-x^2/2\sigma^2 t) ,$$

where

$$\sigma^2 = \lim_{\delta x, \delta t \to 0} (p\delta x^2/q\delta t),$$

which is positive and finite. Thus the scaling factor is again $\{p/q\}^{\frac{1}{2}}$ in comparison with the equivalent result for the simple random walk.

To conclude our work on one-dimensional lattice correlated random walks we note that for fixed t the density p(x,t) is Normal, which is a similar result to the central limit theorem (Theorem 5.6.1) for correlated random walks on the whole of $\mathbb{R}^2$.

6.2 Correlated Random Walk on a Two-Dimensional Square Lattice

We now turn to correlated random walks on an infinite square lattice. In this case steps are again of unit length but the distribution of the turning variables, G(.), is now concentrated on the four values 0, $\pi/2$, π and $3\pi/2$. We will assume that the particle is initially situated at the origin and that the first step is equally likely to be in the positive or negative X- or Y-directions. At each subsequent step the particle moves one unit forwards, backwards, to the right or to the left of its previous step direction with probabilities f, b, r and ℓ respectively ($f+b+r+\ell=1$). In analogy to Section 6.1 we will define

$$p_n(s_1,s_2) \equiv \Pr(\text{particle is at lattice point } (s_1,s_2) \text{ after n steps}) .$$

I have not been able to find exact expressions for the probabilities $\{p_n(s_1,s_2)\}$. The method of conditioning on the number of direction changes which was used for one-dimensional walks (Section 6.1.i) is now too complicated because there are four possible directions and a similar method would require a conditioning on all twelve possible changes in direction. However, we may still use the characteristic function and occupation probability generating function methods to determine the mean and dispersion matrix of the distribution (Section 6.2.ii), the recurrence and mean recurrence time of the walk (Section 6.2.iv) and the asymptotic expected number of lattice points visited (Section 6.2.v). By allowing the distance between lattice points to be decreased as the number of steps is increased a diffusion approximation to the distribution $\{p_n(s_1,s_2)\}$ may be obtained also (Section 6.2.vi).

The main notation to be used in this section is summarised for easy reference in Table 6.2.1.

6.2.i Characteristic function of the probability distribution

As for the one-dimensional walk our first step is to find an expression for the characteristic function

$$\Phi_n(\omega_1,\omega_2) \equiv \sum_{s_1,s_2=-\infty}^{\infty} \exp(is_1\omega_1 + is_2\omega_2)p_n(s_1,s_2) \qquad (6.2.1)$$

Symbol	Interpretation
f,b,r,ℓ	Probability that the particle moves one unit forwards, backwards, to the right or to the left, respectively.
$p_n(s_1,s_2)$	Pr(particle is at (s_1,s_2) after n steps).
E_j $(j=1,2,3,4)$	Particle is in state E_1, E_2, E_3 or E_4 if the previous step was in the positive X-, negative X-, positive Y- or negative Y-direction, respectively.
$p_{nj}(s_1,s_2)$	Pr(particle is at (s_1,s_2) and in state E_j after n steps).
P	$\begin{pmatrix} f & b & r & \ell \\ b & f & \ell & r \\ \ell & r & f & b \\ r & \ell & b & f \end{pmatrix}$
$\Lambda(\omega_1,\omega_2)$	The diagonal matrix $\mathrm{diag}(e^{i\omega_1}, e^{-i\omega_1}, e^{i\omega_2}, e^{-i\omega_2})$.
$\phi_{nj}(\omega_1,\omega_2)$	Characteristic function of the distribution $\{p_{nj}(s_1,s_2)\}$.
$\Phi_n(\omega_1,\omega_2)$	Characteristic function of the distribution $\{p_n(s_1,s_2)\}$.
$\underline{h}_4$	The vector $(1,1,1,1)^T$.
μ_n,Σ_n	Mean and dispersion matrix of the distribution $\{p_n(s_1,s_2)\}$.
λ_j $(j=1,2,3,4)$	Eigenvalues of the matrix P.
$U(z,s_1,s_2)$	Occupation probability generating function, i.e. $U(z,s_1,s_2) \quad \sum_{n=1}^{\infty} z^n p_n(s_1,s_2)$.

Table 6.2.1

Main notation for Section 6.2

(Continued overleaf)

Symbol	Interpretation
$a_1(z)$	$1+2z^2(f^2-b^2)+z^4\{(f^2-b^2)^2-(\ell^2-r^2)^2+4fb(\ell^2+r^2)-4\ell r(f^2+b^2)\}$
$a_2(z)$	$-2zf+2z^3\{f(b^2-f^2)+2fr\ell-b(\ell^2+r^2)\}$
$a_3(z)$	$4z^2(f^2-r\ell)$
$\eta(z)$	$\{a_1(z)-a_3(z)\}^{-\frac{1}{2}}\{a_1(z)-2a_2(z)+a_3(z)\}^{-\frac{1}{2}}$
$\alpha(z)$	$\{a_1(z)+2a_2(z)+a_3(z)\}^{\frac{1}{2}}\{a_1(z)-a_3(z)\}^{-\frac{1}{2}}$
$\beta(z)$	$\{a_1(z)-a_3(z)\}^{\frac{1}{2}}\{a_1(z)-2a_2(z)+a_3(z)\}^{-\frac{1}{2}}$
$\gamma(z)$	$\{a_2(z)+a_3(z)\}\{a_2(z)-a_3(z)\}^{-1}$
$\tau_1(z)$	$2\{a_1(z)a_3(z)-a_2^2(z)\}^{\frac{1}{2}}[\{a_1(z)+a_3(z)\}^2-4a_2(z)]^{-\frac{1}{2}}$
$\tau_2(z)$	$2\{a_2^2(z)-a_1(z)a_3(z)\}^{\frac{1}{2}}\{a_1(z)-a_3(z)\}^{-1}$
$K(.)$	Complete elliptic integral of the first kind.
$\Pi(.\backslash.)$	Complete elliptic integral of the third kind.
$N_E(n)$	Expected number of distinct lattice points visited during the first n steps.
$v_1(t;x,y)$	Probability density function of the particle being situated at (x,y) at time t when the walk consists of a large number of short steps.

Table 6.2.1

Main notation for Section 6.2

(Continued)

so that moments of the distribution $\{p_n(s_1,s_2)\}$ may be determined by differentiation. First we define the particle to be in state E_1, E_2, E_3 or E_4 depending upon whether the previous step was in the positive X-, negative X-, positive Y- or negative Y-direction, respectively. These four states are mutually exclusive and exhaustive, whence if

$$p_{nj}(s_1,s_2) \equiv \Pr(\text{particle is at } (s_1,s_2) \text{ and in state } E_j \text{ after n steps}) ,$$

then

$$p_n(s_1,s_2) = \sum_{j=1}^{4} p_{nj}(s_1,s_2) . \tag{6.2.2}$$

Next an expression for $\Phi_n(\omega_1,\omega_2)$ may be obtained by similar methods to those used in Section 6.1.ii for one-dimensional correlated random walks. By considering the number of lattice points from which the particle may arrive at (s_1,s_2) in one move only, difference equations for $p_{nj}(s_1,s_2)$ $(j=1,2,3,4)$ may be found. This procedure yields

$$\left\{\begin{aligned}
p_{n1}(s_1,s_2) &= fp_{n-1,1}(s_1-1,s_2) + bp_{n-1,2}(s_1-1,s_2) \\
&\quad + rp_{n-1,3}(s_1-1,s_2) + \ell p_{n-1,4}(s_1-1,s_2) \\
p_{n2}(s_1,s_2) &= bp_{n-1,1}(s_1+1,s_2) + fp_{n-1,2}(s_1+1,s_2) \\
&\quad + \ell p_{n-1,3}(s_1+1,s_2) + rp_{n-1,4}(s_1+1,s_2) \\
p_{n3}(s_1,s_2) &= \ell p_{n-1,1}(s_1,s_2-1) + rp_{n-1,2}(s_1,s_2-1) \\
&\quad + fp_{n-1,3}(s_1,s_2-1) + bp_{n-1,4}(s_1,s_2-1) \\
p_{n4}(s_1,s_2) &= rp_{n-1,1}(s_1,s_2+1) + \ell p_{n-1,2}(s_1,s_2+1) \\
&\quad + bp_{n-1,3}(s_1,s_2+1) + fp_{n-1,4}(s_1,s_2+1).
\end{aligned}\right. \tag{6.2.3}$$

After multiplying each of these equations by $\exp(is_1\omega_1 + is_2\omega_2)$ and then summing over all s_1 and s_2 an expression for $\Phi_n(\omega_1,\omega_2)$ may be found by following the method of Section 6.1.ii. The final result is

$$\Phi_n(\omega_1,\omega_2) = \tfrac{1}{4}\underline{h}_4^T(\Lambda(\omega_1,\omega_2)P)^n\underline{h}_4 \,, \tag{6.2.4}$$

where $\underline{h}_4$ denotes the four-dimensional vector with all elements unity,

$$\Lambda(\omega_1,\omega_2) = \begin{pmatrix} \exp(i\omega_1) & 0 & 0 & 0 \\ 0 & \exp(-i\omega_1) & 0 & 0 \\ 0 & 0 & \exp(i\omega_2) & 0 \\ 0 & 0 & 0 & \exp(-i\omega_2) \end{pmatrix} \tag{6.2.5}$$

and where for this section

$$P = \begin{pmatrix} f & b & r & \ell \\ b & f & \ell & r \\ \ell & r & f & b \\ r & \ell & b & f \end{pmatrix}. \tag{6.2.6}$$

Thus the characteristic function of the distribution $\{p_n(s_1,s_2)\}$ may be expressed in vector-matrix notation in a similar manner to the the equivalent characteristic function for the one-dimensional correlated random walk (6.1.9). This is a very useful result because it allows the methods used in the one-dimensional case to be extended to the two-dimensional walk.

6.2.ii Mean and dispersion matrix

Let us denote the mean position of the particle after n steps by $\mu_n = (\mu_{n1},\mu_{n2})^T$ and the 2×2 dispersion matrix by $\Sigma_n = (\sigma^2_{njk})$. Then by differentiating the characteristic function $\Phi_n(\omega_1,\omega_2)$ we see that

$$\mu_{nj} = -i\frac{\partial\Phi_n(\omega_1,\omega_2)}{\partial\omega_j}\bigg|_{\omega_1=\omega_2=0} \qquad (j=1,2), \tag{6.2.7}$$

and

$$\sigma^2_{njk} = - \left. \frac{\partial^2 \Phi_n(\omega_1,\omega_2)}{\partial\omega_j \partial\omega_k} \right|_{\omega_1=\omega_2=0} - \mu_{nj}\mu_{nk} \qquad (j,k = 1,2) . \tag{6.2.8}$$

In analogy to Section 6.1.iii we will write $\partial\Phi_n(0,0)/\partial\omega_j$ and $\partial^2\Phi_n(0,0)/\partial\omega_j\partial\omega_k$ for the derivatives $\partial\Phi_n(\omega_1,\omega_2)/\partial\omega_j$ and $\partial^2\Phi_n(\omega_1,\omega_2)/\partial\omega_j\partial\omega_k$ evaluated at $\omega_1 = \omega_2 = 0$, respectively. Similarly for the matrices of derivatives of $\Lambda(\omega_1,\omega_2)$, which will be written as $\partial\Lambda(0,0)/\partial\omega_j$, etc. The methods which were used in Section 6.1.iii for the one-dimensional walk may be directly extended to the two-dimensional walk. Therefore we will omit many of the details and outine the method only. We have, by analogy to (6.1.14),

$$\frac{\partial\Phi_n(0,0)}{\partial\omega_j} = \tfrac{1}{4}\underline{h}_4^T \{ \frac{\partial\Lambda(0,0)}{\partial\omega_j} \} \underline{h}_4 \qquad (j = 1,2),$$

whence by the definition (6.2.5) of $\Lambda(\omega_1,\omega_2)$ we see that

$$\frac{\partial\Phi_n(0,0)}{\partial\omega_j} = 0 \qquad (j = 1,2).$$

Therefore, from (6.2.7), the mean position of the particle after n steps is again zero.

In order to derive an expression for the dispersion matrix the methods of Section 6.1.iii are again used to obtain

$$\begin{aligned} \frac{\partial^2\Phi_n(0,0)}{\partial\omega_j\partial\omega_k} = -\tfrac{1}{2}n\delta_{j,k} &+ \tfrac{1}{4}\underline{h}_4^T \{ \frac{\partial\Lambda(0,0)}{\partial\omega_j} [\sum_{m=1}^{n-1} (n-m)P^m] \frac{\partial\Lambda(0,0)}{\partial\omega_k} \} \underline{h}_4 \\ &+ \tfrac{1}{4}\underline{h}_4 \{ \frac{\partial\Lambda(0,0)}{\partial\omega_k} [\sum_{m=1}^{n-1} (n-m)P^m] \frac{\partial\Lambda(0,0)}{\partial\omega_j} \} \underline{h}_4, \end{aligned} \tag{6.2.9}$$

for j,k = 1,2 and where $\delta_{j,k}$ is the Kronecker delta function.

The spectral decomposition of the matrix P can be used to simplify (6.2.9). This matrix has eigenvalues $\lambda_1 = 1$, $\lambda_2 = f+b-r-\ell$, $\lambda_3 = (f-b)+i(r-\ell)$ and $\lambda_4 = (f-b)-i(r-\ell)$, and its spectral

decomposition is $\sum_{j=1}^{4} \lambda_j A_j$, where

$$A_1 = \tfrac{1}{4}\begin{bmatrix} 1 & 1 & 1 & 1 \\ 1 & 1 & 1 & 1 \\ 1 & 1 & 1 & 1 \\ 1 & 1 & 1 & 1 \end{bmatrix}, \qquad A_2 = \tfrac{1}{4}\begin{bmatrix} 1 & 1 & -1 & -1 \\ 1 & 1 & -1 & -1 \\ -1 & -1 & 1 & 1 \\ -1 & -1 & 1 & 1 \end{bmatrix},$$

$$A_3 = \tfrac{1}{4}\begin{bmatrix} 1 & -1 & -i & i \\ -1 & 1 & i & -i \\ i & -i & 1 & -1 \\ -i & i & -1 & 1 \end{bmatrix} \quad \text{and} \quad A_4 = \tfrac{1}{4}\begin{bmatrix} 1 & -1 & i & -i \\ -1 & 1 & -i & i \\ -i & i & 1 & -1 \\ i & -i & -1 & 1 \end{bmatrix}.$$

If we use the property that

$$P^m = \sum_{d=1}^{4} \lambda_d^m A_d$$

for any positive integer m expression (6.2.9) may be written as

$$\frac{\partial^2 \Phi_n(0,0)}{\partial\omega_j \partial\omega_k} = -\tfrac{1}{2}n\delta_{j,k} + \tfrac{1}{4}\sum_{d=1}^{4}\Big[\Big\{\sum_{m=1}^{n-1} \lambda_d^{m(n-m)}\Big\} \times \Big\{\underline{h}_4^T \frac{\partial\Lambda(0,0)}{\partial\omega_j} \times A_d \times \frac{\partial\Lambda(0,0)}{\partial\omega_k}\,\underline{h}_4 + \underline{h}_4^T \frac{\partial\Lambda(0,0)}{\partial\omega_k} \times A_d \times \frac{\partial\Lambda(0,0)}{\partial\omega_j}\,\underline{h}_4\Big\}\Big] \tag{6.2.10}$$

for j,k = 1,2.

By inspection we see that

$$\underline{h}_4^T \frac{\partial\Lambda(0,0)}{\partial\omega_j} \times A_d \times \frac{\partial\Lambda(0,0)}{\partial\omega_k}\,\underline{h}_4 = 0 \qquad (j,k,d = 1,2),$$

$$\underline{h}_4^T \frac{\partial\Lambda(0,0)}{\partial\omega_j} \times A_d \times \frac{\partial\Lambda(0,0)}{\partial\omega_j}\,\underline{h}_4 = -1 \qquad (j = 1,2\ ,\ d = 3,4),$$

$$\underline{h}_4^T \frac{\partial \Lambda(0,0)}{\partial \omega_1} \times A_3 \times \frac{\partial \Lambda(0,0)}{\partial \omega_2} \underline{h}_4 = -\underline{h}_4^T \frac{\partial \Lambda(0,0)}{\partial \omega_2} \times A_3 \times \frac{\partial \Lambda(0,0)}{\partial \omega_1} \underline{h}_4 = i ,$$

and

$$\underline{h}_4^T \frac{\partial \Lambda(0,0)}{\partial \omega_1} \times A_4 \times \frac{\partial \Lambda(0,0)}{\partial \omega_2} \underline{h}_4 = -\underline{h}_4^T \frac{\partial \Lambda(0,0)}{\partial \omega_2} \times A_4 \times \frac{\partial \Lambda(0,0)}{\partial \omega_1} \underline{h}_4 = -i .$$

Using these results in (6.2.10) we obtain

$$\frac{\partial^2 \Phi_n(0,0)}{\partial \omega_j^2} = -\tfrac{1}{2}n - \tfrac{1}{2}\{\sum_{m=1}^{n-1} (n-m)\lambda_3^m\} - \tfrac{1}{2}\{\sum_{m=1}^{n-1} (n-m)\lambda_4^m\} \quad (j=1,2) ,$$

and

$$\frac{\partial^2 \Phi_n(0,0)}{\partial \omega_j \partial \omega_k} = 0 \qquad (j \neq k) .$$

Thus the off-diagonal terms of the dispersion matrix are zero and

$$\Sigma_n = \tfrac{1}{2}[\, n\{1+\lambda_3(1-\lambda_3)^{-1}+\lambda_4(1-\lambda_4)^{-1}\} - \lambda_3(1-\lambda_3^n)(1-\lambda_3)^{-2} - \lambda_4(1-\lambda_4^n)(1-\lambda_4)^{-2}]\, I_2 ,$$

where I_2 is the 2×2 identity matrix.

The two coordinates of the particle's position are uncorrelated and, like the one-dimensional case, each has variance asymptotically proportional to n. The constant of proportionality for this walk is $\tfrac{1}{2}\{1+\lambda_3(1-\lambda_3)^{-1}+\lambda_4(1-\lambda_4)^{-1}\}$, which may be rearranged as

$$\frac{\tfrac{1}{2}\{1-(f-b)^2-(r-\ell)^2\}}{\{1-2(f-b)+(f-b)^2+(r-\ell)^2\}}$$

provided that $f \neq 1$.

Therefore if $f = b$ and $r = \ell$ the variance is constant whatever the choice of f. This is a very interesting result for which we can suggest no intuitive explanation. When $f = b$ but $r \neq \ell$ the variance decreases as $|r-\ell|$ increases, perhaps because the probability that the path of the particle forms a closed loop also increases. When $r = \ell$

but $f \neq b$ the variance increases with f because the probability of moving away from the origin without any direction changes increases. The minimum variance occurs when $b = 1$ and the distribution is concentrated on $\{(0,0),(0,1),(0,-1),(1,0),(-1,0)\}$. The maximum variance occurs when $f = 1$ and each of the sites $(n,0)$, $(-n,0)$, $(0,n)$ and $(0,-n)$ is occupied with probability $\frac{1}{4}$.

6.2.iii Occupation probability generating function

Just as for the one-dimensional lattice correlated random walk the recurrence and asymptotic number of lattice points visited may be investigated with the use of the occupation probability generating function

$$U(z,s_1,s_2) \equiv \sum_{n=0}^{\infty} z^n p_n(s_1,s_2) \qquad (0 \leqslant z < 1), \tag{6.2.11}$$

which, by analogy with (6.1.19), is

$$U(z,s_1,s_2) = (4\pi)^{-2} \int_{-\pi}^{\pi} \int_{-\pi}^{\pi} \underline{h}_4^T (I_4 - z\Lambda(\omega_1,\omega_2)P)^{-1} \underline{h}_4 \exp(-i\omega_1 s_1 - i\omega_2 s_2)\, d\omega_1 d\omega_2 , \tag{6.2.12}$$

where I_4 is the 4×4 identity matrix. The existence of $(I_4 - z\Lambda(\omega_1,\omega_2)P)^{-1}$ for all $0 \leqslant z < 1$ is shown by a similar proof to that of Lemma 6.1.1.

I have not been able to derive an expression for $U(z,s_1,s_2)$ for general (s_1,s_2). However, as for the one-dimensional correlated random walk, the value when $s_1 = s_2 = 0$ is most useful and in that case an explicit expression may be derived.

The determinant of the matrix $(I_4 - z\Lambda(\omega_1,\omega_2)$ may be shown to be

$$a_1(z) + a_2(z)\{\cos\omega_1 + \cos\omega_2\} + a_3(z)\cos\omega_1\cos\omega_2 ,$$

where

$$a_1(z) = 1 + 2z^2(f^2-b^2) + z^4\{(f^2-b^2)^2 - (\ell^2-r^2)^2 + 4fb(\ell^2+r^2) - 4\ell r(f^2+b^2)\} , \tag{6.2.13}$$

$$a_2(z) = -2zf + 2z^3\{f(b^2-f^2) + 2fr\ell - b(\ell^2+r^2)\}, \tag{6.2.14}$$

and

(6.2.15) $$a_3(z) = 4z^2(f^2-r\ell).$$

Using this notation we may expand the matrix $(I_4-z\Lambda(\omega_1,\omega_2)P)^{-1}$ to show

$$\underline{h}_4^T(I_4-z\Lambda(\omega_1,\omega_2)P)^{-1}\underline{h}_4 = \frac{4[A_1(z)+\frac{1}{2}A_2(z)\{\cos\omega_1+\cos\omega_2\}+A_3(z)\cos\omega_1\cos\omega_2]}{a_1(z)+a_2(z)\{\cos\omega_1+\cos\omega_2\}+a_3(z)\cos\omega_1\cos\omega_2},$$

where

(6.2.16) $$A_1(z) = 1+z^2(f-b)(1-2r-2\ell),$$

(6.2.17) $$A_2(z) = (1-4f)z+z^3\{(b-f)^2+(\ell-r)^2\}\{2\ell+2r-1\},$$

and

(6.2.18) $$A_3(z) = z^2\{(f-b)(2f-r-\ell)+(r-\ell)^2\}.$$

Therefore upon using expression (6.2.12) and the symmetry in ω_1 and ω_2 of $\underline{h}_4^T(I_4-z\Lambda(\omega_1,\omega_2)P)^{-1}\underline{h}_4$ we have

(6.2.19) $$U(z,0,0) = \tfrac{1}{4}\pi^{-2}\int_{-\pi}^{\pi}\int_{-\pi}^{\pi}\frac{A_1(z)+A_2(z)\cos\omega_1+A_3(z)\cos\omega_1\cos\omega_2}{\{a_1(z)+a_2(z)\cos\omega_1\}+\{a_2(z)+a_3(z)\cos\omega_1\}\cos\omega_2}d\omega_1 d\omega_2 .$$

Integration with respect to ω_2 can be performed with the use of result 3.613.1 of Gradshteyn and Ryzhik (1965) (which has been quoted previously (6.1.22)). This gives

(6.2.20) $$U(z,0,0) = \pi^{-1}\{A_1(z)I_1(z)+A_2(z)I_2(z)+A_3(z)I_3(z)\},$$

where

(6.2.21) $$I_1(z) = \int_0^{\pi}[\{a_1(z)+a_2(z)\cos\omega_1\}^2-\{a_2(z)+a_3(z)\cos\omega_1\}^2]^{-\frac{1}{2}}d\omega_1 ,$$

(6.2.22) $$I_2(z) = \int_0^{\pi}[\{a_1(z)+a_2(z)\cos\omega_1\}^2-\{a_2(z)+a_3(z)\cos\omega_1\}^2]^{-\frac{1}{2}}\cos\omega_1 d\omega_1 ,$$

and

$$I_3(z) = \int_0^{\pi} \cos\omega_1 \{a_2(z)+a_3(z)\cos\omega_1\}^{-1} d\omega_1$$

$$- \int_0^{\pi} \{a_1(z)+a_2(z)\cos\omega_1\}\cos\omega_1 \{a_2(z)+a_3(z)\cos\omega_1\}^{-1}$$

(6.2.23)

$$\times [\{a_1(z)+a_2(z)\cos\omega_1\}^2 - \{a_2(z)+a_3(z)\cos\omega_1\}^2]^{-\frac{1}{2}} d\omega_1 .$$

Each of these three integrals may be evaluated although the algebra becomes quite complicated. Before performing the integrations we will quote the four standard integrals which are required and will introduce some new notation. The standard integrals are as follows.

1 (Gradshteyn and Ryzhik 1965, result 3.152.1).

$$\int_0^{\infty} \{(x^2+u^2)(x^2+v^2)\}^{-\frac{1}{2}} dx = u^{-1} K(\{u^2-v^2\}^{\frac{1}{2}}/u) \qquad (u>v>0) , \tag{6.2.24}$$

where K(.) denotes the complete elliptic integral of the first kind, i.e.

$$K(w) = \int_0^{\frac{1}{2}\pi} (1-w^2\sin^2 x)^{\frac{1}{2}} dx \tag{6.2.25}$$

(Gradshteyn and Ryzhik 1965, definition 8.110).

2 (Gradshteyn and Ryzhik 1965, result 3.157.2).

$$\int_0^{\infty} (g-x^2)^{-1} \{(x^2+u^2)(x^2+v^2)\}^{-\frac{1}{2}} dx = -\{u(u^2+g)\}^{-1} [\Pi(1+gu^{-2} \backslash \{u^2-v^2\}^{\frac{1}{2}}/u)$$

$$- K(\{u^2-v^2\}^{\frac{1}{2}}/u)] \qquad (u^2>v^2) , \tag{6.2.26}$$

where $\Pi(.\backslash.)$ denotes the complete elliptic integral of the third kind, i.e.

$$\Pi(d\backslash w) = \int_0^{\frac{1}{2}\pi} (1+d\sin^2 x)^{-1} (1-w^2\sin^2 x)^{-\frac{1}{2}} dx \tag{6.2.27}$$

(Gradshteyn and Ryzhik 1965, definition 8.110). It should be noted

that several authors use the notation

$$\Pi(d\backslash w) = \int_0^{\frac{1}{2}\pi} (1-d\sin^2 x)^{-1}(1-w^2\sin^2 x)^{-\frac{1}{2}}dx \quad .$$

3 (Gradshteyn and Ryzhik 1965, result 2.553.3).

$$(6.2.28)\quad \int (u+v\cos x)^{-1}dx = \begin{cases} 2(u^2-v^2)^{-\frac{1}{2}}\arctan\{(u^2-v^2)^{\frac{1}{2}}(u+v)^{-1}\tan(\tfrac{1}{2}x)\} & (u^2>v^2) \\ (v^2-u^2)^{-\frac{1}{2}}\log\left\{\dfrac{(v^2-u^2)^{\frac{1}{2}}\tan(\tfrac{1}{2}x)+u+v}{(v^2-u^2)^{\frac{1}{2}}\tan(\tfrac{1}{2}x)-u-v}\right\} & (v^2>u^2) \end{cases} .$$

4 (Gradshteyn and Ryzhik 1965, result 2.554.2).

$$(6.2.29)\quad \int \cos x(u+v\cos x)^{-1}dx = xv^{-1} - uv^{-1}\int (u+v\cos x)^{-1}dx \quad .$$

The new notation is

$$\eta(z) \equiv \{a_1(z)-a_3(z)\}^{-\frac{1}{2}}\{a_1(z)-2a_2(z)+a_3(z)\}^{-\frac{1}{2}} ,$$

$$\alpha(z) \equiv \{a_1(z)+2a_2(z)+a_3(z)\}^{\frac{1}{2}}\{a_1(z)-a_3(z)\}^{-\frac{1}{2}} ,$$

$$\beta(z) \equiv \{a_1(z)-a_3(z)\}^{\frac{1}{2}}\{a_1(z)-2a_2(z)+a_3(z)\}^{-\frac{1}{2}} ,$$

$$\gamma(z) \equiv \{a_2(z)+a_3(z)\}\{a_2(z)-a_3(z)\}^{-1} ,$$

$$\tau_1(z) \equiv 2\{a_1(z)a_3(z)-a_2^2(z)\}^{\frac{1}{2}}[\{a_1(z)+a_3(z)\}^2-4a_2(z)]^{-\frac{1}{2}}$$

and

$$\tau_2(z) \equiv 2\{a_2^2(z)-a_1(z)a_3(z)\}^{\frac{1}{2}}\{a_1(z)-a_3(z)\}^{-1} .$$

We shall also require four inequalities. The first three follow directly from the positivity of the determinant of $(I_4-z\Lambda(\omega_1,\omega_2)P)$ for all ω_1 and ω_2. For this determinant may be written as $a_1(z)+a_2(z)\{\cos\omega_1+\cos\omega_2\}+a_3(z)\cos\omega_1\cos\omega_2$, whence

$$(6.2.30a)\qquad \begin{cases} a_1(z)+2a_2(z)+a_3(z) > 0 & (0 \leqslant z < 1) \\ a_1(z)-2a_2(z)+a_3(z) > 0 & (0 \leqslant z < 1) \\ a_1(z) - a_3(z) > 0 & (0 \leqslant z < 1) \ . \end{cases}$$

The fourth inequality, which is obtained from the definitions of $a_2(z)$ and $a_3(z)$ (6.2.14, 6.2.15), is

$$(6.2.30b)\qquad a_2(z)+a_3(z) < 0 \qquad (0 \leqslant z < 1) \ .$$

Taken together these inequalities show that $\eta(z)$, $\alpha(z)$ and $\beta(z)$ are always real and positive.

Now we can evaluate the three integrals $I_1(z)$, $I_2(z)$ and $I_3(z)$ defined by (6.2.21), (6.2.22) and (6.2.23) respectively.

i) $I_1(z)$

We have

$$I_1(z) = \int_0^{\pi} [\{a_1(z)+a_2(z)\cos\omega_1\}^2-\{a_2(z)+a_3(z)\cos\omega_1\}^2]^{-\frac{1}{2}}d\omega_1 \ ,$$

and if we make the transformation $t = \tan(\frac{1}{2}\omega_1)$ we have

$$I_1(z) = 2\eta(z)\int_0^{\infty} [\{t^2+\alpha^2(z)\}\{t^2+\beta^2(z)\}]^{-\frac{1}{2}}dt \ ,$$

which is in the standard form (6.2.24). Therefore

$$(6.2.31)\qquad I_1(z) = \begin{cases} 2\eta(z)\alpha^{-1}(z)K(\tau_1(z)) & (\alpha^2(z) > \beta^2(z)) \\ 2\eta(z)\beta^{-1}(z)K(\tau_2(z)) & (\beta^2(z) \geqslant \alpha^2(z)) \ , \end{cases}$$

where $K(.)$ is the complete elliptic integral of the first kind (6.2.25).

ii) $I_2(z)$

Similarly, the integral $I_2(z)$ given by (6.2.22) can be written in the standard forms (6.2.24) and (6.2.26) by the use of two elementary transformations, namely $t = \tan(\frac{1}{2}\omega_1)$ first and then $s = 1/t$. The final solution is

$$I_2(z) = \begin{cases} -2\eta(z)[\alpha^{-1}(z)\{\alpha^2(z)-1\}\{K(\tau_1(z))-\Pi(1-\alpha^{-2}(z)\backslash\tau_1(z))\} \\ \quad -\beta^2(z)\{1-\beta^2(z)\}^{-1}\alpha^{-1}(z)\{K(\tau_1(z))-\Pi(1-\beta^2(z)\backslash\tau_1(z))\}] \\ \qquad\qquad (\alpha^2(z) > \beta^2(z)) \\ -2\eta(z)[\beta^{-1}(z)\{\beta^2(z)-1\}\{K(\tau_2(z))-\Pi(1-\beta^{-2}(z)\backslash\tau_2(z))\} \\ \quad -\alpha^2(z)\{1-\alpha^2(z)\}^{-1}\beta^{-1}(z)\{K(\tau_2(z))-\Pi(1-\alpha^2(z)\backslash\tau_2(z))\}] \\ \qquad\qquad (\alpha^2(z) \leqslant \beta^2(z)) \end{cases} \tag{6.2.32}$$

where $\Pi(.\backslash.)$ denotes the complete elliptic integral of the third kind (6.2.27).

iii) $I_3(z)$

We can separate the integral $I_3(z)$, which is given by (6.2.23), into two components, i.e.

$$I_3(z) = J_1(z) + J_2(z) , \tag{6.2.33}$$

where

$$J_1(z) = \int_0^{\pi} \cos\omega_1\{a_2(z)+a_3(z)\cos\omega_1\}^{-1}d\omega_1$$

and

$$J_2(z) = -\int_0^{\pi} \cos\omega_1\{a_1(z)+a_2(z)\cos\omega_1\}\{a_2(z)+a_3(z)\cos\omega_1\}^{-1} \times [\{a_1(z)+a_2(z)\cos\omega_1\}^2-\{a_2(z)+a_3(z)\cos\omega_1\}^2]^{-\frac{1}{2}}d\omega_1 .$$

The integral $J_1(z)$ is in a standard form and may be evaluated with the use of expressions (6.2.28) and (6.2.29). This yields

$$J_1(z) = \begin{cases} \pi\{a_2^2(z)-a_3^2(z)\}^{-\frac{1}{2}}a_3^{-1}(z)[\{a_2^2(z)-a_3^2(z)\}^{\frac{1}{2}}-a_2(z)] \\ \qquad\qquad (a_2(z) > a_3(z),\ a_3(z) \neq 0) \\ \pi a_3^{-1}(z) \qquad\qquad (a_2(z) \leqslant a_3(z),\ a_3(z) \neq 0) \\ 0 \qquad\qquad (a_3(z) = 0) . \end{cases} \tag{6.2.34}$$

We may express the integral $J_2(z)$ in the standard forms (6.2.24) and (6.2.26) by using the two elementary transformations $t = \tan(\tfrac{1}{2}\omega_1)$ and $s = 1/t$. The standard integrals can be evaluated and the final result is

$$J_2(z) = 2\{a_2(z)-a_3(z)\}^{-1}\eta(z)\Big[\{a_1(z)+a_2(z)+\frac{4a_2(z)\gamma(z)}{1-\gamma(z)}\}$$

$$\times \frac{\{K(\tau_1(z))-\Pi(1-\gamma(z)\alpha^{-2}(z)\backslash\tau_1(z))\}}{\alpha(z)\{\alpha^2(z)-\gamma(z)\}}$$

(6.2.35a)

$$+ \frac{\{a_2(z)-a_1(z)\}\beta^2(z)}{\alpha(z)\gamma(z)\{1-\beta^2(z)/\gamma(z)\}}\{K(\tau_1(z))-\Pi(1-\beta^2(z)\gamma^{-1}(z)\backslash\tau_1(z))\}$$

$$- \frac{4a_2(z)\{\alpha^2(z)-1\}}{\{1-\gamma(z)\}\alpha(z)}\{K(\tau_1(z))-\Pi(1-\alpha^{-2}(z)\backslash\tau_1(z))\}\Big]$$

whenever $\alpha^2(z) > \beta^2(z)$, and otherwise

$$J_2(z) = 2\{a_2(z)-a_3(z)\}^{-1}\eta(z)\Big[\{a_1(z)+a_2(z)+\frac{4a_2(z)\gamma(z)}{1-\gamma(z)}\}$$

$$\times \frac{\{K(\tau_2(z))-\Pi(1-\gamma(z)\beta^{-2}(z)\backslash\tau_2(z))\}}{\beta(z)\{\beta^2(z)-\gamma(z)\}}$$

(6.2.35b)

$$+ \frac{\{a_2(z)-a_1(z)\}\alpha^2(z)}{\beta(z)\gamma(z)\{1-\alpha^2(z)/\gamma(z)\}}\{K(\tau_2(z))-\Pi(1-\alpha^2(z)\gamma^{-1}(z)\backslash\tau_2(z))\}$$

$$- \frac{4a_2(z)\{\beta^2(z)-1\}}{\{1-\gamma(z)\}\beta(z)}\{K(\tau_2(z))-\Pi(1-\beta^{-2}(z)\backslash\tau_2(z))\}\Big] \ .$$

If required an expression for $U(z,0,0)$ may now be obtained from results (6.2.31) to (6.2.35). Obviously such an expression will be very difficult to manipulate because each term depends upon the sign of $\beta^2(z) - \alpha^2(z)$. But z is a dummy variable and Lemma 6.2.1 shows that if we choose z sufficiently close to unity then $\beta^2(z) - \alpha^2(z) \geqslant 0$.

Lemma 6.2.1 There is a $z_o < 1$ such that for $z_o < z < 1$

$$\beta^2(z) - \alpha^2(z) \geq 0 .$$

Proof

From the definitions (Table 6.2.1) of $\alpha^2(z)$ and $\beta^2(z)$ we have

$$\beta^2(z)-\alpha^2(z) = \frac{4\{a_2^2(z)-a_1(z)a_3(z)\}}{\{a_1(z)-2a_2(z)+a_3(z)\}\{a_1(z)-a_3(z)\}},$$

and by the inequalities (6.2.30) it follows that $\beta^2(z) - \alpha^2(z) \geq 0$ if and only if $a_2^2(z)-a_1(z)a_3(z) \geq 0$.

Now, we know that $|I_4-P| = 0$ because the matrix P is doubly stochastic (Cox and Miller 1965,p.123). Because $\Lambda(0,0) = I_4$ it follows that $|I_4-z\Lambda(0,0)P| = 0$ at $z = 1$. Therefore by the expansion of $|I_4-z\Lambda(\omega_1,\omega_2)P|$ (6.2.13 to 6.2.15) we have

$$a_1(1)+2a_2(1)+a_2(1) = 0 ,$$

which implies

$$4a_2^2(1) = \{a_1(1)+a_3(1)\}^2 .$$

Let us suppose, for the moment, that $a_1(1) \neq a_3(1)$, whence

$$4a_2^2(1) > \{a_1(1)+a_3(1)\}^2-\{a_1(1)-a_3(1)\}^2 = 4a_1(1)a_3(1) .$$

The function $a_2^2(z) - a_1(z)a_3(z)$ is, by definitions (6.2.13) to (6.2.15), a polynomial in z and can be defined for all z. Choose z_o to be the largest real root below unity of the polynomial and let $z_o = -\infty$ if the polynomial has no real roots below unity. From the above inequality we know that $a_2^2(1) - a_1(1)a_3(1) > 0$ if $a_1(1) \neq a_3(1)$ whence in that case $a_2^2(z) - a_1(z)a_3(z) > 0$ for $z_o < z < 1$ and the lemma is proved.

Now let us suppose that $a_1(1) = a_3(1)$. Except in the trivial case of $b = 1$ the term $a_1(1)$ is always positive and because $a_3(z)$ is a non-decreasing function of z with $a_3(0) = 0$, then $a_1(1) = a_3(1)$ implies that $a_3(z)$ is positive for $z > 0$. In addition, we have $a_2(z) + a_3(z) < 0$ (6.2.30) whence $a_2(z) < 0$ and so $a_2(z) - a_3(z) < 0$

for $0 < z < 1$. Thus

$$a_2^2(z) - a_3^2(z) > 0$$

for $0 < z < 1$. We have assumed that $a_1(1) = a_3(1)$ whence

$$a_2^2(1) - a_1(1)a_3(1) > 0 ,$$

and by the same argument as for the case when $a_1(1) \neq a_3(1)$ the lemma is proved. □

Throughout the following we shall assume that z is chosen to be greater than z_o. Therefore the alternatives when $\alpha^2(z) > \beta^2(z)$ may be neglected and a unified expression for U(z,0,0) obtained. First, we note that $a_2(z) - a_3(z)$ is identically zero only in the trivial case of one of the parameters b, r or ℓ being unity. Otherwise $a_2(z) - a_3(z)$ may be zero for a finite number of values of z only, which we can ignore.

So, after some simplification we obtain

$$\begin{aligned} U(z,0,0) = \pi^{-1}[& B_1(z)K(\tau_2(z)) + B_2(z)\Pi(1-\alpha^2(z)\backslash\tau_2(z)) \\ & + B_3(z)\Pi(1-\alpha^2(z)\gamma^{-1}(z)\backslash\tau_2(z)) + B_4(z)\Pi(1-\beta^{-2}(z)\backslash\tau_2(z)) \\ & + B_5(z)\Pi(1-\gamma(z)\beta^{-2}(z)\backslash\tau_2(z)) + A_3(z)J_1(z)] , \end{aligned} \tag{6.2.36}$$

where

$$\begin{aligned} B_1(z) = & \frac{2A_1(z)}{\{a_1(z)-a_3(z)\}} - A_2(z)[\frac{\{a_1(z)-2a_2(z)+a_3(z)\}}{\{a_1(z)-a_3(z)\}\{a_2(z)-a_3(z)\}} \\ & + \frac{\{a_1(z)+2a_2(z)+a_3(z)\}}{\{a_1(z)-a_3(z)\}\{a_2(z)+a_3(z)\}}] \\ & + A_3(z)[\frac{\{a_1(z)-2a_2(z)+a_3(z)\}\{a_2(z)+a_3(z)\}\{a_2(z)-a_1(z)\}}{\{a_2^2(z)-a_1(z)a_3(z)\}\{a_1(z)-a_3(z)\}\{a_2(z)-a_3(z)\}} \\ & + \frac{\{a_2(z)-a_1(z)\}\{a_1(z)+2a_2(z)+a_3(z)\}}{\{a_1(z)-a_3(z)\}\{a_2^2(z)-a_1(z)a_3(z)\}}] , \end{aligned} \tag{6.2.37}$$

$$(6.2.38)\quad B_2(z) = A_2(z)\left[\frac{\{a_1(z)+2a_2(z)+a_3(z)\}}{\{a_1(z)-a_3(z)\}\{a_2(z)+a_3(z)\}}\right],$$

$$(6.2.39)\quad B_3(z) = A_3(z)\left[\frac{\{a_1(z)+2a_2(z)+a_3(z)\}\{a_1(z)-a_2(z)\}}{\{a_1(z)-a_3(z)\}\{a_2^2(z)-a_1(z)a_3(z)\}}\right],$$

$$(6.2.40)\quad B_4(z) = \begin{cases} \dfrac{\{a_1(z)-2a_2(z)+a_3(z)\}}{\{a_1(z)-a_3(z)\}\{a_2(z)-a_3(z)\}}\left[A_2(z)-2A_3(z)/a_3(z)\right] & (a_3(z)\neq 0) \\ A_2(z)\left[\dfrac{\{a_1(z)-2a_2(z)\}}{a_1(z)a_2(z)}\right] & (a_3(z)=0) \end{cases}$$

and

$$(6.2.41)\quad B_5(z) = \begin{cases} A_3(z)\left[\dfrac{\{2a_2^2(z)+a_2(z)a_3(z)-a_1(z)a_3(z)\}}{\{a_2^2(z)-a_1(z)a_3(z)\}}\right. & \\ \qquad\left.\times\dfrac{\{a_1(z)-2a_2(z)+a_3(z)\}}{a_3(z)\{a_1(z)-a_3(z)\}}\right] & (a_3(z)\neq 0) \\ 0 & (a_3(z)=0). \end{cases}$$

The term $J_1(z)$ is defined by (6.2.34), $K(.)$ and $\Pi(.\backslash.)$ denote the complete elliptic integrals of the first and third kinds respectively and the other terms are defined by (6.2.13) to (6.2.18). Thus we have an expression for $U(z,0,0)$ in terms of known functions, albeit very complicated ones.

However, as for the one-dimensional walk (Sections 6.1.v and 6.1.vi) an asymptotic expression for $U(z,0,0)$ as z increases towards unity is very useful. Furthermore, as z increases expression (6.2.36) simplifies considerably, for $a_1(z)+2a_2(z)+a_3(z) = |I_4-zP|$ and $|I_4-P| = 0$ whence $a_1(z)+2a_2(z)+a_3(z)$ tends to zero as z tends to unity from below. From this result we see that $\alpha^2(z) \to 0$ and $\tau_2(z) \to 1$ as $z \to 1$. In addition, we may replace the elliptic

integrals of the third kind by more simple expressions. For if the parameters of an elliptic integral of the third kind depend on z, say d(z) and w(z), and if w(z) → 1 as z → 1, then for z close to unity

$$\Pi(d(z)\backslash w(z)) \sim \begin{cases} \{1+d(z)\}^{-1} & (d(1) = -1) \\ \{1+d(z)\}^{-1}K(w(z)) & (d(1) \neq -1), \end{cases}$$

(Byrd and Friedman 1954, results 111.01, 112.01, 114.01 and 115.01).

Using these results we finally obtain, for z close to unity,

$$U(z,0,0) \sim \pi^{-1}C(z)K(\tau_2(z)) + D(z) , \tag{6.2.41}$$

where

$$C(z) = B_1(z)+\beta^2(z)B_4(z)+\beta^2(z)\gamma^{-1}(z)B_5(z) \tag{6.2.42}$$

and

$$D(z) = \pi^{-1}\left[\frac{A_2(z)}{a_2(z)+a_3(z)} + A_3(z)\frac{\{a_2^2(z)-a_1(z)a_3(z)\}\{a_2(z)+a_3(z)\}}{\{a_1(z)-a_2(z)\}\{a_2(z)-a_3(z)\}} + A_3(z)J_1(z)\right].$$

We can now proceed to consider the recurrence, mean recurrence time and asymptotic number of lattice points visited by the particle.

6.2.iv Recurrence and first passage times

Correlated random walks on a one dimensional lattice and when not restricted to a subset of $\mathbb{R}^2$ are recurrent (Section 6.1.v and Theorem 5.7.1) and one expects a similar property for walks on a two-dimensional lattice. To prove recurrence we must consider the limiting behaviour of the occupation probability generating function U(z,0,0) as the parameter z increases towards unity, for we know from Lemma 5.7.3 that the walk is recurrent if and only if

$$\lim_{z\uparrow 1} U(z,0,0) = \infty .$$

As z increases towards unity $\tau_2(z)$ tends to unity, whence $K(\tau_2(z))$

tends to infinity (Abramowitz and Stegun 1965, Table 17.5). It is easy to show that both C(z) and D(z) in expression (6.2.41) are finite, whence the walk is recurrent if and only if C(1) is strictly positive.

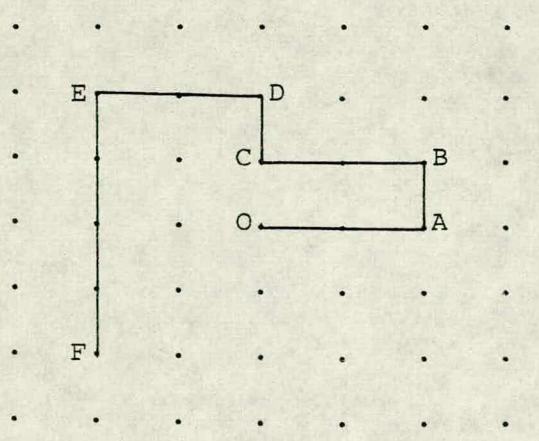
I have not been able to determine the sign of C(1) for general values of f, b, r and ℓ and so have not been able to prove that the walk is recurrent. However, with the use of a simple computer program to determine the appropriate coefficients we have verified that U(z,0,0) does diverge for $f,b,r,\ell = 0.0(0.1)1.0$ provided that $f \neq 1$ and $(f+b+r+\ell) = 1$. Therefore we propose that the two-dimensional lattice correlated random walk is recurrent whenever $f \neq 1$.

It is possible to prove recurrence for the special case $r = \ell$ without using the occupation probability generating function. This is shown in the following lemma.

Lemma 6.2.2 When $r = \ell$ and $f \neq 1$ the correlated random walk on an infinite square lattice is recurrent.

Proof

We are able to prove this result by embedding the original random walk within another random walk whose epochs occur whenever the particle changes direction from moving parallel to one axis (X or Y) to moving parallel to the other. Thus the new walk, which we will call the constrained walk, has steps of variable length and is such that a step parallel to one axis must be followed by a step parallel to the other axis. For example, suppose the diagram below illustrates part of the lattice and that the path marked from O to F



is the path of a particle performing a twelve-step correlated random walk. Then the appropriate constrained walk would consist of the six steps OA, AB, BC, CD, DE and EF. For convenience we shall consider the lengths of the steps of the constrained walk as being negative if the position of the

particle at the end of the step is in the negative direction of the appropriate axis when compared to its position at the beginning of the step. So in the diagram the steps of the constrained walk have lengths 2, 1, -2, 1, -2 and -4 respectively. We shall denote the distribution of step lengths by $H_c(\ell)$ $(\ell = 0, \pm 1, \pm 2, \ldots)$.

Next, consider an ordinary (i.e. independent step) random walk with step lengths governed by $H_c(.)$ but with step directions equally likely to be parallel to either axis. Let us call this the independent random walk. Then if the independent random walk is recurrent so too is the constrained walk. For if the independent walk is recurrent then a particle performing the walk must return to the origin infinitely often. At each return to the origin there is positive probability that the path taken by the particle until the next return satisfies the constraint of steps alternately parallel to the X- and Y-axes. Therefore since there are an infinite number of returns to the origin there must be an infinite number of times that the path between returns satisfies the constraint. We may embed the constrained walk within the independent walk by choosing only those paths between returns to the origin which satisfy the constraint. There are an infinite number of such paths and so the constrained walk must be recurrent.

In turn the recurrence of the constrained walk implies recurrence of the correlated random walk. Therefore we only need to show that a random walk consisting of independent steps, each of which has length distribution $H_c(.)$ and is equally likely to be parallel to either axis, is recurrent.

Now, the probability that the particle performing the correlated random walk changes direction from moving parallel to one axis to moving parallel to the other is $(r + \ell)$ at each step. We have assumed that $r = \ell$ whence it follows that conditional upon such a change in direction there is probability $\frac{1}{2}$ that the next step is in the positive direction of the appropriate axis and is otherwise in the negative direction. Thus the distribution $H_c(.)$ of step lengths of the independent (and constrained) walk is symmetrical about zero. Therefore by Spitzer (1964), Theorem 8.1, the independent random walk is recurrent if the second moment of the distribution $H_c(.)$ is finite.

We shall denote this moment by σ_c^2. If we denote the numbers of positive and negative (unit) steps of the correlated random walk between any two epochs of the constrained walk by ρ and ν respectively, we have

$$\sigma_c^2 = E[(\rho-\nu)^2] \ .$$

Therefore conditioning on the number of consecutive steps parallel to one axis yields

$$\sigma_c^2 = \sum_{n=1}^{\infty} E[(\rho-\nu)^2 \mid (\rho+\nu) = n]$$

$$\times \Pr(\text{exactly n consecutive steps parallel to one axis}) \ ,$$

whence

$$\sigma_c^2 \leqslant \sum_{n=1}^{\infty} n^2 \Pr(\text{exactly n consecutive steps parallel to one axis}) \ .$$

After each step there is probability $r + \ell$ $(= 2r)$ that the next step will not be parallel to the same axis. This probability is independent of all previous steps and so the number of consecutive steps parallel to one axis has a geometric distribution. Thus

$$\sigma_c^2 \leqslant \sum_{n=1}^{\infty} n^2 (1-2r)^{n-1} 2r \ .$$

By the Ratio Theorem (Heading 1970,p.59) we see that the series on the right hand side converges and so σ_c^2 is finite. Hence the independent, constrained and correlated random walks are recurrent and Lemma 6.2.2 is proved. □

Now let us return to the more general correlated random walk, where r and ℓ need not be equal. The mean recurrence time of the one-dimensional correlated random walk has been shown to be infinite provided that the particle is not certain to change direction at every step (Section 6.1.v) and it is interesting to examine whether the two-dimensional walk has similar properties. First we must assume

that the walk is recurrent, i.e.

$$C(z) > 0$$

whenever $z_o < z \leqslant 1$ for some z_o and where $C(z)$ is defined by (6.2.42). As mentioned earlier this has been verified for f,b,r,ℓ = 0.0(0.1)1.0 except when f = 1 so that the assumption is plausible.

Let the expected time until the first return to the origin be m, whence by the methods of Section 6.1.v) we obtain

$$m = \frac{\partial U(z,0,0)}{\partial z}\{U(z,0,0)\}^{-2}\Big|_{z=1} .$$

If $C(z)$ is non-zero this expression may be rearranged with the use of (6.2.41) as

$$m \simeq \pi^{-1}\{C(z)\frac{\partial K(\tau_2(z))}{\partial z} + \frac{\partial C(z)}{\partial z}K(\tau_2(z))\}\{C(z)K(\tau_2(z))\}^{-2}\Big|_{z=1} .$$

Provided that none of the parameters b, r or ℓ are unity we may show that $C(z)$ and $\partial C(z)/\partial z$ are finite, and since $K(\tau_2(z))$ increases to infinity as z increases to unity we have

$$\begin{aligned} m &\simeq \pi^{-1}C^{-1}(z)\frac{\partial K(\tau_2(z))}{\partial z}\{K(\tau_2(z))\}^{-2}\Big|_{z=1} \\ &= \pi^{-1}C^{-1}(z)\frac{\partial K(\tau_2(z))}{\partial \tau_2(z)} \times \frac{\partial \tau_2(z)}{\partial z}\{K(\tau_2(z))\}^{-2}\Big|_{z=1} . \end{aligned} \qquad (6.2.43)$$

The derivative of the elliptic integral is given by result 710.00 of Byrd and Friedman (1954) to be

$$\frac{\partial K(\tau_2(z))}{\partial \tau_2(z)} = [E(\tau_2(z)) - \{1-\tau_2(z)\}^2 K(\tau_2(z))]\tau_2^{-1}(z)\{1-\tau_2(z)\}^{-2} ,$$

where $E(.)$ is the complete elliptic integral of the second kind, i.e.

$$E(w) = \int_0^{\frac{1}{2}\pi} (1-w^2\sin^2 x)^{\frac{1}{2}} dx ,$$

which is finite for all w (Byrd and Friedman 1954, result 110.07).

As z increases to unity the term $\tau_2(z)$ tends to unity from below with a finite, positive derivative. Since for z close to unity

$$K(\tau_2(z)) \simeq \tfrac{1}{2}\log[16\{1-\tau_2^2(z)\}^{-1}]$$

(Byrd and Friedman 1954, result 112.01) we may combine these results in (6.2.43) to show that as $z \to 1$ then $m \to \infty$.

Thus the mean recurrence time is infinite provided that none of the parameters f, b, r or ℓ is unity. If f = 1 the walk is not recurrent, if b = 1 the particle always steps in the opposite direction to the previous step and is certain to return to the origin after two steps, whilst if either r = 1 or ℓ = 1 the path of the particle forms a square with return to the origin certain at the fourth step. But otherwise no matter how high any of the parameters b, r or ℓ and therefore how high the probability of return to the origin within the first few steps, the expected time until the first return is infinite.

6.2.v Asymptotic number of points visited

The asymptotic expected number of distinct lattice points visited by a particle performing a one-dimensional correlated random walk has been found to be proportional to the square root of the number of steps (Section 6.1.vi). When the walk is on a two-dimensional lattice the number of points which may be reached during the first n steps is greater, $(2n+1)^2$ compared to $(2n+1)$, and one expects the particle to visit a greater number of points but it is not obvious what the order of magnitude should be.

An expression for the asymptotic expected number of distinct lattice points visited may be derived from the expression (6.2.41) for U(z,0,0), namely

$$U(z,0,0) \sim \pi^{-1}C(z)K(\tau_2(z)) + D(z) ,$$

and the approximation

$$K(\tau_2(z)) \simeq \tfrac{1}{2}\log[\,16\{1-\tau_2^2(z)\}^{-1}\,]$$

for z close to unity (Byrd and Friedman 1954, result 112.01). Since the method is the same as for the one-dimensional lattice correlated random walk (Section 6.1.vi) we shall quote the final result only: if $N_E(n)$ denotes the expected number of distinct lattice points visited by the particle during the first n steps of the walk, then

$$N_E(n) \sim 2n\pi\{C(1)\log(n)\}^{-1} . \qquad (6.2.44)$$

Thus the expected number of lattice points visited has order of magnitude n/log(n). As expected this is a higher order of magnitude than the one-dimensional equivalent, which was $n^{\frac{1}{2}}$.

When $f = b = r = \ell = \frac{1}{4}$ the correlated random walk is mathematically equivalent to a simple random walk on an infinite square lattice. It is easy to show that with these parameter values $C(1) = 2$ and so $N_E(n) \sim n\pi\{\log(n)\}^{-1}$, which agrees with the result obtained by Dvoretzsky and Erdos (1950) for the simple random walk.

For other parameter values the expression for C(1), namely (6.2.42), is very complicated and the influence of changes in the parameters is not obvious. For this reason we include examples of the coefficient $2\pi C^{-1}(1)$ of n/log(n) in $N_E(n)$ for various choices of f, b, r and ℓ (Table 6.2.2). The coefficient of n in the dispersion matrix of the distribution $\{p_n(s_1,s_2)\}$ is also included for in the one-dimensional case we found the asymptotic number of lattice points visited to be closely related to the variance of the particle's position.

Example 6.2.2.i shows that when $f = b$ and $r = \ell$ the coefficient C(1) is equal to 2 whatever the choice of f. Similarly, the variance is constant whatever the choice of f. As mentioned earlier this is a very interesting result for which we have no explanation.

Example 6.2.2.ii, where $f = \ell$ and $b = r$, indicates that as f, the probability of continuing in the same direction, increases the expected number of lattice points visited at first increases until f is between 0.35 and 0.45 and then decreases. The initial increase is

Example 6.2.2.i $f = b$, $r = \ell = \frac{1}{2}(1-2f)$

f	0.05	0.10	0.15	0.20	0.25	0.30	0.35	0.40	0.45
D	0.50	0.50	0.50	0.50	0.50	0.50	0.50	0.50	0.50
$2\pi/C(1)$	3.14	3.14	3.14	3.14	3.14	3.14	3.14	3.14	3.14

Example 6.2.2.ii $f = \ell$, $b = r = \frac{1}{2}(1-2f)$

f	0.05	0.10	0.15	0.20	0.25	0.30	0.35	0.40	0.45
D	0.16	0.23	0.31	0.40	0.50	0.60	0.68	0.70	0.65
$2\pi/C(1)$	1.01	1.45	1.95	2.52	3.14	3.75	4.25	4.44	4.10

Example 6.2.2.iii $b = r = \ell$, $f = 1-3b$

f	0.00	0.10	0.20	0.30	0.40	0.50	0.60	0.70	0.80	0.90
D	0.25	0.33	0.44	0.57	0.75	1.00	1.38	2.00	3.25	7.00
$2\pi/C(1)$	1.57	2.09	2.74	3.59	4.71	6.28	8.64	12.57	20.42	43.98

Example 6.2.2.iv $f = r = \ell$, $b = 1-3f$

b	0.00	0.10	0.20	0.30	0.40	0.50	0.60	0.70	0.80	0.90
D	1.00	0.75	0.57	0.44	0.33	0.25	0.18	0.13	0.07	0.03
$2\pi/C(1)$	6.28	4.71	3.59	2.75	2.09	1.57	1.14	0.79	0.48	0.22

Example 6.2.2.v $f = b = \ell$, $r = 1-3f$

r	0.00	0.10	0.20	0.30	0.40	0.50	0.60	0.70	0.80	0.90
D	0.40	0.46	0.50	0.50	0.46	0.40	0.32	0.24	0.15	0.07
$2\pi/C(1)$	2.51	2.90	3.11	3.11	2.90	2.51	2.02	1.48	0.94	0.45

The variance of the particle's position is asymptotically proportional to n, the number of steps, whilst the expected number of distinct lattice points visited is proportional to $n/\log(n)$. The coefficients of proportionality, D (say) and $2\pi/C(1)$ respectively, where

$$D = \tfrac{1}{2}\{1-(f-b)^2-(r-\ell)^2\}\{1-2(f-b)+(f-b)^2+(r-\ell)^2\},$$

and C(1) is given by (6.2.42), are tabulated for various parameter values.

Table 6.2.2

Correlated random walk on an infinite square lattice: coefficients of variance and expected number of lattice points visited

probably because of the reduced probability (b) of immediate reversal, whilst the later decrease may be caused by the increased probability of stepping to the left, which increases the probability of the particle's path forming a loop.

Example 6.2.2.iii, where $b = r = \ell$, indicates that as the probability of continuing in a straight line (f) increases , as expected so too does the number of lattice points visited. The highest values of $N_E(n)$ occur when f is close to unity because $N_E(n)$ is inversely proportional to C(1) and C(1) = 0 when f = 1.

Example 6.2.2.iv, where $f = r = \ell$, illustrates that the expected number of lattice points visited decreases as the probability of immediate reversal increases. This is as expected for the minimum value of $N_E(n)$, namely two, occurs when b = 1.

Finally, Example 6.2.2.v, with $f = b = \ell$, shows that as r increases the asymptotic expected number of lattice points visited at first increases and afterwards decreases. The initial increase may be because of the reduction in b and ℓ, and hence reduced probability of the particle immediately returning to a previously visited point or that its path forms an anticlockwise loop. After $r = \frac{1}{4}$ the probability of a clockwise loop becomes important, reducing the expected number of distinct lattice points visited.

In each of Examples 6.2.2.i to 6.2.2.v the coefficient of n, D say, in the dispersion matrix of the distribution $\{p_n(s_1,s_2)\}$ has similar properties to the coefficient $2\pi/C(1)$. When $2\pi/C(1)$ increases as the parameters are altered so too does D, and similarly D decreases when $2\pi/C(1)$ does. On close inspection we see that in all of the illustations $2\pi/C(1)$ is approximately 6.28 times D, i.e. on allowing for rounding errors 2π times D. This suggests that $D = 1/C(1)$ although I have not been able to verify this by algebraic methods because the expression for C(1) is too complicated. Recall that for the one-dimensional lattice correlated random walk we found that the variance of the particle's position was asymptotically (np/q) whilst the asymptotic expected number of lattice points visited was $\{8np/\pi q\}^{\frac{1}{2}}$. Thus for that walk the expected number of lattice points visited was closely related to the standard deviation of the particle's position, whilst for the two-dimensional walk it is the variance which has similar properties to $N_E(n)$. More precisely the coefficient

of n in the dispersion matrix seems to be $(2\pi)^{-1}$ times the coefficient of $n/\log(n)$ in $N_E(n)$. There are no obvious reasons why the variance and expected number of distinct lattice points visited should be so closely related unless perhaps both can be considered as measures of the concentration of $\{p_n(s_1,s_2)\}$ about the origin.

6.2.vi Diffusion approximation

To conclude our work on the two-dimensional lattice correlated random walk we shall consider an approximation to the distribution $\{p_n(s_1,s_2)\}$ when the walk consists of a large number of short steps.

Recall the definitions (Table 6.2.1) of the probabilities $p_{nj}(s_1,s_2)$ of the particle being at (s_1,s_2) and in state E_j after n steps (j=1,2,3,4), and of $p_n(s_1,s_2)$ the probability of being at (s_1,s_2) after n steps irrespective of state. Now let us assume that the distance between neighbouring lattice points is δx in the X-direction and δy in the Y-direction and write $x = s_1\delta x$ and $y = s_2\delta y$. Furthermore, let us assume that the time interval between steps is now δt and write $t = n\delta t$. In addition, write $p_j(t;x,y)$ for $p_{nj}(s_1,s_2)$ and $v_1(t;x,y)$ for $p_n(s_1,s_2)$. Then our purpose is to study the behaviour of $v_1(t;x,y)$ as δx, δy and δt tend to zero.

If $\underline{p}(t;x,y)$ denotes the 4×1 vector with elements $p_j(t;x,y)$ (j=1,2,3,4), expansion of the four difference equations (6.2.3) by Taylor's series yields the vector-matrix equation

$$\underline{p} = P\{\underline{p} - t\frac{\partial \underline{p}}{\partial t}\} + \begin{pmatrix} -f & -b & -r & -\ell \\ b & f & \ell & r \\ 0 & 0 & 0 & 0 \\ 0 & 0 & 0 & 0 \end{pmatrix} \delta x \frac{\partial \underline{p}}{\partial x} + \begin{pmatrix} 0 & 0 & 0 & 0 \\ 0 & 0 & 0 & 0 \\ -\ell & -r & -f & -b \\ r & \ell & b & f \end{pmatrix} \delta y \frac{\partial \underline{p}}{\partial y}$$

$$(6.2.45) \qquad + \tfrac{1}{2} \begin{pmatrix} f & b & r & \ell \\ b & f & \ell & r \\ 0 & 0 & 0 & 0 \\ 0 & 0 & 0 & 0 \end{pmatrix} (\delta x)^2 \frac{\partial^2 \underline{p}}{\partial x^2} + \tfrac{1}{2} \begin{pmatrix} 0 & 0 & 0 & 0 \\ 0 & 0 & 0 & 0 \\ \ell & r & f & b \\ r & \ell & b & f \end{pmatrix} (\delta y)^2 \frac{\partial^2 \underline{p}}{\partial y^2}$$

$$+ O(\delta t^2, \delta x^3, \delta y^3) ,$$

where for brevity we use $\underline{p} \equiv \underline{p}(t;x,y)$ and write $\partial\underline{p}/\partial t$ for the 4×1 vector of partial derivatives of $\underline{p}(t;x,y)$ with respect to t, etc. Here P is again the doubly stochastic matrix defined in Table 6.2.1.

We are interested in $v_1(t;x,y)$, which is given by

$$v_1(t;x,y) = \sum_{j=1}^{4} p_j(t;x,y)$$

and which will be denoted by v_1 for brevity. In order to rearrange (6.2.45) to involve v_1 we require the following terms:

$$v_2 \equiv v_2(t;x,y) \equiv p_1(t;x,y)+p_2(t;x,y)-p_3(t;x,y)-p_4(t;x,y) ,$$

$$v_3 \equiv v_3(t;x,y) \equiv p_1(t;x,y)-p_2(t;x,y)-ip_3(t;x,y)+ip_4(t;x,y)$$

and

$$v_4 \equiv v_4(t;x,y) \equiv p_1(t;x,y)-p_2(t;x,y)+ip_3(t;x,y)-ip_4(t;x,y) ,$$

where $i = \sqrt{(-1)}$. Then by multiplying equation (6.2.45) on the left by the 4×4 matrix of left hand eigenvalues of P, L say, defined by

$$L = \begin{pmatrix} 1 & 1 & 1 & 1 \\ 1 & 1 & -1 & -1 \\ 1 & -1 & -i & i \\ 1 & -1 & i & -i \end{pmatrix} ,$$

the vector-matrix equation can be rearranged as four partial differential equations. These are

$$\begin{aligned} v_1 = \lambda_1 v_1 - \lambda_1 \delta t \frac{\partial v_1}{\partial t} - \tfrac{1}{2}\delta x(\lambda_3 \frac{\partial v_3}{\partial x} + \lambda_4 \frac{\partial v_4}{\partial x}) - \tfrac{1}{2} i \delta y(\lambda_3 \frac{\partial v_3}{\partial y} - \lambda_4 \frac{\partial v_4}{\partial y}) \\ + \tfrac{1}{4}(\delta x)^2(\lambda_1 \frac{\partial^2 v_1}{\partial x^2} + \lambda_2 \frac{\partial^2 v_2}{\partial x^2}) + \tfrac{1}{4}(\delta y)^2(\lambda_1 \frac{\partial^2 v_1}{\partial y^2} - \lambda_2 \frac{\partial^2 v_2}{\partial y^2}) + O(\delta t^2, \delta x^3, \delta y^3), \end{aligned} \tag{6.2.46}$$

$$v_2 = \lambda_2 v_2 - \lambda_2 \delta t \frac{\partial v_2}{\partial t} - \tfrac{1}{2}\delta x(\lambda_3 \frac{\partial v_3}{\partial x} + \lambda_4 \frac{\partial v_4}{\partial x}) + \tfrac{1}{2}i\delta y(\lambda_3 \frac{\partial v_3}{\partial y} - \lambda_4 \frac{\partial v_4}{\partial y})$$

(6.2.47)
$$+ \tfrac{1}{4}(\delta x)^2(\lambda_1 \frac{\partial^2 v_1}{\partial x^2} + \lambda_2 \frac{\partial^2 v_2}{\partial x^2}) - \tfrac{1}{4}(\delta y)^2(\lambda_1 \frac{\partial^2 v_1}{\partial y^2} - \lambda_2 \frac{\partial^2 v_2}{\partial y^2}) + O(\delta t^2, \delta x^3, \delta y^3),$$

$$v_3 = \lambda_3 v_3 - \lambda_3 \delta t \frac{\partial v_3}{\partial t} - \tfrac{1}{2}\delta x(\lambda_1 \frac{\partial v_1}{\partial x} + \lambda_2 \frac{\partial v_2}{\partial x}) + \tfrac{1}{2}i\delta y(\lambda_1 \frac{\partial v_1}{\partial y} - \lambda_2 \frac{\partial v_2}{\partial y})$$

(6.2.48)
$$+ \tfrac{1}{4}(\delta x)^2(\lambda_3 \frac{\partial^2 v_3}{\partial x^2} + \lambda_4 \frac{\partial^2 v_4}{\partial x^2}) + \tfrac{1}{4}(\delta y)^2(\lambda_3 \frac{\partial^2 v_3}{\partial y^2} - \lambda_4 \frac{\partial^2 v_4}{\partial y^2}) + O(\delta t^2, \delta x^3, \delta y^3)$$

and

$$v_4 = \lambda_4 v_4 - \lambda_4 \delta t \frac{\partial v_4}{\partial t} - \tfrac{1}{2}\delta x(\lambda_1 \frac{\partial v_1}{\partial x} + \lambda_2 \frac{\partial v_2}{\partial x}) - \tfrac{1}{2}i\delta y(\lambda_1 \frac{\partial v_1}{\partial y} - \lambda_2 \frac{\partial v_2}{\partial y})$$

(6.2.49)
$$+ \tfrac{1}{4}(\delta x)^2(\lambda_3 \frac{\partial^2 v_3}{\partial x^2} + \lambda_4 \frac{\partial^2 v_4}{\partial x^2}) - \tfrac{1}{4}(\delta y)^2(\lambda_3 \frac{\partial^2 v_3}{\partial y^2} - \lambda_4 \frac{\partial^2 v_4}{\partial y^2}) + O(\delta t^2, \delta x^3, \delta y^3),$$

where $\lambda_1 = 1$, $\lambda_2 = f+b-r-\ell$, $\lambda_3 = f-b+i(r-\ell)$ and $\lambda_4 = f-b-i(r-\ell)$, which are the four eigenvalues of the matrix P.

Now let us choose $\delta y = \delta x$ and $\delta t = \sigma^{-2}(\delta x)^2$ for some positive parameter σ^2. Our objective is to allow δx (and so δy and δt) to tend to zero and so obtain a limiting form for the density $v_1(t;x,y)$. Examination of equations (6.2.47), (6.2.48) and (6.2.49) shows that since λ_2, λ_3 and λ_4 are not unity for genuinely two-dimensional walks, the only solutions which are consistent as δx is decreased to zero must be of the form

$$v_2(t;x,y) \equiv (\delta x)^2 v_2'(t;x,y) ,$$

$$v_3(t;x,y) \equiv (\delta x) v_3'(t;x,y)$$

and

$$v_4(t;x,y) \equiv (\delta x) v_4'(t;x,y) ,$$

for some functions $v_2'(t;x,y)$, $v_3'(t,x,y)$ and $v_4'(t;x,y)$ which are independent of δx. Therefore on dividing each side of (6.2.46) and (6.2.47) by $(\delta x)^2$, and of (6.2.48) and (6.2.49) by (δx), and allowing x to tend to zero we obtain

$$(6.2.50)\qquad \sigma^{-2}\frac{\partial v_1}{\partial t} = -\tfrac{1}{2}(\lambda_3\frac{\partial v_3'}{\partial x}+\lambda_4\frac{\partial v_4'}{\partial x}) - \tfrac{1}{2}i(\lambda_3\frac{\partial v_3'}{\partial y}-\lambda_4\frac{\partial v_4'}{\partial y}) + \tfrac{1}{4}\frac{\partial^2 v_1}{\partial x^2} + \tfrac{1}{4}\frac{\partial^2 v_1}{\partial y^2},$$

$$(6.2.51)\qquad (1-\lambda_2)v_2' = -\tfrac{1}{2}(\lambda_3\frac{\partial v_3'}{\partial x}+\lambda_4\frac{\partial v_4'}{\partial x}) + \tfrac{1}{2}i(\lambda_3\frac{\partial v_3'}{\partial y}-\lambda_4\frac{\partial v_4'}{\partial y}) + \tfrac{1}{4}\frac{\partial^2 v_1}{\partial x^2} - \tfrac{1}{4}\frac{\partial^2 v_1}{\partial y^2},$$

$$(6.2.52)\qquad (1-\lambda_3)v_3' = -\tfrac{1}{2}\frac{\partial v_1}{\partial x} + \tfrac{1}{2}i\frac{\partial v_1}{\partial y}$$

and

$$(6.2.53)\qquad (1-\lambda_4)v_4' = -\tfrac{1}{2}\frac{\partial v_1}{\partial x} - \tfrac{1}{2}i\frac{\partial v_1}{\partial y},$$

where we write v_j' for $v_j'(t;x,y)$ $(j=2,3,4)$.

The function $v_2'(t;x,y)$ does not appear in (6.2.50), (6.2.52) or (6.2.53) and therefore we may ignore equation (6.2.51). Upon using (6.2.52) and (6.2.53) to substitute for v_3' and v_4' in (6.2.50) we obtain the diffusion equation

$$(6.2.54)\qquad 4\sigma^{-2}\frac{\partial v_1}{\partial t} = \{1+\lambda_3(1-\lambda_3)^{-1}+\lambda_4(1-\lambda_4)^{-1}\}\{\frac{\partial^2 v_1}{\partial x^2}+\frac{\partial^2 v_1}{\partial y^2}\}.$$

This is the standard equation for two-dimensional Brownian motion (Feller 1971, p.344), which has solution

$$(6.2.55)\qquad v_1(t;x,y) = \frac{\exp[(\sigma^2 t)^{-1}\{1+\lambda_3(1-\lambda_3)^{-1}+\lambda_4(1-\lambda_4)^{-1}\}^{-1}\{x^2+y^2\}]}{\pi t\sigma^2\{1+\lambda_3(1-\lambda_3)^{-1}+\lambda_4(1-\lambda_4)^{-1}\}}$$

(Pielou 1977, p.170).

Hence in the limit as the number of steps increases whilst the step lengths decrease the distribution of the particle's position becomes Normal with zero mean and dispersion matrix

$$\tfrac{1}{2}\sigma^2 t\{1+\lambda_3(1-\lambda_3)^{-1}+\lambda_4(1-\lambda_4)^{-1}\}I_2 ,$$

where I_2 denotes the 2×2 identity matrix.

When $f = b = r = \ell = \frac{1}{4}$ the correlated random walk is equivalent to a simple random walk on a two-dimensional square lattice. In that case $\lambda_3 = \lambda_4 = 0$ and the limiting distribution has dispersion matrix $\frac{1}{2}\sigma^2 t I_2$. Thus the effect of correlation in step directions is the introduction of a scaling factor $\{1+\lambda_3(1-\lambda_3)^{-1}+\lambda_4(1-\lambda_4)^{-1}\}$. When the ratio of the parameters b,r and ℓ is fixed the scaling factor increases as f, the probability that the particle continues in the same direction as the previous step, increases. Conversely, for fixed values of f and b the scaling factor decreases when $|r-\ell|$ decreases. Therefore the variance of the particle's position is higher when the particle tends to continue in one direction and lower when steps to the right are more likely than steps to the left or vice versa, which has the effect of increasing the probability that the path of the particle forms a loop about the origin.

6.3 Discussion

A theoretical analysis of correlated random walks, whether on lattices or over a continuous space, is difficult because of the complicated algebra involved. Nevertheless several interesting results have been derived.

1. The mean position of a particle undergoing a correlated random walk does not increase with the number of steps except in the trivial case of no direction changes possible (Sections 5.4.i, 6.1.iii and 6.2.ii). Therefore the walk has no preferred direction or drift.
2. Correlated random walks on a one-dimensional lattice and when not restricted to a subset of $\mathbb{R}^2$ are recurrent (Sections 5.7 and 6.1.v). We conjecture that correlated random walks on a two-dimensional lattice are also recurrent although this result has not been proved for all parameter values (Section 6.2.iv).

   An interesting problem, which is not considered in this study, is to ask whether the result that the mean

position is bounded, perhaps with other moment conditions, is sufficient for more general one- and two-dimensional random walks to be recurrent. When walks have independent and identically distributed steps the condition is necessary for recurrence (Spitzer 1964,p.83) but to my knowledge the sufficiency of the condition has never been considered.

3. The variance of the position of a particle performing a correlated random walk is asymptotically proportional to the number of steps (Sections 5.4.ii, 6.1.iii and 6.2.ii). When random walks have independent steps the variance is always proportional to the number of steps.

   With our assumptions (Sections 5.1 and 6.2) on two-dimensional correlated random walks the coordinates of the particle's position are asymptotically uncorrelated when the walk is not restricted to a subset of $\mathbb{R}^2$ and are always uncorrelated when the walk is on a square lattice (Sections 5.4.ii and 6.2.ii). Further investigations are necessary to determine whether similar results are true under other assumptions; for example, in the continuous case when the turning variable distribution is not symmetrical about zero, or in the lattice case when all four directions are not initially equally likely.

4. When walks are restricted to lattices the asymptotic expected number of distinct lattice points visited is closely related to the variance of the particle's position (Sections 6.1.vi and 6.2.v). I have not been able to determine a formal relationship between these two quantities and further work is necessary.

   I have also been unable to derive an expression for the variance of the number of lattice points visited. Such an expression would be useful as it could be used to indicate how many steps are required before the asymptotic expression for the number of lattice points visited becomes close to the true value.

5. The particle's position, with suitable scaling, converges in distribution to a Normal random variable for each of

the three correlated random walks considered (Sections 5.6, 6.1.vii and 6.2.viii). In each case the effect of correlation is to introduce a scaling factor to the limiting variance when compared with independent random walks. The scaling factors are, in the earlier notation:

a)

$$p/q$$

for walks on a one-dimensional lattice;

b)

$$\frac{\frac{1}{2}\{1-(f-b)^2-(r-\ell)^2\}}{\{1-2(f-b)+(f-b)^2+(r-\ell)^2\}}$$

for walks on a two-dimensional lattice; and

c)

$$\{\tfrac{1}{2}\mu_2+\mu_1^2 c/(1-c)\}$$

for walks which are not restricted to a subset of $\mathbb{R}^2$.

Note that the two-dimensional lattice scaling factor is consistent with the two-dimensional continuous space scaling factor. On the lattice $\mu_2 = \mu_1 = 1$ and when deriving c) we assumed that the turning variable distribution was symmetrical about zero, which implies $r = \ell$ and $f-b = c$ in the lattice notation.

Our results may be useful to the applications of correlated random walks which were discussed earlier (Section 5.2) and could also be useful to other areas of investigation where random walks with independent step directions have previously been used as models of physical processes. For example, as suggested by Klein (1952) a correlated random walk model for Brownian motion may be more accurate than the usual simple random walk model (see, for example, Feller 1968,p.354-359). For, owing to its inertia, a particle moving in a certain direction is more likely to be deflected by a small amount on colliding with another particle than to reverse direction. This

can be described by a correlated random walk with suitable parameters but not by a simple random walk. It should be noted that the main use of a simple random walk model of Brownian motion is as a basis for the derivation of a differential equation for the associated diffusion approximation. The same equation (with an unimportant scaling factor) can be obtained by the more intuitively obvious correlated random walk approach (Section 6.2.vi).

CHAPTER 7

BRANCHING CORRELATED RANDOM WALKS

Our study of the correlated random walk was suggested by an examination of the paths of individual roots. Now we shall consider a branching random walk suggested by an examination of entire root systems. In the branching random walk a population of particles evolves in some space in a series of discrete generations. At time n = r the existing rth generation particles split, independently of one another, into a random number of offspring. These offspring instantaneously jump away from their parent's positions to form the (r+1)st generation. The process begins with a number of initial particles whose offspring form the first generation. It should be noted that "generation" is used in a different sense here to "root generation" used in earlier chapters.

A root system observed at a fixed time may be interpreted as a realisation of a branching random walk if the primary root origins are assumed to correspond to the positions of the initial particles, and the straight-line segments of roots are assumed to represent the jumps, or steps, of offspring when moving away from their parent's position. The 5mm diameter points of roots represent the positions of particles which produced no offspring; bends represent the positions of particles which produced one offspring; and any of the types of root branching represent the positions of particles which produced more than one offspring. It is important to note that the temporal development of a root system cannot be described by a branching random walk because the actual growth is not in a series of discrete generations but is continuous.

A branching random walk can describe root distributions however, when: the lengths of the offspring steps are governed by the distributions fitted to the root STEPLEN data (Section 3.4); the directions taken by the offspring are determined by the distributions

fitted to the root angle and azimuth data (Section 3.2); and the number of offspring produced by any particle is drawn from the probability distribution fitted to the root NOFF data (Section 3.4).

A theoretical analysis of this type of branching random walk is very difficult and I have not been able to derive any results. Nevertheless an analysis of a more simple branching random walk which still incorporates the most important factor, correlation in root directions, provides a necessary basis to a more complete analysis and may be useful when root growth in a controlled, homogeneous environment is considered. Moreover, the branching random walk which we will study has several other applications, for example vascular trees (Kamiya, Togawa and Yamamoto 1974), dendritic cells (ten Hoopen and Reuver 1970, 1971) and airways in lungs (Weibel 1963). The process is fully described in Section 7.3. First we will quote the results from the theory of branching processes which will be required (Section 7.1) and describe other related investigations (Section 7.2).

The main notation used in this chapter is summarised for easy reference in Table 7.1.1.

7.1 Branching Processes

The generation sizes of a branching random walk form a branching process. We shall assume that the numbers of particles in each generation form a Galton-Watson process, where the number of offspring produced by any particle is a random variable independently drawn from some distribution $\{p_k: k = 0, 1, 2, \ldots, (p_0+p_1+\ldots) = 1\}$ with mean m. The results which will be used in the sequel are stated without proof. No new results are derived and all proofs are included in either Harris (1963) or Athreya and Ney (1972).

Let us denote the size of the nth generation by $Z^{(n)}$ and the number of initial particles by $Z^{(0)}$. Then

$$E[Z^{(n)}] = m^n Z^{(0)} \tag{7.1.1}$$

and

Symbol	Interpretation
p_k	Pr(any particle produces exactly k offspring).
m, v	Mean and variance of the distribution $\{p_k\}$ respectively.
H(.)	Distribution of step lengths.
G(.)	Distribution of changes in direction between parent and offspring steps.
$F^{(n)}(I;\underline{u},\zeta)$	Probablity that a particle performing a correlated random walk, starting from $\underline{u}$ with initial direction ζ, is in the Borel set I after n steps.
$F^{(n)}(I)$	$F^{(n)}(I;\underline{0},\xi)$.
$\mathcal{L}_n$	The σ-field generated by the first n generations of particles.
$r^{(n)}(k,I)$	Pr(exactly k nth generation particles have positions in I).
$r^{(j,n)}(k,I)$	Pr(exactly k nth generation particles have positions in $I \mid \mathcal{L}_j$).
$M^{(n)}(I)$, $Var^{(n)}(I)$	Mean and variance of the number of nth generation particles with positions in I respectively.

Table 7.1.1

Main notation for Chapter 7

(Continued overleaf)

Symbol	Interpretation
$Z^{(n)}$	Total size of the nth generation.
$Z^{(n)}(I)$	Number of nth generation particles with positions in I.
$W^{(n)}$, $W^{(n)}(I)$	$Z^{(n)}/m^n$ and $Z^{(n)}(I)/m^n$ respectively.
W	$\lim_{n\to\infty} W^{(n)}$.
$\underline{i}_n$	Any nth generation particle.
$\ell(\underline{i}_n), \theta(\underline{i}_n), S(\underline{i}_n)$	Step length and turning variable associated with $\underline{i}_n$ and position of $\underline{i}_n$ respectively.
$\eta(\underline{i}_n)$	Direction of the step taken by $\underline{i}_n$, measured from some fixed direction.
$\sum_{\underline{i}_n}$	Summation over all nth generation particles.
$\underline{i}_k^{(n)}$	Any nth generation descendant of the kth generation particle $\underline{i}_k$ $(k \leqslant n)$.
$Z^{(n)}(\underline{i}_k)$	Number of descendants of $\underline{i}_k$ alive at time n.
$Z^{(n)}(I;\underline{i}_k)$	Number of nth generation descendants of $\underline{i}_k$ with positions in I.
$W^{(n)}(\underline{i}_k), W^{(n)}(I;\underline{i}_k)$	$Z^{(n)}(\underline{i}_k)/m^{n-k}$ and $Z^{(n)}(I;\underline{i}_k)/m^{n-k}$ respectively.

Table 7.1.1

Main notation for Chapter 7

(Continued)

$$\text{(7.1.2)} \qquad \Pr\left(\lim_{n\to\infty} Z^{(n)} = 0\right) = \begin{cases} 1 & \text{if } m < 1 \\ 1 & \text{if } m = 1 \text{ and } p_1 \neq 1 \\ q & \text{otherwise,} \end{cases}$$

where q is the unique non-negative solution less than unity of

$$q = \sum_{k=0}^{\infty} q^k p_k \, .$$

The Galton-Watson process is known as subcritical, critical or supercritical depending upon whether the mean, m, is less than, equal to or greater than unity respectively. Result (7.1.2) implies that subcritical and critical Galton-Watson processes always become extinct, but that there is positive probability that supercritical Galton-Watson processes do not die out. Since we may show that the population size cannot be bounded above and either

$$\lim_{n\to\infty} Z^{(n)} = 0 \quad \text{or} \quad \lim_{n\to\infty} Z^{(n)} = \infty \, ,$$

then a population which does not become extinct must increase indefinitely, although not necessarily monotonically. Throughout the remainder of this chapter we shall assume that $m > 1$. All of our results are conditional upon the survival of the process.

If $Z^{(n)}/m^n \equiv W^{(n)}$ and

$$\lim_{n\to\infty} Z^{(n)} = \infty \, ,$$

then the sequence of random variables $\{W^{(n)}\}$ converges with probability one and in mean square to a positive valued random variable. Paraphrasing this, we say that there is a positive random variable W such that

$$\text{(7.1.3)} \qquad E\left[\left(Z^{(n)}/m^n - W\right)^2\right] \to 0$$

as $n \to \infty$ provided that the population does not become extinct. This result also holds almost surely, i.e.

$$\text{(7.1.4)} \qquad Z^{(n)}/m^n \to W$$

almost surely as $n \to \infty$.

7.2 Related Work

Most authors who have investigated branching random walks have assumed that evolution takes place over the real line, that the generation sizes form a Galton-Watson process arising from one initial particle, and that the offspring steps are independent and identically distributed. All results are conditional upon the non-extinction of the process.

Under these assumptions and with certain restrictions on the offspring distribution $\{p_k\}$ and the mean and variance, μ and σ^2 say, of the offspring step distribution, Harris (1963) suggested an analogue to the central limit theorem. If $Z^{(n)}(I)$ denotes the number of nth generation particles with positions in some set I, and if I(x) denotes the interval of the real line to the left of x, then Harris conjectured that the random variables $Z^{(n)}(I(n\mu+\sigma x\sqrt{n}))/m^n$ should converge in probability to $W\Phi(x)$ as n increases, where W is defined by (7.1.3) and $\Phi(x)$ denotes the standard Normal distribution function. Harris' conjecture was resolved by Stam (1966) and for a more general process, where the time intervals between births are random variables, by Ney (1965a, 1965b). Joffe and Moncayo (1973), Asmussen and Kaplan (1976) and Kaplan and Asmussen (1976) have since proved similar results under less restrictive assumptions and with stronger convergence properties. In Section 7.4 we will extend the methods of Asmussen and Kaplan to include the case when parent and offspring step directions are correlated.

Other results for branching random walks on the real line include laws of large numbers (Biggins 1977b, Bramsom 1978 and Durrett 1979), which are concerned with the tails of the distribution of particle's positions, and investigations into the convergence and continuity properties of certain associated random variables (Biggins 1977a, Biggins and Grey 1979). I have not been able to extend these results to include the case of correlated step directions.

Other types of branching random walks have been studied by several authors: Matthes, Kerstan and Mecke (1978, Chapter 12) give references to work on processes which originate with an infinite number of particles, where the assumption that the branching process is supercritical is no longer necessary; Biggins (1976) considered

a branching random walk where the particles can be of several types; Biggins (1978) and Durrett (1979) allowed the offspring steps to be on $\mathbb{R}^d$ rather than the real line; and Gorostiza and Griego (1979) obtained an analogue to the central limit theorem when the offspring steps were along the real line but incorporated correlation in step directions. To my knowledge no other investigations have been made into the effect of correlated step directions.

7.3 Definitions, Notation and Basic Results

As there is little difficulty in extending the results to higher dimensions we shall consider branching random walks in $\mathbb{R}^2$ only. As there is also little difficulty in extending the results to include any finite number of initial particles we shall assume that the process originates from one initial particle situated at the origin of $\mathbb{R}^2$. To allow us to define the movement of the first generation particles in a similar manner to the movement of subsequent generations we shall associate a direction, ξ, with the initial particle, where ξ is measured anticlockwise from some fixed direction.

At time n = 1 the initial particle produces a random number, k say, of offspring. If $k > 0$ the offspring immediately jump away from the parent, with offspring j (j=1,2,...,k) moving a distance ℓ_j in direction $\xi+\theta_j$. We will assume that k has probability distribution $\{p_k: k = 0, 1, 2,..., (p_0+p_1+...) = 1\}$, with mean and variance m and v respectively. In addition we will assume that the length variables, ℓ_j (j=1,2,...,k), are independently and identically distributed as H(.), and that the turning variables, θ_j (j=1,2,...,k), are independently and identically distributed as G(.). At each subsequent epoch n = 2, 3,... the existing nth generation particles each produce random numbers of offspring, drawn independently from the distribution $\{p_k\}$, which move away from their parent's position to form the (n+1)st generation. The step lengths and angles between offspring and parent steps are mutually independent random variables from the distributions H(.) and G(.) respectively.

Thus the generation sizes form a Galton-Watson process (Section 7.1) and the sequence of steps taken by the ancestors of any nth generation particle forms an n-step two-dimensional correlated random

walk. We will make the same assumptions on the properties of G(.) and H(.) as those made in Chapter 5 (Assumptions 5.1.1). The process will be called a branching correlated random walk .

Let us denote the number of nth generation particles by $Z^{(n)}$, and the number of such particles with positions in some Borel set I by $Z^{(n)}(I)$. Following Harris (1963,p.123) we uniquely label any member of the nth generation (n=1,2,...) by an n-dimensional vector of positive integers $\underline{i}_n = (i_1,i_2,\ldots,i_n)^T$ to describe that particle's line of descent from the original. For example, the second offspring of the third offspring of the initial particle will be denoted by $(3,2)^T$. The length of the step taken by $\underline{i}_n$ will be denoted by $\ell(\underline{i}_n)$ and the angle between that step and the step taken by the parent of $\underline{i}_n$ will be denoted by $\theta(\underline{i}_n)$. The position in $\mathcal{R}^2$ of $\underline{i}_n$ will be denoted by $\underline{S}(\underline{i}_n)$.

We will need several new definitions. Let

$$r^{(n)}(k,I) \equiv \Pr(Z^{(n)}(I) = k) \tag{7.3.1}$$

for any set I and non-negative integers k and n, and let

$$r^{(j,n)}(k,I) \equiv \Pr(Z^{(n)}(I) = k \mid \mathcal{L}_j) \ , \tag{7.3.2}$$

which is the conditional probability of exactly k nth generation particles having positions in I, given the development of the process up to the jth generation ($j \leq n$). The assumption that the process originated with the initial particle situated at the origin of $\mathcal{R}^2$, with associated direction ξ, is implicit in the definitions (7.3.1) and (7.3.2). For other initial positions and associated directions new notation is required. Again writing "starting from $\underline{u},\zeta$" as an abbreviated form of "having started with one initial particle situated at $\underline{u} \in \mathcal{R}^2$, with associated direction ζ", we define

$$r^{(n)}(k,I;\underline{u},\zeta) \equiv \Pr(Z^{(n)}(I)=k, \text{ starting from } \underline{u},\zeta), \tag{7.3.3}$$

and

$$r^{(j,n)}(k,I;\underline{u},\zeta) \equiv \Pr(Z^{(n)}(I)=k, \text{ starting from } \underline{u},\zeta \mid \mathcal{L}_j) \ . \tag{7.3.4}$$

Finally, let $T(I;\underline{u},\zeta)$ be a mapping from a Borel set I to the set of points of I translated by $\underline{u}$ and rotated clockwise about the origin by ζ. More precisely

$$(7.3.5) \qquad T(I;\underline{u},\zeta) \equiv \{\underline{x}: A(\underline{x}+\underline{u}) \in I, \quad A = \begin{pmatrix} \cos\zeta & \sin\zeta \\ -\sin\zeta & \cos\zeta \end{pmatrix} \} .$$

The reason for our definition of this mapping is that with this choice we can express the probabilities $r^{(n)}(.;\underline{u},\zeta)$ and $r^{(j,n)}(.;\underline{u},\zeta)$ as functions of $r^{(n)}(.)$ and $r^{(j,n)}(.)$. For by definitions (7.3.1) to (7.3.5) we have

$$(7.3.6) \quad r^{(n)}(k,I;\underline{u},\zeta) = r^{(n)}(k,T(I;\underline{u},\zeta-\xi);\underline{0},\xi) \equiv r^{(n)}(k,T(I;\underline{u},\zeta-\xi))$$

and

$$(7.3.7) \quad r^{(j,n)}(k,I;\underline{u},\zeta) = r^{(j,n)}(k,T(I;\underline{u},\zeta-\xi);\underline{0},\xi) \equiv r^{(j,n)}(k,T(I;\underline{u},\zeta-\xi)).$$

Now we are able to derive the basic integral equation of the process. Our method is similar to those of Karlin (1966,p.353-356) and Athreya and Ney (1972,p.230-232), who considered branching random walks with independent step directions. The method is to first condition on the number and positions of the first generation particles, then to find an expression for the probability of having exactly k nth generation particles in some set I, and finally to remove the conditioning.

Let us suppose that $Z^{(1)} = N$, which is not zero, and that the positions of the first generation particles are $\underline{u}_j = (\ell_j\cos(\xi+\theta_j), \ell_j\sin(\xi+\theta_j))^T$ (j=1,2,...,N). Then the probability that exactly k_j descendants of any first generation particle j have positions in some set I is $r^{(n-1)}(k;I;\underline{u}_j,\xi+\theta_j)$, independent of the numbers and positions of all descendants of other first generation particles. So by considering the number of ways in which the total number of nth generation particles in I can be k, we obtain

$$r^{(1,n)}(k,I) = \sum_{\substack{k_1,k_2,\ldots,k_N=0 \\ k_1+k_2+\ldots+k_N=k}}^{k} r^{(n-1)}(k_1,I;\underline{u}_1,\xi+\theta_1)$$

$$\times\, r^{(n-1)}(k_2,I;\underline{u}_2,\xi+\theta_2)\ldots r^{(n-1)}(k_N,I;\underline{u}_N,\xi+\theta_N).$$

If we use (7.3.6) this equation can be written as

$$r^{(1,n)}(k,I) = \sum_{\substack{k_1,k_2,..,k_N=0 \\ k_1+k_2+..,k_N}}^{k} r^{(n-1)}(k_1,T(I;\underline{u}_1,\theta_1))$$

$$\times\, r^{(n-1)}(k_2,T(I;\underline{u}_2,\theta_2))\ldots r^{(n-1)}(k_N,T(I;\underline{u}_N,\theta_N)).$$

Now remove the conditioning on the positions of the first generation particles by integration with respect to the length and turning variable distributions H(.) and G(.) respectively. Next sum over all possible values of N. This procedure yields

$$r^{(n)}(k,I) = p_0\delta_{k,0}$$

$$+ \sum_{N=1}^{\infty} p_N \Big[\int\ldots\int_{(\mathbb{R}^2)^N} \{ \sum_{\substack{k_1,k_2,..,k_N=0 \\ k_1+k_2+..+k_N=k}}^{k} r^{(n-1)}(k_1,T(I;\underline{u}_1,\theta_1))\, r^{(n-1)}(k_2,T(I;\underline{u}_2,\theta_2))..$$

(7.3.8)

$$\ldots r^{(n-1)}(k_N,T(I;\underline{u}_N,\theta_N))\}\, dG(\theta_1)\,dH(\ell_1)\,dG(\theta_2)\,dH(\ell_2)\ldots dG(\theta_N)\,dH(\ell_N)\Big],$$

where $\delta_{k,0}$ is the Kronecker delta function.

This is the basic integral equation for the branching correlated random walk. The equation can be simplified by the use of generating functions. For if we define

$$R^{(n)}(I,\omega) \equiv \sum_{k=0}^{\infty} \omega^k r^{(n)}(k,I) \qquad (0 < \omega < 1), \tag{7.3.9}$$

then on multiplication of both sides of (7.3.8) by ω^k and summation over k we have, with $\underline{u} = (\ell\cos\theta,\ell\sin\theta)^T$,

$$(7.3.10)\qquad R^{(n)}(I,\omega) = \sum_{k=0}^{\infty} p_k \{ \int_0^{\infty} \int_0^{2\pi} R^{(n-1)}(T(I;\underline{u},\theta),\omega)\, dG(\theta)\, dH(\ell) \}^k$$

because the offspring are independent of each other.

I have not been able to simplify (7.3.10) further and have not been able to obtain expressions for the probabilities $r^{(n)}(k,I)$. However, the mean number of nth generation particles with positions in I, $M^{(n)}(I)$ say, is easily derived from (7.3.10). First let us define

$$(7.3.11)\qquad A^{(n)}(I,\omega) \equiv \int_0^{\infty} \int_0^{2\pi} R^{(n)}(T(I;\underline{u},\theta),\omega)\, dG(\theta)\, dH(\ell),$$

whence from (7.3.10) we have

$$(7.3.12)\qquad R^{(n)}(I,\omega) = \sum_{k=0}^{\infty} p_k \{A^{(n-1)}(I,\omega)\}^k .$$

We wish to find an expression for the mean number of nth generation particles with positions in some set I, which is given by

$$M^{(n)}(I) = \sum_{k=0}^{\infty} k r^{(n)}(k,I) .$$

From the definition (7.3.9) we see that

$$M^{(n)}(I) = \left. \frac{\partial R^{(n)}(I,\omega)}{\partial \omega} \right|_{\omega=1} .$$

Therefore on differentiating (7.3.12) with respect to ω we have

$$(7.3.13)\qquad M^{(n)}(I) = \sum_{k=0}^{\infty} k p_k \left. \frac{\partial A^{(n-1)}(I,\omega)}{\partial \omega} \right|_{\omega=1} \times \{A^{(n-1)}(I,1)\}^{k-1} .$$

Now, every set I includes either 0, 1, 2,... nth generation particles and so by the definition of $R^{(n)}(I,\omega)$ we have $R^{(n)}(I,1) = 1$. Thus from (7.3.11) we see that $A^{(n)}(I,1) = 1$ and so from (7.3.13) we have

$$(7.3.14)\qquad M^{(n)}(I) = \sum_{k=0}^{\infty} k p_k \left. \frac{\partial A^{(n-1)}(I,\omega)}{\partial \omega} \right|_{\omega=1} .$$

But from (7.3.11) we know that

$$\left.\frac{\partial A^{(n-1)}(i,\omega)}{\partial \omega}\right|_{\omega=1} = \int_0^\infty \int_0^{2\pi} M^{(n-1)}(T(I;\underline{u},\theta))dG(\theta)dH(\ell) \ ,$$

whence on recalling that the mean of the distribution $\{p_k\}$ is m we have the integral difference equation

$$M^{(n)}(I) = m \int_0^\infty \int_0^{2\pi} M^{(n-1)}(T(I;\underline{u},\theta))dG(\theta)dH(\ell) \ . \tag{7.3.15}$$

This equation can be solved recursively. For we know that the mean number of initial particles in the set I is unity if I includes the origin and is otherwise zero. Therefore, from (7.3.15)

$$M^{(1)}(I) = m \iint_I dG(\theta)dH(\ell) \ .$$

Since the integral on the right hand side is just the probability that a particle undergoing a correlated random walk, starting from the origin with initial direction ξ, is in I after one step we may use the notation (of Chapter 5) of $F_n(.)$ for the distribution of such a particle's position after n steps, and so obtain

$$M^{(1)}(I) = mF_1(I).$$

Using this result in (7.3.15) we have

$$M^{(2)}(I) = m^2 \int_0^\infty \int_0^{2\pi} F_1(T(I;\underline{u},\theta))dG(\theta)dH(\ell) \ .$$

But

$$\int_0^\infty \int_0^{2\pi} F_1(T(I;\underline{u},\theta))dG(\theta)dH(\ell) = F_2(I) \ ,$$

and so

$$M^{(2)}(I) = m^2 F_2(I).$$

On continuing this procedure recursively we finally obtain

$$M^{(n)}(I) = m^n F_n(I) \ . \tag{7.3.16}$$

The total expected number of nth generation particles is m^n (7.1.1) and $F_n(I)$ denotes the probability that an n-step correlated random walk ends in I. Hence the the expected number of nth generation particles with positions in some set I may be separated into two terms, one of which depends upon the branching process only and the other depends upon the underlying correlated random walk only. Such a separation of a branching random walk into its two components, branching process and random walk, is often very useful. In particular the results of Section 7.4 are obtained in this manner.

Finding an expression for the variance of the number of nth generation particles with positions in I is more difficult. Let us denote this variance by $\mathrm{Var}^{(n)}(I)$, whence by the definition of the generating function

$$R^{(n)}(I,\omega) \equiv \sum_{k=0}^{\infty} \omega^k r^{(n)}(k,I)$$

we have

$$\mathrm{Var}^{(n)}(I) = \left.\frac{\partial^2 R^{(n)}(i,\omega)}{\partial \omega^2}\right|_{\omega=1} + M^{(n)}(I) - \{M^{(n)}(I)\}^2.$$

With the use of this expression an integral difference equation may be obtained by similar methods to the derivation of an integral difference equation for $M^{(n)}(I)$ (7.3.15). The final equation is

$$\mathrm{Var}^{(n)}(I) - M^{(n)}(I) + \{M^{(n)}(I)\}^2 = (v-m+m^2)\{M^{(n)}(I)/v\}^2$$
$$+ \int_0^{\infty}\int_0^{2\pi} [\mathrm{Var}^{(n-1)}(T(I;\underline{u},\theta)) - M^{(n-1)}(T(I;\underline{u},\theta))$$
$$+ \{M^{(n-1)}(T(I;\underline{u},\theta))\}^2] dG(\theta) dH(\ell) ,$$

where v is the variance of the distribution $\{p_k\}$. I have not been able to solve this equation, even for simple parametric forms of the distributions $\{p_k\}$, G(.) and H(.).

Having been unable to derive exact results for the branching correlated random walk we will now consider the asymptotic behaviour as the population size increases.

7.4 Limiting Results

7.4.i Weak law of large numbers

The weak law of large numbers has been shown to apply to the correlated random walk in the plane (Theorem 5.5.1) and an analogue exists for the branching correlated random walk.

First, the sequence of steps taken by the ancestors of any nth generation particle $\underline{i}_n$ (say) forms an n-step correlated random walk starting from the origin with initial direction ξ. Therefore the expected position of such a particle, which we will write as $(E[S_1(\underline{i}_n)], E[S_2(\underline{i}_n)])^T$, is given by results (5.4.2) and (5.4.3). So if we define the rectangle

$$I_n(\varepsilon_1,\varepsilon_2) \equiv \{(x_1,x_2): \; |x_1 - E[S_1(\underline{i}_n)]| < \varepsilon_1, \; |x_2 - E[S_2(\underline{i}_n)]| < \varepsilon_2 \}$$

for any $\varepsilon_1,\varepsilon_2 > 0$, we have the following theorem.

THEOREM 7.4.1 If G(.) and H(.) satisfy Assumptions 5.1.1 and if

$$m = \sum_{k=0}^{\infty} kp_k > 1 ,$$

then conditional upon the non-extinction of the process there is a positive random variable W such that

$$Z^{(n)}(I_n(\varepsilon_1,\varepsilon_2))/m^n \to W$$

almost surely as n increases for any $\varepsilon_1,\varepsilon_2 > 0$.

Proof

Let us write $\bar{I}_n(\varepsilon_1,\varepsilon_2)$ for the complement of $I_n(\varepsilon_1,\varepsilon_2)$. Then because

$$Z^{(n)} = Z^{(n)}(I_n(\varepsilon_1,\varepsilon_2)) + Z^{(n)}(\bar{I}_n(\varepsilon_1,\varepsilon_2))$$

and $Z^{(n)}/m^n$ converges almost surely to W as n increases (7.1.4), we need to consider the convergence to zero of $Z^{(n)}(\bar{I}_n(\varepsilon_1,\varepsilon_2))/m^n$.

As this variable is never negative, by the first Borel-Cantelli lemma (Kingman and Taylor 1966,p.337) and the definition of almost

sure convergence (Kingman and Taylor 1966,p.312), $Z^{(n)}(\bar{I}_n(\varepsilon_1,\varepsilon_2))/m^n$ will converge almost surely to zero if for every n we can find a positive integer j_n (say), with $j_n \to \infty$ as $n \to \infty$, such that

$$\sum_{n=1}^{\infty} E[Z^{(j_n)}(\bar{I}_{j_n}(\varepsilon_1,\varepsilon_2))/m^{j_n}] < \infty . \tag{7.4.1}$$

This is because if the left hand term is finite then so too is the summation

$$\sum_{n=1}^{\infty} Pr(Z^{(j_n)}(\bar{I}_{j_n}(\varepsilon_1,\varepsilon_2)) > \delta)$$

for any $\delta > 0$. Therefore by the first Borel-Cantelli lemma the event

$$Z^{(j_n)}(\bar{I}_{j_n}(\varepsilon_1,\varepsilon_2)) > \delta$$

occurs for a finite number of indices n only, with probability one. Thus there is a <u>last</u> j_n such that the event is true, and since $j_n \to \infty$ as $n \to \infty$ there is a last n such that

$$Z^{(n)}(\bar{I}_n(\varepsilon_1,\varepsilon_2)) > \delta .$$

This is true for any $\delta > 0$ and so $Z^{(n)}(\bar{I}_n(\varepsilon_1,\varepsilon_2))$ converges almost surely to zero.

Now, by (7.3.16) we have

$$\sum_{n=1}^{\infty} E[Z^{(j_n)}(\bar{I}_{j_n}(\varepsilon_1,\varepsilon_2))/m^{j_n}] = \sum_{n=1}^{\infty} F_{j_n}(\bar{I}_{j_n}(\varepsilon_1,\varepsilon_2)),$$

and from result (5.5.2) we know that there is a positive constant c such that for any positive integer m

$$F_m(\bar{I}_m(\varepsilon_1,\varepsilon_2)) < cm^{-1} .$$

Therefore we can find positive constants c_1 and c_2 (say) such that

$$\sum_{n=1}^{\infty} F_{j_n}(\bar{I}_{j_n}(\varepsilon_1,\varepsilon_2)) < c_1 + c_2 \sum_{n=1}^{\infty} j_n^{-1} . \tag{7.4.2}$$

For any $\alpha > 1$ let us choose j_n as the smallest integer which exceeds n^α. The series on the right hand side of (7.4.2) is then finite, (7.4.1) is true and the proof of Theorem 7.4.1 is complete. □

We now turn to a much more important result, an analogue to the central limit theorem. We shall give two proofs: the first shows mean square convergence and the second almost sure convergence. Although the latter is the stronger convergence (Kingman and Taylor 1966,p.312) the former result is included to demonstrate a more simple method.

7.4.ii A central limit theorem: I, mean square convergence

Our method is similar to, although slightly more simple than, that given by Asmussen and Kaplan (1976) for branching independent random walks on the real line. First we will state our aims and introduce several new terms, then we will prove the result by a series of lemmas and finally we will state the theorem formally.

From result (7.3.16) we know that the mean number of particles with positions in any set can be separated into a branching process term and a random walk term. Intuitively then, one expects that as n increases the proportion of nth generation particles with positions in some set I_n, namely $Z^{(n)}(I_n)/Z^{(n)}$, should converge to the probability that an n-step correlated random walk ends in I_n, which in turn tends to a suitable bivariate Normal probability (Theorem 5.6.1). But since both $Z^{(n)}(I_n)$ and $Z^{(n)}$ are random variables and we know that $Z^{(n)}/m^n$ converges to the random variable W defined by (7.1.3), it is easier to consider the convergence of $Z^{(n)}(I_n)/m^n$.

Let us define, for some non-zero a and b, the two sets

$$I \equiv \{(x_1,x_2): x_1 < a,\ x_2 < b\} \tag{7.4.3}$$

and

$$I_n \equiv \{(x_1,x_2): x_1 < a\sigma\sqrt{n},\ x_2 < b\sigma\sqrt{n}\}\ , \tag{7.4.4}$$

where σ^2 is the limiting variance of a correlated random walk when

scaled by the square root of the number of steps. This was defined by Theorem 5.6.1 to be $\frac{1}{2}\mu_2 + \mu_1^2 c/(1-c)$ in the earlier notation (Table 5.1.1). We seek to show that

$$(7.4.5) \qquad E[\{Z^{(n)}(I_n)/m^n - W\Phi_2(I)\}^2] \to 0$$

as $n \to \infty$, where $\Phi_2(I)$ denotes the standard bivariate Normal distribution.

Before we can prove (7.4.5) we need to introduce some new notation and recall some earlier definitions. Recall (Table 5.1.1) the definitions of $F_n(I_n)$ and $F_n(I_n;\underline{u},\zeta)$ as the probabilities that correlated random walks are in the set I_n after n steps, having started from $\underline{0},\xi$ and $\underline{u},\zeta$ respectively. Now let us define $f_n(\underline{s},\eta)$ as the probability density function of a particle performing a correlated random walk being at $\underline{s}$ with direction η after n steps, having started from $\underline{0},\xi$.

Also recall the notation $\underline{i}_k$ for any kth generation particle, with position $\underline{S}(\underline{i}_k) = (S_1(\underline{i}_k), S_2(\underline{i}_k))^T$, and denote the angle between the step taken by $\underline{i}_k$ in moving away from its parent and some fixed line by $\eta(\underline{i}_k)$. Finally, let $\underline{i}_k^{(n)}$ denote any nth generation descendant of the kth generation particle $\underline{i}_k$ $(k \leq n)$.

We shall use the following conventions:

i) $\underline{u}$ for the vector $(\ell\cos\theta, \ell\sin\theta)^T$ for any ℓ and θ;

ii) $\sum_{\underline{i}_k}$ for summation over all members of the kth generation;

and

iii) $\sum_{\underline{i}_k^{(n)}}$ for summation over all members of the nth generation which are descendants of $\underline{i}_k$.

We also need to define a new function and a new random variable. The new function is

$$(7.4.6) \qquad d_k^{(n)}(I_n;\underline{x},\zeta) \equiv F_k(I_n;\underline{x},\zeta) - F_n(I_n) \qquad (k \leq n),$$

which is the difference between the probabilities that a k-step

correlated random walk starting from $\underline{x},\zeta$ and an n-step correlated random walk starting from $\underline{0},\xi$, end in I_n. Note that by definition

$$F_{n+1}(I_n;\underline{x},\zeta) = \int_0^\infty \int_0^{2\pi} F_n(I_n;\underline{x}+\underline{u},\theta)\,dG(\theta-\zeta)\,dH(\ell) \ ,$$

whence a useful consequence of (7.4.6) is

$$(7.4.7) \qquad d_k^{(n)}(I_n;\underline{x},\zeta) = \int_0^\infty \int_0^{2\pi} d_{k-1}^{(n)}(I_n;\underline{x}+\underline{u},\theta)\,dG(\theta-\zeta)\,dH(\ell) \ .$$

The new random variable is

$$(7.4.8) \qquad D_k^{(n)}(I_n) \equiv \sum_{\underline{i}_k} m^{n-k} d_{n-k}^{(n)}(I_n;\underline{S}(\underline{i}_k),\eta(\underline{i}_k)) \qquad (k \leqslant n) \ ,$$

which, conditional upon the numbers and positions of the kth generation particles, is the expected number of nth generation particles with positions in I_n minus the term $m^{n-k}F_n(I_n)Z^{(k)}$.

Before proceeding with our proof of (7.4.5) we quote the standard results for the mean and variance of a random sum of random variables: if

$$S_N = \sum_{j=1}^{N} X_j \ ,$$

where N has mean μ_N and variance σ_N^2, and is independent of the $\{X_j\}$, a sequence of independent and identically distributed random variables with means μ_X and variances σ_X^2, then

$$(7.4.9) \qquad E[S_n] = \mu_N\mu_X$$

and

$$(7.4.10) \qquad Var(S_N) = \mu_N\sigma_X^2 + \sigma_N^2\mu_X^2$$

(Feller 1968,p.301).

Now we can prove result (7.4.5), that

$$E[\{Z^{(n)}(I_n)/m^n - W\Phi_2(I)\}^2] \to 0$$

as $n \to \infty$. From definitions (7.4.6) and (7.4.8) we have

$$D_n^{(n)}(I_n) = Z^{(n)}(I_n) - Z^{(n)}F_n(I_n), \tag{7.4.11}$$

and as a consequence of the central limit theorem for correlated random walks (Theorem 5.6.1) we have

$$F_n(I_n) \to \Phi_2(I)$$

as $n \to \infty$. The random variable W is defined to be the limit as $n \to \infty$ of $Z^{(n)}/m^n$ (7.1.3). Therefore upon rearranging (7.4.11) and dividing each side by m^n we see that result (7.4.5) will be proved if we can show that

$$m^{-2n}E[\{D_n^{(n)}(I_n)\}^2] \to 0 \tag{7.4.12}$$

as $n \to \infty$.

The method of proof of (7.4.12) depends on expanding $E[\{D_n^{(n)}(I_n)\}^2]$ by succesively conditioning on the number and positions of the preceding generation particles. Because the arguments become rather involved the proof is separated into four technical lemmas. We start with an expansion of $E[\{D_n^{(n)}(I_n)\}^2]$.

Lemma 7.4.1 For any positive integer n

$$E[\{D_n^{(n)}(I_n)\}^2] = \sum_{k=1}^{n} E[\mathrm{Var}(D_k^{(n)}(I_n) \mid \mathcal{L}_{k-1})] .$$

Proof

By first conditioning on the numbers and positions of the (n-1)st generation particles and then removing the conditioning, we have

$$E[\{D_n^{(n)}(I_n)\}^2] = E[E[\{D_n^{(n)}(I_n)\}^2 \mid \mathcal{L}_{n-1}]] .$$

So because the expected value of the square of a random variable may be expressed as its variance plus the square of its mean,

$$E[\{D_n^{(n)}(I_n)\}^2] = E[\mathrm{Var}(D_n^{(n)}(I_n) \mid \mathcal{L}_{n-1}] + E[\{E[D_n^{(n)}(I_n) \mid \mathcal{L}_{n-1}]\}^2]. \tag{7.4.13}$$

Now let us proceed recursively, at each stage expanding the last term

on the right hand side. For by definition (7.4.8) we have, for any $k \leq n$,

$$E[D_k^{(n)}(I_n) \mid \mathcal{L}_{k-1}] = E[\{\sum_{\underline{i}_k} m^{n-k} d_{n-k}^{(n)}(I_n; \underline{S}(\underline{i}_k), \eta(\underline{i}_k))\} \mid \mathcal{L}_{k-1}] ,$$

where $d_{n-k}^{(n)}(I_n; \underline{S}(\underline{i}_k), \eta(\underline{i}_k))$ is defined by (7.4.6). Since the term in braces is a random sum we may use result (7.4.9) to take expectations of the number and positions of the kth generation particles conditional upon $\mathcal{L}_{k-1}$. This yields

$$E[D_k^{(n)}(I_n) \mid \mathcal{L}_{k-1}] = \sum_{\underline{i}_{k-1}} m^{n-k+1} \{\int_0^\infty \int_0^{2\pi} d_{n-k}^{(n)}(I_n; \underline{S}(\underline{i}_{k-1}) + \underline{u}, \theta) \, dG(\theta - \eta(\underline{i}_{k-1})) \, dH(\ell)\} , \tag{7.4.14}$$

whence from (7.4.7)

$$E[D_k^{(n)}(I_n) \mid \mathcal{L}_{k-1}] = \sum_{\underline{i}_{k-1}} m^{n-k+1} d_{n-k+1}^{(n)}(I_n; \underline{S}(\underline{i}_{k-1}), \eta(\underline{i}_{k-1})) ,$$

and upon using definition (7.4.8)

$$E[D_k^{(n)}(I_n) \mid \mathcal{L}_{k-1}] = D_{k-1}^{(n)}(I_n) . \tag{7.4.15}$$

This relationship can be used recursively in (7.4.13) to complete the proof of Lemma 7.4.1.

□

The second technical lemma is concerned with the expansion of any one of the components $\mathrm{Var}(D_k^{(n)}(I_n) \mid \mathcal{L}_{k-1})$.

Lemma 7.4.2 For any positive integers k and n with $k < n$,

$$\mathrm{Var}(D_n^{(n)}(I_n) \mid \mathcal{L}_{k-1})$$

$$= \sum_{\underline{i}_{k-1}} m^{2n-2k+1} [\int_0^\infty \int_0^{2\pi} \{d_{n-k}^{(n)}(I_n; \underline{S}(\underline{i}_{k-1}) + \underline{u}, \theta)\}^2 dG(\theta - \eta(\underline{i}_{k-1})) \, dH(\ell)$$

$$- (1 - m^{-1}v)\{d_{n-k+1}^{(n)}(I_n; \underline{S}(\underline{i}_{k-1}), \eta(\underline{i}_{k-1}))\}^2] ,$$

where v denotes the variance of the offspring distribution $\{p_k\}$.

Proof

Because the offspring of any two particles behave independently, and $D_k^{(n)}(I_n)$ involves a summation over all members of the kth generation, we may use definition (7.4.8) to expand $\mathrm{Var}(D_k^{(n)}(I_n) \mid \mathcal{L}_{k-1})$ into components derived from the individual members of the kth generation, i.e.

$$\mathrm{Var}(D_k^{(n)}(I_n) \mid \mathcal{L}_{k-1}) = \sum_{\underline{i}_{k-1}} \mathrm{Var}\Big(\{ \sum_{\underline{i}_{k-1}^{(k)}} m^{n-k} d_{n-k}^{(n)}(I_n; \underline{S}(\underline{i}_{k-1}^{(k)}), \eta(\underline{i}_{k-1}^{(k)}))\} \mid \mathcal{L}_{k-1}\Big) ,$$

where $\underline{i}_{k-1}^{(k)}$ denotes any kth generation offspring of the (k-1)st generation particle $\underline{i}_{k-1}$.

The term in braces is a random sum whence result (7.4.10) for the variance of a random sum can be used to give

$$\mathrm{Var}(D_k^{(n)}(I_n) \mid \mathcal{L}_{k-1}) = \sum_{\underline{i}_{k-1}} m^{2n-2k} \{ m\mathrm{Var}(d_{n-k}^{(n)}(I_n; \underline{S}(\underline{i}_{k-1}^{(k)}), \eta(\underline{i}_{k-1}^{(k)})) \mid \mathcal{L}_{k-1})$$

$$+ v E[d_{n-k}^{(n)}(I_n; \underline{S}(\underline{i}_{k-1}^{(k)}), \eta(\underline{i}_{k-1}^{(k)})) \mid \mathcal{L}_{k-1}]^2 \} .$$

The right hand side may now be expanded with the use of (7.4.7) to complete the proof of Lemma 7.4.2. □

Now we return to the expansion of $E[\{D_n^{(n)}(I_n)\}^2]$ (Lemma 7.4.1) and use Lemma 7.4.2 to obtain the following result.

Lemma 7.4.3 For any positive integer n

$$E[\{D_n^{(n)}(I_n)\}^2] = \sum_{k=1}^{n} m^{2n-k} A_k^{(n)}(I_n) ,$$

where

$$A_k^{(n)}(I_n) = \iint_{\mathcal{R}^2} \int_0^{2\pi} \{d_{n-k}^{(n)}(I_n; \underline{s}, \eta)\}^2 f_k(\underline{s}, \eta) d\eta d\underline{s}$$

$$- (1-m^{-1}v) \iint_{\mathcal{R}^2} \int_0^{2\pi} \{d_{n-k+1}^{(n)}(I_n; \underline{s}, \eta)\}^2 f_{k-1}(\underline{s}, \eta) d\eta d\underline{s} .$$

Here $f_k(\underline{s}, \eta)$ denotes the probability density function of a k-step

correlated random walk starting from $\underline{0},\xi$ ending at $\underline{s}$ with direction η.

Proof

From Lemma 7.4.2 we have

$$\mathrm{Var}(D_k^{(n)}(I_n)\,|\,\mathcal{L}_{k-1})$$

$$= \sum_{\underline{i}_{k-1}} m^{2n-2k+1}\Big[\int_0^\infty\int_0^{2\pi}\{d_{n-k}^{(n)}(I_n;\underline{S}(\underline{i}_{k-1})+\underline{u},\theta)\}^2 dG(\theta-\eta(\underline{i}_{k-1}))dH(\ell)$$

$$- (1-m^{-1}v)\{d_{n-k+1}^{(n)}(I_n\ \underline{S}(\underline{i}_{k-1}),\eta(\underline{i}_{k-1}))\}^2\Big] .$$

If we remove the conditioning with respect to $\mathcal{L}_{k-1}$, the term on the right hand side is a random sum of random variables and we may use result (7.4.9) to take expectations. This procedure yields

$$E[\mathrm{Var}(D_k^{(n)}(I_n)\,|\,\mathcal{L}_{k-1})]$$

$$= m^{2n-k}\iint_{\mathcal{R}^2}\int_0^{2\pi}\Big[\int_0^\infty\int_0^{2\pi}\{d_{n-k}^{(n)}(I_n;\underline{s}+\underline{u},\theta)\}^2 dG(\theta-\eta)dH(\ell)\Big] f_{k-1}(\underline{s},\eta)d\eta d\underline{s}$$

$$- m^{2n-k}(1-m^{-1}v)\iint_{\mathcal{R}^2}\int_0^{2\pi}\{d_{n-k+1}^{(n)}(I_n;\underline{s},\eta)\}^2 f_{k-1}(\underline{s},\eta)d\eta d\underline{s} .$$

Therefore since

$$\iint_{\mathcal{R}^2}\int_0^{2\pi}\Big[\int_0^\infty\int_0^{2\pi} g(\underline{s}+\underline{u},\theta)dG(\theta-\eta)dH(\ell)\Big] f_{k-1}(\underline{s},\eta)d\eta d\underline{s} = \iint_{\mathcal{R}^2}\int_0^{2\pi} g(\underline{s},\eta)f_k(\underline{s},\eta)d\eta d\underline{s}$$

for any function $g(.,.)$, we have

$$E[\mathrm{Var}(D_k^{(n)}(I_n)\,|\,\mathcal{L}_{k-1})] = m^{2n-k}A_k^{(n)}(I_n) .$$

Lemma 7.4.1, which states that

$$E[\{D_n^{(n)}(I_n)\}^2] = \sum_{k=1}^{n} E[\mathrm{Var}(D_k^{(n)}(I_n)\,|\,\mathcal{L}_{k-1})]$$

now completes the proof of Lemma 7.4.3.

□

The final result which we require is concerned with the convergence to zero of the terms $\{A_k^{(n)}(I_n)\}$ when k is fixed but n tends to infinity.

Lemma 7.4.4 For any positive integer k the term

$$A_k^{(n)}(I_n) = \iint_{\mathbb{R}^2} \int_0^{2\pi} \{d_{n-k}^{(n)}(I_n;\underline{s},\eta)\}^2 f_k(\underline{s},\eta)\,d\eta\,d\underline{s}$$

$$- (1-m^{-1}v) \iint_{\mathbb{R}^2} \int_0^{2\pi} \{d_{n-k+1}^{(n)}(I_n;\underline{s},\eta)\}^2 f_{k-1}(\underline{s},\eta)\,d\eta\,d\underline{s}$$

tends to zero as n tends to infinity.

Proof

The central limit theorem for correlated random walks (Theorem 5.6.1) may be used to show that for all $\underline{s}$ and η

$$F_{n-k}(I_n;\underline{s},\eta) \to \Phi_2(I) \tag{7.4.16}$$

as n tends to infinity whilst k is fixed. (This explains our choice of the sets I_n and I for any a and b (7.4.3, 7.4.4)). Therefore the function

$$d_{n-k}^{(n)}(I_n;\underline{s},\eta) = F_{n-k}(I_n;\underline{s},\eta) - F_n(I_n)$$

must tend to zero as n increases to infinity. This function is a difference between two probabilities and so has modulus less than or equal to one. Thus

$$\{d_{n-k}^{(n)}(I_n;\underline{s},\eta)\}^2 \leqslant \left|d_{n-k}^{(n)}(I_n;\underline{s},\eta)\right| \leqslant 1\,, \tag{7.4.17}$$

and the left hand term must also tend to zero as n increases. Therefore we can use the dominated convergence principle (Feller 1971, p.111) to show that because the two integrands in the definition of $A_k^{(n)}(I_n)$ above each tend to zero as n increases to infinity, then so too does $A_k^{(n)}(I_n)$. This completes the proof of Lemma 7.4.4.

□

Note that since $A_k^{(n)}(I_n)$ is a variance (Lemmas 7.4.2 and 7.4.3), and $\{d_k^{(n)}(I_n;\underline{s},\eta)^2\} \leqslant 1$ (7.4.17), then

$$0 \leqslant A_k^{(n)}(I_n) \leqslant \max(1, m^{-1}v) .$$

Together with Lemma 7.4.4 and our assumption that $m > 1$, these bounds are sufficient to show that as n tends to infinity

$$\sum_{k=1}^{n} m^{-k} A_k^{(n)}(I_n) \to 0 .$$

Hence result (7.4.12), namely

$$m^{-2n} E[\{D_n^{(n)}(I_n)\}^2] \to 0$$

as n tends to infinity, follows directly from Lemma 7.4.3. Therefore upon using (7.4.11), i.e.

$$D_n^{(n)}(I_n) = Z^{(n)}(I_n) - Z^{(n)}F_n(I_n) ,$$

the central limit theorem for correlated random walks (Theorem 5.6.1) and the definition of the random variable W, we have proved the following analogue to the central limit theorem.

THEOREM 7.4.2 If Assumptions 5.1.1 are satisfied by G(.) and H(.), and if $m > 1$ and $v < \infty$, then there is a positive random variable W such that if the branching correlated random walk does not become extinct

$$E[\{Z^{(n)}(I_n)/m^n - W\Phi_2(I)\}^2] \to 0$$

as $n \to \infty$, where I and I_n are the sets defined by (7.4.3) and (7.4.4) respectively.

7.4.iii A central limit theorem: II, almost sure convergence

The mean square convergence of Theorem 7.4.2 may be strengthened to almost sure convergence. The method which we use to prove this is similar to that given by Kaplan and Asmussen (1976) for branching independent random walks on the real line, and so we will omit some

details. So, our aim is to prove that $Z^{(n)}(I_n)/m^n$ converges almost surely to $W\Phi_2(I)$ as n increases. As in the previous section first we will introduce some necessary new notation, then we will prove the result by a series of lemmas, and finally we will give a formal statement of the theorem.

Let us denote the number of descendants of the kth generation particle $\underline{i}_k$ which are alive at time n (n > k) by $Z^{(n)}(\underline{i}_k)$, and the number of such particles with positions in some set I by $Z^{(n)}(I;\underline{i}_k)$. No confusion will arise between these definitions and our earlier definition of $Z^{(n)}(I)$ to be the number of nth generation particles with positions in I, because the useage will be clear from the context. Also let

$$W^{(n)}(\underline{i}_k) \equiv Z^{(n)}(\underline{i}_k)/m^{n-k}$$

and

$$W^{(n)}(I;\underline{i}_k) \equiv Z^{(n)}(I;\underline{i}_k)/m^{n-k} .$$

In addition, throughout the following we will use the definitions (7.4.3) and (7.4.4) of the two sets I and I_n respectively.

Now we may proceed with our proof. For each positive integer n define k(n) as some integer between zero and n, such that both k(n) and n - k(n) tend to infinity with n. For example, k(n) could be the integer part of $n^{\frac{1}{2}}$ or $n^{\frac{1}{4}}$. Then because

$$Z^{(n)}(I_n) = \sum_{\underline{i}_{k(n)}} Z^{(n)}(I_n;\underline{i}_{k(n)}),$$

we may write

$$W^{(n)}(I_n) \equiv Z^{(n)}(I_n)/m^n = m^{-k(n)} \sum_{\underline{i}_{k(n)}} W^{(n)}(I_n;\underline{i}_{k(n)}).$$

Now let us introduce the zero term

$$m^{-k(n)} \sum_{\underline{i}_{k(n)}} \{E[W^{(n)}(I_n;\underline{i}_{k(n)})] - E[W^{(n)}(I_n;\underline{i}_{k(n)})] - \Phi_2(I)\} + W^{(k(n))}\Phi_2(I)$$

to the right hand term above to obtain

$$Z^{(n)}(I_n)/m^n = m^{-k(n)} \sum_{\underline{i}_{k(n)}} \{W^{(n)}(I_n;\underline{i}_{k(n)}) - E[W^{(n)}(I_n;\underline{i}_{k(n)})]\}$$

(7.4.18)

$$+ m^{-k(n)} \sum_{\underline{i}_{k(n)}} \{E[W^{(n)}(I_n;\underline{i}_{k(n)})] - \Phi_2(I)\} + W^{(k(n))}\Phi_2(I).$$

We have defined $k(n)$ such that $k(n) \to \infty$ as $n \to \infty$, whence as n tends to infinity $W^{(k(n))} \equiv Z^{(k(n))}/m^{k(n)}$ converges almost surely to the random variable W defined by (7.1.4). Thus to prove that $Z^{(n)}(I_n)/m^n$ converges almost surely to $W\Phi_2(I)$ we need to show that

$$(7.4.19) \quad m^{-k(n)} \sum_{\underline{i}_{k(n)}} \{W^{(n)}(I_n;\underline{i}_{k(n)}) - E[W^{(n)}(I_n;\underline{i}_{k(n)})]\} \to 0$$

almost surely and

$$(7.4.20) \quad m^{-k(n)} \sum_{\underline{i}_{k(n)}} \{E[W^{(n)}(I_n;\underline{i}_{k(n)})] - \Phi_2(I)\} \to 0$$

almost surely.

The former result (7.4.19) is shown by the following lemma.

Lemma 7.4.5 If there is an $\varepsilon > 0$ such that

$$\sum_{k=1}^{\infty} k\{\log(k)\}^{1+\varepsilon} p_k < \infty ,$$

then for all choices of $k(n)$ such that $k(n) \to \infty$ and $(n-k(n)) \to \infty$ as $n \to \infty$,

$$m^{-k(n)} \sum_{\underline{i}_{k(n)}} \{W^{(n)}(I_n;\underline{i}_{k(n)}) - E[W^{(n)}(I_n;\underline{i}_{k(n)})]\} \to 0$$

almost surely provided that the process does not become extinct.

Proof

By the definition of almost sure convergence (Kingman and Taylor 1966,p.312) and the first Borel-Cantelli lemma (Kingman and Taylor 1966,p.337) we only need to show that for every $\delta > 0$

$$\sum_{n=1}^{\infty} \Pr\left(\left| m^{-k(n)} \sum_{\underline{i}_{k(n)}} \{W^{(n)}(I_n;\underline{i}_{k(n)}) - E[W^{(n)}(I_n;\underline{i}_{k(n)})]\}\right| > \delta\right) < \infty .$$

The number of nth generation descendants of $\underline{i}_{-k(n)}$ with positions in any set cannot exceed the total number of nth generation descendants of $\underline{i}_{-k(n)}$, i.e.

$$Z^{(n)}(I_n;\underline{i}_{-k(n)}) \leqslant Z^{(n)}(\underline{i}_{-k(n)}) ,$$

whence

$$W^{(n)}(I_n;\underline{i}_{-k(n)}) \leqslant W^{(n)}(\underline{i}_{-k(n)}),$$

and so

$$\sum_{n=1}^{\infty} \Pr\Big(\Big| m^{-k(n)} \sum_{\underline{i}_{-k(n)}} \{ W^{(n)}(I_n;\underline{i}_{-k(n)}) - E[W^{(n)}(I_n;\underline{i}_{-k(n)})] \} \Big| > \delta \Big)$$

$$\leqslant \sum_{n=1}^{\infty} \Pr\Big(m^{-k(n)} \sum_{\underline{i}_{-k(n)}} \{ W^{(n)}(\underline{i}_{-k(n)}) + E[W^{(n)}(\underline{i}_{-k(n)})] \} > \delta \Big) .$$

Moreover, because $W^{(n)}(\underline{i}_{-k(n)})$ has the same distribution as $W^{(n-k(n))}$ we have

$$\sum_{n=1}^{\infty} \Pr\Big(m^{-k(n)} \sum_{\underline{i}_{-k(n)}} \{ W^{(n)}(\underline{i}_{-k(n)}) + E[W^{(n)}(\underline{i}_{-k(n)})] \} > \delta \Big)$$

$$\leqslant \sum_{n=1}^{\infty} \Pr\Big(m^{-k(n)} \sum_{\underline{i}_{-k(n)}}^{\infty} \{ M + E[M] \} > \delta \Big) ,$$

where

$$M = \sup_n (W^{(n)}) .$$

The term on the right hand side of the last inequality is independent of the underlying correlated random walk and dimensionality, and depends on the distribution $\{p_k\}$ only. As we make the same assumptions on $\{p_k\}$ as Kaplan and Asmussen (1976), their Lemmas 1, 2 and 4 may be used to show that the term is finite and complete the proof of Lemma 7.4.5.

□

To prove the second result (7.4.20) required for the almost sure

convergence of $Z^{(n)}(I_n)/m^n$ we need three preparatory technical lemmas. First, let us define the set $I(c_1,c_2)$ for any c_1 and c_2 by

$$I(c_1,c_2) \equiv \{ (x_1,x_2): x_1 < c_1, x_2 < c_2 \} .$$

We shall still use our earlier definitions (7.4.3 and 7.4.4) of the sets I and I_n, which, in the new notation, are equivalent to $I(a,b)$ and $I(a\sigma\sqrt{n},b\sigma\sqrt{n})$ respectively. Also, recall the definition of $\Phi_2(.)$ as the standard Normal distribution, i.e.

$$\Phi_2(I(c_1,c_2)) \equiv \Pr(Y_1 < c_1)\Pr(Y_2 < c_2) , \tag{7.4.21}$$

where Y_1 and Y_2 are two independent standard Normal random variables.

The first technical lemma is a simple result for the distribution $\Phi_2(.)$.

Lemma 7.4.6 For any c_1, c_2, c_3 or c_4

$$\Phi_2(I(c_1-c_3,c_2-c_4)) \leqslant \Phi_2(I(c_1,c_2)) + \tfrac{1}{2}\pi^{-1}|c_3||c_4| + (2\pi)^{-\frac{1}{2}}\{|c_3| + |c_4|\} .$$

Proof

For any random variable Y we have

$$\Pr(Y < c_1-c_3) \leqslant \Pr(Y < c_1+|c_3|) = \Pr(Y < c_1) + \Pr(c_1 \leqslant Y < c_1+|c_3|) . \tag{7.4.22}$$

Furthermore, if Y has the standard Normal distribution

$$\Pr(c_1 \leqslant Y < c_1+|c_3|) = \int_{c_1}^{c_1+|c_3|} (2\pi)^{-\frac{1}{2}}\exp(-\tfrac{1}{2}y^2)dy ,$$

which has maximum (over all c_1) when c_1 is equal to $-\frac{1}{2}|c_3|$, i.e.

$$\Pr(c_1 \leqslant Y < c_1+|c_3|) \leqslant \int_{-\frac{1}{2}|c_3|}^{\frac{1}{2}|c_3|} (2\pi)^{-\frac{1}{2}}\exp(-\tfrac{1}{2}y^2)dy .$$

Therefore since $\exp(-\frac{1}{2}y^2)$ is not greater than unity we have

$$\Pr(c_1 \leqslant Y < c_1+|c_3|) \leqslant (2\pi)^{-\frac{1}{2}}|c_3| .$$

A similar result is true when c_1 and c_3 are replaced by c_2 and c_4

respectively. Thus we can complete the proof of Lemma 7.4.6 by using these results together with (7.4.22) in the definition (7.4.21). □

Before we state the second technical lemma let us choose the integers $k(n)$. For some $0 < \beta < \frac{1}{2}$ choose a positive number α such that $\alpha\beta^{-1} < 1$. Thus for each positive integer n we can find another positive integer j_n (say) such that $j_n^\alpha \leq n^\beta < (j_n+1)^\alpha$, and we will choose $k(n)$ to be the largest integer which does not exceed j_n^α. More precisely

$$k(n) = \sup \{k: k \leq j_n^\alpha,\ j_n^\alpha \leq n^\beta < (j_n+1)^\alpha\} . \tag{7.4.23}$$

It is easy to show that this choice of $k(n)$ satisfies the criteria that $0 \leq k(n) \leq n$ and both $k(n)$ and $n - k(n)$ tend to infinity with n. First, we know that $n^\beta \geq 0$ whence $k(n) \geq 0$, and because $\beta < \frac{1}{2}$ and $k(n) \leq n^\beta$ it follows that $k(n) \leq n$. Next, from the definition (7.4.23) we see that $\{k(n)+1\}^{1/\alpha}+1 \geq n^{\beta/\alpha}$ and as $\beta/\alpha > 1$ we see that $k(n)$ must tend to infinity with n. Finally, $\{n-k(n)\} > \{n-n^\beta\}$ and $0 < \beta < \frac{1}{2}$ whence $n - k(n)$ tends to infinity with n.

Throughout the remainder of this section we will assume that $k(n)$ is chosen by (7.4.23).

The second technical lemma is concerned with the convergence to zero of a certain random variable.

Lemma 7.4.7 Denote the position of the $k(n)$th generation particle $\underline{i}_{k(n)}$ by

$$\underline{S}(\underline{i}_{k(n)}) \equiv (S_1(\underline{i}_{k(n)}), S_2(\underline{i}_{k(n)}))^T .$$

With $k(n)$ chosen by (7.4.23) the random variables

$$m^{-k(n)} \sum_{\underline{i}_{k(n)}} |S_1(\underline{i}_{k(n)}) \times S_2(\underline{i}_{k(n)})| / \{n-k(n)\}$$

converge almost surely to zero as n tends to infinity.

Proof

By the first Borel-Cantelli lemma (Kingman and Taylor 1966,p.337)

and the definition of almost sure convergence (Kingman and Taylor 1966, p.312) we require that for any $\delta > 0$,

$$(7.4.24)\quad \sum_{k(n)=1}^{\infty} \Pr(\{m^{-k(n)} \sum_{\underline{i}_{k(n)}} |S_1(\underline{i}_{k(n)}) \times S_2(\underline{i}_{k(n)})|/(n-k(n))\} > \delta) < \infty .$$

Since the term in braces is non-negative and $\Pr(Y > \delta) < E[Y]/\delta$ for any non-negative random variable Y, (7.4.24) will be true if

$$(7.4.25)\quad \sum_{k(n)=1}^{\infty} E[\, m^{-k(n)} \sum_{\underline{i}_{k(n)}} |S_1(\underline{i}_{k(n)}) \times S_2(\underline{i}_{k(n)})|/(n-k(n))] < \infty .$$

The expected position of any particle existing at time $k(n)$ is the same as that of a particle performing a $k(n)$-step correlated random walk starting from $\underline{0},\xi$. Moreover, the expected size of the $k(n)$th generation is $m^{k(n)}$. Therefore by using (7.4.9) to take expectations of the random sum

$$\sum_{\underline{i}_{k(n)}} |S_1(\underline{i}_{k(n)}) \times S_2(\underline{i}_{k(n)})|$$

we have

$$E[\, m^{-k(n)} \sum_{\underline{i}_{k(n)}} |S_1(\underline{i}_{k(n)}) \times S_2(\underline{i}_{k(n)})|/(n-k(n))]$$

$$(7.4.26)\qquad = E[|S_{k(n)1} \times S_{k(n)2}|]/(n-k(n)) ,$$

where we use $S_{k(n)1}$ and $S_{k(n)2}$ to denote the coordinates of a particle after $k(n)$ steps of a correlated random walk.

Now, for any positive integer k the term $E[\{|S_{k1}| - |S_{k2}|\}^2]$ is non-negative, whence upon expanding the square we see that

$$E[|S_{k1} \times S_{k2}|] \leqslant \tfrac{1}{2}E[S_{k1}^2 + S_{k2}^2] .$$

Therefore with the use of the moment results for correlated random walks (Section 5.4) we can find a positive number c such that

$$E[|S_{k1} \times S_{k2}|] \leqslant ck .$$

This result may be used together with (7.4.26) to show that

$$\sum_{k(n)=1}^{\infty} E\left[m^{-k(n)} \sum_{\underline{i}_{k(n)}} |S_1(\underline{i}_{k(n)}) \times S_2(\underline{i}_{k(n)})|/(n-k(n))\right] \leqslant c \sum_{k(n)=1}^{\infty} k(n)/(n-k(n)).$$

If we recall the definition (7.4.23) of k(n) we see that the right hand side above is finite if

$$\sum_{k=1}^{\infty} k/(k^{1/\beta}-k) < \infty ,$$

which is true because $\beta < \frac{1}{2}$. Thus (7.4.25) is true, (7.4.24) is true and the proof of Lemma 7.4.7 is complete.

□

The proof of the final preparatory lemma is similar to that of Lemma 7.4.7 and will be omitted. The lemma is as follows.

Lemma 7.4.8 With k(n) chosen by (7.4.23) for any positive integer n, and with the position of the k(n)th generation particle $\underline{i}_{k(n)}$ denoted by $(S_1(\underline{i}_{k(n)}), S_2(\underline{i}_{k(n)}))^T$, the random variables

$$m^{-k(n)} \sum_{\underline{i}_{k(n)}} |S_1(\underline{i}_{k(n)})|/\{n-k(n)\}^{\frac{1}{2}} \text{ and } m^{-k(n)} \sum_{\underline{i}_{k(n)}} |S_2(\underline{i}_{k(n)})|/\{n-k(n)\}^{\frac{1}{2}}$$

each converge almost surely to zero as n tends to infinity.

□

Now we may prove result (7.4.20) and so complete the proof of the central limit analogue.

Lemma 7.4.9 With k(n) defined by (7.4.23) for any positive integer n, the random variable

$$m^{-k(n)} \sum_{\underline{i}_{k(n)}} \{E[W^{(n)}(I_n; \underline{i}_{k(n)})] - \Phi_2(I)\}$$

converges almost surely to zero as n tends to infinity.

Proof

Throughout this proof the terms $an^{\frac{1}{2}}/\{n-k(n)\}^{\frac{1}{2}}$ and $bn^{\frac{1}{2}}/\{n-k(n)\}^{\frac{1}{2}}$ will be denoted by a_n and b_n respectively, where a and b are as chosen

in the definitions of the sets I and I_n (7.4.3 and 7.4.4).

Let us consider the random variable

$$B_n \equiv m^{-k(n)} \sum_{\underline{i}_{k(n)}} \{E[W^{(n)}(I_n;\underline{i}_{k(n)})] - \Phi_2(I)\} ,$$

which, by the definition of $W^{(n)}(I_n;\underline{i}_{k(n)})$, may be written as

$$B_n = m^{-k(n)} \sum_{\underline{i}_{k(n)}} \{E[Z^{(n)}(I_n;\underline{i}_{k(n)})]/m^{n-k(n)} - \Phi_2(I)\} .$$

The expected number of nth generation descendants of $\underline{i}_{k(n)}$ with positions in I_n, namely $E[Z^{(n)}(I_n;\underline{i}_{k(n)})]$, is given by (7.3.16) as $m^{n-k(n)}F_{n-k(n)}(I_n;\underline{S}(\underline{i}_{k(n)}),\eta(\underline{i}_{k(n)}))$. Thus

$$B_n = m^{-k(n)} \sum_{\underline{i}_{k(n)}} \{F_{n-k(n)}(I_n;\underline{S}(\underline{i}_{k(n)}),\eta(\underline{i}_{k(n)})) - \Phi_2(I)\} .$$

Now introduce the zero term

$$m^{-k(n)} \sum_{\underline{i}_{k(n)}} [\Phi_2(I(a_n - S_1(\underline{i}_{k(n)})/\{\sigma\sqrt{(n-k(n))}\}, b_n - S_2(\underline{i}_{k(n)})/\{\sigma\sqrt{(n-k(n))}\}))$$

$$- \Phi_2(I(a_n - S_1(\underline{i}_{k(n)})/\{\sigma\sqrt{(n-k(n))}\}, b_n - S_2(\underline{i}_{k(n)})/\{\sigma\sqrt{(n-k(n))}\}))]$$

to the right hand side to give

$$B_n = m^{-k(n)} \sum_{\underline{i}_{k(n)}} [\Phi_2(I(a_n - S_1(\underline{i}_{k(n)})/\{\sigma\sqrt{(n-k(n))}\}, b_n - S_2(\underline{i}_{k(n)})/\{\sigma\sqrt{(n-k(n))}\}))$$

$$- \Phi_2(I)] + m^{-k(n)} \sum_{\underline{i}_{k(n)}} [F_{n-k(n)}(I_n;\underline{S}(\underline{i}_{k(n)}),\eta(\underline{i}_{k(n)}))$$

$$- \Phi_2(I(a_n - S_1(\underline{i}_{k(n)})/\{\sigma\sqrt{(n-k(n))}\}, b_n - S_2(\underline{i}_{k(n)})/\{\sigma\sqrt{(n-k(n))}\}))] . \qquad (7.4.27)$$

If we define

$$\Delta_n \equiv \sup_{\substack{\underline{s} \in \mathbb{R}^2 \\ 0<\eta<2\pi}} \{ |F_{n-k(n)}(I_n;\underline{s},\eta) - \Phi_2(I(a_n,b_n))| \} ,$$

we can take the modulus of each side of (7.4.27) to yield

$$|B_n| \leq m^{-k(n)} \sum_{\underline{i}_{k(n)}} [|\Phi_2(I(a_n - S_1(\underline{i}_{k(n)})/\{\sigma\sqrt{(n-k(n))}\}, b_n - S_2(\underline{i}_{k(n)})/\{\sigma\sqrt{(n-k(n))}\}))$$

(7.4.28)

$$- \Phi_2(I)|] + W^{(k(n))}\Delta_n ,$$

where $W^{(k(n))}$ is the random variable $Z^{(k(n))}/m^{k(n)}$.

As a consequence of the central limit theorem for correlated random walks (Theorem 5.6.1) and the choice of k(n) (7.4.23) such that n - k(n) tends to infinity with n, we see that Δ_n, which is not random, tends to zero as n increases. The random variable $W^{(k(n))}$ converges almost surely as n increases to infinity (7.1.4), whence $W^{(k(n))}\Delta_n$ converges almost surely to zero. As Lemma 7.4.9 will be proved if we can show that B_n converges almost surely to zero it follows that we need to consider the first term on the right hand side of (7.4.28) only, i.e.

$$m^{-k(n)} \sum_{\underline{i}_{k(n)}} [|\Phi_2(I(a_n - S_1(\underline{i}_{k(n)})/\{\sigma\sqrt{(n-k(n))}\}, b_n - S_2(\underline{i}_{k(n)})/\{\sigma\sqrt{(n-k(n))}\}))$$

$$- \Phi_2(I)|] .$$

First let us use Lemma 7.4.6 to write

$$\Phi_2(I(a_n - S_1(\underline{i}_{k(n)})/\{\sigma\sqrt{(n-k(n))}\}, b_n - S_2(\underline{i}_{k(n)})/\{\sigma\sqrt{(n-k(n))}\})) \leq \Phi_2(I(a_n, b_n))$$

(7.4.29)

$$+ \tfrac{1}{2}\pi^{-1}|S_1(\underline{i}_{k(n)}) \times S_2(\underline{i}_{k(n)})|/\{\sigma^2(n-k(n))\}$$

$$+ (2\pi)^{-\frac{1}{2}}\{|S_1(\underline{i}_{k(n)})| + |S_2(\underline{i}_{k(n)})|\}/\{\sigma\sqrt{(n-k(n))}\} ,$$

and then note that as n tends to infinity

(7.4.30)

$$\Phi_2(I(a_n, b_n)) \to \Phi_2(I) .$$

Therefore we only need to consider the random variables

$$\tfrac{1}{2}\pi^{-1}m^{-k(n)} \sum_{\underline{i}_{k(n)}} |S_1(\underline{i}_{k(n)}) \times S_2(\underline{i}_{k(n)})|/\{\sigma^2(n-k(n))\}$$

and

$$(2\pi)^{-\frac{1}{2}} m^{-k(n)} \sum_{\underline{i}_{k(n)}} \{|S_1(\underline{i}_{k(n)})| + |S_2(\underline{i}_{k(n)})|\}/\{\sigma\sqrt{(n-k(n))}\} .$$

Lemmas 7.4.7 and 7.4.8 show that each of these converge almost surely to zero as n increases. Thus from (7.4.28), (7.4.29) and (7.4.30) we see that B_n converges almost surely to zero and the proof is complete.

□

We have proved the results (7.4.19) and (7.4.20) to be true and so we may state the following theorem.

THEOREM 7.4.3 If Assumptions 5.1.1 are satisfied by G(.) and H(.), and if $m > 1$ and for some $\varepsilon > 0$

$$\sum_{k=1}^{\infty} k\{\log(k)\}^{1+\varepsilon} p_k < \infty ,$$

then there is a positive random variable W such that if the branching correlated random walk does not become extinct

$$Z^{(n)}(I_n)/m^n \to W\Phi_2(I)$$

almost surely as n tends to infinity, where I and I_n are the sets defined by (7.4.3) and (7.4.4) respectively.

7.5 Asymptotic Shape

7.5.i The shape of a spatial population distribution

Our central limit theorem analogues (Theorems 7.4.2 and 7.4.3) do not apply to the extremities of the distribution of particle positions, which must be considered separately. Whilst several authors (for example Biggins 1977b or Bramsom 1978) have investigated the tails of the distribution for branching independent-step random walks on the real line, their methods cannot be used for populations evolving in higher dimensions where there is no unique ordering of the particle positions. Biggins (1978) however, has investigated the

shape of d-dimensional branching independent-step random walks (for any positive integer d) by considering the convex hull of the set of nth generation particle positions scaled by n. The convex hull of a collection of points is the smallest closed convex set containing all points: a convex set, C say, has the property that if x_1 and x_2 are points in C then the line from x_1 to x_2 is wholly contained in C. Biggins showed that as n increases the convex hull converges to a certain convex set whose boundary satisfies a given expression. A similar investigation into the convergence of the convex hulls of a population evolving as a branching correlated random walk would be useful, but unfortunately Biggins' method cannot be extended to include the case of correlated step directions. This is because Biggins' method involves certain convolution properties which are not true when step directions are correlated. I have not been able to develop any other method of studying the convergence of the convex hulls by theoretical analysis.

An alternative to a formal theoretical analysis is to study the convex hulls formed when a number of branching correlated random walks are simulated by computer. To my knowledge there have been no previous simulation studies of any type of branching random walk.

7.5.ii Computer simulation of branching correlated random walks

Before the evolution of branching correlated random walks can be simulated we must choose:

i) a stopping rule;

ii) the parametric form of the distributions $\{p_k\}$, G(.) and H(.);

iii) the number of simulations to be performed; and

iv) a method of comparing simulated populations,

Our choices are described below.

Stopping rule

Our purpose is to investigate the asymptotic shape of the convex hulls of the population distribution, but obviously an infinite number of generations cannot be simulated. Therefore the evolution must be terminated either after a fixed number of generations or when

the population reaches a specified size. Because the variance of the population size distribution has the same order of magnitude as the square of its mean (Harris 1963,p.6), simulation of a fixed number of generations would result in a wide range of population sizes. Therefore we preferred to simulate the evolution until the population size reached a fixed number, which was restricted to 10,000 by computing capacity. We then considered the convex hull of the Mth generation, where

$$M = \sup\,(n: Z^{(n)} \leqslant 10{,}000) \ .$$

Parametric forms of the distributions $\{p_k\}$, G(.) and H(.)

The step length distribution H(.) has a scaling effect only on the convex hull. Therefore in our simulations only one length distribution was considered, namely that of the fourth power of a standard Normal random variable. This distribution was suggested by our analysis of the root STEPLEN data (Section 3.4).

The offspring distribution $\{p_k\}$ may affect the convergence of the convex hulls. We considered three such distributions; each had mean 1.05 so that the expected population size did not reach 10,000 until after almost 200 generations. The distributions, which were labelled A, B and C for reference, were:

	p_0	p_1	p_2	p_3	p_k $(k > 3)$
A	0.00	0.95	0.05	0.00	0.00
B	0.00	0.97	0.01	0.02	0.00
C	0.05	0.89	0.02	0.04	0.00

Distribution A allows only one or two offspring to be produced by any particle, B also allows three and C includes a positive probability of death. When distribution C was used in the simulations and a population became extinct before the number of particles had reached 10,000, then that simulation was discarded and another was performed. Thus our results are conditional upon the non-extinction of the process.

Our main interest is in the effect of correlation between step directions. This may be studied by changing the variance of the

turning variable distribution G(.). If that variance is low then there is a high correlation between the parent and offspring step directions; whilst if the variance is high G(.) is almost equivalent to the circular uniform distribution, as is the distribution of offspring step directions whatever the parent step direction (Mardia 1972,p.51). We chose G(.) to be the zero mean wrapped Normal distribution with variance σ^2, and performed simulations at each of the values $\sigma^2 = 0.1(0.1)1.0$ (radians)^2.

Number of simulations

Three offspring distributions and ten turning variable distributions were chosen. Because of computing time restrictions five branching correlated random walks only could be simulated at each combination of distributions.

Comparison of populations

To my knowledge no method of comparing convex hulls has been suggested previously. In this study the convex hulls of the 150 simulated populations were compared by visually examining graph plots and with the use of crinkliness coefficients (Mollison 1972). The crinkliness coefficient of a convex hull is the ratio of its perimeter to that of a circle enclosing an identical area. Circles have minimum boundary length of all sets enclosing a like area, whence crinkliness coefficients are at least unity, with values close to one indicating shapes similar to a circle.

The development of only a finite number of generations could be simulated and so the results may be distorted by an occasional outlying particle. Therefore the crinkliness coefficients of the outer ten convex peels (Green and Silverman 1979) of each simulated population were also calculated. The first convex peel of a set of points is simply the convex hull, the second convex peel is the convex hull of the points remaining after those on the first convex peel have been removed, and so on. When the population size is near 10,000 ten convex peels include only a small proportion of the total number of points, yet should be sufficient to illustrate any effect of outlying particles.

The properties of the crinkliness coefficient of the convex hull

of a spatial population distribution are unknown. In particular it is not clear whether the crinkliness coefficients converge as the population size increases, even if the convex hulls converge. In order to investigate the convergence of the crinkliness coefficients an additional twenty branching correlated random walks were simulated, using the offspring distribution A, at each of σ^2 = 0.1, 0.3 and 0.5 (radians)^2. In each case the crinkliness coefficients of the outer ten convex peels of the the M_jth generation particle positions were calculated for j = 1, 2,...,10, where

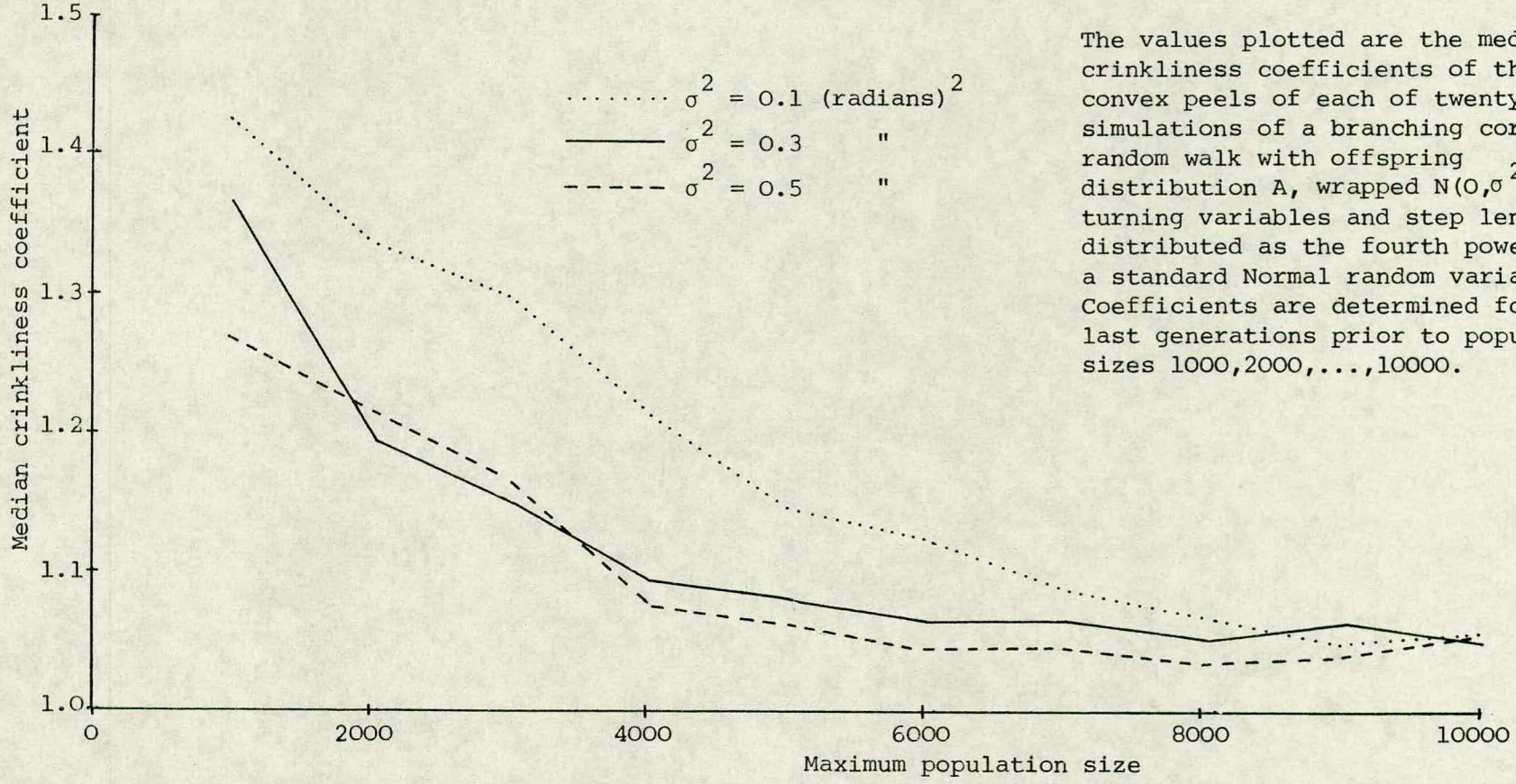
$$M_j = \sup\ (n:\ Z^{(n)} < 1000j)\ .$$

All simulations were performed with the use of a FORTRAN program incorporating a convex peeling routine (Green and Silverman 1979). Each population was evolved from one initial particle situated at the origin of the plane and with associated direction (ξ) parallel to the X-axis.

7.5.iii Results

The median crinkliness coefficients of the convex peels of the twenty simulations at each of σ^2 = 0.1, 0.3 and 0.5 (radians)^2, were high at low population sizes but decreased to a fairly stable value as the population size increased (Figure 7.5.1). The rate of decline was slowest at σ^2 = 0.1 (radians)^2, which caused offspring and parent step directions to be similar, but the final median coefficients at each choice of σ^2 were similar: in each case near to 1.05. The range of the crinkliness coefficients over the ten convex peels also decreased as the population size increased (Figure 7.5.2). Again the rate of decline was slowest when σ^2 = 0.1 (radians)^2 but the final values were similar. Although not conclusive, these data suggest that the crinkliness coefficients converge, and that the coefficients of populations of more than 8000 particles are stable.

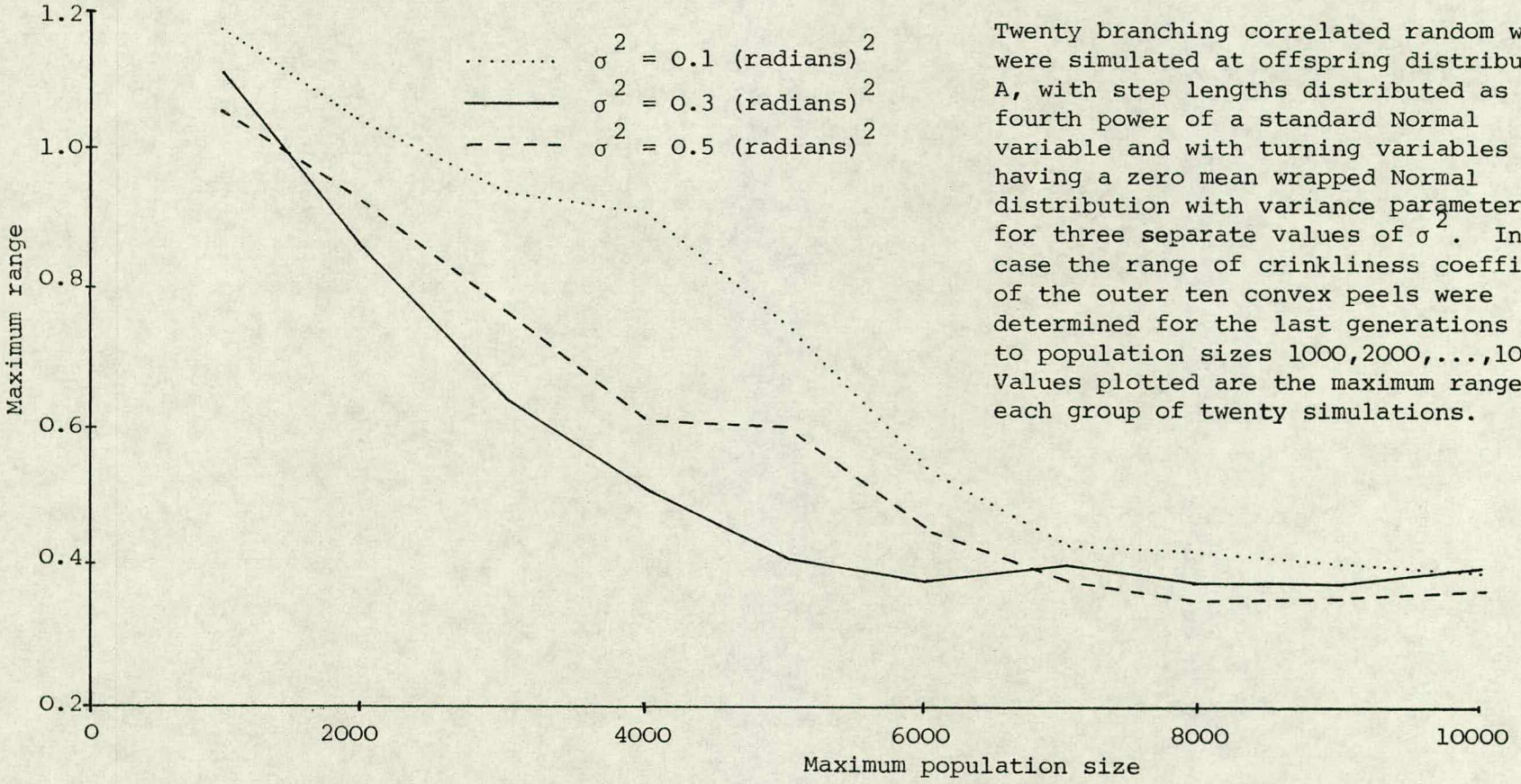
The final population sizes of the 150 branching correlated random walks simulated at the 30 combinations of offspring and turning variable distributions all exceeded 9300 (after between 140 and 250 generations). Therefore the crinkliness coefficients may be used to



The values plotted are the median crinkliness coefficients of the ten convex peels of each of twenty simulations of a branching correlated random walk with offspring distribution A, wrapped $N(0,\sigma^2)$ turning variables and step lengths distributed as the fourth power of a standard Normal random variable. Coefficients are determined for the last generations prior to population sizes 1000,2000,...,10000.

Figure 7.5.1

Convergence of the crinkliness coefficients



Twenty branching correlated random walks were simulated at offspring distribution A, with step lengths distributed as the fourth power of a standard Normal variable and with turning variables having a zero mean wrapped Normal distribution with variance parameter σ^2, for three separate values of σ^2. In each case the range of crinkliness coefficients of the outer ten convex peels were determined for the last generations prior to population sizes 1000,2000,...,10000. Values plotted are the maximum ranges of each group of twenty simulations.

Figure 7.5.2

Maximum ranges of crinkliness coefficients

compare the convex hulls of the final populations and so analyse the influence of the three offspring distributions and the ten turning variable distributions.

Examination of the crinkliness coefficients showed that there were no obvious differences between the coefficients of different offspring distributions and no systematic variation between peels or values of σ^2 (Tables 7.5.1 and 7.5.2). A log-log transformation was used to transform the data to be approximately Normal; and a standard split-plot analysis of variance, with the convex peels as subplots and the offspring and turning variable distributions as treatments, showed no significant (10%) differences between peels, offspring distributions or turning variable distributions.

Graph plots of the spatial patterns of the final populations were examined visually. These showed that, as expected, the spatial distributions of particles included a heavily populated central region and a more sparsely populated periphery (for example Figures 7.5.3 to 7.5.6). The centre of the distribution was not always located at the position of the initial particle, i.e. the origin of the plane, especially at low values of σ^2. This could be because when the variance of the turning variable distribution is low the steps taken during the first few generations are in similar directions, leading to a cluster of particles some distance from the origin. At higher generations the influence of the direction associated with the initial particle becomes less important and the population spreads out around the cluster formed during the first few generations. We found no clusters of particles separated from the main body of the distribution, and that the particles were evenly spread around the central heavily populated region.

Our results suggest that a population evolving as a branching correlated random walk spreads out evenly in all directions. If, as suggested by the convergence of the crinkliness coefficients (Figures 7.5.1 and 7.5.2), the convex hull of the particles positions converges when scaled by the number of generations, then it follows that the asymptotic shape will be close to a circle. However, our simulations were restricted by computing capacity and our results are inconclusive. Furthermore, our choice of parametric forms for the offspring and turning variable distributions may have led to misleading

		Turning variable parameter σ^2									
		0.1	0.2	0.3	0.4	0.5	0.6	0.7	0.8	0.9	1.0
Offspring distribution	A	1.06	1.02	1.02	1.04	1.03	1.05	1.03	1.06	1.02	1.03
	B	1.03	1.02	1.06	1.02	1.03	1.04	1.02	1.02	1.05	1.02
	C	1.04	1.05	1.02	1.05	1.06	1.03	1.02	1.02	1.02	1.04

The tabulated values are the median crinkliness coefficients of ten convex peels of five replicates. The offspring distributions are:

A: $p_0 = 0.00,\ p_1 = 0.95,\ p_2 = 0.05,\ p_3 = 0.00,\ p_k = 0.00\ (k > 3)$

B: $p_0 = 0.00,\ p_1 = 0.97,\ p_2 = 0.01,\ p_3 = 0.02,\ p_k = 0.00\ (k > 3)$

C: $p_0 = 0.05,\ p_1 = 0.89,\ p_2 = 0.02,\ p_3 = 0.04,\ p_k = 0.00\ (k > 3)$.

The turning variable distributions are wrapped $N(0,\sigma^2)$.

Table 7.5.1

Crinkliness coefficients: offspring distributions v turning variable distributions

		Convex peel									
		1	2	3	4	5	6	7	8	9	10
Offspring distribution	A	1.03	1.04	1.03	1.03	1.05	1.03	1.02	1.06	1.03	1.02
	B	1.04	1.04	1.03	1.02	1.05	1.02	1.02	1.03	1.05	1.03
	C	1.02	1.05	1.04	1.03	1.02	1.02	1.03	1.04	1.02	1.03

The tabulated values are the median crinkliness coefficients of five replicates at each of $\sigma^2 = 0.1(0.1)1.0$. The offspring distributions are:

A: $p_0 = 0.00,\ p_1 = 0.95,\ p_2 = 0.05,\ p_3 = 0.00,\ p_k = 0.00\ (k > 3)$

B: $p_0 = 0.00,\ p_1 = 0.97,\ p_2 = 0.01,\ p_3 = 0.02,\ p_k = 0.00\ (k > 3)$

C: $p_0 = 0.05,\ p_1 = 0.89,\ p_3 = 0.02,\ p_3 = 0.04,\ p_k = 0.00\ (k > 3)$.

Table 7.5.2

Crinkliness coefficients: offspring distributions v convex peels

Offspring distribution A
$\sigma^2 = 0.1$ (radians)^2

Number of generations = 187
Population size = 9748

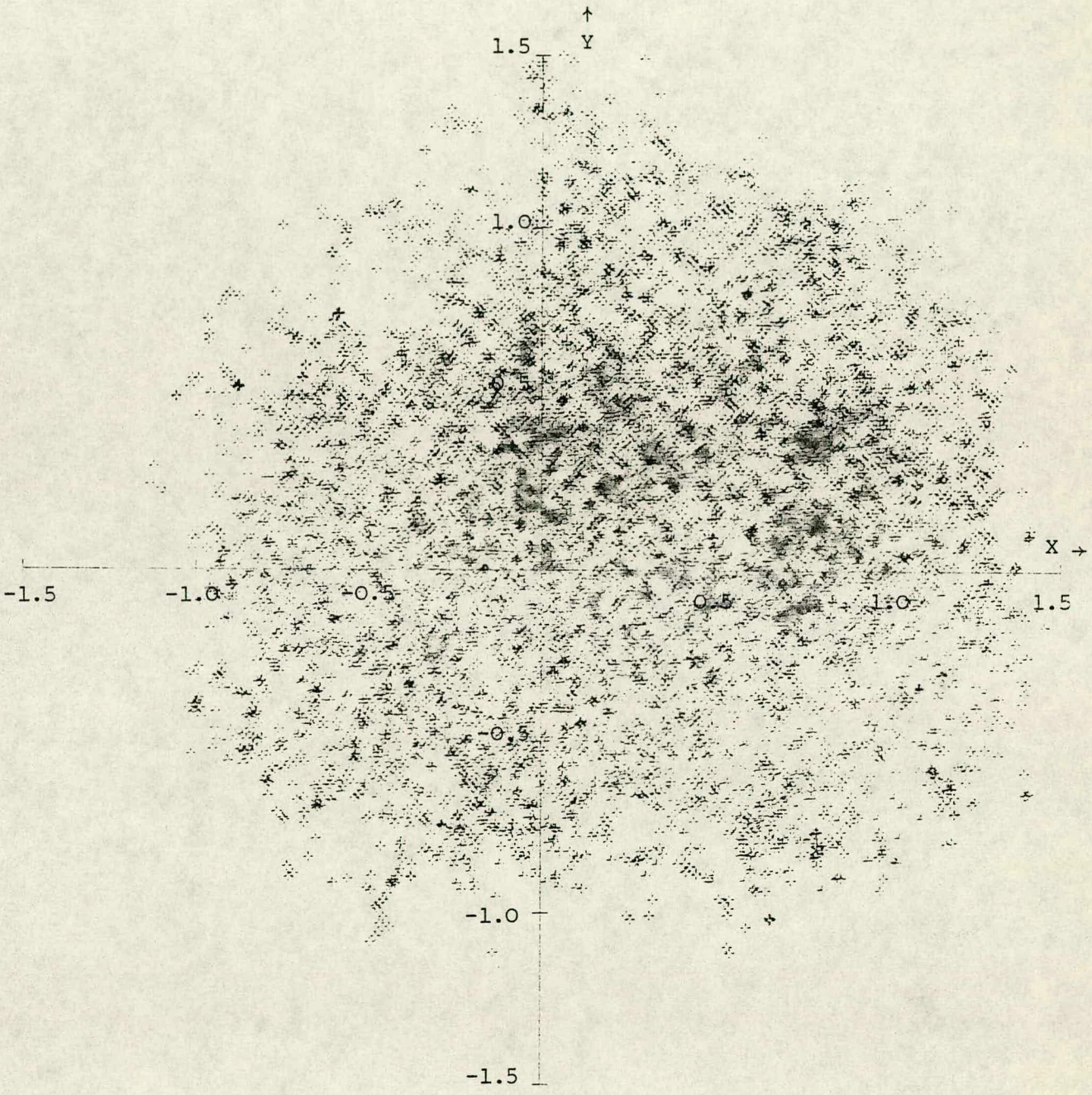


Figure 7.5.3

Population evolved as a branching correlated random walk (scaled by the number of generations)

Offspring distribution B
σ^2 = 0.4 (radians)^2

Number of generations = 214
Population size = 9521

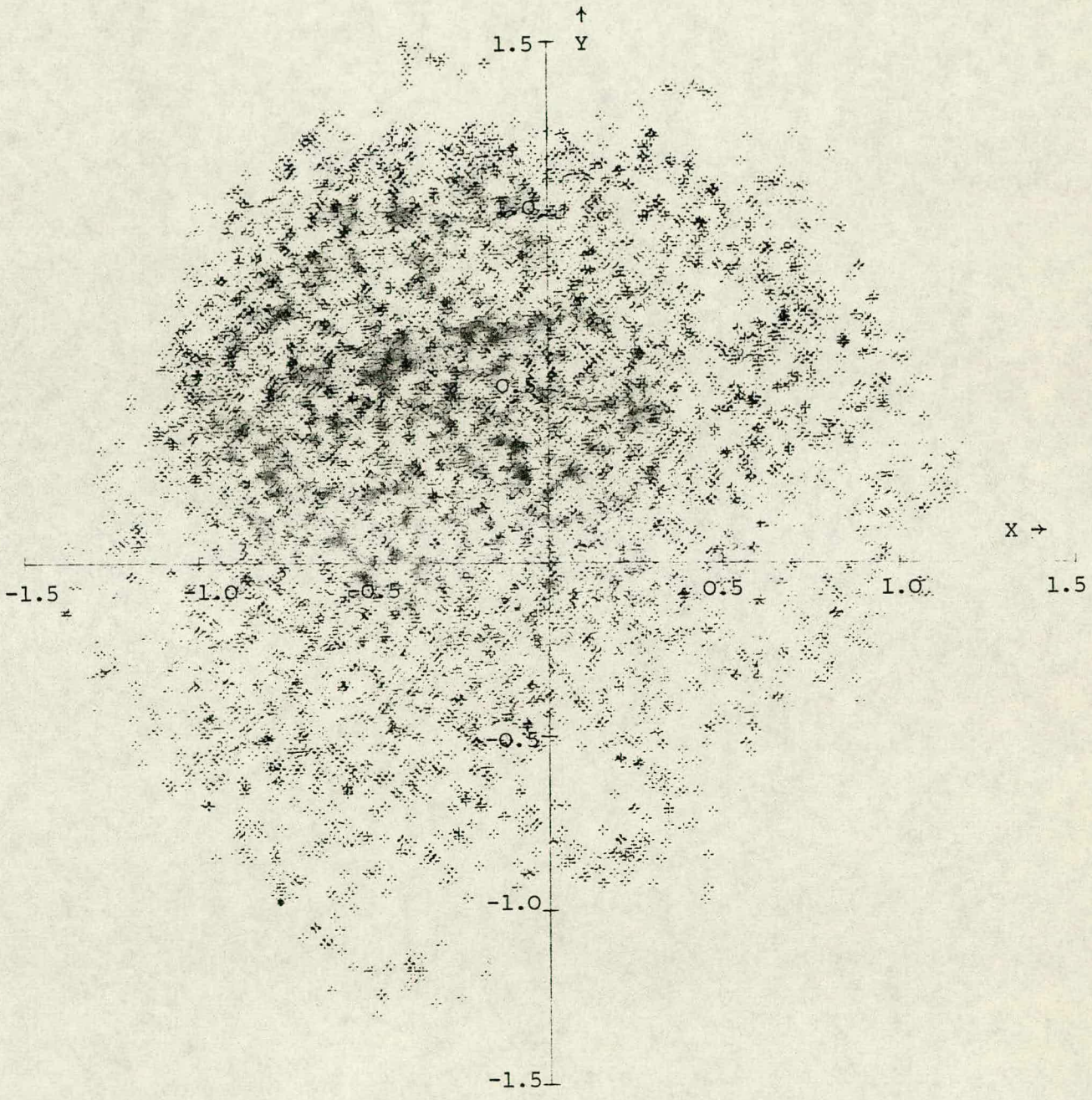


Figure 7.5.4

Population evolved as a branching correlated random walk (scaled by the number of generations)

Offspring distribution C
σ^2 = 0.7 (radians)^2

Number of generations = 228
Population size = 9897

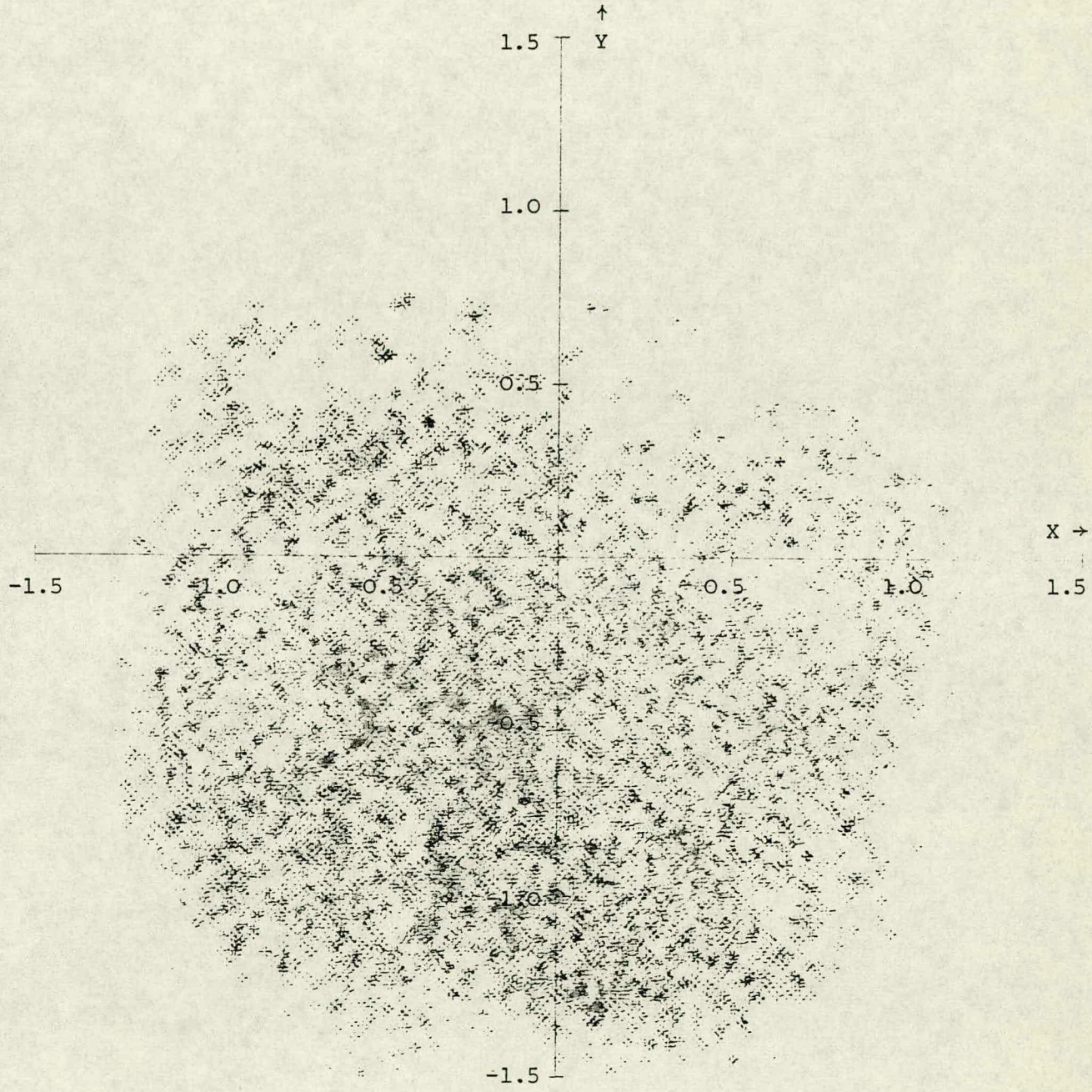


Figure 7.5.5

Population evolved as a branching correlated random walk (scaled by the number of generations)

Offspring distribution A
σ^2 = 1.0 (radians)^2

Number of generations = 171
Population size = 9645

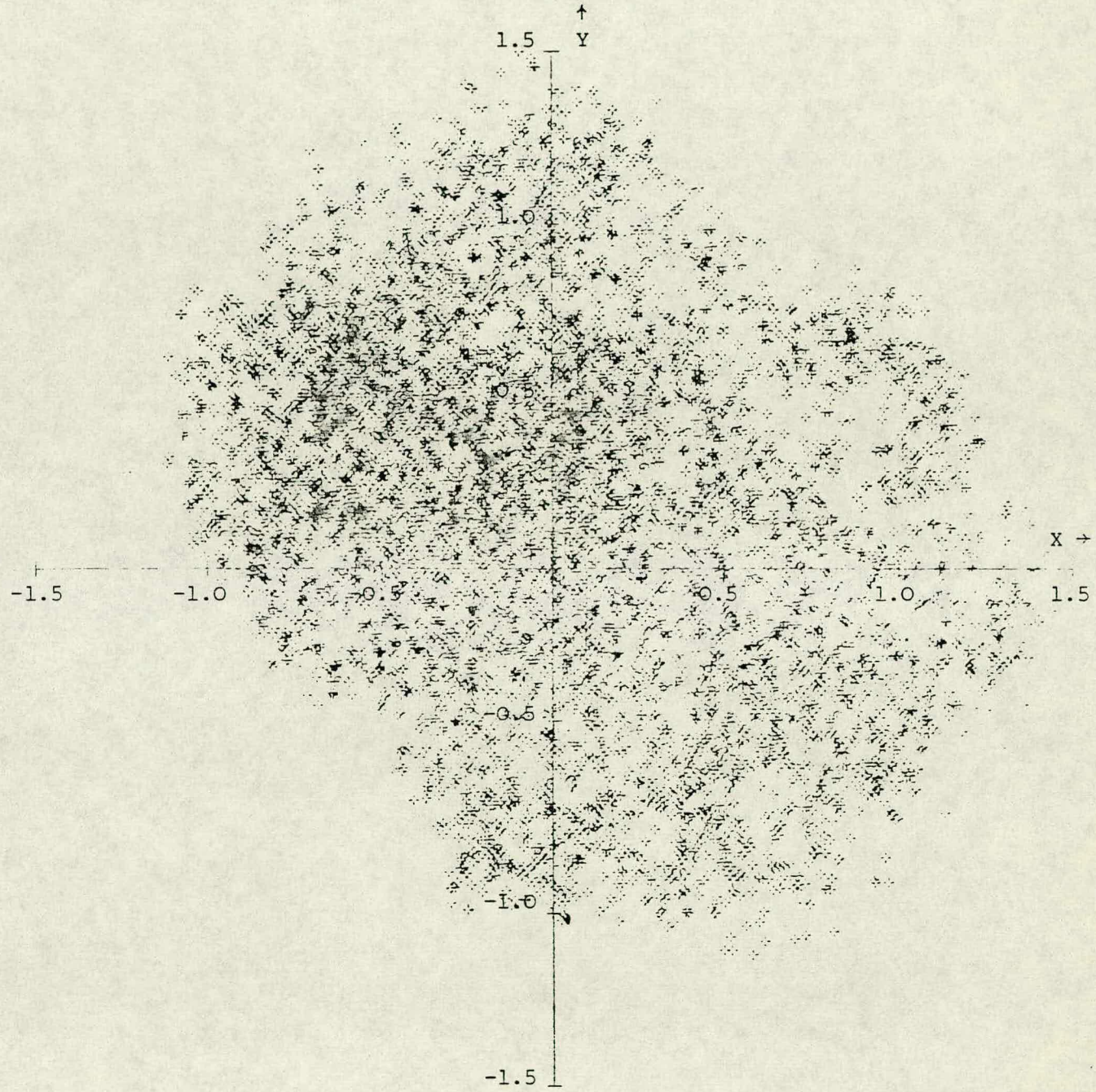


Figure 7.5.6

Population evolved as a branching correlated random walk (scaled by the number of generations)

results: there may be other distributions for which the population spreads in a more asymmetrical manner.

7.6 Discussion

A mathematical analysis of the branching correlated random walk is very difficult because the basic integral of the process (7.3.8) is so complicated. Nevertheless an expression for the mean number of nth generation particles with positions in any set and an analogue to the central limit theorem have been obtained. In each case the branching correlated random walk can be separated into its two component processes, namely a branching process and a correlated random walk. For the expected number of nth generation particles with positions in any set is just the total expected number of nth generation particles times the probability that an n-step correlated random walk ends in the set (7.3.16); and the central limit theorem states that $Z^{(n)}(I_n)/m^n$ converges to $W\Phi_2(I)$ as n increases (Theorems 7.4.2 and 7.4.3), where W is obtained from the branching process only (7.1.4) and $\Phi_2(I)$ is obtained from the central limit theorem for correlated random walks (Theorem 5.6.1). Further work is necessary to determine whether the variance of the number of particles in any set, or the tails of the limiting spatial distribution, may be separated into branching process and correlated random walk terms also.

It is possible that results on the spatial distribution of the particles existing after a small number of generations may be obtained by computer simulation, but asymptotic results for large populations are difficult to obtain by simulation techniques because of computing capacity restrictions (Section 7.5.ii). Moreover, the development of the process is determined by three probability distributions, $\{p_k\}$, G(.) and H(.), and unless a wide variety of parametric forms are considered results obtained by simulation may be misleading. However, on the basis of our simulations (Section 7.5) we conjecture that a population evolving as a branching correlated random walk spreads isotropically whatever the form of the of the offspring, length and turning variable distributions (except for trivial cases). Such a result is plausible on recalling the recurrence of the correlated random walk (Theorem 5.7.1), which implies that there can be no

preferred direction. Intuitively then, one expects that if the convex hull of the particles' positions converges when scaled by the number of generations, it should converge either to a random shape, in a similar manner to the convergence of $Z^{(n)}/m^n$ to a random variable W (7.1.4), or to a circle. Our results suggest the latter, that the convex hull converges to a circle, although the rate of convergence may depend upon the distributions $\{p_k\}$, G(.) and H(.). Our results are inconclusive however and a formal theoretical analysis is necessary.

One method of analysis is to consider the branching correlated random walk as a multitype branching random walk, where there can be several types of particle (Mode 1971,p.1). The number of types may be finite, countably infinite or uncountably infinite, and the numbers, types and steps of offspring may depend upon the type of parent. A branching correlated random walk is equivalent to a multitype branching random walk if we call the direction of the step taken by any particle its type. In that case the offspring types depend upon the type of parent but conditional upon the type of particle the number of offspring it produces and the steps that they take in moving away from the parent's position are independent of each other and of the parent.

When the turning variable distribution is concentrated on a circular lattice only a finite number of step directions, and hence types, are possible. In that case the results of Biggins (1976) for multitype branching random walks may be used to show that the convex hull of the particles positions, scaled by the number of generations, converges to a convex set C say. I have not been able to extend Biggins' method to allow G(.) to be more general and have not been able to determine the shape of C for even simple parametric forms of $\{p_k\}$, G(.) and H(.).

CHAPTER 8

FURTHER WORK

To conclude the thesis we suggest several specific areas for further research.

8.1 Internal Control of Root Growth

We have suggested that the development of a structural root system may be inherently regular, and that the observed variability of rooting patterns may have been caused by growth in a heterogeneous environment (Sections 3.5 and 4.5). Further understanding of root growth must now be obtained through detailed laboratory experiments. In particular, examination of root systems grown in a controlled, homogeneous environment will be useful in assessing how root morphology is modified by the environment. Attempts have already been made to study root growth in a controlled environment using seedlings (Deans and Henderson, unpublished) but examination of mature root systems will be more useful. Practical difficulties associated with such experiments are considerable however because of the time required to develop a structural root system and the problem of maintaining a homogeneous environment large enough to allow the root system to spread without restrictions.

The most interesting physiological problems arising from our work are to determine the mechanisms which caused roots to have alternate azimuth changes and regularly spaced laterals (Chapter 3). Root growth directions are both tropic, i.e. responsive to external stimuli such as moisture gradients, and nastic, i.e. determined by internal factors (Wilkins 1969,p.277-300). We suggest that the alternate azimuth changes may be induced by a nastic factor, although detailed experiments are required. Experiments are also necessary to examine the internal factor which controls the positions of lateral branches. Shoot apices are known to have a controlling effect on the positions, orientation and development of lateral shoots and perhaps root apices also have this apical dominance property (Wilkins 1969, p.165-204).

8.2 External Control of Root Growth

As well as experiments on the root growth mechanisms further work is required to determine how silvicultural techniques may be designed to improve windthrow resistance and so increase forest yield. First, it is important that the relationship between root morphology and tree stability should be studied. Some attempts have been made to examine the relationship between the gross dimensions of root systems and tree stability (for example, Faulkner and Malcolm 1972) but more detailed work is required. For whilst it is intuitively obvious that trees with large, evenly spread root systems will be more stable than those with smaller or non-isotropic root systems, no attempts have been made to find whether optimum rooting patterns exist.

If an optimum rooting pattern can be found then an important problem is to encourage root systems to form that optimum. One possible technique, namely selective fertilization, was suggested by Coutts and Phillipson (1975). They found that fertilization caused rooting density to increase and suggested that root morphology could be controlled by fertilizing certain soil areas only. It is not clear whether this technique is practicable however, and field trials are required. Field trials are also required to determine the optimum spacing of ploughing ditches, which restrict root spread (Chapter 2) but improve drainage.

8.3 Modelling Root Distributions

A stochastic model of the development of root systems will be very useful to root growth studies, especially because of the necessarily long-term nature of field experiments. But as mentioned earlier (Sections 4.1 and 4.4.iii) further understanding of root growth must be obtained before a model can be specified. We have suggested that until then an empirical model of root distribution at a fixed time, such as the reconstruction model (Section 4.1), may be useful to many investigations. Two examples of the use of the reconstruction model have been given, namely its use in assessing the accuracy of sampling schemes and the performance of descriptive statistics (Sections 4.3.iii and 4.4), and other applications should now be considered. In

particular, we suggest that simulation using the reconstruction model should be used to study the distribution of the maximum extent of root systems, for knowledge of this distribution is important when considering the optimum spacing of trees and the positions of ploughing ditches.

It is possible that the distribution of the maximum extent of roots may be obtained by a theoretical analysis. But as seen in Chapter 7 a theoretical analysis of even simple root distribution models is very difficult and much further work is necessary. We suggest that an analysis should proceed in a series of stages, with at each stage a more realistic model being introduced. For example, beginning with the branching correlated random walk (Chapter 7) the next stage may be to introduce reflecting barriers (Cox and Miller 1965,p.70-72) to represent root behaviour at the ditch sides. Next, the alternate azimuth changes may be taken into account, and so on. At each stage the methods developed to analyse the previous model should be extended to the current model.

8.4 Correlation in the Random Walk

The effect of correlation between the steps of a random walk is a very interesting and important problem which should be considered further. For whilst we have obtained several results for a specific type of correlated random walk (Chapters 5 and 6) there are many other classical random walk results which should be extended (see, for example, Petrov 1975). In particular, we suggest that analogues to the classical laws of large deviations (Petrov 1975,p.217-255) should be obtained, for the extreme value properties of the correlated random walk have not been considered in our work. Moreover, if laws of large deviations can be derived for the correlated random walk then perhaps analogues may be obtained for the branching correlated random walk.

In addition, it will be useful to investigate random walks with other types of correlation between steps. For example, in Section 6.1.iv we introduced a one-dimensional lattice random walk where the probability of a direction change depended on the previous direction. This type of random walk should be studied in detail as it subsumes both classical random walks and the correlated random walk which we

have investigated. It is interesting to note that attempts have been made to study the asymptotic properties of correlated random walks without specifying the type of correlation (Revesz 1968,p.137-143). Few results have been obtained however, for analysis of such general correlated random walks is very difficult. It may be better to study specific types of correlation individually, so that more precise results can be obtained.

Several interesting mathematical problems arise from our work. First, in Chapter 6 we found that the variance of the position of a particle performing a lattice correlated random walk is closely related to the asymptotic expected number of lattice points visited. There are no obvious reasons for this relationship and further work is required to determine whether other types of random walk have similar properties. A second problem is to determine whether one- and two-dimensional random walks with bounded means are always recurrent. In Chapters 5 and 6 we found that the correlated random walks which we studied, whose means did not increase with the number of steps, were recurrent and it may be that a bounded mean, with certain moment conditions on the individual steps, is a sufficient condition for recurrence. Finally, an interesting mathematical problem arising from our interpretation of a root path as a random walk, is to study random walks where the steps are considered as <u>links</u> of a chain rather than instantaneous jumps. Then it may be possible to find, for example, the distribution of the total length of an n-link chain within a fixed distance of the origin. This may be used as a basis for a theoretical investigation into the properties of length curves (Section 4.4).

APPENDIX 1

IMP PROGRAM TO SIMULATE ROOT DISTRIBUTION

```
%COMMENT    THIS PROGRAM SIMULATES THE STRUCTURAL ROOT
%COMMENT    DISTRIBUTIONS OF SITKA SPRUCE, USING A METHOD BASED
%COMMENT    ON THE PATH RECONSTRUCTION VARIABLES (CHAPTER 3).  SEE
%COMMENT    THE FLOW CHART (FIGURE 4.2.1) FOR A DESCRIPTION OF THE
%COMMENT    PROGRAM.  THE INPUT STREAM IS ST44, THE OUTPUT STREAMS
%COMMENT    ARE:
%COMMENT    ST45, FOR THE MAXIMUM DIMENSIONS AND NUMBER OF ROOTS;
%COMMENT    ST46, FOR AN ARRAY OF THE NUMBER OF STRAIGHT-LINE
%COMMENT          SEGMENTS OF EACH ROOT (USED IN GRAPH PLOTTING);
%COMMENT    ST47, FOR AN ORDERED LIST OF THE 3-D COORDINATES OF
%COMMENT          ROOT ORIGINS, BENDS, BRANCHING POINTS AND FORKS;
%COMMENT    ST48, FOR THE LENGTH CURVES OF EACH ROOT SYSTEM.
%COMMENT    THE EXTERNAL ROUTINES AND FUNCTIONS CALLED BY THE
%COMMENT    PROGRAM ARE INCLUDED BELOW, TOGETHER WITH A SEPARATE
%COMMENT    PROGRAM USED FOR PLOTTING THE SIMULATED ROOT SYSTEMS.


%BEGIN

%COMMENT    PARAMETER DECLARATIONS.

%REAL ALT,ANG,ANG1,ANP1,ANP2,ANSD1,ANSD2,AZ,AZ1,AZ2,AZ3,AZLAST
%REAL AZM1,AZM2,AZM3,AZM4,AZP,AZSD1,AZSD2,AZSD3,AZSD4,BEA,BESD
%REAL BRA,BRB,BRSD,STEMRAD,ENDA,ILM,ILSD,ILTR,INSD,L,MAXX,MAXY
%REAL MAXZ,MINX,MINY,MINZ,R,STSD,THETA1,THETA2,UNIF,X,X1,X2
%REAL Y,Y1,Y2,Z,Z1,Z2
%INTEGER AZI,BEPI,BRPI,CHANGE,CURRPOS,DIM,ENTY,GENER,I,IIJ
%INTEGER IN1,INROOT,INT,LAB,LAST,LN,MAXRTS,NBE,NBR
%INTEGER NPTS,NSIMS,NUMPTS,SIG,STI,TA,TY
%REALARRAY GENA(1:6)
%REALARRAY TOTA(1:12),TOTRD(1:15),TOTD(1:8)
%INTEGERARRAY GENI(1:6)
```

```
%COMMENT     EXTERNAL SUBROUTINES AND FUNCTIONS REQUIRED. "RANDOM"
%COMMENT     IS A SYSTEM RANDOM NUMBER GENERATOR (EDINBURGH
%COMMENT     REGIONAL COMPUTING CENTRE, 2900 SYSTEM MANUAL),
%COMMENT     ALL OTHER EXTERNAL FUNCTIONS AND SUBROUTINES
%COMMENT     ARE LISTED BELOW THE MAIN PROGRAM.

%EXTERNALREALFNSPEC RANDOM(%INTEGERNAME INT,%INTEGER N)
%EXTERNALREALFNSPEC GENLEN(%INTEGER GENER,GI,%REAL GA%C
,%INTEGERNAME INT)
%EXTERNALINTEGERFNSPEC ENDTYPE(%INTEGER GENER,%REAL ENDA,R,%C
%INTEGERNAME INT)
%EXTERNALINTEGERFNSPEC NBRAN(%INTEGER GENER%C
,%REAL R,BRA,BRB,%INTEGERNAME INT)
%EXTERNALINTEGERFNSPEC NBEND(%REAL R,BEA,%INTEGERNAME INT)
%EXTERNALROUTINESPEC PROPS(%INTEGER PROP1,NPROP,%INTEGERNAME%C
INT,%REALARRAYNAME P,%REAL PROPSD)
%EXTERNALROUTINESPEC SORT(%INTEGER NBE,NBR,%C
%REALARRAYNAME PBR,PBE,PALL,%C
%INTEGERARRAYNAME TYPES,%INTEGER ENTY)
%EXTERNALREALFNSPEC INAZ(%INTEGER INI,%INTEGERNAME INT,%REAL %C
STAZ,INSD)
%EXTERNALREALFNSPEC STEMAZ(%INTEGER STI,INROOT,STJ,%INTEGERNAME %C
INT,%REAL STSD)
%EXTERNALREALFNSPEC AZIM(%INTEGER AZI,TA,%INTEGERNAME INT,%REAL %C
AZM1,AZM2,AZM3,AZM4,AZSD1,AZSD2,AZSD3,AZSD4,AZP)
%EXTERNALROUTINESPEC CLASSIFY(%REAL X1,Y1,X2,Y2,%REALARRAYNAME %C
TOTA,TOTRD,TOTD)
%EXTERNALROUTINESPEC TRACE(%INTEGERNAME INT,NUMPTS,%C
%REALNAME X1,Y1,Z1,X2,Y2,Z2,AZ,AZL,%REALARRAYNAME TOTA,TOTRD,TOTD)
%EXTERNALREALFNSPEC ANGLE(%INTEGER TYPE,%REAL ANG,ANSD1,ANSD2,%C
ANP1,ANP2,Z,%INTEGERNAME INT,CHANGE)

SELECTINPUT(44)
SELECTOUTPUT(47)

%COMMENT     READ INPUT.  FOR INTERPRETATION OF THE PARAMETERS SEE
%COMMENT     THE FUNCTION LISTINGS BELOW.

READ(NSIMS);      %COMMENT  THE NUMBER OF SYSTEMS TO BE SIMULATED.

READ(INT);        %COMMENT  DUMMY VARIABLE FOR RANDOM NUMBER
                  %COMMENT  GENERATOR.

READ(MAXRTS);     %COMMENT  MAXIMUM POSSIBLE NUMBER OF ROOTS IN ANY
                  %COMMENT  SYSTEM.  IF THIS NUMBER IS EXCEEDED THE
                  %COMMENT  PROGRAM FAILS.

READ(INROOT);     %COMMENT  THE NUMBER OF PRIMARY ROOTS.

READ(STEMRAD);    %COMMENT  THE STEM RADIUS.

%COMMENT  READ THE "GENLEN" PARAMETERS.
%CYCLE I=1,1,6;READ(GENI(I));READ(GENA(I));%REPEAT
```

```
%COMMENT  READ THE "ENDTYPE" PARAMETER.
READ(ENDA)

%COMMENT  READ THE "INAZ" PARAMETERS.
READ(INI)
READ(INSD)

%COMMENT  READ THE "STEMAZ" PARAMETERS
READ(STI)
READ(STSD)

%COMMENT  READ THE "AZIM" PARAMETERS.
READ(AZI)
READ(AZM1)
READ(AZM2)
READ(AZM3)
READ(AZM4)
READ(AZSD1)
READ(AZSD2)
READ(AZSD3)
READ(AZSD4)
READ(AZP)
READ(ALT)

%COMMENT  READ THE "NBEND" AND "DISTBEND" PARAMETERS.
READ(BEA)
READ(BEPI)
READ(BESD)

%COMMENT  READ THE "NBRAN" AND "DISTBRAN" PARAMETERS.
READ(BRA)
READ(BRB)
READ(BRPI)
READ(BRSD)

%COMMENT  READ THE "ANGLE" PARAMETERS.

READ(ANSD1)
READ(ANSD2)
READ(ANP1)
READ(ANP2)

%COMMENT  NOW BEGIN THE SIMULATIONS.

%CYCLE IIJ=1,1,NSIMS
%BEGIN
%REALARRAY STARTZ,STARTANG,STARTX,STARTY,STARTAZ(1:MAXRTS)
%INTEGERARRAY STARTL,SIZE,STARTGEN(1:MAXRTS)
SELECTOUTPUT(47)
```

```
%COMMENT  SET LENGTH CURVES AND "START" ARRAYS TO ZERO.

%CYCLE I=1,1,8;TOTD(I)=0;%REPEAT
%CYCLE I=1,1,12;TOTA(I)=0;%REPEAT
%CYCLE I=1,1,15;TOTRD(I)=0;%REPEAT
%CYCLE I=1,1,MAXRTS
STARTL(I)=0
STARTX(I)=0
STARTY(I)=0
STARTZ(I)=0
STARTANG(I)=0
STARTAZ(I)=0
STARTGEN(I)=0
SIZE(I)=1
%REPEAT

%COMMENT  FIND THE INITIAL COORDINATES OF THE
%COMMENT  PRIMARY ROOTS AND ADD TO THE "START" ARRAYS.

%CYCLE I=1,1,INROOT
THETA1=STEMAZ(STI,INROOT,I,INT,STSD)
THETA2=INAZ(INI,INT,THETA1,INSD)
X1=STEMRAD*COS(THETA1)
Y1=STEMRAD*SIN(THETA1)
Z1=13*Y1/55+1
STARTL(I)=0
STARTX(I)=X1
STARTY(I)=Y1
STARTZ(I)=Z1
STARTANG(I)=-PI/18+RANDOM(INT,1)*PI/7
%IF Y1 < 15 %THEN STARTANG(I)=-MOD(STARTANG(I))
STARTAZ(I)=THETA2
STARTGEN(I)=1
%REPEAT

%COMMENT  BEGIN TO CYCLE THROUGH THE "START" ARRAY, AT EACH
%COMMENT  RETURN CHECKING WHETHER ANY MORE ROOTS EXIST.

CURRPOS=1
DIN=INROOT
LAB=1
MAXX=0;MAXY=0;MINX=0;MINY=0;MAXZ=0;MINZ=0
%WHILE (STARTX(CURRPOS)#0 %OR STARTY(CURRPOS)#0 %OR %C
STARTZ(CURRPOS)#0 %OR STARTANG(CURRPOS)#0 %C
%OR STARTAZ(CURRPOS)#0) %AND CURRPOS<MAXRTS %CYCLE
NEWLINE
NEWLINE
```

```
%COMMENT  FIND THE INITIAL COORDINATES OF THE CURRENT ROOT.

X=STARTX(CURRPOS)
Y=STARTY(CURRPOS)
Z=STARTZ(CURRPOS)
ANG=STARTANG(CURRPOS)
AZ=STARTAZ(CURRPOS)
GENER=STARTGEN(CURRPOS)
TY=1
LAST=STARTL(CURRPOS)
PRINT(X,4,1)
PRINT(Y,4,1)
PRINT(Z,4,1)
NEWLINE

%COMMENT  GENERATE THE TOTAL LENGTH AND END TYPE OF THE ROOT.

R=GENLEN(GENER,GENI(GENER),GENA(GENER),INT)
ENTY=ENDTYPE(GENER,ENDA,R,INT)

%COMMENT  DISTRIBUTE A NUMBER  OF BENDS AND BRANCHING POINTS
%COMMENT  ALONG THE ROOT LENGTH AND SORT INTO ORDER.

NBE=NBEND(R,BEA,INT)
NBR=NBRAN(GENER,R,BRA,BRB,INT)
NPTS=NBE+NBR+1
SIZE(CURRPOS)=NPTS+1
%BEGIN
%REALARRAY PBR(1:(NBR+1)),PBE(1:(NBE+1))
%REALARRAY PALL,RALL(1:NPTS)
%INTEGERARRAY TYPES(1:NPTS)
PBR(NBR+1)=1;PBE(NBE+1)=1
%IF NBR>0 %THEN PROPS(BRPI,NBR,INT,PBR,BRSD)
%IF NBE>0 %THEN PROPS(BEPI,NBE,INT,PBE,BESD)
SORT(NBE,NBR,PBR,PBE,PALL,TYPES,ENTY)
RALL(1)=R*PALL(1)

%COMMENT  NOW MOVE ALONG THE ROOT PATH UNTIL THE END-POINT
%COMMENT  (5MM OR FORK) IS REACHED. AT EACH BEND AND BRANCHING
%COMMENT  POINT GENERATE  THE APPROPRIATE DIRECTION CHANGES. AT
%COMMENT  BRANCHING POINTS (AND ALSO AT THE FINAL FORK IF THE
%COMMENT  ROOT DOES NOT END AT THE 5MM LEVEL) RECORD THE INITIAL
%COMMENT  COORDINATES AND DIRECTIONS OF THE NEW ROOTS.
%COMMENT  AT EACH BEND AND BRANCHING POINT,AFTER THE PARENT ROOT
%COMMENT  DIRECTION HAS BEEN MODIFIED CALCULATE THE "ATTEMPTED"
%COMMENT  COORDINATES OF THE NEXT POINT ON THE ROOT.  THEN USE
%COMMENT  THE SUBROUTINE "TRACE" TO CHECK WHETHER THE NEXT
%COMMENT  SEGMENT CROSSES ANY OF THE SOIL BOUNDARIES (FIGURE
%COMMENT  4.5.1).  IF SO "TRACE" AUTOMATICALLY CHANGES THE ROOT
%COMMENT  DIRECTION AT THE BOUNDARY.  "TRACE" ALSO CALLS THE
%COMMENT  SUBROUTINE "CLASSIFY" TO UPDATE THE LENGTH CURVES,
%COMMENT  TAKING ANY DIRECTION CHANGES INTO ACCOUNT.
%COMMENT  THE MAXIMUM AND MINIMUM X,Y AND Z COORDINATES REACHED
%COMMENT  ARE ALSO UPDATED AT EVERY POINT.
```

```
%IF NPTS>1 %START
%CYCLE I=2,1,NPTS
RALL(I)=R*(PALL(I)-PALL(I-1))
%REPEAT
%FINISH
%CYCLE I=1,1,NPTS

%COMMENT  CALCULATE THE "ATTEMPTED" POSITION OF THE NEXT POINT
%COMMENT  ON THE ROOT AND USE "TRACE" TO AMEND IF NECESSARY.
%COMMENT  IF "TRACE" INTRODUCES ANY NEW BENDS THEN AMEND THE
%COMMENT  NUMBER OF POINTS ON THE ROOT (I.E. THE ARRAY "SIZE").

X2=X+RALL(I)*COS(AZ)*COS(ANG)
Y2=Y+RALL(I)*SIN(AZ)*COS(ANG)
Z2=Z+RALL(I)*SIN(ANG)
NUMPTS=0
TRACE(INT,NUMPTS,X,Y,Z,X2,Y2,Z2,AZ,ANG,TOTA,TOTRD,TOTD)
SIZE(CURRPOS)=SIZE(CURRPOS)+NUMPTS
ANG1=ANG
CHANGE=0
ANG=ANGLE(2,ANG,ANSD1,ANSD2,ANP1,ANP2,Z2,INT,CHANGE)
Z=Z2;X=X2;Y=Y2

%COMMENT  IF CURRENT POINT IS A BEND (TYPE=1) THEN GENERATE A
%COMMENT  DIRECTION CHANGE, TAKING INTO ACCOUNT THE TENDENCY FOR
%COMMENT  DIRECTION CHANGES TO BE ALTERNATELY CLOCKWISE
%COMMENT  AND ANTICLOCKWISE (BY USING THE PARAMETER "LAST"
%COMMENT  TO RECORD THE SIGN OF ANY PREVIOUS DIRCTION CHANGE).
%COMMENT  THE PROBABILITY THAT A DIRECTION CHANGE HAS OPPOSITE
%COMMENT  SIGN TO THE LAST IS "ALT".

%IF TYPES(I)=1 %THEN SIG=1 %ELSE SIG=0
AZLAST=AZIM(AZ1,2+SIG,INT,AZM1,AZM2,AZM3,AZM4,AZSD1,AZSD2,%C
AZSD3,AZSD3,AZSD4,AZP)
UNIF=RANDOM(INT,1)
%IF LAST#0 %START
%IF UNIF>ALT %THEN AZLAST=LAST*MOD(AZLAST) %ELSESTART
AZLAST=-LAST*MOD(AZLAST)
%FINISH
%FINISH
%IF AZLAST>0 %THEN LAST=1 %ELSE LAST=-1
AZ3=AZ
AZ=AZ+AZLAST
%IF AZ<0 %THEN SIG=-1 %ELSE SIG=1
AZ=(MOD(AZ)-2*PI*(INT PT(MOD(AZ)/(2*PI))))*SIG
%IF AZ<0 %THEN AZ=2*PI+AZ
%IF X>MAXX %THEN MAXX=X
%IF X<MINX %THEN MINX=X
%IF Y>MAXY %THEN MAXY=Y
%IF Y<MINY %THEN MINY=Y
%IF Z>MAXZ %THEN MAXZ=Z
%IF Z<MINZ %THEN MINZ=Z
TY=2
```

```
%COMMENT  IF CURRENT POINT IS A LATERAL BRANCHING POINT (TYPE=2)
%COMMENT  THEN GENERATE THE NEW DIRECTION OF BOTH PARENT AND
%COMMENT  LATERAL AND RECORD THE LATERAL POSITION.

%IF TYPES(I)=2 %START
AZ1=AZIM(AZI,1,INT,AZM1,AZM2,AZM3,AZM4,AZSD1,AZSD2,AZSD3,AZSD4%C
,AZP)
%IF AZ1>0 %THEN LN=1 %ELSE LN=-1
AZ2=AZ3+AZ1
%IF AZ2<0 %THEN SIG=-1 %ELSE SIG=1
AZ2=(MOD(AZ2)-2*PI*(INT PT(MOD(AZ2)/(2*PI))))*SIG
%IF AZ2<0 %THEN AZ2=2*PI+AZ2
DIM=DIM+1
STARTL(DIM)=LN
STARTAZ(DIM)=AZ2
STARTX(DIM)=X
STARTY(DIM)=Y
STARTZ(DIM)=Z
CHANGE=0
STARTANG(DIM)=ANGLE(1,ANG1,ANSD1,ANSD2,ANP1,ANP2,Z,INT,CHANGE)
STARTGEN(DIM)=GENER+1
%FINISH

%COMMENT  IF THE FINAL POINT OF THE ROOT IS A FORK (TYPE=3)
%COMMENT  THEN GENERATE THE INITIAL DIRECTIONS OF THE NEW ROOTS
%COMMENT  AND RECORD WITH THE INITIAL COORDINATES.

%IF TYPES(I)=3 %START
AZ1=AZIM(AZI,3,INT,AZM1,AZM2,AZM3,AZSD1,AZSD2,AZSD3,AZSD4,AZP)
AZ2=AZ3+AZ1
AZ3=AZ3-AZ1
%IF AZ2<0 %THEN SIG=1 %ELSE SIG=0
AZ2=AZ2-2*PI*(INT PT(AZ2/(2*PI)))-2*PI*SIG
%IF AZ2<0 %THEN AZ2=2*PI+AZ2
DIM=DIM+1
STARTL(DIM)=1
STARTAZ(DIM)=AZ2
STARTX(DIM)=X
STARTY(DIM)=Y
STARTZ(DIM)=Z
STARTANG(DIM)=ANG1
STARTGEN(DIM)=GENER+1
%IF AZ3<0 %THEN SIG=1 %ELSE SIG=0
AZ3=AZ3-2*PI*(INT PT(AZ3/(2*PI)))-2*PI*SIG
%IF AZ3<0 %THEN AZ3=2*PI+AZ3
DIM=DIM+1
STARTL(DIM)=-1
STARTAZ(DIM)=AZ3
STARTX(DIM)=X
STARTY(DIM)=Y
STARTZ(DIM)=Z
STARTANG(DIM)=STARTANG(DIM-1)
STARTGEN(DIM)=GENER+1
%FINISH
%REPEAT
%END
```

```
%COMMENT  MOVE TO THE NEXT POSITION IN THE "START" ARRAY AND
%COMMENT  REPEAT.

CURRPOS=CURRPOS+1
LAB=LAB+1
%REPEAT


%COMMENT  FINALLY, PRINT THE OUTPUT.  THE POSITIONS OF ALL ROOT
%COMMENT  ORIGINS, BENDS, BRANCHING POINTS, FORKS AND SMM POINTS
%COMMENT  WERE PRINTED DURING THE GENERATION OF THE ROOT PATHS.


%BEGIN
SELECTOUTPUT(45)
PRINT(MAXX,4,1)
PRINT(MINX,4,1)
PRINT(MAXY,4,1)
PRINT(MINY,4,1)
PRINT(MAXZ,4,1)
PRINT(MINZ,4,1)
NEWLINE
PRINT(DIM,3,0)
NEWLINE
SELECTOUTPUT(46)
%CYCLE I=1,1,DIM
PRINT(SIZE(I),3,0)
%REPEAT
NEWLINE
%END
%BEGIN
SELECTOUTPUT(48)
%CYCLE I=1,1,12
PRINT(TOTA(I),3,1)
%REPEAT
NEWLINE
%CYCLE I=1,1,15
PRINT(TOTRD(I),3,1)
%REPEAT
NEWLINE
%CYCLE I=1,1,8
PRINT(TOTD(I),3,1)
%REPEAT
NEWLINE
%END
%END
%REPEAT
%ENDOFPROGRAM

%COMMENT          **********
```

```
%COMMENT          EXTERNAL ROUTINES AND FUNCTIONS


%COMMENT  FUNCTION TO GENERATE THE "STEMAZ" VALUE OF THE STJ'TH
%COMMENT  OF "INROOT" ROOTS.  THE OPTION IS CHOSEN BY STI.  IF
%COMMENT  STI=1 THEN STEMAZ=(STJ-1)*2*PI/INROOT.  IF STI=2 THEN
%COMMENT  STEMAZ=(STJ-1)*2*PI/INROOT+(A WRAPPED N(0,STSD**2)
%COMMENT  DEVIATION).  IF STI=3 STEMAZ IS ASSUMED TO BE
%COMMENT  UNIFORMLY DISTRIBUTED ON THE CIRCLE.

%EXTERNALREALFN STEMAZ(%INTEGER STI,INROOT,STJ,%INTEGERNAME %C
INT,%REAL STSD)
%REAL RV,TEM,SIGN
%IF STI=1 %THEN %RESULT=(STJ-1)*2*PI/INROOT %ELSESTART
%IF STI=2 %START
RV=(RANDOM(INT,12)-6)*STSD
TEM=((STJ-1)*2*PI/INROOT+RV)
%IF TEM<0 %THEN SIGN=2*PI %ELSE SIGN=0
%RESULT=TEM-(INT PT(TEM/(2*PI))*2*PI)-SIGN
%FINISHELSESTART
%RESULT=RANDOM(INT,1)*2*PI
%FINISH
%FINISH
%END

%COMMENT          --------------------


%COMMENT  FUNCTION TO GENERATE THE INITIAL AZIMUTH OF A PRIMARY
%COMMENT  ROOT WITH CORRESPONDING "STEMAZ" VALUE "STAZ".  THE
%COMMENT  OPTION IS CHOSEN BY INI.  IF INI=1 THEN INAZ=STAZ.
%COMMENT  IF INI=2 THEN INAZ=STAZ+(A WRAPPED N(0,INSD**2) VARIABLE).
%COMMENT  IF INI=3 THEN INAZ IS ASSUMED TO BE  UNIFORMLY
%COMMENT  DISTRIBUTED ON THE CIRCLE.

%EXTERNALREALFN INAZ(%INTEGER INI,%INTEGERNAME INT,%REAL %C
STAZ,INSD)
%REAL RV,TEM,SIGN
%IF INI=1 %THENRESULT=STAZ %ELSESTART
%IF INI=2 %START
RV=(RANDOM(INT,12)-6)*INSD
TEM=(STAZ+RV)
%IF TEM<0 %THEN SIGN=2*PI %ELSE SIGN=0
%RESULT=TEM-2*PI*(INT PT(TEM/(2*PI)))-SIGN
%FINISHELSESTART
%IF INI=3 %START
%RESULT=RANDOM(INT,1)*2*PI
%FINISH
%FINISH
%FINISH
%END

%COMMENT          --------------------
```

```
%COMMENT  FUNCTION TO GENERATE THE LENGTH OF A ROOT OF GENERATION
%COMMENT  "GENER".  IF GENER=1 THE FUNCTION GENERATES A U(0,GA)
%COMMENT   VARIABLE, OTHERWISE THE FUNCTION GENERATES A GAMMA
%COMMENT  (GI,GA) VARIABLE.

%EXTERNALREALFN GENLEN(%INTEGER GENER,GI,%REAL GA,%C
%INTEGERNAME INT)
%INTEGER K
%REAL TEM
%IF GENER=1 %START
TEM=GA*RANDOM(INT,1)
%FINISHELSESTART
TEM=1
%CYCLE K=1,1,GI
TEM=TEM*RANDOM(INT,1)
%REPEAT
TEM=-LOG(TEM)/GA
%FINISH
%RESULT=TEM
%END

%COMMENT          --------------------


%COMMENT  FUNCTION TO GENERATE THE END-TYPE OF A GENERATION
%COMMENT  "GENER" ROOT OF LENGTH "R". TWO TYPES ARE CONSIDERED,
%COMMENT  5MM POINTS (ENDTYPE=0) AND FORKS (ENDTYPE=3).  THE
%COMMENT  MODEL IS
%COMMENT                    1                        GENER=6 OR R>50
%COMMENT  PR(ENDTYPE=0)=
%COMMENT                   1-EXP(-ENDA*(GENER-1))  OTHERWISE.

%EXTERNALINTEGERFN ENDTYPE(%INTEGER GENER,%C
%REAL ENDA,R,%INTEGERNAME INT)
%REAL TEM,RV
%INTEGER K
%IF GENER=6 %THEN TEM=1 %ELSE TEM=1-EXP(-ENDA*(GENER-1))
%IF ER>50 %THEN TEM=1
RV=RANDOM(INT,1)
%IF RV<TEM %THEN K=0 %ELSE K=3
%RESULT=K
%END

%COMMENT          --------------------
```

```
%COMMENT  FUNCTION TO GENERATE A NUMBER OF BRANCHES FOR
%COMMENT  DISTRIBUTION ALONG A ROOT OF GENERATION "GENER" AND
%COMMENT  LENGTH "R".  THE MODEL FOR NBRAN IS POISSON WITH
%COMMENT  PARAMETER BRA*R FOR FIRST GENERATION ROOTS
%COMMENT  POISSON WITH PARAMETER BRB*R FOR SECOND TO FIFTH
%COMMENT  GENERATION ROOTS AND OTHERWISE IDENTICALLY ZERO

%EXTERNALINTEGERFN NBRAN(%INTEGER GENER,%REAL R,BRA,BRB,%C
%INTEGERNAME INT)
%REAL RV,TEM,PAR
%INTEGER NJ
%IF GENER=1 %THEN PAR=BRA*R %ELSE PAR=BRB*R
NJ=0
%IF GENER<6 %START
RV=RANDOM(INT,1)
TEM=EXP(-PAR)
%WHILE TEM>RV %CYCLE
NJ=NJ+1
TEM=TEM*PAR/NJ+TEM
%REPEAT
%FINISH
%RESULT=NJ
%END

%COMMENT          --------------------


%COMMENT  FUNCTION TO GENERATE A NUMBER OF BENDS FOR
%COMMENT  DISTRIBUTION ALONG A ROOT OF LENGTH "R". NBEND IS
%COMMENT  A POISSON RANDOM VARIABLE WITH PARAMETER BEA*R.

%EXTERNALINTEGERFN NBEND(%REAL R,BEA,%INTEGERNAME INT)
%INTEGER K
%REAL RV,TEM,PAR
RV=RANDOM(INT,1)
PAR=BEA*R
K=0
TEM=EXP(-PAR)
%WHILE TEM<RV %CYCLE
K=K+1
TEM=TEM*PAR/K+TEM
%REPEAT
%RESULT=K
%END

%COMMENT          --------------------
```

```
%COMMENT  ROUTINE TO DISTRIBUTE A NUMBER OF BENDS OR LATERALS
%COMMENT  ALONG A ROOT'S LENGTH.  THE POSITIONS OF THE BENDS OR
%COMMENT  LATERALS ARE EXPRESSED, IN THE ARRAY P, AS
%COMMENT  PROPORTIONS OF THE ROOT'S LENGTH.  TWO OPTIONS ARE
%COMMENT  POSSIBLE, CHOSEN BY "PROPI".  IF PROPI=1 THE POINTS
%COMMENT  ARE ALMOST REGULARLY SPACED ALONG THE ROOT, WITH
%COMMENT  N(0,PROPSD**2) DEVIATIONS FROM PERFECT REGULARITY.
%COMMENT  IF PROPI=2  THE POINTS ARE UNIFORMLY DISTRIBUTED
%COMMENT  ALONG THE ROOT.

%EXTERNALROUTINE PROPS(%INTEGER PROPI,NPROP,%INTEGERNAME INT,%C
%REALARRAYNAME P,%REAL PROPSD)
%INTEGER K
%IF PROPI=1 %START
%CYCLE K=1,1,NPROP
P(K)=K/(NPROP+1)+(RANDOM(INT,12)-6)*PROPSD
%IF P(K)<0 %THEN P(K)=0
%IF P(K)>1 %THEN P(K)=1
%REPEAT
%FINISHELSESTART
%CYCLE K=1,1,NPROP
P(K)=RANDOM(INT,1)
%REPEAT
%FINISH
%END

%COMMENT          ----------
```

```
%COMMENT  TECHNICAL SUBROUTINE TO ORDER THE POSITIONS OF
%COMMENT  NBE BENDS AND  NBR BRANCHING POINTS ALONG THE ROOT.
%COMMENT  THE ROUTINE EXPRESSES THE POSITIONS AS PROPORTIONS
%COMMENT  OF THE ROOT LENGTH IN THE ORDERED ARRAY PALL.  THE
%COMMENT  ROUTINE ALSO CONSTRUCTS THE ARRAY "TYPES" TO MARK
%COMMENT  WHETHER A POINT IN "PALL" CORRESPONDS TO A BEND OR
%COMMENT  BRANCHING POINT, USING THE CODE 1 FOR BEND AND 2 FOR
%COMMENT  BRANCHING POINT.  THE LAST ELEMENT OF THE ARRAY
%COMMENT  "TYPES" CORRESPONDS TO THE END-TYPE OF THE ROOT,
%COMMENT  0 AT 5MM POINTS AND 3 AT FORKS.

%EXTERNALROUTINE SORT(%INTEGER NBE,NBR,%C
%REALARRAYNAME PBR,PBE,PALL,%INTEGERARRAYNAME TYPES,%INTEGER ENTY)
%INTEGER K,K1,K2,MARK
K=NBE+NBR+1
%BEGIN
%INTEGERARRAY TYT,ORDER(1:K)
%REALARRAY SS,ST(1:K)
%IF NBEND>0 %START
%CYCLE K1=1,1,NBEND
ST(K1)=PBE(K1)
TYT(K1)=1
%REPEAT
%FINISH
%CYCLE K1=NBE+1,1,K
%IF K1=K %THEN TYT(K1)=ENTY %AND ST(K1)=1 %ELSE TYT(K1)=2 %AND%C
 ST(K1)=PBR(K1-NBE)
%REPEAT
%CYCLE K1=1,1,K
MARK=1
%CYCLE K2=1,1,K
%IF ST(K2)<ST(MARK) %THEN MARK=K2
%REPEAT
SS(K1)=ST(MARK)
ORDER(K1)=TYT(MARK)
ST(MARK)=1.1
%REPEAT
%CYCLE K1=1,1,K
TYPES(K1)=ORDER(K1)
PALL(K1)=SS(K1)
%REPEAT
%END
%END

%COMMENT          ----------------------
```

```
%COMMENT  FUNCTION TO GENERATE THE NEXT ANGLE OF
%COMMENT  A ROOT OF CURRENT ANGLE "ANG" AND DEPTH "Z".
%COMMENT  AT BENDS,BRANCHING POINTS AND FORKS THE MODEL IS
%COMMENT              ANGLE=ANG+D(I)*MOD(E(J))
%COMMENT  WHERE I=1 IF ANG>0 AND IS OTHERWISE 2, AND J=1 IF Z<15
%COMMENT  AND IS OTHERWISE 2.  HERE D(1)=1 WITH PROBABILITY ANP1
%COMMENT  AND IS OTHERWISE -1, WHILST D(2)=1 WITH PROBABILITY
%COMMENT  ANP2 AND IS OTHERWISE -1.  E(1),E(2) ARE WRAPPED
%COMMENT  N(0,ANSD1**2) AND N(0,ANSD2**2) VARIABLES RESPECTIVELY.
%COMMENT  FOR LATERAL ROOTS THE MODEL IS
%COMMENT              ANGLE=ANG+D*U
%COMMENT  WHERE D=1 WITH PROBABILITY 1 IF ANG>0 AND 1-ANG*0.262
%COMMENT  IF ANG>0, AND OTHERWISE D=-1.  U IS A U(0,PI/3)
%COMMENT  VARIABLE.

%EXTERNALREALFN ANGLE(%INTEGER TYPE,%REAL ANG,ANSD1,ANSD2,ANP1,%C
ANP2,Z,%INTEGERNAME INT,CHANGE)
%INTEGER SIGN
%REAL PAR,TEM,RV,TPI,PR
TPI=2*PI
%IF TYPE=2 %START
%IF Z<15 %THEN TEM=ANSD1 %ELSE TEM=ANSD2
RV=(RANDOM(INT,12)-6)*(TEM)
%IF RV>0 %THEN SIGN=1 %ELSE SIGN=-1
RV=MOD(RV)
RV=(RV-TPI*INT PT(RV/TPI))*SIGN
%IF RV>PI %THEN RV=PI-RV
%IF RV<-PI %THEN RV=-PI-RV
%IF ANG>0 %THEN PAR=ANP1 %ELSE PAR=ANP2
%IF RANDOM(INT,1)<PAR %THEN RV=MOD(RV) %ELSE RV=-MOD(RV)
RV=ANG+RV
%IF RV>PI %THEN RV=PI-RV
%IF RV<-PI %THEN RV=-PI-RV
TEM=RV
%FINISHELSESTART
RV=RANDOM(INT,1)*PI/3
%IF ANG<0 %THEN PR=1 %ELSE PR=1-ANG*0.262
%IF RANDOM(INT,1)>PR %THEN SIGN=-1 %ELSE SIGN=1
TEM=ANG+SIGN*RV
%FINISH
%IF TEM>PI/2 %THEN TEM=PI-TEM %AND CHANGE=1
%IF TEM<-PI/2 %THEN TEM=-PI-TEM %AND CHANGE=1
%RESULT=RES
%END

%COMMENT          --------------------
```

```
%COMMENT  FUNCTION TO GENERATE CHANGES IN AZIMUTH AT BENDS,
%COMMENT  LATERALS AND FORKS.  THREE OPTIONS ARE POSSIBLE,
%COMMENT  CHOSEN BY AZI.
%COMMENT  1) AZI=1.
%COMMENT  IN THIS CASE THE GENERAL MODEL IS
%COMMENT    AZIM=D*MOD(E)
%COMMENT  WHERE D=1 WITH PROBABILITY PA AND IS OTHERWISE
%COMMENT  -1 AND WHERE E IS A WRAPPED N(AZM,AZSD**2) VARIABLE.
%COMMENT  THE VALUES OF AZM AND AZSD DEPEND UPON THE TYPE OF
%COMMENT  POINT, WITH
%COMMENT            POINT                    AZM    AZSD
%COMMENT          NEW LATERAL                AZM1   AZSD1
%COMMENT          PARENT ROOT AT LATERAL     AZM2   AZSD2
%COMMENT          NEW ROOT AT FORK           AZM3   AZSD3
%COMMENT          BEND                       AZM4   AZSD4
%COMMENT  2)AZI=2.
%COMMENT  AZIM HAS ABSOLUTE VALUE AZM WITH PROBABILITY AZP
%COMMENT  AND OTHERWISE AZSD.  THE VALUES OF AZM AND AZSD ARE AS
%COMMENT  ABOVE.  IN EACH CASE THE SIGN OF AZIM IS EQUALLY
%COMMENT  LIKELY TO BE POSITIVE OR NEGATIVE.
%COMMENT  3)AZI=3.
%COMMENT  AZIM IS UNIFORMLY DISTRIBUTED ON THE CIRCLE.
%COMMENT  THE TENDENCY FOR DIRECTION CHANGES TO BE ALTERNATELY
%COMMENT  CLOCKWISE AND ANTICLOCKWISE IS WRITTEN INTO THE
%COMMENT  MAIN PROGRAM, NOT THE FUNCTION.

%EXTERNALREALFN AZIM(%INTEGER AZI,TA,%INTEGERNAME INT,%REAL %C
AZM1,AZM2,AZM3,AZM4,AZSD1,AZSD2,AZSD3,AZSD4,AZP)
%REAL TEM,RV,SIGN,AZM,AZSD
%IF TA=1 %THEN AZSD=AZSD1 %AND AZM=AZM1
%IF TA=2 %THEN AZSD=AZSD2 %AND AZM=AZM2
%IF TA=3 %THEN AZSD=AZSD3 %AND AZM=AZM3
%IF TA=4 %THEN AZSD=AZSD4 %AND AZM=AZM4
%IF AZI=1 %START
RV=(RANDOM(INT,12)-6)*AZSD+AZM
%IF RV<0 %THEN SIGN=-1 %ELSE SIGN=1
RV=(MOD(RV)-2*PI*INT PT(MOD(RV)/2*PI))*SIGN
TEM=RV
%FINISHELSESTART
%IF AZI=2 %START
RV=RANDOM(INT,1)
%IF RV<AZP %THEN TEM=AZM %ELSE TEM=AZSD
RV=RANDOM(INT,1)
%IF RV<0.5 %THEN TEM=2*PI-TEM
%FINISHELSESTART
TEM=RANDOM(INT,1)*2*PI
%FINISH
%FINISH
RV=RANDOM(INT,1)
%IF RV>0.5 %THEN TEM=-TEM
%IF TEM<0 %THEN TEM=2*PI+TEM
%RESULT=TEM
%END

%COMMENT          ------------------
```

```
%COMMENT  TECHNICAL SUBROUTINE TO ENSURE THAT ALL ROOT GROWTH
%COMMENT  TAKES PLACE WITHIN THE SOIL BOUNDARIES (FIGURE 3.5.1)
%COMMENT  BEHAVIOUR  ON REACHING ANY BOUNDARY IS ASSUMED TO BE
%COMMENT  AS SUMMARISED IN TABLE 3.5.1.
%COMMENT  THE ROUTINE CALLS THE SUBROUTINE "CLASSIFY" TO AMEND
%COMMENT  THE LENGTH CURVES.

%EXTERNALROUTINE TRACE(%INTEGERNAME INT,NUMPTS,%REALNAME %C
X1,Y1,Z1,X3,Y3,Z3,AZ,ANGV,%REALARRAYNAME TOTA,TOTRD,TOTD)
%REAL ZMAX,YMAX,YMIN,ZMIN,XI,XN,YI,YN,ZI,ZN,D1,D2,R1,R2,TV,SV
%INTEGER INTERCEPT,THIS,FACE,DIR
INTERCEPT=1;NUMPTS=0
%WHILE INTERCEPT=1 %CYCLE
%IF Z3>=Z1 %THEN ZMAX=Z3 %AND ZMIN=Z1 %ELSE ZMAX=Z1 %AND ZMIN=Z3
%IF Y3>=Y1 %THEN YMAX=Y3 %AND YMIN=Y1 %ELSE YMAX=Y1 %AND YMIN=Y3
D1=10000;XN=X3;YN=Y3;ZN=Z3;INTERCEPT=0;FACE=0
R1=SQRT((X3-X1)**2+(Y3-Y1)**2+(Z3-Z1)**2)

%COMMENT  FIRST FIND THE NEAREST BOUNDARY (IF ANY) WHICH IS
%COMMENT  INTERCEPTED BY THE STRAIGHT-LINE SEGIMENT.

THIS=0
%IF Y1#Y3 %AND YMAX>55   %AND YMIN<=55 %START
YI=55
ZI=(55-Y1)*(Z3-Z1)/(Y3-Y1)+Z1
XI=(55-Y1)*(X3-X1)/(Y3-Y1)+X1
%IF -75<=ZI %AND ZI>=40 %THEN THIS=1 %AND INTERCEPT=1 %ELSE THIS=0
%FINISH
%IF THIS=1 %START
D2=(XI-X1)**2+(YI-Y1)**2+(ZI-Z1)**2
%IF D2<=D1 %START
D1=D2
XN=XI;YN=YI;ZN=ZI
FACE=1
%FINISH
%FINISH

THIS=0
%IF Z3#Z1 %AND ZMIN<=40 %AND ZMAX>40 %START
ZI=40
YI=(40-Z1)*(Y3-Y1)/(Z3-Z1)+Y1
XI=(40-Z1)*(X3-X1)/(Z3-Z1)+X1
%IF -75<=YI %AND YI<=55 %THEN THIS=1 %AND INTERCEPT=1 %ELSE %C
THIS=0
%FINISH
%IF THIS=1 %START
D2=(XI-X1)**2+(YI-Y1)**2+(ZI-Z1)**2
%IF D2<=D1 %START
D1=D2
XN=XI;YN=YI;ZN=ZI;FACE=2
%FINISH
%FINISH
```

```
THIS=0
%IF Y3#Y1 %AND YMAX>=-75 %AND YMIN<-75 %START
YI=-75
ZI=(-75-Y1)*(Z3-Z1)/(Y3-Y1)+Z1
XI=(-75-Y1)*(X3-X1)/(Y3-Y1)+X1
%IF 13<=ZI %AND ZI<=40 %THEN THIS=1 %AND INTERCEPT=1 %ELSE THIS=0
%FINISH
%IF THIS=1 %START
D2=(XI-X1)**2+(YI-Y1)**2+(ZI-Z1)**2
%IF D2<=D1 %START
D1=D2
XN=XI;YN=YI;ZN=ZI
FACE=3
%FINISH
%FINISH

THIS=0
%IF Z3#Z1  %AND ZMIN<13 %AND ZMAX>=13 %START
ZI=13
YI=(13-Z1)*(Y3-Y1)/(Z3-Z1)+Y1
XI=(13-Z1)*(X3-X1)/(Z3-Z1)+X1
%IF -75<=YI %AND YI<=-40  %THEN THIS=1 %AND INTERCEPT=1 %ELSE THIS=0
%FINISH
%IF THIS=1 %START
D2=(XI-X1)**2+(YI-Y1)**2+(ZI-Z1)**2
%IF D2<=D1 %START
D1=D2
XN=XI;YN=YI;ZN=ZI
FACE=4
%FINISH
%FINISH
```

```
THIS=0
%IF ((Z3-Z1)*15#-17*(Y3-Y1)) %AND (Y3#Y1 %OR Z3#Z1) %START
%IF Y3=Y1 %START
YI=Y1
ZI=-17*YI/15-85/3-4
XI=(ZI-Z1)*(X3-X1)/(Z3-Z1)+X1
%FINISHELSESTART
%IF Z3=Z1 %START
ZI=Z3
YI=-(Z3+85/3+4)*15/17
XI=(YI-Y1)*(X3-X1)/(Y3-Y1)+X1
%FINISHELSESTART
YI=(-Y1*(Z3-Z1)/(Y3-Y1)+Z1+85/3+4)/(-17/15-(Z3-Z1)/(Y3-Y1))
ZI=-17*YI/15-85/3-4
XI=(ZI-Z1)*(X3-X1)/(Z3-Z1)+X1
%FINISH
%FINISH
%IF -40<=YI %AND YI<=-25 %AND -4<=ZI %AND ZI<=13 %AND YMIN<=YI %C
  %THEN THIS=1
%IF THIS=1 %AND YI<=YMAX %AND ZMIN<=ZI %AND %C
ZI<=ZMAX %THEN THIS=1 %AND INTERCEPT=1 %ELSE THIS=0
%FINISH
%IF THIS=1 %START
D2=(XI-X1)**2+(YI-Y1)**2+(ZI-Z1)**2
%IF D2<=D1 %START
D1=D2
XN=XI;YN=YI;ZN=ZI
FACE=5
%FINISH
%FINISH

THIS=0
%IF Z3#Z1 %AND ZMIN<-4 %AND ZMAX>=-4  %START
ZI=-4
YI=(-4-Z1)*(Y3-Y1)/(Z3-Z1)+Y1
XI=(-4-Z1)*(X3-X1)/(Z3-Z1)+X1
%IF -25<=YI %AND YI<=-15 %THEN THIS=1 %AND INTERCEPT=1 %ELSE %C
THIS=0
%FINISH
%IF THIS=1 %START
D2=(XI-X1)**2+(YI-Y1)**2+(ZI-Z1)**2
%IF D2<=D1 %START
D1=D2
XN=XI;YN=YI;ZN=ZI
FACE=6
%FINISH
%FINISH
```

```
THIS=0
%IF (Z3-Z1)*55#(Y3-Y1)*13 %AND (Y3#Y1 %OR Z3#Z1) %START
%IF Y3=Y1 %START
YI=Y3
ZI=13*YI/55
XI=(ZI-Z1)*(X3-X1)/(Z3-Z1)+X1
%FINISHELSESTART
%IF Z3=Z1 %START
ZI=Z1
YI=55*ZI/13
XI=(YI-Y1)*(X3-X1)/(Y3-Y1)+X1
%FINISHELSESTART
YI=(-Y1*(Z3-Z1)/(Y3-Y1)+Z1)/(13/55-(Z3-Z1)/(Y3-Y1))
ZI=13*YI/55
XI=(ZI-Z1)*(X3-X1)/(Z3-Z1)+X1
%FINISH
%FINISH
%IF -15<=YI %AND YI<=55 %AND -4<=ZI %AND ZI<=13 %AND ZMIN<ZI %C
%THEN THIS=1
%IF %AND ZI<=ZMAX %AND YMIN<=YI %AND YI<=YMAX %THEN THIS=1 %C
THIS=1%AND INTERCEPT=1 %ELSE THIS=0
%FINISH
%IF THIS=1 %START
D2=(XI-X1)**2+(YI-Y1)**2+(ZI-Z1)**2
%IF D2<=D1 %START
D1=D2
XN=XI;YN=YI;ZN=ZI
FACE=7
%FINISH
%FINISH

%COMMENT  IF ANY BOUNDARIES ARE INTERCEPTED THEN MOVE TO THE
%COMMENT  FIRST INTERCEPT, PRINT THE COORDINATES, CLASSIFY THE
%COMMENT  LENGTH OF THE LAST SEGMENT AND GENERATE AN APPROPRIATE
%COMMENT  CHANGE IN DIRECTION.
%COMMENT  FIND THE "ATTEMPTED" NEXT POINT AND REPEAT THE
%COMMENT  PROCEDURE OF SEEKING ANY INTERCEPTS, ETC.

%IF INTERCEPT=1 %START
%IF D1>0.5 %START
PRINT(XN,4,1)
PRINT(YN,4,1)
PRINT(ZN,4,1)
NEWLINE
NUMPTS=NUMPTS+1
CLASSIFY(X1,Y1,Z1,XN,YN,ZN,TOTA,TOTRD,TOTD)
%FINISH
%IF XN>X1 %THEN DIR=1 %ELSESTART
%IF XN=X1 %THEN DIR=0 %ELSE DIR=-1
%FINISH
X1=XN;Y1=YN;Z1=ZN
TV=RANDOM(INT,12)-6
```

```
%IF FACE=1 %OR FACE=3 %START
%IF FACE=1 %THEN SV=-1 %ELSE SV=1
ANGV=PI/2-RANDOM(INT,1)*PI/9
%IF DIR=1 %THEN AZ=SV*MOD(TV*0.3)
%IF DIR=0 %THEN AZ=SV*PI/2+TV*0.3
%IF DIR=-1 %THEN AZ=SV*(PI-MOD(TV*0.3))
%FINISH
%IF FACE=2 %START
ANGV=-MOD(RANDOM(INT,1)*PI/12)
%IF Y1<-70 %OR Y1>50 %START
%IF DIR=1 %THEN AZ=-MOD(RANDOM(INT,1)*0.5)
%IF DIR=0 %THEN AZ=-PI/2+TV*0.3
%IF DIR=-1 %THEN AZ=-PI+RANDOM(INT,1)*0.5
%IF Y1<-70 %THEN AZ=-AZ
%FINISH
%FINISH
%IF FACE=4 %OR FACE=6 %THEN ANGV=MOD(RANDOM(INT,1))*PI/12
%IF FACE=5 %THEN ANGV=5*PI/18+RANDOM(INT,1)*0.2
%IF FACE=7 %THEN ANGV=17*PI/180+RANDOM(INT,1)*0.2
R2=R1-SQRT(D1)
X3=X1+R2*COS(ANGV)*COS(AZ)
Y3=Y1+R2*COS(ANGV)*SIN(AZ)
Z3=Z1+R2*SIN(ANGV)
%FINISH
%REPEAT

%COMMENT  IF THERE ARE NO MORE INTERCEPTS THEN PRINT THE
%COMMENT  CURRENT COORDINATES AND CLASSIFY THE LENGTH OF THE
%COMMENT  FINAL SEGMENT

PRINT(X3,4,1)
PRINT(Y3,4,1)
PRINT(Z3,4,1)
NEWLINE
CLASSIFY(X1,Y1,Z1,X3,Y3,Z3,TOTA,TOTRD,TOTD)
%END

%COMMENT          --------------------
```

```
%COMMENT  TECHNICAL SUBROUTINE TO AMEND THE LENGTH CURVES
%COMMENT  - TOTA (30' ARCS), TOTRD (10CM RADIAL DISTANCE GROUPS)
%COMMENT  AND TOTD (10CM DEPTH GROUPS) -  TO ACCOUNT FOR
%COMMENT  THE STRAIGHT-LINE SEGMENT BETWEEN THE POINTS (X1,Y1,Z1)
%COMMENT  AND (X2,Y2,Z2)

%EXTERNALROUTINE CLASSIFY(%REAL X1,Y1,Z1,X2,Y2,Z2,%REALARRAYNAME%C
TOTA,TOTRD,TOTD)
%REAL XX1,XXN,XMAX,XMIN,YY1,YYN,YMAX,YMIN,ZZ1,ZZN,ZMAX,ZMIN,RN
%INTEGER LOW,UPP,HI
%INTEGERARRAY CCT(1:36)
%REALARRAY CT(1:4),AX,AY(1:36)
%REAL CZ3,CZ4,CZT,CA,CB,CD,CC,CU,CV,CX,CXT,CX3,CX4,CX5,CY,CYT,CY.
%REAL CY4,CY5,CR,CR2,CR3,CR4,CRAD,CTHETA
%INTEGER CS,CLL,CMM,CL,CI,CJ,CN,CM
%IF MOD(X1-X2)<0.0001 %AND MOD(Y1-Y2)< 0.0001 %START
CR=MOD(Z2-Z1)
CI=1
%CYCLE CJ=1,1,14
%IF X1>CJ*10 %THEN CI=CI+1
%REPEAT
TOTRD(CI)=TOTRD(CI)+CR
CTHETA=ARCTAN(X1,Y1)
%IF CTHETA<0 %THEN CTHETA=2*PI+CTHETA
CI=1
%CYCLE CJ=1,1,11
%IF CTHETA>CJ*PI/6 %THEN CI=CI+1
%REPEAT
TOTA(CI)=TOTA(CI)+CR
%FINISHELSESTART
CT(1)=SQRT(3);CT(2)=SQRT(1/3);CT(3)=-CT(1);CT(4)=-CT(2)
CX=X2-X1
CY=Y2-Y1
%CYCLE CL=1,1,15
%IF MOD(CX)<0.0001 %START
AX(CL)=X1
AX(CL+15)=X1
%IF MOD(CY)<0.0001 %START
AY(CL)=Y1
AY(CL+15)=Y1
%FINISHELSESTART
%IF ((10*CL)**2-X1**2)<0.0001 %START
AY(CL)=10000
AY(CL+15)=10000
%FINISHELSESTART
AY(CL)=SQRT((10*CL)**2-X1**2)
AY(CL+15)=-AY(CL)
%FINISH
%FINISH
%FINISHELSESTART
%IF MOD(CY)<0.0001 %START
AY(CL)=Y1
AY(CL+15)=Y1
%IF (10*CL)**2-Y1**2<0.0001 %START
```

```
AX(CL)=10000
AX(CL+15)=10000
%FINISHELSESTART
AX(CL)=SQRT((10*CL)**2-Y1**2)
AX(CL+15)=-AX(CL)
%FINISH
%FINISHELSESTART
CA=1+CY**2/CX**2
CB=CY*(Y1-X1*CY/CX)/CX
CC=(X1*CY/CX-Y1)**2-(10*CL)**2
CD=CB**2-CA*CC
%IF CD<0.0001 %START
AX(CL)=10000
AX(CL+15)=10000
AY(CL)=10000
AY(CL+15)=10000
%FINISHELSESTART
AX(CL)=(-CB+SQRT(CD))/CA
AX(CL+15)=(-CB-SQRT(CD))/CA
AY(CL)=CY*(AX(CL)-X1)/CX+Y1
AY(CL+15)=CY*(AX(CL+15)-X1)/CX+Y1
%FINISH
%FINISH
%FINISH
%REPEAT
AX(31)=0
%IF MOD(CX)>0.0001 %THEN AY(31)=CY*(-X1)/CX+Y1 %ELSE AY(31)=10000
AY(32)=0
%IF MOD(CY)>0.0001 %THEN AX(32)=CX*(-Y1)/CY+X1 %ELSE AX(32)=10000
%CYCLE CN=1,1,4
%IF MOD(CX)<0.0001 %START
%IF MOD(CY)<0.0001 %START
AX(32+CN)=10000
AY(32+CN)=10000
%FINISHELSESTART
AX(32+CN)=X1
AY(32+CN)=AX(32+CN)/CT(CN)
%FINISH
%FINISHELSESTART
%IF MOD(CY)<0.0001 %START
AY(32+CN)=Y1
AX(32+CN)=AY(32+CN)*CT(CN)
%FINISHELSESTART
%IF MOD(CY*CT(CN)-CX)<0.0001 %START
AX(32+CN)=10000
AY(32+CN)=10000
%FINISHELSESTART
AY(32+CN)=(X1*CY-CX*Y1)/(CY*CT(CN)-CX)
AX(32+CN)=CT(CN)*AY(32+CN)
%FINISH
%FINISH
%FINISH
```

```
%REPEAT
CS=0
%CYCLE CL=1,1,36
CU=(AX(CL)-X1)**2+(AY(CL)-Y1)**2
CV=(AX(CL)-X2)**2+(AY(CL)-Y2)**2
%IF (SQRT(CU)+SQRT(CV))< SQRT(CX**2+CY**2)+0.001 %START
CS=CS+1
CCT(CL)=1
%FINISHELSESTART
CCT(CL)=0
%FINISH
%REPEAT
CZ3=Z1;CX3=X1;CY3=Y1
%BEGIN
%REALARRAY BCX,BCY(1:CS+1)
CMM=0
%CYCLE CL=1,1,36
%IF CCT(CL)=1 %START
CMM=CMM+1
BCX(CMM)=AX(CL)
BCY(CMM)=AY(CL)
%FINISH
%REPEAT
BCX(CS+1)=X2
BCY(CS+1)=Y2
%CYCLE CL=1,1,CS+1
CR2=10000;CLL=CS+1
%CYCLE CM=1,1,CS+1
CR3=(BCX(CM)-CX3)**2+(BCY(CM)-CY3)**2
%IF CR3< CR2 %START
CLL=CM
CR2=CR3
%FINISH
%REPEAT
CX4=BCX(CLL)
CY4=BCY(CLL)
%IF MOD(X2-X1)< 0.0001 %THEN %C
CZT=(CY4-Y1)/(Y2-Y1) %ELSE CZT=(CX4-X1)/(X2-X1)
CZ4=Z1+(Z2-Z1)*CZT
CZT=CZ4-CZ3
CXT=CX4-CX3
CYT=CY4-CY3
CX5=(CX4+CX3)/2
%IF MOD(CX5-CX3)<0.0001 %THEN CY5=(CY4+CY3)/2 %ELSE %C
 CY5=CYT*(CX5-CX3)/CXT+CY3
CRAD=SQRT(CX5**2+CY5**2)
%IF CX5>0.0001 %START
CTHETA=ARCSIN((-CY5)/CRAD)
%IF CTHETA<0 %THEN CTHETA=2*PI+CTHETA
%FINISHELSESTART
%IF MOD(CX5)<0.0001 %START
%IF CY>0 %THEN CTHETA=3*PI/2 %ELSE CTHETA=PI/2
%FINISHELSESTART
CTHETA=PI+ARCSIN(CY5/CRAD)
%FINISH
%FINISH
```

```
CI=1
%CYCLE CN=1,1,11
%IF CTHETA>CN*PI/6 %THEN CI=CI+1
%REPEAT
CJ=1
%CYCLE CN=1,1,14
%IF CRAD>(10*CN) %THEN CJ=CJ+1
%REPEAT
CR4=SQRT(CXT**2+CYT**2+CZT**2)
TOTA(CI)=TOTA(CI)+CR4
TOTRD(CJ)=TOTRD(CJ)+CR4
CX3=CX4;BCX(CLL)=10000
CY3=CY4;BCY(CLL)=10000
CZ3=CZ4
%REPEAT
%IF Z1<Z2 %THEN ZMAX=Z2 %AND ZMIN=Z1 %ELSE ZMIN=Z2 %AND ZMAX=Z1
%IF ZMAX=Z2 %START
XMAX=X2;YMAX=Y2
XMIN=X1;YMIN=Y1
%FINISHELSESTART
XMAX=X1;YMAX=Y1
XMIN=X2;YMIN=Y2
%FINISH
%IF ZMIN<0 %THEN LOW=1 %ELSE LOW=INT PT(ZMIN/10)+1
%IF ZMAX<0 %THEN UPP=1 %ELSE UPP=INT PT(ZMAX/10)+1
%IF UPP>8 %THEN UPP=8
%IF LOW>8 %THEN LOW=8
%IF LOW=UPP %START
RN=SQRT((X2-X1)**2+(Y2-Y1)**2+(Z2-Z1)**2)
TOTD(LOW)=TOTD(LOW)+RN
%FINISHELSESTART
XX1=XMIN;YY1=YMIN;ZZ1=ZMIN
%CYCLE HI=LOW,1,(UPP-1)
ZZN=HI*10
XXN=(ZZN-Z1)*(X2-X1)/(Z2-Z1)+X1
YYN=(ZZN-Z1)*(X2-X1)/(Z2-Z1)+Y1
RN=SQRT((XXN-XX1)**2+(YYN-YY1)**2+(ZZN-ZZ1)**2)
TOTD(HI)=TOTD(HI)+RN
XX1=XXN;YY1=YYN;ZZ1=ZZN
%REPEAT
RN=SQRT((XMAX-XX1)**2+(YMAX-YY1)**2+(ZMAX-ZZ1)**2)
TOTD(UPP)=TOTD(UPP)+RN
%FINISH
%END
%FINISH
%END


%COMMENT          **********************
```

```
%COMMENT  A SEPARATE PROGRAM PLOTS X-Y, Y-Z AND X-Z VIEWS OF THE
%COMMENT  NSIM SIMULATED ROOT SYSTEMS.  THE EXTERNAL ROUTINES
%COMMENT  CALLED BY THIS PROGRAM ARE DESCRIBED IN THE EDINBURGH
%COMMENT  REGIONAL COMPUTING CENTRE GRAPHICS MANUAL (1977). THE
%COMMENT  INPUT STREAMS ARE AS FOR THE MAIN SIMULATION PROGRAM,
%COMMENT  THE OUTPUT STREAM IS SQ77.


%BEGIN
%INTEGER NSIMS,M,T,I,J,K,L,U,S
%REAL A,B,C,D
%EXTERNALROUTINESPEC GRAPHPAPER(%LONGREAL XLNGTH,%INTEGER IUNITS)
%EXTERNALROUTINESPEC CLOSEPLOTTER
%EXTERNALROUTINESPEC OPENPLOTTER(%INTEGER N)
%EXTERNALROUTINESPEC PLOTSTRING(%STRING (255) S)
%EXTERNALROUTINESPEC SETPLOT(%LONGREAL XMIN,YMIN,XMAX,YMAX,%C
%INTEGER IUNITS)
%EXTERNALROUTINESPEC SCALE(%LONGREAL XORIGIN,YORIGIN,XSCALE,%C
YSCALE,THETA)
%EXTERNALROUTINESPEC LINEGRAPH(%LONGREALARRAYNAME X,Y,%C
%INTEGER M,N,%LONGREAL DASH,GAP,%INTEGER ICODE,%LONGREAL SIZE)
SELECTINPUT(44)
READ(NSIMS)
OPENPLOTTER(77)
GRAPHPAPER(212,M'CMS')
PLOTSTRING('OUTPUT FILE NAME')
%CYCLE I=1,1,NSIMS
SELECTINPUT(45)

%COMMENT  THE MAIN PROGRAM OUTPUTS SOME VALUES WHICH ARE
%COMMENT  UNNECESSARY FOR PLOTTING.

READ(A);READ(A);READ(A);READ(A);READ(A);READ(A)

READ(L);      %COMMENT  THE NUMBER OF ROOTS.

%BEGIN
%INTEGERARRAY N(1:L)
SELECTINPUT(46)
T=0
%CYCLE J=1,1,L

READ(N(J));  %COMMENT  THE NUMBER OF POINTS ON ROOT J
```

```
T=T+N(J)
%REPEAT
%BEGIN
%LONGREALARRAY X,Y,Z(1:T)
SELECTINPUT(47)

%COMMENT  NOW READ THE (X,Y,Z) COORDINATES OF ALL BENDS, BRANCHING
%COMMENT  POINTS, FORKS, ROOT ORIGINS AND 5MM POINTS.

%CYCLE J=1,1,T
READ(X(J))
READ(Y(J))
READ(Z(J))
Z(J)=-Z(J)
%REPEAT
K=1
SETPLOT(0,0,40,80,M'CMS')

%COMMENT  PLOT THE X-Y VIEW.
SCALE(20,20,0.1,0.1,0)
%CYCLE J=1,1,L
U=K+N(J)-1
LINEGRAPH(X,Y,K,U,1,0,0,0.1)
K=U+1
%REPEAT
K=1
SETPLOT(0,40,40,80,M'CMSV')

%COMMENT  PLOT THE Y-Z VIEW.
SCALE(20,20,0.1,0.1,0)
%CYCLE J=1,1,L
U=K+N(J)-1
LINEGRAPH(Y,Z,K,U,1,0,0,0.1)
K=U+1
%REPEAT
K=1
SETPLOT(0,0,40,80,M'CMS')

%COMMENT  PLOT THE X-Z VIEW
SCALE(20,20,0.1,0.1,0)
%CYCLE J=1,1,L
U=K+N(J)-1
LINEGRAPH(X,Z,K,U,1,0,0,0.1)
K=U+1
%REPEAT
%END
%END
%REPEAT
CLOSEPLOTTER
%ENDOFPROGRAM
```

APPENDIX 2

EXPECTED VALUE OF R_n^4

In this appendix we will derive an exact expression for the expected value of R_n^4, where R_n denotes the distance of a particle from the origin after n steps of a correlated random walk. The assumptions and notation which will be used are those of Chapter 5. Recall that the step lengths are denoted by ℓ_j $(j=1,2,\ldots)$, that the turning variables are denoted by θ_j $(j=1,2,\ldots)$, that $\mu_r = E[\ell_j^r]$, $c = E[\cos\theta_j]$, $\eta = E[\exp(i2\theta_j)]$ and $\nu = E[\exp(-i2\theta_j)]$. The only results that will be required are

$$E[\cos(\theta_j+\ldots+\theta_k)] = c^{k-j+1} \qquad (k \geq j), \tag{A2.1}$$

$$E[\sin(\theta_j+\ldots+\theta_k)] = 0 \qquad (k \geq j) \tag{A2.2}$$

and

$$E[R_n^2] = n\mu_2 + \frac{2\mu_1^2 c}{(1-c)}\{n - \frac{(1-c^n)}{(1-c)}\} \tag{A2.3}$$

$$\equiv a_1(n)\mu_2 + a_2(n)\mu_1^2 \qquad \text{(say)}.$$

These results are all proved in Section 5.4.

Because the derivation of the expression is very laborious we shall illustrate the method but will omit many details. We will require five preparatory lemmas: the proof of the first is simply induction and is omitted.

Lemma A2.1 For any positive integers j and k with $k \geq j$,

$$E[\cos(2\theta_j+2\theta_{j+1}+\ldots+2\theta_k)] = \tfrac{1}{2}(\eta^{k-j+1}+\nu^{k-j+1}),$$

$$E[\sin(2\theta_j+2\theta_{j+1}+\ldots+2\theta_k)] = -\tfrac{1}{2}i(\eta^{k-j+1}-\nu^{k-j+1})$$

and

$$E[\cos^2(\theta_j+\theta_{j+1}+\ldots+\theta_k)] = \tfrac{1}{2} + \tfrac{1}{4}(\eta^{k-j+1}+\nu^{k-j+1}) \ .$$

□

The remaining lemmas are all concerned with properties of the function

$$(A2.4) \quad g_n \equiv \ell_1\cos(\theta_1+\theta_2+\ldots+\theta_n) + \ell_2\cos(\theta_2+\theta_3+\ldots+\theta_n) + \ldots + \ell_n\cos\theta_n \ .$$

The proof of Lemma A2.2 is also omitted as the result follows directly from the definition of g_n.

Lemma A2.2 For any positive integer n,

$$E[g_n] = \mu_1 c(1-c^n)/(1-c) \equiv a_3(n)\mu_1 \qquad \text{(say)} \ .$$

□

The next lemma is more complicated.

Lemma A2.3 For any positive integer n,

$$E[g_n^2] = \tfrac{1}{2}\mu_2\Big[2n + \frac{\eta(1-\eta^n)}{(1-\eta)} + \frac{\nu(1-\nu^n)}{(1-\nu)}\Big]$$

$$+ \mu_1^2\Big[\frac{c}{(1-c)}\Big\{n - \frac{(1-c^n)}{(1-c)}\Big\} + \frac{\eta c}{2(1-\eta)}\Big\{\frac{(1-c^{n-1})}{(1-c)} - \frac{\eta(c^{n-1}-\eta^{n-1})}{(c-\eta)}\Big\}$$

$$+ \frac{\nu c}{2(1-\nu)}\Big\{\frac{(1-c^{n-1})}{(1-c)} - \frac{\nu(c^{n-1}-\nu^{n-1})}{(c-\nu)}\Big\}\Big]$$

$$\equiv a_4(n)\mu_2 + a_5(n)\mu_1^2 \qquad \text{(say)} \ .$$

Proof

Upon squaring each side of A2.4 we have

$$g_n^2 = \sum_{j=1}^{n} \ell_j^2\cos^2(\theta_j+\ldots+\theta_n) + 2\sum_{j=1}^{n-1}\sum_{k=j+1}^{n} \ell_j\ell_k\cos(\theta_j+\ldots+\theta_n)\cos(\theta_k+\ldots+\theta_n) \ .$$

For any two integers j and k with k > j we can write

$$\cos(\theta_j+\ldots+\theta_n) = \cos(\theta_j+\ldots+\theta_{k-1})\cos(\theta_k+\ldots+\theta_n)$$

$$- \sin(\theta_j+\ldots+\theta_{k-1})\sin(\theta_k+\ldots+\theta_n) ,$$

whence taking expectations of the expansion of g_n^2 yields

$$E[g_n^2] = \mu_2 \sum_{j=1}^{n} E[\cos^2(\theta_j+\ldots+\theta_n)] + 2\mu_1^2 \sum_{j=1}^{n-1} \sum_{k=j+1}^{n} c^{k-j} E[\cos^2(\theta_k+\ldots+\theta_n)] .$$

Hence upon using Lemma A2.1 we have

$$E[g_n^2] = \mu_2 \sum_{j=1}^{n} \{\tfrac{1}{2}+\tfrac{1}{4}(\eta^{n-j+1}+\nu^{n-j+1})\} + 2\mu_1^2 \sum_{j=1}^{n-1} \sum_{k=j+1}^{n} c^{k-j}\{\tfrac{1}{2}+\tfrac{1}{4}(\eta^{n-k+1}+\nu^{n-k+1})\} .$$

The first term on the right hand side is easily summed and shown to be equal to $a_4(n)$. Summing the second term over k yields

$$2\mu_1^2 \sum_{j=1}^{n-1} \sum_{k=j+1}^{n} c^{k-j}\{\tfrac{1}{2}+\tfrac{1}{4}(\eta^{n-k+1}+\nu^{n-k+1})\}$$

$$= 2\mu_1^2 \sum_{j=1}^{n-1} \left\{ \frac{c(1-c^{n-j})}{2(1-c)} + \frac{c\eta(\eta^{n-j}-c^{n-j})}{4(\eta-c)} + \frac{c\nu(\nu^{n-j}-c^{n-j})}{4(\nu-c)} \right\} .$$

Performing the summation on the right hand side completes the proof of Lemma A2.3. □

The fourth preparatory lemma which we require is quite simple.

Lemma A2.4 For any positive integer n,

$$E[g_n \sum_{j=1}^{n} \ell_j^2] = \{\mu_3 + (n-1)\mu_2\mu_1\}c(1-c^n)/(1-c)$$

$$\equiv a_6(n)\mu_3 + a_7(n)\mu_2\mu_1 \qquad \text{(say)}.$$

Proof

From the definition (A2.4) of the function g_n we have

$$g_n \sum_{j=1}^{n} \ell_j^2 = \sum_{k=1}^{n} \{ \sum_{j=1}^{n} \ell_j^2 \} \ell_k \cos(\theta_k + \ldots + \theta_n) ,$$

and the result follows if we take expectations and sum. □

The final preparatory lemma is concerned with products of g_n and g_j for $j < n$.

Lemma A2.5 For any positive integer n,

$$\sum_{j=1}^{n-1} E[g_n g_j \ell_{j+1}] = a_8(n)\mu_2\mu_1 + a_9(n)\mu_1^3 ,$$

where

$$a_8(n) \equiv \tfrac{1}{4}\Big[\frac{2c}{(1-c)} \{ n - \frac{(1-c^n)}{(1-c)} + \frac{2c(1-c^{n-1})}{(1-c)} - 2(n-1)c^n \}$$

$$+ \frac{\eta c}{(1-\eta)} \{ \frac{(1-c^{n-1})}{(1-c)} - \frac{\eta(c^{n-1}-\eta^{n-1})}{(c-\eta)} \} + \frac{\nu c}{(1-\nu)} \{ \frac{(1-c^{n-1})}{(1-c)} - \frac{\nu(c^{n-1}-\nu^{n-1})}{(c-\nu)} \} \Big]$$

and

$$a_9(n) \equiv \frac{c^2}{(1-c)^2} \{ (2n-1)(1+c^{n-1}) + \frac{2c^{n-1}(1+c)-3-c}{(1-c)} \}$$

$$+ \frac{\eta}{2(1-\eta)} \{ \frac{c^2(1-c^{n-1})}{(1-c)^2} - \frac{(n-1)c^n}{(1-c)} - \frac{(n-1)\eta^n}{(c-\eta)} + \frac{c^2\eta(c^{n-1}-\eta^{n-1})}{(c-\eta)^2} \}$$

$$+ \frac{\nu}{2(1-\nu)} \{ \frac{c^2(1-c^{n-1})}{(1-c)^2} - \frac{(n-1)c^n}{(1-c)} - \frac{(n-1)\nu^n}{(c-\nu)} + \frac{c^2\nu(c^{n-1}-\nu^{n-1})}{(c-\nu)^2} \} .$$

Proof

First let us consider $g_n g_j \ell_{j+1}$ for some fixed integer $j < n$. The terms of g_n which also appear in g_j may be separated from the others to give

$$g_n g_j \ell_{j+1} = \{g_j \cos(\theta_{j+1}+\ldots+\theta_n) - g_j \sin(\theta_{j+1}+\ldots+\theta_n) + \ell_{j+1}\cos(\theta_{j+1}+\ldots+\theta_n)$$

(A2.5)
$$+ \sum_{k=j+2}^{n} \ell_k \cos(\theta_k+\ldots+\theta_n)\} g_j \ell_{j+1} .$$

Because the length and turning variables are identically distributed we have

$$E[\sum_{k=j+2}^{n} \ell_j \cos(\theta_k+\ldots+\theta_n)] = E[\sum_{k=1}^{n-j-1} \ell_k \cos(\theta_k+\ldots+\theta_{n-j-1})] = E[g_{n-j-1}] .$$

Therefore we can take expectations of each side of (A2.5) to yield

$$E[g_n g_j \ell_{j+1}] = \mu_1 c^{n-j} E[g_j^2] + \mu_2 c^{n-j} E[g_j] + \mu_1 E[g_j] E[g_{n-j-1}] .$$

Thus using Lemmas A2.2 and A2.3 and summing gives

$$\sum_{j=1}^{n-1} E[g_n g_j \ell_{j+1}] = \sum_{j=1}^{n-1} \{\mu_2\mu_1 c^{n-j} a_4(j) + \mu_1^3 c^{n-j} a_5(j) + \mu_2\mu_1 c^{n-j} a_3(j)$$

$$+ \mu_1^3 a_3(j) a_3(n-j-1)\} .$$

The proof of Lemma A2.5 can now be completed by direct summation. □

The preparatory lemmas are complete and we may now derive an expression for $E[R_n^4]$. First let us use the definitions of R_n and g_n to expand R_n^2 and give

(A2.6)
$$R_n^2 = \sum_{j=1}^{n} \ell_j^2 + \sum_{j=1}^{n-1} \ell_{j+1} g_j ,$$

which may be written as

$$R_n^2 = R_{n-1}^2 + \ell_n^2 + \ell_n g_{n-1} .$$

Thus by squaring each side we have

$$R_n^4 = R_{n-1}^4 + 2R_{n-1}^2 \ell_n^2 + \ell_n^4 + 2R_{n-1}^2 \ell_n g_{n-1} + 2\ell_n^3 g_{n-1} + \ell_n^2 g_{n-1}^2 ,$$

which may be rearranged with the use of (A2.6) as

$$R_n^4 = R_{n-1}^4 + 2R_{n-1}^2 \ell_n^2 + \ell_n^4 + 2\ell_n g_{n-1} \sum_{j=1}^{n-1} \ell_j^2 + 2\ell_n g_{n-1} \sum_{j=1}^{n-1} \ell_{j+1} g_j + 2\ell_n^3 g_{n-1} + \ell_n^2 g_{n-1}^2 .$$

Now take expectations of each side and use the preparatory lemmas to show that

$$E[R_n^4] = E[R_{n-1}^4] + \mu_4 + \mu_3\mu_1\{2a_3(n-1)+2a_6(n-1)\} + \mu_2^2\{2a_1(n-1)+a_4(n-1)\}$$

$$+ \mu_2\mu_1^2\{2a_2(n-1)+a_5(n-1)+2a_7(n-1)+2a_8(n-1)\} + 2\mu_1^4 a_9(n-1) .$$

An expression for $E[R_n^4]$ may now be found recursively, because we know that $E[R_1^4] = E[\ell_1^4] = \mu_4$. The final result is

$$E[R_1^4] = n\mu_4 + b_1(n)\mu_3\mu_1 + b_2(n)\mu_2^2 + b_3(n)\mu_2\mu_1^2 + b_4(n)\mu_1^4 ,$$

where

$$b_1(n) = \frac{4c}{(1-c)}\{(n-1) - c(1-c^{n-1})/(1-c)\} ,$$

$$b_2(n) = \tfrac{1}{4}\Big[5n(n-1) + \frac{\eta}{(1-\eta)}\Big\{(n-1) - \frac{\eta(1-\eta^{n-1})}{(1-\eta)}\Big\} + \frac{\nu}{(1-\nu)}\Big\{(n-1) - \frac{\nu(1-\nu^{n-1})}{(1-\nu)}\Big\}\Big] ,$$

$$b_3(n) = \frac{4cn(n-1)}{(1-c)} + \frac{c(n-1)}{(1-c)}\Big\{\frac{\eta}{(1-\eta)} + \frac{\nu}{(1-\nu)} + \frac{4(c^n+c-2)}{(1-c)}\Big\}$$

$$+ \frac{4c^2(1-c^{n-1})}{(1-c)^2} - \frac{\eta c(1-c^{n-1})}{(1-c)^2(c-\eta)} - \frac{\nu c(1-c^{n-1})}{(1-c)^2(c-\nu)}$$

$$+ \frac{\eta^2 c(1-\eta^{n-1})}{(1-\eta)^2(c-\eta)} + \frac{\nu^2 c(1-\nu^{n-1})}{(1-\nu)^2(c-\nu)}$$

and

$$b_4(n) = \frac{2c^2 n(n-1)}{(1-c)^2} + \frac{(n-1)c^2}{(1-c)^2}\left[\left\{\frac{\eta}{(1-\eta)} + \frac{\nu}{(1-\nu)}\right\}(1+c^{n-2}) - \frac{4(2+c^{n-1})}{(1-c)}\right]$$

$$+ \frac{c^2(1-c^{n-1})}{(1-c)^3}\left[\frac{6(1+c)}{(1-c)} + \frac{\eta}{(1-\eta)}\left\{\frac{\eta(1-c)^2}{(c-\eta)^2} - 2\right\} + \frac{\nu}{(1-\nu)}\left\{\frac{\nu(1-c)^2}{(c-\nu)^2} - 2\right\}\right]$$

$$+ \frac{\eta}{(1-\eta)^2(c-\eta)}\left[(n-1)\eta^n + \frac{\eta(1-\eta^{n-1})}{(1-\eta)(c-\eta)}\{\eta^2 - c^2 + \eta c^2 - \eta c\}\right]$$

$$+ \frac{\nu}{(1-\nu)^2(c-\nu)}\left[(n-1)\nu^n + \frac{\nu(1-\nu^{n-1})}{(1-\nu)(c-\nu)}\{\nu^2 - c^2 + \nu c^2 - \nu c\}\right] .$$

Note that for large n we have

$$E[R_n^4]/n^2 \sim 5\mu_2^2/4 + 4c\mu_2\mu_1^2/(1-c) + 2c^2\mu_1^4/(1-c)^2 ,$$

whence there is a positive number a_o (say) such that

$$E[R_n^4] \leq a_o n^2$$

for all n greater than some n_o. This result is used in our proof of the central limit theorem for correlated random walks (Section 5.6).

APPENDIX 3

ROSEN'S CENTRAL LIMIT THEOREM FOR SUMS OF DEPENDENT MULTIVARIATE RANDOM VARIABLES APPLIED TO THE CORRELATED RANDOM WALK

In this appendix we will present an outline of Rosen's (1967) central limit theorem for sums of dependent multivariate random variables, and will illustrate how the theorem can be applied to the correlated random walk. The assumptions, notation and conventions are as for Chapter 5.

A3.1 Rosen's Theorem

Rosen's theorem is concerned with partial sums of the double sequence of (possibly dependent) random d-dimensional variables

$$\begin{array}{llll} \underset{-}{Y}_{11}, & \underset{-}{Y}_{12}, & \cdots\cdots, & \underset{-}{Y}_{1n_1} \\ \underset{-}{Y}_{21}, & \underset{-}{Y}_{22}, & \cdots\cdots, & \underset{-}{Y}_{2n_2} \\ \vdots & \vdots & & \vdots \\ \underset{-}{Y}_{k1}, & \underset{-}{Y}_{k2}, & \cdots\cdots, & \underset{-}{Y}_{kn_k} \\ \vdots & \vdots & & \vdots \end{array} \qquad \text{(A3.1.1)}$$

where $n_k \to \infty$ as $k \to \infty$. Let

$$\underset{-}{Z}_{\alpha,k} = \sum_{j=1}^{[\alpha n_k]} \underset{-}{Y}_{kj} \qquad (0 \leqslant \alpha \leqslant 1) ,$$

which is a partial sum of the kth row of (A3.1.1), and denote the distribution function of $\underset{-}{Z}_{\alpha,k}$ by $G_{\alpha,k}(.)$. Also let $\underset{-}{Z}_{(\alpha+\Delta),k} - \underset{-}{Z}_{\alpha,k}$ $(0 \leqslant \alpha < \alpha+\Delta < 1)$ have distribution function $G^{(k)}_{\alpha,\Delta}(.)$.

Now impose the following four conditions.

Condition R1 There is a function $\kappa(s)$, which is bounded on $0 \leq s \leq 1$, and which tends to zero as s tends to zero, such that

$$\overline{\lim_{k\to\infty}} E[\| \sum_{j=[\beta n_k]}^{[\alpha n_k]} \underline{Y}_{kj} \|_2^2] \leq \kappa(\alpha-\beta) \qquad (0 \leq \beta < \alpha \leq 1) .$$

Condition R2 There is a $d \times d$ function matrix $M(\alpha)$, defined and continuous for $0 \leq \alpha \leq 1$, such that

$$\lim_{\Delta\downarrow 0} \frac{1}{\Delta} \overline{\lim_{k\to\infty}} E[\| E[\sum_{j=[\alpha n_k]}^{[(\alpha+\Delta)n_k]} \underline{Y}_{kj} \mid \mathcal{L}_{[\alpha n_k]}] - \Delta M(\alpha)\underline{Z}_{\alpha,k}\|_1] = 0 .$$

Condition R3 There is a $d \times d$ function matrix $D(\alpha)$, defined and continuous for $0 \leq \alpha \leq 1$, such that

$$\lim_{\Delta\downarrow 0} \frac{1}{\Delta} \overline{\lim_{k\to\infty}} E[\| E[\Big(\sum_{j=[\alpha n_k]}^{[(\alpha+\Delta)n_k]} \underline{Y}_{kj}\Big)\Big(\sum_{j=[\alpha n_k]}^{[(\alpha+\Delta)n_k]} \underline{Y}_{kj}\Big)^T \mid \mathcal{L}_{[\alpha n_k]}] - \Delta D(\alpha)\|_1] = 0 .$$

Condition R4 For every $\varepsilon > 0$ and for $r = 1, 2, \ldots, d$,

$$\lim_{\Delta\downarrow 0} \frac{1}{\Delta} \overline{\lim_{k\to\infty}} \int_{|z_r|>\varepsilon} z_r^2 dG_{\alpha,\Delta}^{(k)}(\underline{z}) = 0 ,$$

where $\underline{z} = (z_1, z_2, \ldots, z_d)^T$.

Rosen used condition R1 to show that as k increases the distributions $G_{\alpha,k}(.)$ converge to a limit, $G_\alpha(.)$ say, with characteristic function

$$\psi(\underline{t},\alpha) \equiv \int_{\mathcal{R}^d} \exp(i\underline{t}^T\underline{x}) dG_\alpha(\underline{x})$$

for $\underline{t} \in \mathcal{R}^d$. Also using R1 Rosen showed that $\psi(\underline{t},\alpha)$ is continuous and differentiable in α. Next, using R2-R4 he showed that $\psi(\underline{t},\alpha)$ satisfies the partial differential equation

$$\frac{\partial\psi(\underline{t},\alpha)}{\partial\alpha} = \underline{t}^T M(\alpha) \Big(\frac{\partial\psi(\underline{t},\alpha)}{\partial t_1}, \ldots, \frac{\partial\psi(\underline{t},\alpha)}{\partial t_d}\Big)^T - \tfrac{1}{2}\underline{t}^T D(\alpha)\underline{t}\psi(\underline{t},\alpha)$$

for $0 \leqslant \alpha \leqslant 1$, $\underline{t} \in \mathbb{R}^d$, and with boundary value $\psi(\underline{t},0) = 1$.

Rosen then used R3 to show that the unique solution to the above equation with boundary value $\psi(\underline{t},0) = 1$ is

$$\psi(\underline{t},\alpha) = \exp(-\tfrac{1}{2}\underline{t}^T \Lambda(\alpha)\underline{t}) \ ,$$

where $\Lambda(\alpha)$ is the unique solution of

$$\frac{d\Lambda(\alpha)}{d\alpha} = M(\alpha)\Lambda(\alpha) + (M(\alpha)\Lambda(\alpha))^T + D(\alpha) \qquad (0 \leqslant \alpha \leqslant 1).$$

But $\exp(-\tfrac{1}{2}\underline{t}^T \Lambda(\alpha)\underline{t})$ is well known to be the characteristic function of a Normal random variable. Therefore by the inversion theorem (Kingman and Taylor 1966,p.326-327), when conditions R1 to R4 are satisfied the random variable $Z_{\alpha,k}$ converges in distribution to a d-dimensional, zero mean Normal random variable with dispersion matrix $\Lambda(\alpha)$ as k tends to infinity.

A3.2 Correlated Random Walk Modification of Rosen's Theorem

Recall that $\underline{X}_n$ denotes the nth step of a particle performing a correlated random walk. Then the double sequence of random variables which we shall consider is

(A3.2.1)
$$\begin{array}{llll} \underline{X}_1 & & & \\ \underline{X}_1/\sqrt{2}, & \underline{X}_2/\sqrt{2} & & \\ \underline{X}_1/\sqrt{3}, & \underline{X}_2/\sqrt{3}, & \underline{X}_3/\sqrt{3} & \\ \vdots & \vdots & \vdots & \\ \underline{X}_1/\sqrt{k}, & \underline{X}_2/\sqrt{k}, & \underline{X}_3/\sqrt{k}, \ \ldots\ldots, & \underline{X}_4/\sqrt{k} \\ \vdots & \vdots & \vdots & \end{array}$$

which is equivalent to Rosen's sequence (A3.1.1) with $\underline{Y}_{kj}$ replaced by $\underline{X}_j/\sqrt{k}$ and n_k replaced by k. Rosen's theorem is concerned with sums such as

$$\sum_{j=1}^{[\alpha n_k]} \underline{Y}_{kj} \ ,$$

which are now equivalent to (in the notation of Chapter 5) $\underline{S}_{[\alpha k]}/\sqrt{k}$, i.e.

the particle's position after $[\alpha k]$ steps $(0 \leqslant \alpha \leqslant 1)$ when scaled by $\sqrt{k}$. Similarly, the partial sums such as

$$\sum_{j=[\beta k]}^{[\alpha k]} \underline{Y}_{kj} \qquad (0 \leqslant \beta < \alpha \leqslant 1)$$

are now equivalent to $\underline{S}_{[\alpha k]}^{[\alpha k]} / \sqrt{k}$.

Thus we see that the conditions C1, C3 and C4 imposed in Section 5.6 are identical to Rosen's conditions R1, R3 and R4 respectively, but that conditions C2 and R2 are dissimilar. Therefore to show that the central limit theorem applies to the correlated random walk we may use Rosen's method with suitable modifications whenever R2 is evoked. From Section A3.1 we see that R2 is evoked only in the derivation of a differential equation satisfied by $\psi(\underline{t},\alpha)$, the characteristic function of the limiting distribution of $\underline{S}_{[\alpha k]} / \sqrt{k}$, i.e.

$$\text{(A3.2.2)} \qquad \psi(\underline{t},\alpha) = \overline{\lim_{k\to\infty}} \, E[\exp(i\underline{t}^T \underline{S}_{[\alpha k]} / \sqrt{k})] \ ,$$

where $\underline{t} \equiv (t_1, t_2)^T$.

We begin with

$$\frac{\partial \psi(\underline{t},\alpha)}{\partial \alpha} = \lim_{\Delta \downarrow 0} [\{\psi(\underline{t},\alpha+\Delta) - \psi(\underline{t},\alpha)\}/\Delta] \qquad (0 \leqslant \alpha < \alpha+\Delta \leqslant 1),$$

and use (A3.2.2) to replace $\psi(.,.)$ in the right hand side. This procedure yields

$$\frac{\partial \psi(\underline{t},\alpha)}{\partial \alpha} = \lim_{\Delta \downarrow 0} \frac{1}{\Delta} \overline{\lim_{k\to\infty}} \, E[\exp(i\underline{t}^T \underline{S}_{[(\alpha+\Delta)k]} / \sqrt{k}) - \exp(i\underline{t}^T \underline{S}_{[\alpha k]} / \sqrt{k})] \ .$$

If we use the notation of Section 5.6 we may write

$$\underline{S}_{[(\alpha+\Delta)k]} = \underline{S}_{[\alpha k]} + \underline{S}_{[\alpha k]}^{[(\alpha+\Delta)k]} \ ,$$

whence

$$\frac{\partial \psi(\underline{t},\alpha)}{\partial \alpha} = \lim_{\Delta \downarrow 0} \frac{1}{\Delta} \overline{\lim_{k\to\infty}} \, E[\exp(i\underline{t}^T \underline{S}_{[\alpha k]} / \sqrt{k}) \{\exp(i\underline{t}^T \underline{S}_{[\alpha k]}^{[(\alpha+\Delta)k]} / \sqrt{k}) - 1\}] \ .$$

Now let us introduce the zero term

$$\tfrac{1}{2}\underline{t}^T D(\alpha)\underline{t}\{\overline{\lim_{k\to\infty}} E[\exp(i\underline{t}^T \underline{S}_{[\alpha k]}/\sqrt{k})]\} - \tfrac{1}{2}t^T D(\alpha)\underline{t}\{\overline{\lim_{k\to\infty}} E[\exp(i\underline{t}^T \underline{S}_{[\alpha k]}/\sqrt{k})]\}$$

to the right hand side and so obtain

$$\text{(A3.2.4)}\qquad \frac{\partial\psi(\underline{t},\alpha)}{\partial\alpha} = -\tfrac{1}{2}\underline{t}^T D(\alpha)\underline{t}\{\overline{\lim_{k\to\infty}} E[\exp(i\underline{t}^T \underline{S}_{[\alpha k]}/\sqrt{k})]\} + \overline{\lim_{\Delta\downarrow 0}} \frac{1}{\Delta} \lim_{k\to\infty} A_k$$

where

$$\text{(A3.2.5)}\qquad A_k = E[\exp(i\underline{t}^T \underline{S}_{[\alpha k]}/\sqrt{k})\{\exp(i\underline{t}^T \underline{S}_{[\alpha k]}^{[(\alpha+\Delta)k]}/\sqrt{k}) - 1 + \tfrac{1}{2}\Delta\underline{t}^T D(\alpha)\underline{t}\}] \ .$$

If we write

$$\exp(i\underline{t}^T \underline{S}_{[\alpha k]}^{[(\alpha+\Delta)k]}/\sqrt{k}) = 1 + i\underline{t}^T \underline{S}_{[\alpha k]}^{[(\alpha+\Delta)k]}/\sqrt{k} - \tfrac{1}{2}\underline{t}^T (\underline{S}_{[\alpha k]}^{[(\alpha+\Delta)k]})(\underline{S}_{[\alpha k]}^{[(\alpha+\Delta)k]})^T \underline{t}/k$$

$$+ H(\underline{t}^T \underline{S}_{[\alpha k]}^{[(\alpha+\Delta)k]}/\sqrt{k}) \ ,$$

then (A3.2.5) becomes

$$A_k = E[\exp(i\underline{t}^T \underline{S}_{[\alpha k]}/\sqrt{k}) H(\underline{t}^T \underline{S}_{[\alpha k]}^{[(\alpha+\Delta)k]}/\sqrt{k})]$$

$$- \tfrac{1}{2}E[\exp(i\underline{t}^T \underline{S}_{[\alpha k]}/\sqrt{k})\underline{t}^T\{(\underline{S}_{[\alpha k]}^{[(\alpha+\Delta)k]})(\underline{S}_{[\alpha k]}^{[(\alpha+\Delta)k]})^T/k - \Delta D(\alpha)\}\underline{t}]$$

$$+ iE[\exp(i\underline{t}^T \underline{S}_{[\alpha k]}/\sqrt{k})\underline{t}^T \underline{S}_{[\alpha k]}^{[(\alpha+\Delta)k]}/\sqrt{k}]$$

$$\equiv B_k^{(1)} - \tfrac{1}{2}B_k^{(2)} + iB_k^{(3)} \qquad \text{(say)} \ .$$

Now, Rosen's results (2.15) and (2.19) do not evoke condition R2 and can be used to show that

$$\text{(A3.2.6)}\qquad \lim_{\Delta\downarrow 0} \frac{1}{\Delta} \overline{\lim_{k\to\infty}} B_k^{(1)} = \lim_{\Delta\downarrow 0} \frac{1}{\Delta} \overline{\lim_{k\to\infty}} B_k^{(2)} = 0 \ .$$

Therefore we need consider $B_k^{(3)}$ only. We have

$$B_k^{(3)} = E[\exp(i\underline{t}^T \underline{S}_{[\alpha k]}/\sqrt{k})\underline{t}^T \underline{S}_{[\alpha k]}^{[(\alpha+\Delta)k]}/\sqrt{k}] \ ,$$

which, by first conditioning on $\mathcal{L}_{[\alpha k]}$ and then removing the conditioning, may be wriiten as

$$B_k^{(3)} = E[\exp(i\underline{t}^T \underline{S}_{[\alpha k]}/\sqrt{k}) E[\underline{t}^T \underline{S}_{[\alpha k]}^{[(\alpha+\Delta)k]}/\sqrt{k} \mid \mathcal{L}_{[\alpha k]}]] ,$$

and so

$$-|E[E[\underline{t}^T \underline{S}_{[\alpha k]}^{[(\alpha+\Delta)k]}/\sqrt{k} \mid \mathcal{L}_{[\alpha k]}]]| \leq B_k^{(3)} \leq |E[E[\underline{t}^T \underline{S}_{[\alpha k]}^{[(\alpha+\Delta)k]}/\sqrt{k} \mid \mathcal{L}_{[\alpha k]}]]| .$$

Because $\underline{t} = (t_1, t_2)^T$ and $t_i < \infty$ $(i=1,2)$, the condition C2 implies

$$\lim_{\Delta \downarrow 0} \frac{1}{\Delta} \overline{\lim_{k \to \infty}} B_k^{(3)} = 0 , \tag{A3.2.7}$$

whence from (A3.2.6) and (A3.2.7) we see that

$$\lim_{\Delta \downarrow 0} \frac{1}{\Delta} \overline{\lim_{k \to \infty}} A_k = 0 .$$

Thus upon using (A3.2.4) and (A3.2.2) we have

$$\frac{\partial \psi(\underline{t},\alpha)}{\partial \alpha} = -\tfrac{1}{2}\underline{t}^T D(\alpha)\underline{t}\psi(\underline{t},\alpha) . \tag{A3.2.8}$$

It is easy to show that the unique solution of (A3.2.8) with boundary condition $\psi(\underline{t},0) = 1$ is

$$\psi(\underline{t},\alpha) = \exp\{-\tfrac{1}{2}\underline{t}^T D(\alpha)\underline{t}\} .$$

Thus if conditions C1 to C4 are satisfied by the correlated random walk, as k increases $\underline{S}_{[\alpha k]}/\sqrt{k}$ converges in distribution to a Normal random variable with mean zero and dispersion matrix $D(\alpha)$.

REFERENCES

ABRAMOWITZ, M. and STEGUN, I.A. (1965). Handbook of Mathematical Functions. Dover, New York.

ALDHOUSE, J.R. (1972). Nursery practice. Bull. For. Comm. Lond. 43.

ASMUSSEN, S. and KAPLAN, N. (1976). Branching random walks I. Stoch. Proc. and Appl. 4, 1-13.

ATHREYA, K.B. and NEY, P.E. (1972). Branching Processes. Springer-Verlag, Berlin.

ATKINSON, D., NAYLOR, D. and COLDRICK, G.A. (1976). The effect of tree spacing on the apple root system. Hortic. Res. 16, 89-105.

BAILEY, N.T.J. (1964). The Elements of Stochastic Processes. Wiley, New York.

BANNAN, M.W. (1940). The root systems of northern Ontario conifers growing in sand. Am. J. Botany 27, 108-114.

BARTLETT, M.S. (1975). Appendix to the paradox of probability in physics. In Probability, Statistics and Time. Chapman and Hall, London.

BARTLETT, M.S. (1978). A note on random walks at constant speed. Adv. Appl. Prob. 10, 704-707.

BERGMANN, F. and HAGGSTROM, B. (1976). Some important facts concerning planting with rooted forest plants. Forestry Chronicle, 52, 266-273.

BIGGINS, J.D. (1976). Asymptotic Properties of the Branching Random Walk. Ph.D. Thesis, Univ. Oxford.

BIGGINS, J.D. (1977a). Martingale convergence in the branching random walk. J. Appl. Prob. 14, 25-37.

BIGGINS, J.D. (1977b). Chernoff's theorem in the branching random walk. J. Appl. Prob. 14, 630-636.

BIGGINS, J.D. (1978). The asymptotic shape of the branching random walk. Adv. Appl. Prob. 10, 62-84.

BIGGINS, J.D. and GREY, D.R. (1979). Continuity of limit random variables in the branching random walk. J. Appl. Prob. 16, 740-749.

BOWEN, G.D. (1964). Root distribution of Pinus radiata. CSIRO Divisional Report 1/64.

BOX, G.E.P. and COX, D.R. (1964). An analysis of transformations. J. Roy. Stat. Soc. B 26, 211-252.

BRAMSOM, M.D. (1978). Minimal displacement of branching random walk. Z. Wahrscheinlichkeitsth. 45, 89-108.

BYRD, P.F. and FRIEDMAN, M.D. (1954). Handbook of Elliptic Integrals for Engineers and Physicists. Springer-Verlag, Berlin.

CANE, V.R. (1967). Random walks and physical processes. Bull. Int. Stat. Inst. 42, 622-639.

CANE, V.R. (1975). Diffusion models with relativity effects. In Perspectives in Probability and Statistics: Papers in Honour of M.S. Bartlett on the Occasion of his Sixty-fifth Birthday, ed. J. Gani. Distributed by Academic Press, London, for the Applied Probability Trust, Sheffield, 263-273.

CHANDRASEKHAR, S. (1943). Stochastic problems in physics and astronomy. Rev. Modern Physics 15, 1-89.

CHUNG, K.L. and FUCHS, W.H.J. (1951). On the distribution of values of sums of random variables. Mem. Am. Math. Soc. 6, 1-12.

CHUNG, K.L. and ORNSTEIN, D. (1962). On the recurrence of sums of random variables. Bull. Am. Math. Soc. 68, 30-32.

COCHRANE, L.A. (1977). Statistical Models for the Branching of Sitka Spruce. Ph.D. Thesis, Heriot-Watt University, Edinburgh.

COCHRANE, L.A. and FORD, E.D. (1978). Growth of a Sitka spruce plantation: analysis and stochastic description of the development of the branching structure. J. Appl. Ecology 15, 227-244.

COHEN, D. (1967). Computer simulation of biological pattern generation processes. Nature 216, 246-248.

COUTTS, M.P. and PHILLIPSON, J.J. (1975). The influence of mineral nutrition on the development of individual roots of Sitka spruce. Aboricult. J. 2, 406-410.

COX, D.R. and MILLER, H.D. (1965). The Theory of Stochastic Processes. Methuen, London.

DALEY, D.J. (1979). Lattice valued random walks with Markov chain dependent steps. Math. Proc. Camb. Phil. Soc. 86, 115-126.

DANIELS, H.E. (1952). The statistical theory of stiff chains. Proc. Roy. Soc. Edin. A 43, 290-311.

DAY, W.R. (1962). Notes on the development of the root system with Sitka spruce. Scot. For. 16, 72-83.

DEANS, J.D. (1979). Fluctuations in the soil environment and fine root growth in a young Sitka spruce plantation. Plant and Soil 52, 195-208.

DEANS, J.D. (1981). Dynamics of coarse root production in a young plantation of Picea sitchensis. Forestry (to appear).

DOMB, C. and FISHER, M.E. (1958). On random walks with restricted reversals. Proc. Camb. Phil. Soc. 54, 48-59.

DOMB, C., GILLIS, J. and WILMERS, G. (1965). On the shape and configuration of polymer molecules. Proc. Phys. Soc. 85, 625-645.

DURRETT, R. (1979). Maxima of branching random walks vs independent random walks. Stoch. Proc. and Appl. 9, 117-135.

DVORETZSKY, A. and ERDOS, P. (1950). Some problems on random walk in space. Proc. 2nd Berkely Symp. Math., Stats. and Prob., Univ. California Press, Berkely, 353-367.

EDINBURGH REGIONAL COMPUTING CENTRE (1977). Graphics Manual. Univ. Edinburgh.

EDINBURGH REGIONAL COMPUTING CENTRE (1978). System Library Manual for Edinburgh 2900 Compilers. Univ. Edinburgh.

EDWARDS, S.F. (1965). Statistical mechanics of polymers with excluded volume. Proc. Phys. Soc. 85, 613-624.

EIS, S. (1974). Root system morphology of western hemlock, western red cedar and Douglas fir. Can. J. For. Res. 4, 28-38.

EYRING, H. (1932). The resultant electric moment of complex molecules. Phys. Rev. 39, 746-748.

FAULKNER, M.E. and MALCOLM, D.C. (1972). Soil physical factors affecting root morphology and stability of Scots pine on upland heaths. Forestry 45, 23-36.

FAYLE, D.C.F. (1965). Rooting habit of sugar maple and yellow birch. Dep. Forestry Pub. 1120.

FAYLE, D.C.F. (1968). Radial growth in tree roots. Fac. of Forestry Univ. Toronto Tech. Rep. 9, 1-183.

FAYLE, D.C.F. (1975). Extension and longitudinal growth during the development of red pine root systems. Can. J. For. Res. 5, 608-625.

FELLER, W. (1968). An Introduction to Probability Theory and its Applications, Vol. 1, 3rd edn. Wiley, New York.

FELLER, W. (1971). An Introduction to Probability Theory and its Applications, Vol. 2, 2nd edn. Wiley, New York.

FIXMAN, M. and SKOLNICK, J. (1976). Moments and distribution function of polymer chains. J. Chem. Phys. 65, 1700-1707.

FLORY, P.J. (1962). Principles of Polymer Chemistry. Cornell Univ. Press, Ithaca, New York.

FORD, E.D. and DEANS, J.D. (1977). Growth of a Sitka spruce plantation: spatial distribution and seasonal fluctuations of lengths, weights and carbohydrate contents of fine roots. Plant and Soil 47, 463-485.

FRASER, A.I. and GARDINER, J.B.H. (1967). Rooting and stability in Sitka spruce. Bull. For. Comm. Lond. 40.

FREED, K.F. (1971). Weiner integrals and models of stiff polymer chains. J. Chem. Phys. 54, 1453-1463.

GILLIS, J. (1955). Correlated random walk. Proc. Camb. Phil. Soc. 51, 639-651.

GOLDSTEIN, S. (1951). On diffusion by discontinuous muvements and on the telegraph equation. Quart. J. Mech. 4, 129-156.

GOROSTIZA, L.G. (1973). An invariance principle for a class of d-dimensional polygonal random functions. Trans. Am. Math. Soc. 177, 413-445.

GOROSTIZA, L.G. and GRIEGO, R.J. (1979). Convergence of branching transport processes to branching Brownian motion. Stoch. Proc. and Appl. 8, 269-276.

GOUDSMIT, S. and SAUNDERSON, J.L. (1940). Multiple scattering of electrons. Phys. Rev. 57, 24-29.

GRADSHTEYN, I.S. and RYZHIK, I.M. (1965). Tables of Integrals, Series and Products. Academic Press, London.

GREEN, P.J. and SILVERMAN, B.W. (1979). Constructing the convex hull of a set of points in the plane. Computer J. 22, 262-266.

HARDY, G.H. (1949). Divergent Series. Clarendon Press, Oxford.

HARRIS, T.E. (1963). The Theory of Branching Processes. Springer-Verlag, Berlin.

HEADING, J. (1970). Mathematical Methods in Science and Engineering, 2nd edn. Edward Arnold, London.

HERMANS, J.J. and Ullman, R. (1952). Statistics of stiff chains with applications to light scattering. Physica 18, 951-971.

HILTON, R.J. and KHATAMAIN, H. (1973). Diurnal variation in elongation rates of woody plants. Can. J. Plant Sci. 53, 699-700.

HONDA, H. (1971). Description of the form of trees by parameters of the tree-like body. J. Theor. Biol. 31, 331-338.

ten HOOPEN, M. and REUVER, H.A. (1970). Quantification of dentritic trees. Prog. Rep. 2, Inst. Med. Phys., Utrecht, Netherlands.

ten HOOPEN, M. and REUVER, H.A. (1971). Growth patterns of neuronal dendrites - an attempted probabilistic description. Kybernetik 8, 234-239.

HORSLEY, S.B. and WILSON, B.F. (1971). Development of the woody portion of the root system of Betula papyrifera. Am. J. Bot. 58, 141-147.

JAIN, G.C. (1971). Some results in a correlated random walk. Can. Math. Bull. 14, 341-347.

JAIN, G.C. (1973). On the expected number of visits of a particle before absorbtion in a correlated random walk. Can. Math. Bull. 16, 389-395.

JOFFE, A. and MONCAYO, A.R. (1973). Random variables, trees and branching random walks. Adv. Math. 10, 401-416.

JOHNSON, N.L. (1966). Paths and chains of straight line segments. Technometrics 8, 303-317.

KAC, M. (1959). Probability and Related Topics in Physical Sciences. Lectures in Applied Mathematics, Vol. 1. Interscience, New York.

KAMIYA, A., TOGAWA, T. and YAMAMOTO, A. (1974). Theoretical relationships between the optimal models of the vascular tree. Bull. Math. Biol. 36, 311-323.

KAPLAN, N. and ASMUSSEN, S. (1976). Branching random walks II. Stoch. Proc. and Appl. 4, 15-31.

KARLIN, S. (1966). A First Course in Stochastic Processes. Academic Press, London.

KENDALL, M.G. (1948). The Advanced Theory of Statistics, Vol 1, 4th edn. Griffin, London.

KENDALL, M.G. and STUART, A. (1961). The Advanced Theory of Statistics, Vol 2, 1st edn. Griffin, London.

KESTEN, H., KOZLOV, M.V. and SPITZER, F. (1975). A limit law for random walk in a random environment. Comp. Math. 30, 145-168.

KINGMAN, J.F.C. and TAYLOR, S.J. (1966). Introduction to Measure and Probability. Cambridge University Press.

KLEIN, G. (1952). A generalization of the random walk problem. Proc. Roy. Soc. Edin. A 63, 268-279.

KOCHENDERFER, J.N. (1973). Root distribution under some forest types common to West Virginia. Ecol. 54, 445-448.

KOZLOWSKI, T.T. (1949). Light and water in relation to growth and competition of Piedmont forest tree species. Ecol. Monogr. 19, 207-231.

KOZLOWSKI, T.T. (1971). Growth and Development of Trees, Vol 2. Academic Press, London.

LUTZ, H.J., ELY, J.B. and LITTLE, S. (1937). The influence of soil profile horizons on root distribution of white pine. Yale Univ. Sch. Forestry Bull. 44.

LYR, H. and HOFFMANN, G. (1967). Growth rates and growth periodicity of tree roots. Int. Rev. For. Res. 2, 181-206.

MARDIA, K.V. (1972). Statistics of Directional Data. Academic Press, London.

MASON, R.G., BHAR, D.S. and HILTON, R.J. (1970). Root growth studies on Mugho pine. Can. J. Bot. 48, 43-47.

MATTHES, K., KERSTAN, J. and MECKE, J. (1978). Infinitely Divisible Point Processes. Wiley, New York.

McCULLY, M.E. (1975). The development of lateral roots. In The Development and Function of Roots, ed. J.G. Torrey and D.T. Clarkson. Academic Press, London, 105-124.

McMINN, R.G. (1963). Characteristics of Douglas fir root systems. Can. J. Bot. 41, 105-122.

MODE, C.J. (1971). Multitype Branching Processes: Theory and Applications. American Elsevier, New York.

MOHAN, C. (1955). The gambler's ruin problem with correlation. Biometrika 42, 486-493.

MOLLISON, D. (1972). Conjecture on the spread of infection in two dimensions disproved. Nature 240, 467-468.

MONTROLL, E.W. (1964). Random walks on lattices. Proc. Symp. Appl. Math. of Am. Math. Soc. 16, 193-220.

MORAN, P.A.P. (1948). Statistical distribution of the length of a rubber molecule. Proc. Camb. Phil. Soc. 44, 342-344.

MOYAL, J.E. (1950). The momentum and sign of fast cosmic ray particles. Phil. Mag. 41, 1058-1077.

NAIN, R.B. and KANWAR SEN (1980). Transition probability matrices for correlated random walks. J. Appl. Prob. 17, 253-258.

NELDER, J.A. and MEAD, R. (1965). A simplex method for function minimisation. Computer J. 7, 308-313.

NEY, P.E. (1965a). The limit distribution of a binary cascade process. J. Math. Anal. and Appl. 10, 30-36.

NEY, P.E. (1965b). The convergence of a random distribution function associated with a branching process. J. Math. Anal. and Appl. 12, 316-327.

OLKIN, I. and PRATT, J.W. (1958). A multivariate Tchebycheff inequality. Annals Math. Stat. 29, 226-236.

PEARSON, K. (1905). Problem of the random walk. Nature 72, 294.

PETROV, V.V. (1975). Sums of Independent Random Variables. Springer-Verlag, Berlin.

PIELOU, E.C. (1977). Mathematical Ecology, 2nd edn. Wiley, New York.

PONDER, H.G. and KENWORTHY, A.L. (1976). Trickle irrigation of shade trees growing in the nursery II. Influence on root distribution. J. Am. Soc. Hortic. Sci. 101, 104-107.

POTTER, M.K. and LAMB, K.M. (1974). Root development of radiata pine in the gravel soils of Eyrewell Forest, Canterbury. New Zealand J. For. 19, 264-275.

RAYLEIGH, Lord (1919). Random vibrations and flights in one, two and three dimensions. Phil. Mag. 6th Series 37, 321-347.

RENSHAW, E. and HENDERSON, R. (1981). The correlated random walk. J. Appl. Prob. (to appear).

REVESZ, P. (1968). The Laws of Large Numbers. Academic Press, London.

REYNOLDS, E.R.C. (1975). Tree rootlets and their distribution. In The Development and Function of Roots, ed. J.G. Torrey and D.T. Clarkson. Academic Press, London, 163-177.

ROSEN, B. (1967). On asymptotic Normality of sums of dependent random vectors. Z. Wahrscheinlichkeitsth. 7, 95-102.

SAVILL, P.S. (1976). The effects of drainage and ploughing of surface water gleys on rooting and windthrow of Sitka spruce in Northern Ireland. Forestry 49, 133-141.

SETH, A. (1963). The correlated unrestricted random walk. J. Roy. Stat. Soc. B 25, 394-400.

SETH, S.K. and SRIVASTAVA, P.B.L. (1972). Effect of profile morphology on root development of Sal (Shorea robusta) seedlings. Indian Forester 98, 155-167.

SKELLAM, J.G. (1973). The formation and interpretation of mathematical models of diffusionary processes in population biology. In The Mathematical Theory of the Dynamics of Biological Populations, ed. M.S. Bartlett and R.W. Hiorns. Academic Press, London, 63-85.

SNEDECOR, G.W. and COCHRANE, W.G. (1967). Statistical Methods, 6th edn. Iowa State University Press.

SPITZER, F. (1964). Principles of Random Walk. Van Nostrand, Princeton, New Jersey.

STAM, A.J. (1966). On a conjecture by Harris. Z. Wahrscheinlichkeitsth. 5, 202-206.

STEPHENS, M.A. (1963). Random Walk on a circle. Biometrika 50, 385-390.

STEVENS, C.L. (1931). Root growth of white pine. Yale Univ. Sch. Forestry Bull. 32.

TCHEN, C.M. (1952). Random flight with multiple partial correlations. J. Chem. Phys. 20, 214-217.

TORREY, J.G. and CLARKSON, D.T. (1975). The Development and Function of Roots. Academic Press, London.

UENO, M. and YOSHIHARA, K. (1967). Living root systems distinguished by the use of carbon-14. Nature 213, 530-532.

VAADIA, Y. and ITAI, C. (1969). Interrelationships of growth with reference to the distribution of growth substances. In Root Growth, Proceedings of the Fifteenth Easter School in Agricultural Science, University of Nottingham, 1968. Butterworths, London, 65-67.

WALLER, H.D. and OLSEN, J.S. (1967). Prompt transfers of cesium-137 to the soils of a tagged Liriodendron forest. Ecology 48, 15-25.

WANG, T.T. (1952). Root development of the dominant, the intermediate and the suppressed trees in a Cryptomenia stand. National Taiwan Univ. Forestry Exp. Stat. Tech. Bull. 3.

WAREING, P.F. (1971). The physiology of conifers I. The growth of the shoot and root. J. Roy. Hortic. Soc. 96, 394-403.

WATSON, G.N. (1952). A Treatise on the Theory of Bessel Functions. Cambridge University Press.

WEIBEL, E.R. (1963). Morphometry of the Human Lung. Springer-Verlag, Berlin.

WILCOX, H.E. (1968). Morphological studies of the root of red pine I. Growth characteristics and patterns of branching. Am. J. Bot. 55, 247-254.

WILDE, S.A. (1958). Forest Soils. Ronald Press, New York.

WILKINS, M.B. (1969). Physiology of Plant Growth and Development. McGraw-Hill, London.

WILSON, B.F. (1967). Root growth around barriers. Bot. Gaz. 128, 79-82.

WILSON, B.F. (1970). Evidence for injury as a cause of tree root branching. Can. J. Bot. 48, 1497-1498.

ZIMMERMANN, M.H. and BROWN, C.L. (1971). Trees: Structure and Function. Springer-Verlag, Berlin.